

## Table of contents

<b>Abstract .....</b>	<b>5</b>
<b>Acknowledgements .....</b>	<b>6</b>
<b>Abbreviations .....</b>	<b>7</b>
1. <b>Plant Stem cells.....</b>	<b>10</b>
1.1 Definition and function of plant stem cells .....	10
1.2 Organisation and regulation of the <i>Arabidopsis</i> SAM .....	11
1.3 Organisation and regulation of the <i>Arabidopsis</i> RAM.....	15
1.4 Endogenous and exogenous stresses endured by plant stem cells, and links to DNA damage .....	18
2. <b>Cellular responses to DNA damage in animals and plants .....</b>	<b>20</b>
2.1 DNA damage responses in animal cells .....	20
2.1.1 The different types of DNA damage .....	20
2.1.2 DNA damage sensing and the importance of ATM.....	21
2.1.3 Transduction of the DNA damage signal.....	23
2.1.4 The repair of a double strand break.....	23
2.1.5 Apoptosis as a consequence of DNA damage .....	24
2.1.5.1 Different DNA damage thresholds.....	24
2.1.5.2 A major role for p53 in DNA damage induced apoptosis .....	25
2.1.5.3 Action of other effectors of apoptosis .....	26
2.1.5.4 Mechanism of apoptosis .....	26
2.2 DNA damage responses in plant cells .....	27
2.2.1 Homologs of the DDR response in plant stem cells .....	27
2.2.2 DNA damage repair pathways in plants .....	27
2.2.3 Specific DNA repair effectors and pathways in plants .....	29
2.2.4 Programmed cell death as a response to DNA damage in plant stem cells..	31
3. <b>The emerging roles of chromatin state, silencing mechanisms and         small interfering RNAs (siRNAs) in the DDR .....</b>	<b>33</b>
3.1 Chromatin remodelling and the DDR .....	34
3.1.1 Phosphorylation of H2AX.....	34
3.1.2 ATP dependent chromatin remodelling .....	35
3.1.3 Histone chaperones .....	36
3.1.4 Re-establishment of chromatin state following repair .....	36
3.2 Chromatin silencing and the DDR.....	37
3.3 A role for ncRNAs (noncoding RNAs) in the DDR .....	37
4. <b>siRNA pathways in plants.....</b>	<b>39</b>
5. <b>Transposons, stem cells and DNA damage .....</b>	<b>43</b>
5.1 Transposon silencing in plants .....	43
5.2 Transposon control in plant stem cells .....	44
5.3 DNA damage induced by transposons .....	45
6. <b>Objectives of this project.....</b>	<b>46</b>
1. <b>Introduction .....</b>	<b>48</b>
2. <b>Results .....</b>	<b>50</b>
2.1 Death of root initials is altered by cycloheximide in response to zeocin in root meristems.....	50
2.2 Developmental PCD mutants have a limited effect on PCD in response to zeocin in root meristems .....	53
2.2.1 A cell death marker linked to xylogenesis is not expressed in the root in response to zeocin treatment .....	53
2.2.2 A possible link between <i>ACL5</i> and zeocin response in the root meristem...56	56
2.2.3 A mutant protein involved in cell death in vascular tissues is not involved in PCD in response to zeocin in the root meristem .....	58

2.3 PCD in response to zeocin is not affected in a mitogen-activated protein kinase phosphatase mutant in the root meristem.....	60
2.4 A possible involvement of the Poly (ADP)-ribose pathway in PCD in response to zeocin .....	62
2.5 PCD in response to zeocin is not affected in a mutant and an over-expressor line for a plasmodesmal-localized $\beta$ -1,3 glucanases in the root meristem.....	66
<b>3. Discussion .....</b>	<b>68</b>
<b>Chapter 3 Forward genetics approach to identify components of the ATM pathway leading to PCD in response to DNA damage .....</b>	<b>73</b>
<b>1. Introduction .....</b>	<b>73</b>
<b>2. Results .....</b>	<b>74</b>
2.1 Design of the forward genetics screen.....	74
2.2 Identification of several stable mutants.....	80
2.3 The mutant line 396 is a new <i>sog1</i> allele .....	83
2.4 PCD in response to X-ray irradiation in stable mutants.....	85
2.5 Test of PCD response in different <i>Arabidopsis</i> accessions and identification of an <i>Arabidopsis</i> ecotype showing decreased cell death in response to zeocin .....	87
<b>3. Discussion .....</b>	<b>99</b>
<b>Chapter 4 ATM dependent silencing in response to a recombination event .....</b>	<b>104</b>
<b>1. Introduction .....</b>	<b>104</b>
<b>2. Results .....</b>	<b>108</b>
2.1 Loss of GFP expression following a recombination event was due to ATM- and SOG1-dependent transgene silencing.....	108
2.1.1 GFP fluorescence cannot be observed in true leaves following a recombination event at the cotyledon stage .....	108
2.1.2 The loss of GFP fluorescence is dependent on ATM and SOG1.....	108
2.1.3 GFP fluorescence was lost in a pattern that suggested gene silencing .....	111
2.1.4 Cre-catalysed recombination was not prevented in the GFPmosaic line... .....	116
2.1.5 The loss of GFP fluorescence was associated with loss of GFP expression .....	118
2.1.6 Searching for the hallmarks of DNA damage following the Cre-catalysed recombination: Silencing was prevented when the NHEJ pathway is disabled.....	120
2.2 ATM-dependent production of small RNAs.....	122
2.3 Characterisation of the pathway leading to ATM dependent silencing .....	125
2.4 Development of reporter lines for inducible DSBs.....	130
<b>3. Discussion .....</b>	<b>134</b>
<b>Chapter 5 Investigation of the link between DNA damage and transposon activity .....</b>	<b>141</b>
<b>1. Introduction .....</b>	<b>141</b>
<b>2. Results .....</b>	<b>142</b>
2.1 A class of genomically unstable mutants displays spontaneous cell death .....	142
2.2 Partial enhancement of the <i>bru1-2</i> phenotype in <i>atm-2</i> background and partial rescue in <i>sog1</i> background .....	146
2.3 <i>ddm1</i> , but not other genes required for transcriptional gene silencing, displays spontaneous cell death in the root initials.....	149
2.4 ATM-dependent reactivation of retrotransposons .....	154
2.4.1 Possible generational transposition event in the <i>atm</i> mutant.....	155
2.4.2 Detection of ONSEN expression by <i>in situ</i> hybridisation following heat- stress .....	158

<b>3. Discussion .....</b>	<b>160</b>
<b>Chapter 6 General Discussion .....</b>	<b>165</b>
1. Summary of results .....	165
2. Perspectives and future work .....	169
<b>Material and Methods.....</b>	<b>172</b>
1. Materials.....	172
1.1 Plant lines .....	172
1.1.1 Mutant lines .....	172
1.1.2 Transgenic lines.....	173
1.2 Oligonucleotides.....	173
1.2.1 Genotyping oligonucleotides.....	173
1.2.2 Other oligonucleotides.....	174
1.3 Plasmids .....	175
1.4 Other material .....	175
2. Methods.....	175
2.1 Propagation and manipulation of plants .....	175
2.1.1 Seed sterilization .....	175
2.1.1.1 Gas seed sterilization .....	175
2.1.1.2 Liquid sterilisation .....	176
2.1.2 Growth conditions.....	176
2.1.2.1 <i>In vitro</i> culture.....	176
2.1.2.2 Controlled Environment Room (CER) culture .....	176
2.1.3 Crosses .....	177
2.1.4 Heat Shock.....	177
2.1.5 Heat stress for transposon movement.....	177
2.1.6 DNA damaging treatments.....	177
2.1.7 GUS staining.....	178
2.2 Manipulation of nucleic acids .....	178
2.2.1 Isolation of plant genomic DNA.....	178
2.2.1.1 Rapid extraction in 96 well plates for genotyping .....	178
2.2.1.2 Clean genomic DNA extraction .....	179
2.2.2 Isolation of small volumes of plant total RNA.....	179
2.2.3 Modified TRI protocol for small RNA Northern blotting.....	180
2.2.4 Enrichment for the small RNA fraction of plant RNA .....	181
2.2.5 Cloning procedures.....	181
2.2.5.1 Restriction enzyme digestion.....	181
2.2.5.2 Dephosphorylation .....	181
2.2.5.3 Ligation.....	182
2.2.5.4 Purification of nucleic acids following enzymatic reactions .....	182
2.2.5.5 Transformation of electrocompetent bacteria.....	182
2.2.5.6 Miniprep of plasmidic DNA .....	183
2.2.5.7 Sequencing.....	183
2.2.6 Polymerase chain reaction based techniques.....	183
2.2.6.1 Polymerase chain reaction (PCR) .....	183
2.2.6.2 Production of Taq .....	184
2.2.6.3 Gel purification of PCR products .....	185
2.2.6.4 Semi-quantitative RT-PCR .....	185
2.2.6.5 Quantitative PCR .....	185
2.2.6.6 Transposon display.....	187
2.2.7 Radiolabelling of nucleic acids.....	188
2.2.7.1 End-labelled oligonucleotide .....	188
2.2.7.2 Riboprobe.....	188
2.2.8 Gel electrophoresis of nucleic acids .....	189
2.2.8.1 Agarose gels .....	189
2.2.8.2 Polyacrylamide-urea gels.....	189
2.2.9 Hybridisation of nucleic acids.....	190

2.2.9.1	Northern blotting of small RNAs.....	190
2.2.9.2	<i>in situ</i> hybridisation.....	191
2.3	Imaging techniques .....	197
2.3.1	Confocal microscopy.....	197
2.3.2	Fluorescence stereomicroscopy .....	198
2.3.2.1	Screening.....	198
2.3.2.2	GFP expression and GUS staining .....	198
2.4	Statistical analysis.....	198
<b>References</b> .....	<b>201</b>	

## Abstract

Plants are sessile organisms that cannot escape environmental hazards, which induce DNA damage and cause mutations. Plants are also subject to DNA damage caused by endogenous processes such as transposon movement. Plant stem cell populations in particular must be protected from genotoxicity, as they are the origin of all organs, together with the germline. In accordance with this premise, plant stem cells were found to be hypersensitive to Double Strand Breaks (DSBs), leading to their specific killing *via* the *ATAXIA TELANGIECTASIA MUTATED* (ATM) and *SUPPRESSOR OF GAMMA RESPONSE 1* (SOG1) genes. However, the components of the pathway leading to programmed cell death (PCD) in response to DSBs in plant stem cells are still unknown, and the *in vivo* DNA damaging agents relevant to this mechanism have not been characterised, providing the starting point of this thesis. Here, a candidate gene approach and a forward genetics screen in the root stem cells did not yield new factors of the pathway leading to PCD in root stem cells. However, a specific ecotype showed an absence of DSBs-induced PCD, revealing natural variation in stem cell responses to DSBs. In relation to responses to endogenous DNA damage in plant stem cells, I identified several chromatin-silencing mutants showing spontaneous PCD in the root meristem, and studied the link between transposon silencing and the ATM/SOG1 pathway. Finally, by characterising responses to Cre-catalysed recombination in the shoot meristem, I uncovered an unexpected link between the DNA damage response pathway and chromatin silencing. This silencing was dependent on ATM/SOG1, linked to the production of 24-nt siRNA, and required the RNA polymerase IV and ARGONAUTE 6. My work links DNA damage responses to chromatin silencing in *Arabidopsis* stem cells.

## Acknowledgements

I decided to try to get into a PhD programme at JIC after an amazing summer project in the lab of Dr Phil Wigge. I was so fortunate to be selected for the rotation PhD programme and my thank you goes to the selection committee for offering me this chance, the John Innes Foundation for offering me a studentship, and especially Mike Merrick who was so supportive during my time at JIC.

Of course, my deepest gratitude goes to my supervisor Dr Robert Sablowski. His guidance, support and enthusiasm throughout this project have been invaluable and I feel like I have grown so much as a scientist thanks to his advice and always-constructive criticism. Thank you to Dr Silvia Costa from my supervisory community for her availability and input. Thank you to Dr Richard Morris for teaching me modelling and to Dr Kay Denyer for sharing her knowledge of plant chemistry with me. Thank you to Pr Peter Shaw and Dr Karel Riha for accepting to be my examiners.

A massive thank you to the present and past members of the Sablowski lab and the CDB department and beyond that I met during my stay. I found the friendly yet competitive environment to be very inspiring, and it felt extremely fulfilling to be surrounded by such talented and passionate people. Special thanks to Max Bush for his invaluable technical assistance, Nicolas Arnaud, Mathilde Seguela-Arnaud, Neil Mcenzie and the members of the Dean Lab. A big thank you to members of the support teams of JIC, especially the irreplaceable Cindy Cooper and Tim Wells for taking such good care of the plants.

Finally, this experience enabled me to meet incredible friends for all over the world and I want to thank them for such great moments of science and fun spent together, especially Scott Berry, Jacqueline Blesing, Jack Dumenil and above all my very best friend Charlotte Miller. This could not have been done without you!

I would have never been able to conduct this project without the infallible support of my husband Fabrice, my parents Elisabeth and Laurent, and my sisters Lucie and Marie. I will never forget it.

## Abbreviations

53BP1	P53 BINDING PROTEIN 1
ACL5	ACAULIS 5
ACR4	ARABIDOPSIS CRINKLY 4
AGO	ARGONAUTE
ARF	AUXIN RESPONSE FACTOR
ARR	ARABIDOPSIS RESPONSE REGULATORs
AS	ASYMETRIC LEAVES
ASF1	ANTI-SILENCING FUNCTION 1
ATM	ATAXIA-TELANGIECTASIA MUTATED
<i>AtNUDX7</i>	NUCLEOSIDE DIPHOSPHATES LINKED TO SOME MOIETY X 7
ATR	ATAXIA-TELANGIECTASIA MUTATED AND RAD3-RELATED
BAK	BLC-2 ANTAGONIST/KILLER
BAX	BLC-2 ASSOCIATED X PROTEIN
BER	Base excision repair
BP	BREVIPEDICELLUS
BRCA1	BREAST CANCER ASSOCIATED FACTOR 1
BRU	BRUSHY
CAF1	chromatin assembly factor1
CDC	CELL DIVISION CYCLE
CDK	Cyclin dependent kinases
ChIP	Chromatin immunoprecipitation
CHK	Checkpoint kinase
CK	Cytokinin
CLV	CLAVATA
CLE	CLV3/EMBRYO SURROUNDING REGION
CMT3	CHROMOMETHYLASE 3
Col	Columbia
CPD	cyclobutane pyrimidine dimers
CtBP	C-terminal BONDING PROTEIN
CZ	Central zone
DDR	DNA damage response
DNA-PK	DNA dependent protein kinase
dNTP	Deoxynucleotide triphosphate
DCL3	DICER-LIKE3
dc-SAM	decarboxylated S-adenosyl methionine
DDM1	DECREASE IN DNA METHYLATION 1
DRM2	DOMAINS REARRANGED METHYLTRANSFERASE 2
DSB	Double strand break
DTT	Dithioteitol
EDTA	Ethylenediaminetetraacetic Acid
ESCs	Embryonic stem cells
EMS	Ethyl Methane Sulfonate
FAS	FASCIATA
GA	Gibberellins
GFP	Green fluorescent protein
GM	Germination media

GUS	$\beta$ -glucuronidase
GWAS	Genome Wide Association Scanning
HST	Hasty
HIPK2	HOMEODOMAIN INTERACTING PROTEIN KINASE 2
HR	Homologous recombination
HSP	HEAT SHOCK PROTEIN
IAB	5-iodo-6-amino-1, 2-benzopyrone
IPT7	ISOPENTENYL TRANSFERASE 7
IR	Ionizing radiation
KAPP	KINASE ASSOCIATED PROTEIN PHOSPHATASE
KNOX	Class 1 KNOTTED-like HOMEOBOX
KRP	KIP-RELATED PROTEIN
LB	Lysogeny broth
L- <i>er</i>	<i>Landsberg erecta</i>
LIGIV	DNA ligase IV
lnc-RNA	long non-coding RNA
LOG	LONELY GUY
MAPK	Mitogen Activated Protein Kinase
Mb	Megabases
miRNA	microRNA
MMS	Methyl methanesulfonate
MOM1	MORPHEUS MOLECULE 1
MRE11	Meiotic recombination 11
MRN	MRE11/RAD50/NBS1 complex
MULE	Mutator-like element
NER	Nucleotide Excision Repair
NHEJ	Non homologous end joining
MSH2	MUT S HOMOLOG 2
OC	Organising centre
PANDA	p21-associated lncRNA DNA damage activated
PARP	POLY- (ADP-RIBOSE) POLYMERASE
PARG	POLY- (ADP) RIBOSE GLUCOHYDROLASE
PdBg	Plasmodesmal-localized $\beta$ -1, 3 glucanases
PIKK	PHOSPHOINOSITIDE 3-KINASE-LIKE KINASE
PCD	Programmed cell death
PCR	Polymerase chain reaction
PdBGs	Plasmodesmal $\beta$ -1, 3 glucanases
PI	Propidium iodide
PIN	PIN-FORMED
PLT	PLETHORA
PNK	Polynucleotide Kinase
PTGS	Post Transcriptional Gene Silencing
PUMA	p53 UPREGULATED MODULATOR OF APOPTOSIS
PZ	Peripheral zone
QC	Quiescent centre
RAM	Root apical meristem
RISC	RNA-induced silencing complex
RB	RETINOBLASTOMA
RBR	RETINOBLASTOMA Related

RdDM	RNA-directed DNA methylation
RDR	RNA DEPENDENT RNA POLYMERASE
ROS	Reactive oxygen species
RPA	Replication binding protein A
RT	Reverse transcription
ReV	ReVersionless
RZ	Rib zone
SAM	Shoot apical meristem
SCR	SCARECROW
SGS3	SUPPRESSOR OF GENE SILENCING 3
SHR	SHORTROOT
SPD	SPLAYED
SOG1	SUPPRESSOR OF GAMMA RESPONSE 1
SIM/SMR	SIAMESE/SIAMESE-RELATED
siRNA	short-interfering RNA
SRP2	SERPIN 2
SSB	single strand break
SSC	Saline Sodium Citrate
ssDNA	Single stranded DNA
STM	SHOOTMERISTEMLESS
SWI/SNF	SWItch/Sucrose NonFermentable
TBE	Tris Borate EDTA
TE	Transposable Element
TGS	Transcriptional Gene Silencing
UV	Ultraviolet
VAD1	VASCULAR ASSOCIATED DEATH 1
WOX5	WUSCHEL-RELATED HOMEOBOX PROTEIN 5
WS	Wassilewskija
WT	Wild type
WUS	WUSCHEL
XCP2	XYLEM CYSTEINE PROTEASE 2
X-Gluc	5-bromo-4-chloro-3-indolyl- $\beta$ -D-glucuronide
ZLL	ZWILLE

## Chapter 1 General Introduction

### 1. Plant Stem cells

#### 1.1 Definition and function of plant stem cells

One of the most important aspects of plant developmental plasticity is their ability to continuously produce new organs, sometimes for centuries in the case of perennial trees. This ability to produce most of their organs post-embryonically is due to the pluripotent stem cells present in the shoot and root meristems. Stem cells can be defined by their ability to form a self-maintaining reserve of undifferentiated cells, while providing a supply of precursors for the differentiation of tissues (Sablowski, 2004).

The shoot apical meristem (SAM) is involved in the development of all aerial parts of the plants, and the root apical meristem (RAM) leads to the formation of the root system for water and nutrient absorption. Two other meristematic regions, most prominent in perennial trees, lead to the formation of the vascular cambium, which supports increases in the diameter of stems and trunks, and the cork cambium, which enables bark replenishment (Aichinger et al., 2012).

On the other hand, in animals, body plans and organs are established in the embryo and post-embryonic growth occurs mostly through an increase of the size of the organism, with the exception of pools of somatic stem cells localized in particular organs and tissues enabling the replacement of dying cells and providing a certain form of plasticity, such as hematopoietic stem cells or neural stem cells (Altman and Das, 1965; Chaudhary and Roninson, 1991).

Stem cells in plants and animals share common characteristics. They are undifferentiated cells maintained in specific locations called stem cell niches, where extracellular signals ensure that the pool of stem cells

remains undifferentiated and dividing. As daughter cells are displaced from the stem cell niche by rounds of cell divisions, they exit the region within reach of the maintenance signal and can start to differentiate (Sablowski, 2007). I will summarise below the signalling pathways involved in the maintenance of stem cell niches in both the shoot and the root of *Arabidopsis thaliana*.

## 1.2 Organisation and regulation of the *Arabidopsis* SAM

The shoot apical meristem is involved in the development of all aerial parts of the plant (figure 1.1).

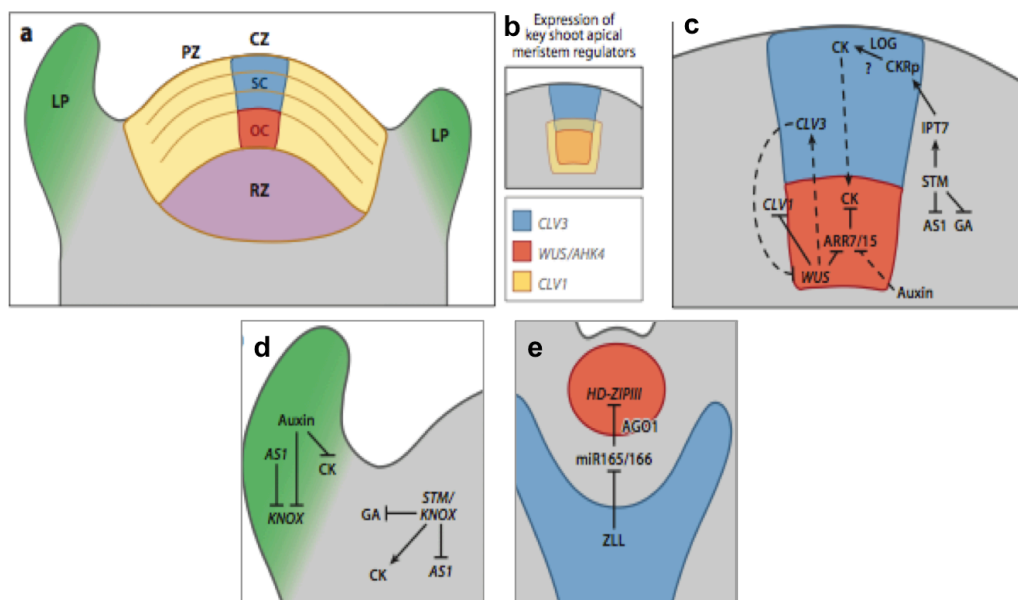


**Figure 1.1: Organisation and regulation of the *Arabidopsis* SAM.** (a) Structure of the SAM. CZ: Central Zone, LP: Leaf primordium, OC: Organising Centre, PZ: Peripheral Zone, RZ: Rib Zone, SC: Stem Cells. (b) Expression patterns of key stem cell regulators: *CLV1* and *3* (*CLAVATA 1* and *3*), *WUS* (*WUSCHEL*). (c) A pool of stem cells (blue) is maintained by a *WUS/CLV3* negative-feedback loop. STM activates *IPT7*, which catalyses cytokinin biosynthesis; LOG might convert inactive cytokinin (CKRp) into active cytokinin. Higher sensitivity to CK in the OC is achieved by localized expression of AHK4 and repression of ARR7/15. (d) Regulation of organ boundaries. AS1 and auxin repress the meristem-promoting activities of KNOX genes and cytokinin (CK) in the leaf primordium, whereas STM and related KNOX genes repress AS1 in the meristem, activate CK biosynthesis, and repress gibberellic acid (GA) biosynthesis. (e) ZLL/AGO10 is expressed in the vasculature underlying the shoot meristem, where it sequesters miR165/166.

miR165/166 to prevent downregulation of meristematic HD-ZIPIII genes in the shoot meristem. (Adapted from (Aichinger et al., 2012)).

It was discovered in 1940 that the shoot meristem of dicotyledonous seed plants consists of three layers of clonal cells: the outer L1 giving rise to the epidermis, the sub epidermal L2 and the internal L3. This organization is different in monocotyledons (two layers) and gymnosperms (one layer) (Satina et al., 1940; Aichinger et al., 2012). The stem cell niche of the SAM spans all three layers and is located in the apical region of the meristem, called the central zone (CZ, Figure 1.1 a). As the dividing cells are displaced from the central zone, they enter the peripheral zone (PZ), giving rise to lateral organs, or the underlying rib zone (RZ) giving rise to the stem. These cells function in a so-called population mode, meaning that their division is not strictly asymmetric, with the division of a stem cell generating a new stem cell and a differentiating cell; instead, the fate of a new cell depends on its position (Laux, 2003).

Thus the maintenance of the SAM depends on the coordination of two processes that are antagonistic: the initiation of new organs, first the stem and rosette leaves, then the cauline leaves and floral buds, and the renewal of the stem cell population. This maintenance depends on signals emerging from the organizing centre (OC) situated directly below the stem cell population. The *WUSCHEL* and *CLAVATA* family genes play an important role in this maintenance (Figure 1.1 b and c). The *wus* mutant lacks a shoot meristem at the seedling stage and shows differentiated cells at the position of the stem cells, whereas overexpression of *WUS* leads to enlarged meristems (Lenhard et al., 2002; Yadav et al., 2010). This suggests that *WUS* is required to prevent differentiation of stem cells and is sufficient to promote stem cell identity, whereas the *CLAVATA* genes (*CLV1, 2* and *3*) are required for organ initiation, as *clv* mutants accumulate undifferentiated cells at the shoot meristem (Clark et al., 1996). On the other hand, overexpression of *CLV3* leads to a decrease in mitotic activity, together with

a reduction of the size of the SAM and a decrease in *WUS* transcript accumulation (Yadav et al., 2010).

The existence of a feedback loop between the *WUS* and *CLV* genes was demonstrated, limiting *WUS* expression and consequently the size of the stem cell population (Lenhard et al., 2002). As described above, *WUS* is expressed in the OC but the *WUS* protein migrates to the CZ where it directly binds to the *CLV3* promoter, leading to *CLV3* expression. In turn, signalling of *CLV3* in the OC through the *CLV1/2* receptor complex represses *WUS* at the transcript level (Brand et al., 2002). The expression of *CLV3* depends only on *WUS* in the embryonic shoot meristem, but at later developmental stages, *WUS* and *STM* (*SHOOTMERISTEMLESS*), which is another homeobox protein, also promote *CLV3* expression. *STM* is expressed in both the PZ and the CZ, maintains cell division and delays differentiation (Schoof et al., 2000) (Brand et al., 2002) (Yadav et al., 2011).

This mechanism links the maintenance of the stem cell niche with a second pathway involving *STM* and other genes of the *KNOTTED-LIKE (KNOX)* class genes. *stm-1* mutants are unable to initiate meristems postembryonically (Long et al., 1996). *KNOX* genes are expressed in the SAM but downregulated in differentiated cells (Barton and Poethig, 1993). *STM* promotes the maintenance of stem cells by repression of the differentiation genes *AS1* and *AS2* (*ASYMMETRIC LEAVES1 and 2*) (Figure 1.1 d). Another *KNOX* gene, *BREVIPEDICELUS (BP)*, promotes meristem maintenance in the absence of *STM*, showing a redundancy of *KNOX* gene action to maintain the stem cell niche in the SAM. *STM* and *BP* rely on *PENNYWISE* to maintain stem cell fate. Indeed, *KNOX* proteins interact directly with *PENNYWISE* and *pennywise* mutants enhance the meristem defects seen in weak alleles of *stm* (Byrne et al., 2003) (Scofield and Murray, 2006).

Phytohormones are also part of the regulation of the maintenance of the SAM. *STM* directly promotes the expression of the cytokinin biosynthetic

enzyme IPT7 (isopentenyl transferase 7) (Figure 1.1 c) and exogenous application of cytokinins or expression of a cytokinin biosynthetic gene under the control of the *STM* promoter both rescue the *stm* mutant phenotype, showing that activation of cytokinin synthesis is crucial for *STM* action (Jasinski et al., 2005; Yanai et al., 2005). The ortholog of the rice *LONELY GUY (LOG)* gene might convert inactive cytokinin into active cytokinin, as in rice, *LOG* encodes the enzyme catalyzing the final step of cytokinin biosynthesis and is specifically expressed in the stem cell domain. In *Arabidopsis*, *LOG* expression was reported in the SAM (Yadav et al., 2009). Overexpression of *BP* also leads to elevated cytokinin levels in the plant. *STM* also downregulates Gibberellic Acid (GA) levels through a direct repression of biosynthesis genes and upregulation of degradation genes (Figure 1.1 d). Also, in the OC, *WUS* down-regulates the inhibitors of cytokinin signal transduction *ARR7* and *ARR15* (ARABIDOPSIS RESPONSE REGULATORs), the Jasmonate Response Factor *JAZ5* and auxin function through modulation of auxin transport and response genes (Figure 1.1 d) (Zhao et al., 2010; Aichinger et al., 2012).

Finally, non-coding RNAs also play a role in SAM maintenance. Notably, *ZLL/AGO10* mutants have pleiotropic meristem phenotypes, ranging from flat apices of differentiated cells to a pin-like terminal organ instead of a functional SAM. However, *WUS* is still expressed in *zll* embryos, overexpression of *WUS* in the *zll* mutants does not lead to an accumulation of undifferentiated cells, and *CLV3* expression is still initiated. It was suggested that *ZLL* is required to enable stem cell signalling via *WUS*. The cause of the *zll* mutant phenotype is due to the loss of miRNA 165/166 and the subsequent loss of expression of their target HDZIPIII genes, such as *PHABULOSA*, *PHAVOLUTA* and *REVOLUTA* (McConnell et al., 2001; Emery et al., 2003), which are key meristem regulators, but how they play a role in meristem maintenance is still unclear (Figure 1.1 e) (Aichinger et al., 2012).

The signals described above maintain shoot stem cell identity, however, it is still unclear what this identity means in terms of molecular mechanisms. Recent evidence suggests a specialized chromatin structure in plant stem cells, as seen in animals. For instance, the subunits of the chromatin assembly factor 1 (CAF1) FAS1 and FAS2 (FASCIATA 1 and 2) restrict *WUS* and *SCARECROW* (*SCR*) activity (regulator of the RAM, see below): indeed, the *fas* mutants are defective in the maintenance of the expression states of *WUS* and *SCR*. Their pattern of misexpression is also not constant and the degree of misexpression becomes more severe with time (Kaya et al., 2001). Also, the *SWI2/SNF2* (SWItch/Sucrose NonFermentable) chromatin remodelling gene *PICKLE* interacts with *AS1*, indicating a role for chromatin remodelling in stem cell maintenance. Orthologs of *AS1* in other plants include *PHANTASTICA* from *Antirrhinum* and *ROUGH SHEATH 2* from maize. These genes share a MYB domain found in the *SWI3* family of proteins in yeast, which interact with the chromatin remodellers from the *SWI2/SNF2* family (Byrne et al., 2002) (Phelps-Durr et al., 2005).

### 1.3 Organisation and regulation of the *Arabidopsis* RAM

The *Arabidopsis* root growth originates at the tip of the root. At the centre of RAM is the quiescent centre (QC, figure 1.2 a), where cells rarely divide. The root stem cells surround the QC, together defining a region of the RAM that is functionally similar to the CZ of the SAM. Contrary to the SAM, however, cellular divisions in the *Arabidopsis* root stem cell niche are asymmetric, replenishing the daughter cell that stays in contact with the QC, and producing another cell called root initial. The latter undergoes several rounds of division before differentiation, giving rise to the highly organized cell files surrounding the QC: the root, stele, ground tissue, endodermis and cortex, epidermis, root cap and columella (figure 1.2 a).

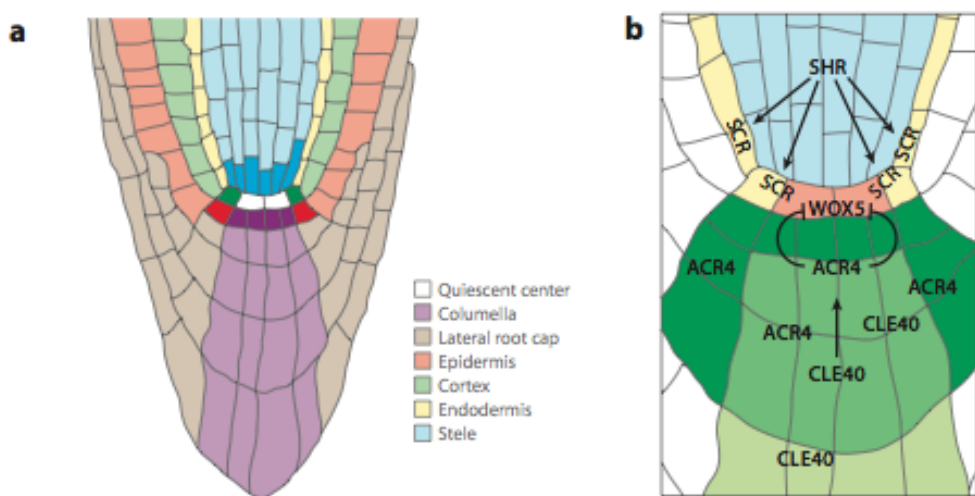


**Figure 1.2: Organisation and regulation of the *Arabidopsis* RAM.** (a) Organisation of the stem cell niche. Intense colours represent stem cells, whereas paler colours mark the cell files originated by each type of stem cell. (b) Action of SHR/SCR and CLE40/ACR4. SHR is expressed in the stele and moves to the endodermis and quiescent centre. SCR is required for nuclear localization of SHR, and SHR activates SCR expression. CLE40 is expressed in the columella and acts via its putative receptor, ACR4. CLE40/ACR4 might function to repress WOX51 expression in an indirect manner (Adapted from (Aichinger et al., 2012)).

The organised cell files of the RAM could suggest a lineage-based mechanism to maintain cell identity. However, as in the shoot, cell identity in the RAM also depends on position: after ablation of individual cells, neighbouring cells are displaced to a different cell file, switch fate and differentiate according to signals received from older cells (Dolan et al., 1993; Scheres et al., 1997).

This simple structure of the *Arabidopsis* RAM, together with its easy accessibility via confocal microscopy, makes it an ideal model to study developmental responses specifically in stem cells (Aichinger et al., 2012).

The quiescence of the QC is caused by a prolonged G1 phase. However, the regulators of cell differentiation in the RAM are not as clearly characterized as in the SAM. Notably, the RETINOBLASTOMA protein (RBR) was shown to suppress cell divisions in the QC, as loss of RBR function cause more cell

divisions and delays differentiation, whereas increased RBR activity causes premature differentiation (Wildwater et al., 2005).

The RAM expresses a *WUS* homolog called *WOX5* (*WUSCHEL-RELATED HOMEOBOX PROTEIN 5*) specifically in the QC. *wox5* mutations lead to the differentiation of QC cells, whereas overexpression of *WOX5* in the columella leads to the generation of stem cells and blocks differentiation. *WOX5* is also required to maintain proximal stem cells, acting redundantly with the SHORTROOT (SHR)/SCARECROW (SCR) and PLETHORA (PLT) pathways (Figure 1.2 b). Much like the CLV3 peptide, several CLE peptides (from the CLV3/EMBRYO-SURROUNDING REGION gene family) promote the differentiation of cells exiting the QC maintenance signal. CLE40 promotes the differentiation of columella cells via the receptor-like kinase ARABIDOPSIS CRINKLY 4 (ACR4) (Stahl et al., 2009). *SHR* is a transcription factor expressed in the stele and moves to the surrounding cells where it activates *SCR* expression (Gallagher et al., 2004). Reciprocally, *SCR* is required for the nuclear localization of *SHR* and mutations in either of the genes result in irregular morphology of the stem cell niche, lack of *WOX5* expression and an eventual collapse of the meristem (Sozzani et al., 2010).

On top of these short-range maintenance signals, the phytohormone auxin plays a crucial role of the control of the root stem cell niche. Indeed, the QC is marked by an auxin maximum. Elegant computer modelling studies coupled to the discovery of the polar localization of the PIN auxin transporter to one side of a cell suggest that auxin accumulates via two transport direction in the vasculature: one rootward towards the QC and one shootward to the root cap and epidermis (Grieneisen et al., 2007). The *PLETHORA* (PLT) genes mediate the function of auxin in the RAM. These transcription factors have additive effects and manipulation of their expression levels suggest a dose-dependent action: the highest expression is found in the QC, whereas intermediate levels are found in the proximal meristem and low levels correlate with differentiation. However, the direct

targets of PLT proteins are still unknown. One attractive hypothesis is that PLT activity is involved in a positive feedback loop stabilizing the auxin maxima at the root tip, as PLT activity enhances PIN (PINOID) expression. Auxin also plays a different role in the columella, where it promotes differentiation via ARF10 and ARF16, showing that auxin plays a role in both promoting and restricting the stem cell niche (Aida et al., 2004; Grieneisen et al., 2007).

The genes and signals described above maintain the meristems under the favourable growth conditions provided in the lab. Plants growing in a natural environment, however, are often subject to environmental fluctuation and stresses, which affect meristem and stem cell functions. These stresses and their consequences are described below.

#### 1.4 Endogenous and exogenous stresses endured by plant stem cells, and links to DNA damage

Plants are exposed to a multitude of environmental hazards due to their sessile nature such as ozone pollution, drought and desiccation, high salinity or heavy metals in the soil. All of these hazards lead to oxidative stress that leads to DNA damage via the generation of Reactive Oxygen Species (ROS) that then cleave the DNA, creating notably double strand breaks (DSBs) (Bray and West, 2005), which are the most severe form of DNA damage, and can be potentially lethal for the cell.

Also, as higher plants rely on photosynthesis to ensure growth, they are therefore heavily exposed to light, including UV-B solar radiations. Consequently, UV-damage is one of the major identified causes of DNA damage in plants. Field crops are known to suffer from continuous UV induced damage. The UV light that is not absorbed by the waxy leaf surfaces or cell walls and flavonoids induces the formation of Cyclobutane Pyrimidine Dimers (CPDs) (Kimura et al., 2004).

Then, one of the developmental steps of plant development that is the most subject to DNA damage is the seed stage. Indeed, dehydration and rehydration of the seeds during seed development and germination respectively leads to oxidative stress, which leads to DNA damage *via* base modification or DNA breaks (Dandoy et al., 1987; Waterworth et al., 2010).

Finally, biotic stresses such as fungi and bacteria induce DNA damage via the hypersensitive response, which includes an oxidative burst (Lorrain et al., 2004). ROS are also the primary cause of single-strand breaks (SSBs) in the DNA of plant cells, either directly, through destruction of deoxyribose units, or by covalent modification of bases (Fong et al., 2013).

Additionally, genomic instability can have endogenous sources, such as replication stress caused by stalled replication forks (Curtis and Hays, 2007). Also, as telomeres age, they shorten and become uncapped, and the exposure of chromosome ends can lead to their end-to-end ligation, which leads to mitotic defects and is potentially lethal for the cell (Riha, 2001). Frequently, vital processes such as replication, transcription and even repair itself require chromatin modifications, which leads to periods where DNA vulnerability might be enhanced. Finally, ROS continually arise within plant cells as a result of normal oxidative cellular processes and present a continuous danger to the integrity and viability of the cell, even in the absence of external stresses (Huefner et al., 2011; Waterworth et al., 2011; Shiloh and Ziv, 2013; Yoshiyama et al., 2013b).

As described above, all organs of a plant originate and grow postembryonically from the stem cell pools in the RAM, the lateral root meristems, the SAM, the secondary floral meristems and the cambium meristems. This means that their maintenance is crucial at the organism level. But plants also lack a reserve germline, as gametes descend from the SAM cells during flowering. Therefore, plant stem cells must have evolved special features to keep the stem cell niches safe, and specifically the stem cell genome against deleterious mutations caused by the aforementioned

stresses (Slotkin et al., 2009). For instance, it was shown that under conditions of phosphate starvation, cell divisions of QC cells do occur and QC derivatives can replace stem cells (Sánchez-Calderón et al., 2005). Also, the QC is more active in older roots of *Arabidopsis thaliana*, and mitosis is induced by altered hormone levels, showing that the QC can be described as responsive organizer competent to replenish stem cells when necessary (González-García et al., 2011; Aichinger et al., 2012).

More specifically in relation to DNA damage, it was shown that plant stem cells are hypersensitive to DSBs and this sensitivity leads to their programmed killing via identified DNA damage response (DDR) pathways (Fulcher and Sablowski, 2009; Furukawa et al., 2010). The responses to DNA damage and the specificity of plant stem cells responses to DNA breaks is described below.

## 2. Cellular responses to DNA damage in animals and plants

### 2.1 DNA damage responses in animal cells

The response of animal cells to DNA damage has been studied extensively, especially in the light of the link between DNA breaks and the onset of cancer (Wyllie et al., 2000).

Cells are protected against genomic instability in different ways, depending on the severity of the damage.

#### 2.1.1 The different types of DNA damage

The different types of DNA damage a cell can suffer from include DSBs, SSBs, base modifications, DNA crosslinks and stalling of replication forks in S phase. Here, I will concentrate mostly of DSBs, which are the most severe form of DNA damage and can jeopardize the survival of the whole organism (Bitomsky and Hofmann, 2009).

### 2.1.2 DNA damage sensing and the importance of ATM

The response to DSBs causes one of the broadest cellular response cascades to any stimuli and begins seconds after the DSB occurs (figure 1.3).

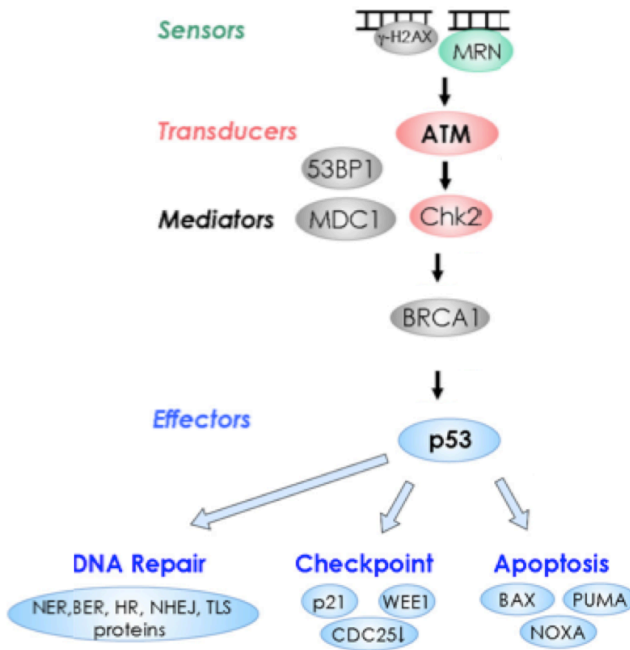


Figure 1.3: **DNA damage signalling**. Sensors shown in green, signal transducing kinases shown in red, mediators shown in grey, and effectors shown in blue, leading to DNA repair, cell-cycle checkpoint, or apoptosis (adapted from (Yoshiyama et al., 2013a)).

The first phase of DSB response is the recruitment of a group of proteins called sensors, forming large foci that are visible with fluorescence microscopy. The sensors transmit the signal to transducers. The very first signal transduction in response to DNA damage is the activation of kinases from the PIKK (phosphoinositide 3-kinase-like kinase) family that relay the signal to numerous downstream effectors. Some of the effectors also act as sensors creating a feedback loop to maintain and enhance the response (Yoshiyama et al., 2013a).

The best-characterised PIKK family sensor is ATM (Ataxia-Telangiectasia Mutated). ATM becomes fully activated by autophosphorylation (Bakkenist and Kastan, 2003) and subsequently activates the checkpoint kinases CHK1 and 2 by phosphorylation to transmit the DNA damage signal to downstream factors (Smith et al., 2010). ATM is a large protein of 350 kDa composed of more than 3,000 residues belonging to the PI3K protein kinase family. The PI3K-domain comprises 10% of the protein. The other numerous domains likely modulate the mode of action and broad substrate specificity of ATM, but very few domains have been fully characterized (Shiloh and Ziv, 2013).

Another player of the PIKKs protein family in response to genotoxic stress is ATR (ATM AND RAD-3 RELATED), which plays a role in replication fork stability. Here, single-stranded DNA becomes opsonised by the replication protein A, which then recruits ATR (Polo and Jackson, 2011). Finally, DNA-PKc (DNA-dependent protein kinase catalytic subunit) is a third member of the PIKKs protein family and binds to the Ku70-Ku80 heterodimer, which is essential for non-homologous end-joining of the broken DNA ends (see below) (Norbury and Zhivotovsky, 2004).

ATM is recruited to the site of damage by a sensor complex containing the MRE11 (Meiotic recombination 11), Rad50 and Nbs1 proteins (the MRN complex). The MRN forms a physical bridge spanning the DSB ends. The nuclease component of the MRN, MRE11 takes part in DSB end resection. The interaction between Nbs1 and ATM is crucial to the ATM recruitment and retention at the site of the DSB. Two major sensor proteins, 53BP1 (p53 BINDING PROTEIN 1) and BRCA1 (BREAST CANCER ASSOCIATED FACTOR 1) are also required at the site of damage for the onset of the DDR to occur. BRCA1 is notably required for the ATM/ATR dependent phosphorylation of p53 that plays a major role in apoptosis (see below). Once the integrity of the DNA is restored, the complex disassembles (Ward et al., 2003; Yamada and Coffman, 2005).

### 2.1.3 Transduction of the DNA damage signal

Depending on the cell type and the extent of the damage, decisions are taken within the DDR whether the damage is repairable or not. Mild DNA damage is first handled via cell cycle arrest through the up-regulation of cyclin dependent kinases inhibitors, such as p21, followed by a repair of the lesions (Bunz et al., 1998).

The signal transduction process starts with the induction of numerous post-translational modifications, including phosphorylation, ubiquitylation, sumoylation, acetylation, methylation and poly (ADP)-ribosylation of the recruited proteins, but also some of the histones situated in the vicinity of the break. The most notable histone change is the phosphorylation of the tail of histone H2AX on serine 139. Chromatin relaxation is also part of the signal transduction process and enables repair of the lesion (see 3.)(Dinant et al., 2008).

### 2.1.4 The repair of a double strand break

DSB repair is mediated by two pathways: the non-homologous end-joining (NHEJ) or Homologous Recombination (HR) pathway (figure 1.4).

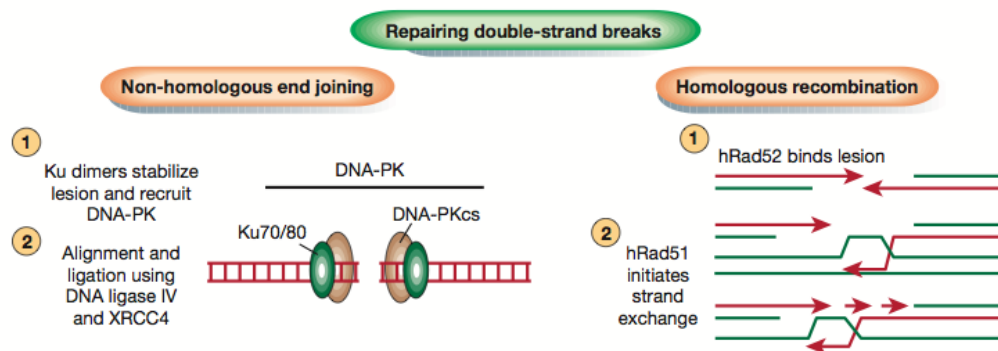


Figure 1.4: **Double-strand break (DSB) repair.** Two competing repair processes called homologous recombination and non-homologous end-joining (NHEJ) target DSBs. Homologous recombination uses a sister

chromatid or homologue to patch up the damage, whereas NHEJ is less accurate and simply joins DNA ends together (Wyllie et al., 2000).

NHEJ is the preferred mechanism for DSB repair in animal cells, but can leave microdeletions at the DNA junctions, together with larger deletions in non-templated fill-in DNA synthesis mechanisms. In this pathway, the Ku70-Ku80 heterodimer recognizes the ends formed by ends and bind to the DNA ends, protecting and stabilising them (Ramsden, 1998) (Walker et al., 2001). Subsequently, the DNA-PKcs binds to these stabilised ends (T Carter, 1990). This complex then promotes rejoining of the two ends by the DNA ligase IV (LIG4) (Lindahl, 1996). On the other hand, HR involves recombination between the damaged DNA molecule and an intact homologous molecule.

### 2.1.5 Apoptosis as a consequence of DNA damage

#### 2.1.5.1 Different DNA damage thresholds

It is thought that in different organisms, organs, tissues or cell types have different DNA damage thresholds to which they can resist. Specifically in animals, once this DNA damage threshold is reached, cycle arrest and DNA repair does not occur and the cell switches to apoptosis, which is a specific form of programmed cell death. The reason why a cell would undergo apoptosis instead of DNA repair or cell cycle arrest is therefore not only linked to the level of DNA damage, but also the cell type (Wyllie et al., 2000).

For instance, the post-replicative epithelial cells of the adult intestinal crypt are resistant to apoptosis in response to ionizing radiations, which induces DSBs in all cells, whereas the replicative cells of the same lineage are acutely sensitive just a few hours earlier in their life history. In this context, the threshold for apoptosis was shown to be lower for stem cells and their descendants than for other cell types. For instance, if the threshold is absent in *Drosophila* embryos that carry a mutation for the *REAPER* gene, which

plays a central role in apoptosis, their resistance to cell death after ionizing radiation is enhanced by 1000 fold (White et al., 1994) .

### 2.1.5.2 A major role for p53 in DNA damage induced apoptosis

The tumour suppressor protein p53 is a transcription factor playing a major role in DNA damage induced apoptosis in animals. Indeed, up to 50% of all human tumours show mutations in the p53 gene resulting in loss of p53 expression or the production of an inactive protein (Vogelstein et al., 2000). The primary role of p53 is transcriptional activation of apoptotic genes, from the very first steps in cell-cycle regulation. The major steps in p53 activation are described in figure 5.1.

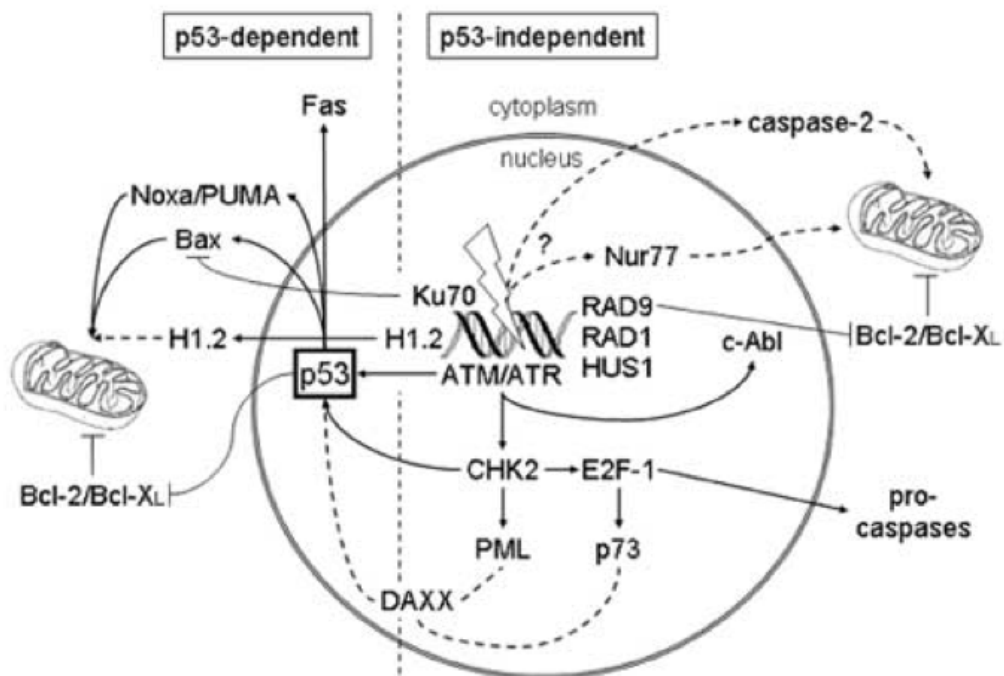


**Figure 1.5: Overview of DNA damage signalling in apoptosis.** Early damage sensing in the nucleus involves the ATM and ATR protein kinases, the RAD1-RAD9-HUS1 (9-1-1) complex, and their downstream effector CHK2. Once CHK2 is activated, the signalling processes can be grouped into p53-dependent (left) and p53-independent events (right). The activities of p53 include transcriptional activation of the genes encoding Bax, Noxa, PUMA and Fas, as well as direct effects on mitochondrial permeabilisation

and mediating the release of histone H1.2 from the nucleus. The proapoptotic effects of Bax are antagonized by the release of nuclear Ku70 into the cytoplasm. The p53-independent pathways include CHK2- mediated signalling to PML, and redirection of E2F-1 towards proapoptotic transcriptional target genes, including those encoding p73 and procaspases. ATM also phosphorylates c-Abl, which promotes the neutralisation of the antiapoptotic Bcl-2 and Bcl-XL byRAD9. Caspase-2 and Nurr77 transduce p53-independent damage signals from the nucleus to mitochondria in less well- defined ways (Norbury and Zhivotovsky, 2004).

#### 2.1.5.3 Action of other effectors of apoptosis

Other effectors play an important role in the onset of apoptosis, either in a p53 dependent or independent manner. Notably, p73 is an unstable molecule marked for proteasome degradation in unstressed cells (Rossi et al., 2005), but accumulates in response to DNA damage and targets pro-apoptotic genes similar to those regulated by p53 (Irwin et al., 2000; Lissy et al., 2000; Dobbelstein et al., 2005).

E2F-1 activity is also crucial for p53 dependent and independent apoptosis. E2F-1 is a transcription factor released from the RETINOBLASTOMA protein as the latter becomes phosphorylated during the progression from G1 to the S phase of the cell cycle. E2F-1 forms a heterodimer with its co-factor DP-1. Like p53, E2F-1 is inactivated by HDM2/MDM2, releasing DP-1 in the nucleus. It is now known that E2F-1 can initiate apoptosis in a p53-null background, and this could be linked to the p73 pathway (Bitomsky and Hofmann, 2009).

#### 2.1.5.4 Mechanism of apoptosis

Apoptosis is the most prevailing mechanism of programmed cell death in animals. It entails engulfment of the dying cell, which limits consequences on neighbouring cells, as the organelles are recycled when the neighbouring cells absorb them. Apoptosis is characterized by three morphological features of the dying cells: the fragmentation of the nucleus, the formation of

lytic bodies called apoptotic bodies, and the degradation of those bodies in the lysosome of the neighbouring live cell. Other features are characteristic of apoptosis, but can also be regulators of autophagic PCD or can also be absent from truly apoptotic systems, such as the action of caspases, chromatin condensation and DNA laddering (van Doorn and Woltering, 2005; Mace and Riedl, 2010).

## 2.2 DNA damage responses in plant cells

### 2.2.1 Homologs of the DDR response in plant stem cells

Plants possess homologues of most of the genes involved in the DDR, including ATM and ATR. In *Arabidopsis*, *atm* and *atr* mutants are hypersensitive to DSB-inducing agents and replication-blocking agents, respectively (Garcia et al., 2003; Culligan et al., 2004). Such hypersensitivity is similar to that of mammalian mutants of *ATM* and dominant negative mutants of *ATR*, indicating conserved functions between plants and mammals. However, counterparts of the signal transducers CHK1, CHK2 and p53 are absent in *Arabidopsis*, suggesting that plants deploy a unique system to transmit the DNA damage signal to downstream effectors (Yoshiyama et al., 2013a).

### 2.2.2 DNA damage repair pathways in plants

Plants possess different DNA repair pathways depending on the type of damage. Specifically, photoreactivation is a major DNA damage repair pathway in plants. It is carried out by photolyases using the energy of light to cleave CPDs provoked by UV-irradiations (Kimura et al., 2004).

The nucleotide excision repair (NER) pathway recognises and repairs various types of DNA damage. It involves the recognition of the DNA damage, the unravelling of the double helix, excision of the damaged

nucleotides and filling of the single stranded gap by DNA synthesis. Base excision repair (BER) also occurs when bases are modified or damaged and are removed by DNA glycosylases. The mismatch repair pathway restores the correct match in mismatched base pairs formed by incorporation of an incorrect base by the DNA polymerase or during recombination (Kimura and Sakaguchi, 2006). In particular the MSH2 (MUT S HOMOLOG 2) protein is crucial to the protection of the genome against genomic instability, as the mutant shows pleiotropic effects over generations, such as germination efficiency, abnormal morphology and reduced fertility (Hoffman et al., 2004). This shows that uncorrected mismatch events lead to an accumulation of mutations and as a consequence the loss of many cellular functions.

When UV damage cannot be repaired via the NER pathway and DNA synthesis cannot be mediated by the DNA polymerase  $\delta/\epsilon$ , new polymerases act instead *via* trans-lesion synthesis. The DNA polymerases,  $\zeta$ ,  $\eta$ ,  $\iota$ ,  $\kappa$ , and ReV1 (ReVersionless 1) synthesise DNA to overcome the DNA damage. However, their fidelity is low and can lead to point mutations. Notably, REV3, which encodes the catalytic subunit of DNA polymerase  $\zeta$ , was shown to be required for DNA damage tolerance in both yeast and *Arabidopsis* (Nelson et al., 1996; Kunz et al., 2000; Wang et al., 2011). In particular, the *rev3* mutant is hypersensitive to UV-irradiation,  $\gamma$  irradiation and the cross-linking agent mitomycin (Wang et al., 2011).

The repair of DSBs is also crucial in plant cells due to potential lethality of unrepaired DSBs. Plants possess homologs of the MRN complex, together with homologs of RAD51, Ku70, Ku80 and LIG4. Ku80-ku70 is also thought to function in telomere maintenance (Zellinger et al., 2007). Like in animals, DSBs are mostly repaired via the NHEJ pathway in plants. As described above, *Arabidopsis* does not possess CHK1 and 2 homologs. However, some of the substrates of those kinases (BRCA1 and E2F) are present in plants,

suggesting that other kinases may work as functional homologs of CHK1 and 2 (Yoshiyama et al., 2013b).

Cell-cycle arrest also functions as a response to DNA damage in Arabidopsis (Preuss and Britt, 2003), although no homologs of p21 have been identified. Instead, proteins from the Kip-related protein (KRP) and SIAMESE/SIAMESE-RELATED (SIM/SMR) family are strongly induced by DNA damaging treatments and may be involved in cell cycle arrest in response to DNA damage (De Veylder et al., 2001). Gamma irradiation of Arabidopsis plants results in an increase in the numbers of cells in G2, suggesting the presence of a DNA damage responsive G2/M checkpoint in plants (Culligan et al., 2004).

### 2.2.3 Specific DNA repair effectors and pathways in plants

Plants have also evolved responses to DNA damage that do not exist in animals (figure 1.6).

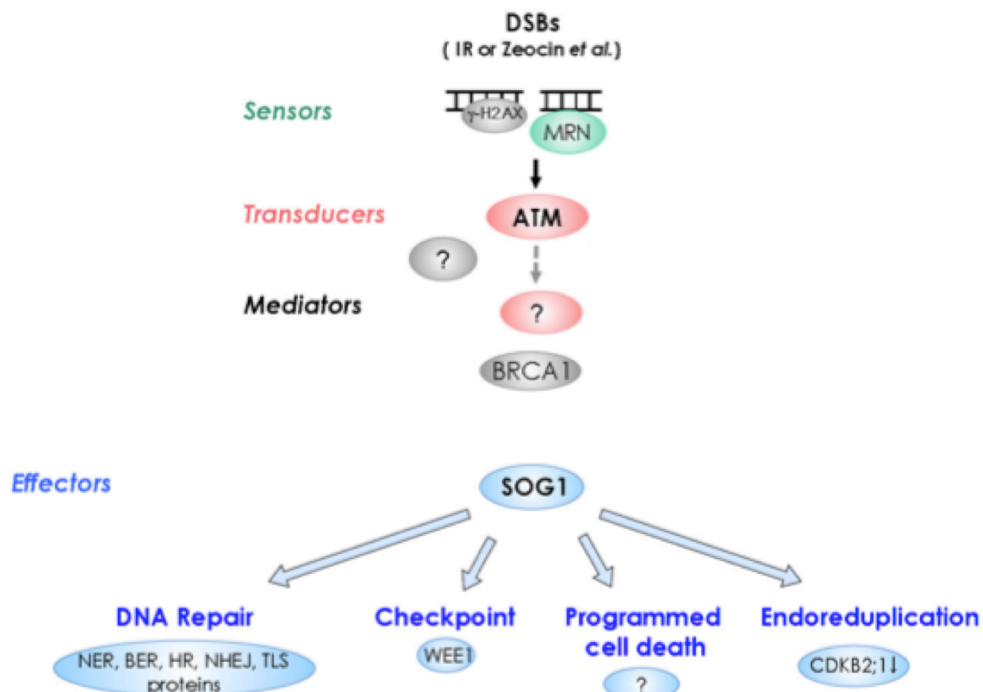


**Figure 1.6: DNA damage response pathways in plants.** DNA damage signal through the sensors shown in green, signal transducing kinases

shown in red, mediators shown in grey, and effectors shown in blue, leading to DNA repair, cell-cycle checkpoint, programmed cell death, and endoreduplication. Dashed lines denote hypothetical situations (adapted from (Yoshiyama et al., 2013a)).

Specifically, a central regulator of DNA damage responses in plants that does not exist in animals is the SOG1 (SUPPRESSOR OF GAMMA RESPONSE 1) transcription factor. SOG1 was discovered by a forward genetics screen looking for mutants that would not show the expected response to gamma ray irradiation (Yoshiyama et al., 2009). It was later shown to be expressed in meristematic tissues such as the SAM and RAM. A small amount of SOG1 is phosphorylated even when no DNA damage is occurring. Hyperphosphorylated SOG1 is detectable 1 hour after gamma-irradiation, suggesting that a rapid modification of SOG1 occurs upon DNA damage. It was also shown that DNA-damage induced hyperphosphorylation of SOG1 is ATM dependent, whereas ATR does not have a main role in zeocin-induced SOG1 phosphorylation. SOG1 is also implicated in the DSB response in particular and not in responses to replication stress. SOG1 plays a role in cell cycle arrest, the transcriptional response and cell death induction in response to DSBs. The similarity in the ATM dependent phosphorylation of SOG1 and p53 prompted the idea that SOG1 is the evolutionary equivalent of p53 and plays the same role as guardian of the genome, even though the 2 proteins share no similarity (Yoshiyama et al., 2013a).

Also, endoreduplication may play a part in the DDR in plants. Endoreduplication involves genome replication without cell division. It was shown in drosophila that mitotic cells respond to damage resulting from stalled replication forks by either arresting the cell cycle or inducing apoptosis, but endocycling cells do neither. By having a muted response to p53 activation and express proapoptotic genes at a lower level than diploid cells (Mehrotra et al., 2008). It was also shown that DSBs caused by depletion of CAF 1 does not affect endocycle progression (Klapholz et al., 2009). Thus, polyploid cells have evolved a mechanism to buffer against the

DNA damage that accumulates during endocycle progression (Lee et al., 2009b).

Similarly to *Drosophila*, it has been recently reported that DSBs caused by depletion of CAF 1 lead to endoreduplication cycles during leaf development. Also, zeocin treatment increases endoreduplication in leaves and roots. This shows that cells with compromised DNA can exit the mitotic cell cycle by switching to the endocycle instead, but the reason for this cellular decision is still unclear. It was hypothesised that the endocycle would allow continued growth in spite of DNA damage by avoiding the deleterious or lethal consequences of defective chromosome segregation during mitosis. The cell enlargement caused by endoreduplication can compensate for the loss of cell number when mitosis cannot occur and therefore sustain growth and tissue structure (Adachi et al., 2011).

#### 2.2.4 Programmed cell death as a response to DNA damage in plant stem cells

True apoptosis does not appear to happen in plants, even though apoptotic-like features of plant cells undergoing PCD have been described. Indeed, the engulfment and later degradation of apoptotic bodies in another cell is not found in plants and it was suggested that the presence of the cell wall prevents phagocytosis. Also, plants lack the apoptotic effector p53. There are also no orthologous caspases in *Arabidopsis*, although plants possess metacaspases (MC), which have been proposed as functionally related to animal caspases in their role in cell death. For instance, expression of *MC8* correlates with cell death and the *mc8* mutant displays reduced sensitivity to DNA damage, but the protein did not cleave known caspase substrates (Coll et al., 2010; Watanabe and Lam, 2011). Also, ATMCP2-d mutants exhibit reduced sensitivity to herbicides that induce oxidative stress, leading to DNA damage (Watanabe and Lam, 2011).

Higher plants have been shown to be more tolerant to DNA damage than mammalian cells, both due to a lower induction of DNA damage but also a more efficient repair of DSBs (Yokota et al., 2005). It was also shown that mutation rates in perennial trees are not very high (Klekowski, 1997), indicating that protection mechanisms are in place to maintain the integrity of the genome of somatic cells. But as plants lack a reserve germline and considering that the stem cell pool can sometimes stay alive for centuries, it has been assumed that plant stem cells in particular may have evolved specific coping mechanisms to avoid a high mutation load caused by DNA breaks.

Indeed, it was discovered in our lab and in another study that plant stem cells display an hypersensitivity to DSBs induced by radiomimetic drugs (Fulcher and Sablowski, 2009) (Furukawa et al., 2010). This sensitivity leads to their selective death under the control of ATM, ATR and SOG1, as no cell death in response to zeocin was observed in the stem cells of those mutants. Interestingly, the study by Furukawa and colleagues showed that *atm* and *atr* mutant plants only show a delayed response to DNA damage compared to the wild type (WT), where *sog1* mutants show no cell death even with an increase of the length of the DNA damage treatment, suggesting that some multiple pathways converge on SOG1 during DNA damage responses in stem cells.

These studies provided the first description of cell death as a downstream response to DNA damage in plants, as previous experiments had only characterized cell cycle arrest mechanisms and DNA repair programmes activation downstream of ATM/ATR (Fulcher and Sablowski, 2009). However, as plants lack the regulators and executioners of apoptosis described above, the programmed cell death induced by DNA damage in stem cells remains uncharacterised. The first clue regarding the type of cell death that is occurring is the morphology of the dying cells in response to zeocin, where the nuclei of dying stem cells remains in a single piece, the

various organelles disappear until the cytoplasm lost its structure, and finally the cell collapses (Fulcher and Sablowski, 2009). This morphology of the dying cells resembles the features of autolysis, which has been well documented in mechanisms of developmental PCD, such as xylogenesis, or the dehiscence of anthers (van Doorn and Woltering, 2005). More recently, the newly characterized and poorly described paraptosis pathway (Sperandio et al., 2010) was identified in response to DNA damage in *Arabidopsis* cell cultures (Smetana et al., 2012). These features suggest that plants have evolved a parallel pathway relying on ATM to induce PCD in stem cells in response to DNA damage.

An interesting aspect of differential responses to DNA damage in plant and animals can be more broadly linked to the growth strategy of plants. Indeed, mutations in *ATM* and *ATR* in plants have little phenotypic consequences, whereas mutation of *ATM* in humans leads to the Louis-Bar syndrome, characterized by poor coordination (ataxia) together with small, dilated blood vessels (telangiectasia). Also, mutations in genes such as *BRCA1* are associated with cancer onset in animals, but plants do not develop tumours in mutants for those genes. Finally, cell-cycle control disruption can lead to cancer in animals but does not lead to tumour formation in plants. Because plants can post-embryonically form new organs from their stem cell pools, even if some tissues or organs are lost due to damage, these can be newly developed without the cell-lineage issues that animal cells have. The option of endoreduplication, allowing tissue growth in the absence of mitosis, may provide plants with a decreased sensitivity to DDR effects.

3. The emerging roles of chromatin state, silencing mechanisms and small interfering RNAs (siRNAs) in the DDR

It has been known for many years that the state of the chromatin is changed during a DNA break to allow sensors and effectors of the DDR to access the damaged region (Lydall and Whitehall, 2005; Dinant et al., 2008; Fernandez-

Capetillo and Murga, 2008). But over the last decade a growing number of studies linked the DDR to more profound chromatin modifications and to silencing mechanisms, including a direct role of siRNAs in the DNA repair mechanism (Tran et al., 2005; Lee et al., 2009a; Shanbhag et al., 2010; Francia et al., 2012; Wei et al., 2012; Wei et al., 2013).

### 3.1 Chromatin remodelling and the DDR

The DNA of eukaryotic organisms is assembled into chromatin, which can achieve a huge degree of compaction thanks to several levels of chromatin organisation. The primary unit is the nucleosome, which comprises the DNA, wrapped around two copies of the histones H2A, H2B, H3 and H4. The nucleosomes have been proposed to be organised into a 30 nm fibre, which is compacted further to form the chromonema fibres of 60-130 nm (Lydall and Whitehall, 2005).

This compaction level requires the remodelling and modification of chromatin to achieve DNA-dependent cellular processes. Chromatin remodelling can be divided into three main categories: the modification of histones and the incorporation of histone variants, ATP dependent remodelling, and the action of histone chaperones (Lydall and Whitehall, 2005), which are described below specifically in the context of DNA damage sensing and repair.

#### 3.1.1 Phosphorylation of H2AX

Histones are subject to a wide range of post-translational modifications including acetylation, methylation, phosphorylation, ubiquitylation and ribosylation. In response to DNA damage, some histone modifications that are involved in transcription also play a role in repair. Others, such as the phosphorylation of H2AX, appear to be unique to the DDR. Here, we will focus in this last modification.

The hallmark of histone modification in the DDR is the phosphorylation of histone H2AX by ATM and DNA-PKcs (in the case of animals). H2AX phosphorylation can span Mb (Megabases) of DNA around the break in mammals. The phosphorylated form is called  $\gamma$ H2AX; in the absence of  $\gamma$ H2AX, Nbs1 and BRCA1, 53BP fail to accumulate in the MRN foci. It was shown in *Saccharomyces cerevisiae* that rapid accumulation of  $\gamma$ H2AX is accompanied by a rapid recruitment of MRE11.  $\gamma$ H2AX accumulation form large foci (50kb) around the break. However, very little  $\gamma$ H2AX can be detected in chromatin within 1-2kb of the break, contrary to repair proteins. This shows that the localization of the repair proteins is unlikely to be the main function of this histone modification (Shroff et al., 2004).

### 3.1.2 ATP dependent chromatin remodelling

As chromatin compaction affects the access of repair proteins to the site of DSBs, the majority of identified chromatin remodelling activities lead to a more relaxed, open chromatin. The increase of chromatin accessibility at DSBs sites is now known to be one of the initial responses that are activated by DNA damage.

Thus, differences in DNA repair efficiencies among cell types and break localisation can be linked to differential chromatin states. In particular, DNA repair efficiency is decreased at the nuclear periphery in subtelomeric regions, which have a more compact chromatin state. Also it was observed that embryonic stem cells show a decompacted chromatin, and this could be linked to their higher responsiveness to DNA damage, providing a possible mechanism for maintaining an intact genome in those cells. These mechanisms are still not clearly identified in plant stem cells. It would be interesting to know if the same mechanisms of differential chromatin states are occurring in stem cell niches vs. differentiated cells (Zhu, 2009).

ATP-dependent chromatin remodelling linked to the DDR involves the SWR1, RSC, INO80, Rad54 and SWI/SNF proteins. Indeed, mutations in INO80 or the SWI/SNF complex have been reported to limit the signalling and repair of the DSB. More globally, it was also shown that ATM-mediated phosphorylation events might have a more global role in promoting the relaxation of chromatin throughout the nucleus, notably through the phosphorylation of KAP1. This low-profile role of ATM may be necessary for the resolution of aberrant DNA structures occasionally formed during DNA-dependent cellular events (Goodarzi et al., 2010; Shiloh and Ziv, 2013) (Fernandez-Capetillo and Murga, 2008).

### 3.1.3 Histone chaperones

ASF1 (anti-silencing function 1) is a key histone H3/H4 chaperone that promotes nucleosome assembly together with CAF1 in a NER-dependent manner upon UV irradiation in mammals (Dinant et al., 2008) (Lydall and Whitehall, 2005; Lario et al., 2013). It was shown that ASF1A and B are both targets of E2F in Arabidopsis, and their levels are also increased following UV-B treatment. They physically interact with N-terminal acetylated histones H3 and H4, and with acetyltransferases of the HAM subfamily, which are known to be involved in cell cycle control and DNA repair. ASF1A and ASF1B are regulated by cell cycle progression and are involved in DNA repair after UV-B irradiation (Battu et al., 2011; Lario et al., 2013).

### 3.1.4 Re-establishment of chromatin state following repair

Finally, once the DNA break has been repaired, the timely re-establishment of chromatin structure is a crucial step for to maintain DNA integrity. This mechanism is assured by two remodelling activities: the recruitment of chromatin-modifying enzymes with the opposite activity of those acting during repair, and the eviction and replacement of modified histones (Lydall and Whitehall, 2005).

### 3.2 Chromatin silencing and the DDR

On top of the characterized chromatin remodelling activities required for efficient repair of DSBs, several studies linking DNA damage responses with silencing mechanisms have been recently published.

One of the first clues linking DNA damage responses with silencing mechanisms showed that normal repair of a DSB can cause heritable silencing by recruitment of proteins involved in silencing in CpG island-containing promoters (O'Hagan et al., 2008). More recently, it was shown that in the context of a DSB in mammalian cell culture, ATM prevents RNA polymerase II elongation at the site of DSB and several chromatin marks are dependent on ATM, especially the ubiquitylation of histone H2A, leading to chromatin condensation, whereas if deubiquitylation is induced, transcription is restored. The conclusion is that DSBs induce transcriptional silencing in *cis* through chromatin modifications, and this can occur multiple kb away from the damage (Shanbhag et al., 2010).

### 3.3 A role for ncRNAs (noncoding RNAs) in the DDR

Recently, post transcriptional regulation of the DDR signalling network have been uncovered, notably involving non-coding RNAs (Gonfloni, 2013). Indeed, it was first thought that only protein-coding genes played a role in the DDR. But miRNAs (miRNAs) were the first non-protein components shown to be involved in the DDR, as overexpression of mir24, which targets H2AX, led to a decrease of H2AX levels, resulting in higher sensitivity of the cells to IR (Lal et al., 2009). Subsequently, several other miRNAs were identified as regulators of ATM, BRCA1 and p53 levels. Also, the lncRNA (long non-coding RNA) PANDA (p21-associated lncRNA DNA damage activated), is induced after DNA damage and regulates apoptosis (Liu and Lu, 2012; Ba and Qi, 2013).

piRNAs (piwi-RNAs) are the largest class of small ncRNA molecules that are expressed in animal cells and do not exist in plants. piRNAs associate with ARGONAUTE-like proteins of the Piwi family. Loss of Piwi proteins leads to germline-specific apoptosis, which may be triggered by DNA damage linked to loss of transposon silencing and their subsequent remobilisation (Wan et al., 2013) (Castañeda et al., 2011; Fang et al., 2012) (Klattenhoff and Theurkauf, 2008).

In plants, several studies showed the importance of siRNAs for an efficient repair of DNA damage. It was shown that *dcl3* (*DICER-LIKE3*) and *rdr6* (*RNA DEPENDENT RNA POLYMERASE 6*) *Arabidopsis* mutants, which are impaired in *trans* activating siRNA biogenesis, were more sensitive to MMS (methylmethane sulfonate), whereas mutants impaired in natural antisense siRNA and heterochromatic siRNA were more tolerant, suggesting a link between DNA damage response and the biogenesis of various siRNAs (Yao et al., 2010).

Furthermore, two new classes in non-coding RNAs have been described as having a role in DNA repair itself. First, in the filamentous fungi *Neurospora crassa*, small RNAs interacting with the QDE2 argonaute protein were identified and called qiRNAs. Their biogenesis requires DNA-damage-induced pre-siRNAs as precursors and *Neurospora* RNA interference mutants showed increased sensitivity to DNA damage, suggesting a role for qiRNAs in the DDR by inhibiting protein translation (Lee et al., 2009a). Second, siRNAs linked to DNA repair and called diRNAs have been identified in plants and animals. Wei and colleagues (Wei et al., 2012), showed that siRNAs generated from sequences flanking a DSB are important for efficient repair, but this repair is not mediated by the chromatin remodelling pathway or through the regulation of known repair genes. The exact function of these diRNAs is unclear, but one theory is that they may help

generate either an open or closed chromatin structure at the break site (O'Hagan, 2013).

Two other studies conducted in *Drosophila* and vertebrates further characterised this new pathway. The inactivation of the RNases DICER and DROSHA, which are implicated in the generation of small double stranded RNA products in animals, but not the downstream elements of the RNAi pathway, was reported to lead to impaired DDR caused by oncogene-induced DNA replication stress or IR. The inactivation reduced the formation and DDR foci containing signalling factors, such as the activated form of ATM. ATM autophosphorylation and activation were also impaired upon DICER or DROSHA inactivation and the G1/S and G2/M cell cycle checkpoints were lost, leading to an escape from apoptosis. This role of DICER and DROSHA in efficient repair was also shown to required the formation of site-specific DICER-and DROSHA-dependent small RNAs, named DDRNAs, which act in a MRE11–RAD50–NBS1- complex-dependent manner (Francia et al., 2012) (Fagagna, 2013). A similar mechanism was characterised in *Drosophila*, with the generation of small RNAs at DNA ends in the context of a DSB. The small RNA response was amplified in the vicinity of the break by active transcription, showing that breaks are sites of transcription initiation, a novel aspect of the cellular DSB response. These small RNAs were also shown to repress homologous sequences in *trans*. Therefore, on top of their putative function in DNA repair mechanisms, these small RNAs may exert a quality control function by clearing potentially truncated messages from genes in the vicinity of the break (Michalik et al., 2012).

#### 4. siRNA pathways in plants

Gene silencing pathways play crucial roles in regulating development and the response to biotic and abiotic stresses. RNA silencing also plays a role in endogenous processes. Indeed, genes, transposons and repetitive sequences

are regulated by RNA silencing. Small RNAs play a major role in these transcriptional and posttranscriptional mechanisms and are very diverse in plants. Here I summarise the diversity of silencing pathways identified in plants, as siRNAs were shown to play a role in the DDR response (figure 1.8).

The two main pathways identified in plants are transcriptional gene silencing (TGS), which prevents transcription through modification of DNA methylation and chromatin modifications, or post-transcriptional gene silencing (PTGS) through mRNA cleavage or translational repression.

The argonaute (AGO) protein-small RNA complex constitutes the core of the RNA-induced silencing complex (RISC) that uses base pairing to silence complementary mRNA at the posttranscriptional level or genomic loci producing complementary RNA at the transcriptional level (Martínez de Alba et al., 2013). The sequence specificity of any RNA silencing reaction is provided by the guide RNA, while the precise nature of silencing depends on the properties of the associated AGO protein (Poulsen et al., 2013).

The small RNA population of WT plants grown under standard conditions is currently believed to consist of 10% miRNAs and 90% siRNAs (Martínez de Alba et al., 2013).

miRNAs have the particularity of deriving from their own loci. The active miRNA is produced from a single stranded primary transcript called pre-miRNA that fold into loops. PolII transcribes the pre-miRNA from the miRNA locus. The DCL-like1 protein processes pre-miRNA into functional miRNAs. They are then exported into the cytoplasm by the exportin-5 homologue Hasty (HST). One strand of the miRNA duplex is then incorporated into the RISC complex containing an AGO protein. The RISC complex targets RNA sequences complementary to the miRNA and provokes the cleavage of the target RNA. The AGO protein, mostly AGO1 in the case of miRNAs, acts as the RNA slicer. Moreover, miRNAs sometimes direct DNA methylation or inhibit

translation (Thieme et al., 2012a; Martínez de Alba et al., 2013; Zhang et al., 2013).

siRNAs derive from true dsRNAs, resulting from the folding of long inverted repeats, convergent transcription or the action of RNA dependent RNA polymerases (RDRs). Their categories include *trans*-acting siRNAs (ta-siRNA), natural antisense transcript-derived siRNAs (nat-siRNA), endogenous siRNAs (endo-siRNA), DNA-Dependent RNA Polymerase IV (PolIV)/PolV siRNAs (p4/p5-siRNA) and Needed for RDR2 Independent DNA Methylation (NERD) siRNAs (Jamalkandi and Masoudi-Nejad, 2009).

ta-siRNAs derive from long non-coding transcripts of trans-acting siRNA (TAS) genes that contain miRNA-binding sites. Those transcripts are produced by PolII and transferred to miRNA/AGO catalytic centres where they are cleaved by the miRNAs miR173, miR390 and miR828, producing tasiRNAs. After the cleavage, the RNA binding suppressor of gene silencing 3 (SGS3) protein stabilises the cleavage products and enables the recruitment of RDR6, which catalyses the synthesis of a complementary RNA strand. Then, DCL4 processes the dsRNA into 21-nt ta-siRNAs. Similarly to miRNAs, only one strand of the duplex associates with AGO1 to guide cleavage of target mRNAs. Like most miRNAs, ta-siRNAs are involved in developmental processes (McCue et al., 2012).

Natural antisense transcripts-derived siRNAs (nat-siRNAs) originate from dsRNA precursors that result from natural antisense transcripts. *cis*-nat-siRNAs are transcribed from genes encoding the complementary strand of DNA at the same locus. On the other hand, *trans*-nat-siRNAs are transcribed from two different genomic loci. Their production requires a DCL together with the activity of PolIV, RDR6 and SGS3. Primary nat-siRNAs are loaded onto a yet unidentified AGO protein to direct the cleavage of the constitutively expressed complementary transcript. Then, the cleaved transcript is converted into dsRNA in a PolIV and RDR6 dependent manner.

Further processing of the dsRNA in a DCL1-dependent fashion generate 21-nt nat- siRNAs, which target the expressed transcripts (Martínez de Alba et al., 2013).

endoIR-siRNAs derive from single-stranded hairpin precursors that are transcribed from different loci found throughout the genome. These structures differ from *MIR* genes as they are much larger. Like pre-miRNAs, endoIR-siRNA precursors fold to form molecules with perfect or near-perfect complementarity, which makes them substrates of DCL2, DCL3 and DCL4 instead of DCL1. 24-nt endoIR-siRNAs have the particularity to trigger *de novo* methylation at a distance. Their function is still unknown but it has been proposed that they could be used in adaptation to the environment and also in trans-generational memory (Vazquez, 2006).

DNA-dependent RNA polymerases IV/V-derived siRNAs (p4/p5-siRNAs), also called heterochromatic siRNAs (hc-siRNAs) are the most abundant class of small RNAs in *Arabidopsis* and are derived from transposons and other repetitive sequences. They are 24-nt in length and their biogenesis depends on the plant-specific DNA-dependent RNA polymerases, PolIV and PolV. They associate with AGO4, AGO6 or AGO9 depending on their localisation: AGO4 is widely expressed, whereas AGO6 is expressed in shoot and root apical meristems, and AGO9 in reproductive tissues. These AGO proteins act in RNA-directed DNA methylation (RdDM), in which the complex formed by AGO protein and the siRNA guides DNA methyltransferase to the sites of their production, triggering *de novo* methylation. This process results in transcriptional silencing of transposons and repeats (Vazquez, 2006; Eun et al., 2011; Martínez de Alba et al., 2013).

The biogenesis of p4/p5-siRNAs starts with the production of ssRNA transcripts by PolIV and their subsequent transformation into dsRNA via RDR2. Those dsRNAs are then processed by DCL3 into 24-nt siRNAs duplexes that are methylated by HEN1. One strand of the duplex is loaded

into a RISC-like complex, which contains AGO4, AGO6 or AGO9 and directs CG and non-CG DNA methylation at specific DNA target loci by interacting with PolV-derived scaffold transcripts. Indeed, the PolV transcripts serve as scaffold molecules to recruit the *de novo* DNA methyltransferase DOMAINS REARRANGED METHYLTRANSFERASE 2 (DRM2) at its DNA target loci, via interaction with MORPHEUS MOLECULE 1 (MOM1). The maintenance of methylation of those targets then requires chromomethylase 3 (CMT3) and DNA methyltransferase 1 (MET1) (Martínez de Alba et al., 2013).

## 5. Transposons, stem cells and DNA damage

The emerging link between chromatin remodelling, silencing pathways and the DDR raises the question of how frequently DDR could be activated by normal cellular processes, in comparison to DDR induced by external factors. Notably, piRNAs are responsible for transposon silencing in the germline of animals, where transposon movement could potentially lead to deleterious mutations that would be passed onto the next generation (Fang et al., 2012). Here I summarise the known mechanisms by which transposons are silenced in plants, and how their mobilisation could be sensed as a DNA break by the cell.

### 5.1 Transposon silencing in plants

Barbara McClintock first discovered the existence of transposable elements (TEs) in the 1950s. Since then it has been revealed that even though the number of protein coding genes remains roughly the same between species, the size of the genome greatly varies in size, and the source of this difference is the non coding portion of the genome, mostly composed of transposable elements. Therefore transposons have the potential to accumulate in large numbers and appear to be a major force that shapes genomes over evolutionary time.

Arabidopsis contributed interesting insights into the control of transposon activity, even though the Arabidopsis genome is transposon-poor (17% of the genome compared to 85% in maize for instance (Buisine et al., 2008). One of the first transposon control factors identified was involved in DNA methylation. *DECREASE IN DNA METHYLATION 1 (DDM1)* encodes a putative chromatin remodelling protein. *ddm1* and subsequently other epigenetic mutants such as *cmt3* and *met1* were shown to release transcriptional silencing of transposons (Cao et al., 2003; Blevins et al., 2009). The study of these mutants shed light on several layers of repression in transposon transcription. These features include DNA methylation, dimethylation of histone H3K9 and the action of heterochromatic 24 nt siRNAs that guide the RdDM machinery (Cui et al., 2013).

Transposon expression often occurs in response to stress. For instance, recent studies using tiling arrays showed that transposons with strong repressive epigenetic marks could be transcribed under heat shock (Lang-Mladek et al., 2010). The mechanisms underlying this reactivation are not yet understood.

The transcription of some transposons in epigenetic mutants or in cell culture is accompanied by the production of 21-nt siRNAs, a hallmark of PTGS (Post Transcriptional Gene Silencing). Also, it was shown that 24-nt siRNAs generated from the mother plant are important in restricting the transposition of the heat shock inducible retrotransposon ONSEN (Ito et al., 2011). Further experiments are needed to reveal whether additional transposons are under the same epigenetic control for their transposition and how these 24-nt siRNAs exert their “anti-transposition” function (Fedoroff, 2012) (Bucher et al., 2012).

## 5.2 Transposon control in plant stem cells

For a transposon to stably increase its copy number, the neoinsertions have to occur in germ cells or in their progenitors, which are present in the shoot meristem and in developing reproductive organs.

In the case of male germ cells (the sperm nuclei in the pollen grain), it was shown that the accompanying vegetative nuclei undergo DNA demethylation, leading to the release of transposon silencing and their subsequent transcriptional activation. Consistent with the reactivation of transposons, in the case of the MULE (Mutator-like element) element, neoinsertions were detected in the vegetative nucleus, but these were not transmitted (Slotkin et al., 2009). It was suggested that this “unmasking” of transposons in the vegetative cell leads to the migration of 21nt siRNA, which migrate from the vegetative nucleus to the sperm nuclei, thereby reinforcing transposon silencing in the germ cells.

The endosperm is also a source of PolIV-dependent 24-nt siRNAs that are required to silence transposons. Additionally, the sporophytic maternal tissues play a role in transposon silencing and could be a source of mobile siRNAs targeting transposable elements in the female gametes. But as *MET1* expression is repressed in ovules and *DDM1* expression is not detected in the male gametes, unknown mechanisms should play a role in maintaining transposon silencing at these specific developmental stages (Lisch, 2009; Bucher et al., 2012). Interestingly in maize, post-transcriptional gene silencing is crucial for the silencing of a DNA transposon in meristems. However, the meristem-specific transposon control is not clear yet in *Arabidopsis* (Slotkin and Martienssen, 2007).

### 5.3 DNA damage induced by transposons

There are two main classes of TEs in eukaryotes, including plants. They are called retrotransposons (or class I elements), which use an RNA intermediate for replication, whereas DNA transposons (class II elements) use a DNA intermediate and function by a so-called “cut and paste”

mechanism. Retrotransposons are further subdivided into long terminal repeat (LTR) and non-LTR elements, based on the presence or absence of LTR sequences in the element. Retrotransposons do not jump *per se*, they keep their original position and increase their copy number in the genome (la Chaux et al., 2012; Wang et al., 2013).

Transposon movement has been shown to induce DNA breaks that need to be repaired via the NHEJ pathway. This was shown in *Arabidopsis* for class II transposable elements (Huefner et al., 2011), and also with during excision and reinsertion of the sleeping beauty transposon in mammalian cells (Yant and Kay, 2003) (Izsvák et al., 2004). It was also shown that reinsertion of the human LINE-1 retrotransposon into the genome leads to DNA damage and apoptosis in cancer cells (Belgnaoui et al., 2006) (Gasior et al., 2006). The insertion of retroviral DNA in the host genome was also shown to require DNA repair (Skalka and Katz, 2005).

## 6. Objectives of this project

Several independent studies have shown that plant stem cells are hypersensitive to DNA damage and the induction of DSBs leads to their specific killing via the ATM pathway. However, several important questions regarding this mechanism remain unanswered and formed the premise of this PhD project. First, the factors of the ATM pathway leading to programmed cell death are still unknown, and the type of cell death is not characterized. Also, the *in vivo* DNA damaging agents that lead to PCD in plant stem cells and that potentially directed the evolution of this mechanism are still unknown.

Following on from these observations, one of my aims was to identify new components downstream of the ATM pathway leading to PCD in *Arabidopsis* meristems, using a combination of reverse and forward genetics. Based on the idea that stem cells have characteristic chromatin states and that

## Chapter 1

### General Introduction

chromatin modification affects DNA damage responses, I also aimed to investigate the links between chromatin states and DNA damage responses in plant stem cells. Finally, considering that a prominent function of chromatin silencing is to control transposon activity and that transposons are potential causes of DNA damage, my final aim was to explore the links between transposon activity and DNA damage responses in plant stem cells.

Candidate Gene approach to identify components of the ATM pathway  
leading to PCD in response to DNA damage

**Chapter 2 Candidate Gene approach to identify components of the ATM pathway leading to PCD in response to DNA damage**

1. Introduction

Plants are sessile organisms and therefore cannot escape environmental hazards. They evolved a vast array of coping mechanisms to protect themselves from biotic and abiotic stresses. One of them is their mode of growth, as they keep several pools of meristematic cells that produce new cells to sustain growth throughout the life of the plant. Indeed, all organs of a plant are created postembryonically from those pluripotent cells present in the root and shoot meristematic regions. This enable them to constantly produce new tissues and organs, and their stem cell pools can stay alive for centuries in the case of perennial trees (Aichinger et al., 2012).

Plants are reliant on photosynthesis to ensure growth, and therefore require exposure to sunlight. This means that they are exposed to high levels of UV-B solar radiations. These are responsible for high levels of DNA damage (see Chapter 1). The repair mechanisms of UV-B induced lesions have been studied in *Arabidopsis*, rice, maize and wheat (Kimura et al., 2004).

But plants are also exposed to other environmental hazards that lead to oxidative stress and consequently DNA damage, such as: ozone pollution, desiccation through drought or salinity, or heavy metals in the soil (Waterworth et al., 2011). Genomic instability also arises from endogenous sources in both plant and animal cells, for instance replication stress caused by stalled replication forks and proof-reading problems (Yoshiyama et al., 2013a), or in response to uncapped telomeres (Shiloh and Ziv, 2013). Another source of genotoxicity is transposon movement (Huefner et al., 2011). For a full description see chapter 1.

The mode of growth and reproduction of higher plants provides the opportunity for mutations to arise in the genome of somatic cells through DNA damage and be passed onto the next generation. Indeed, plants lack a reserve germ line, as gametes arise from the meristematic cells on the shoot

Chapter 2

Candidate Gene approach to identify components of the ATM pathway  
leading to PCD in response to DNA damage

meristem during flowering. Therefore these cells will have passed through numerous rounds of DNA replication and cell division before gamete production, when somatic mutations can pass to the germ line (Bray and West, 2005).

Therefore, plant stem cells must have evolved specific mechanisms to safeguard their genome against DNA damaging agents. For example, it was discovered that plant stem cells are hypersensitive to DNA damage such as double stranded breaks (DSBs) induced by radiomimetic drugs (Fulcher and Sablowski, 2009) (Furukawa et al., 2010) (Smetana et al., 2012). This sensitivity leads to their selective death under the control of the ATM and kinases, together with the SOG1 transcription factor. As described in chapter 1, these studies provided the first description of cell death as a downstream response to DNA damage in plants, as previous experiments had only characterized cell cycle arrest mechanisms and DNA repair programmes activation downstream of ATM/ATR (Fulcher and Sablowski, 2009).

On the contrary, PCD *via* apoptosis in response to DNA damage was extensively studied in animal cells such as mammalian cell cultures, *Drosophila* and *Caenorhabditis elegans*. ATM acts as a chief mobilizer of the cellular response to DNA lesions and depending on the severity of the damage and the cell type (stem cells presenting a suicidal tendency) can lead to apoptosis notably *via* the check-point kinases CHK1 and 2, the tumour-suppressor protein p53 and the activation of caspases (Wyllie et al., 2000) (Norbury and Zhivotovsky, 2004) (Yamada and Coffman, 2005). As plants lack the regulators and executioners of apoptosis described above, and the final phagocytosis of dead cells by their neighbours is prevented by the cell wall (van Doorn and Woltering, 2005), the programmed cell death induced by DNA damage in stem cells remains uncharacterised. Studies describe the features of dying cells in response to DNA damage as having autophagic features, resembling developmental PCD and the newly discovered, poorly characterized paraptosis pathway (Fulcher and Sablowski, 2009) (Smetana et al., 2012).

Chapter 2

Candidate Gene approach to identify components of the ATM pathway  
leading to PCD in response to DNA damage

The first objective of this work was therefore to use a candidate gene strategy to identify new components of the ATM/ATR/SOG1 pathway leading to PCD in response to DNA damage in stem cells. We took a broad approach covering known DNA damage response genes not linked previously to PCD in plants and known PCD pathways in plants not linked previously to DNA damage responses.

In all these experiments, cell death was induced treating *Arabidopsis* seedlings with zeocin as previously described (Fulcher and Sablowski, 2009) (Furukawa et al., 2010). Zeocin is an antibiotic that intercalates into the DNA and induces DSBs (Chankova et al., 2007). This candidate-based approach failed to gather conclusive evidence to better understand the PCD pathway downstream of ATM/SOG1 or the type of cell death involved, leading me to a forward genetic approach described in chapter 3.

## 2. Results

### 2.1 Death of root initials is altered by cycloheximide in response to zeocin in root meristems

In order to test whether *de novo* protein synthesis is required in the hypersensitivity of stem cells to DNA damage, we used cycloheximide, which inhibits the elongation phase of eukaryotic translation by binding the ribosome and inhibiting the translocation phase, where a new codon moves into the A site of the ribosome (Schneider-Poetsch et al., 2010). After treatment for 24 hours with zeocin, cell death was observed in plants that were not treated with cycloheximide (figure 2.1 B), but less death was observed with the cycloheximide treatment (figure 2.1 D). Cycloheximide treated plants also displayed dead cells higher up in the root (figure 2.1 C

Candidate Gene approach to identify components of the ATM pathway  
leading to PCD in response to DNA damage

and D), indicating that the cycloheximide treatment could be inducing a form of stress. The observation that zeocin failed to increase the frequency of cell death in the presence of cycloheximide compared to the wild type suggests that cell death induced by zeocin requires intermediate steps of gene expression and *de novo* protein synthesis.

Candidate Gene approach to identify components of the ATM pathway  
leading to PCD in response to DNA damage

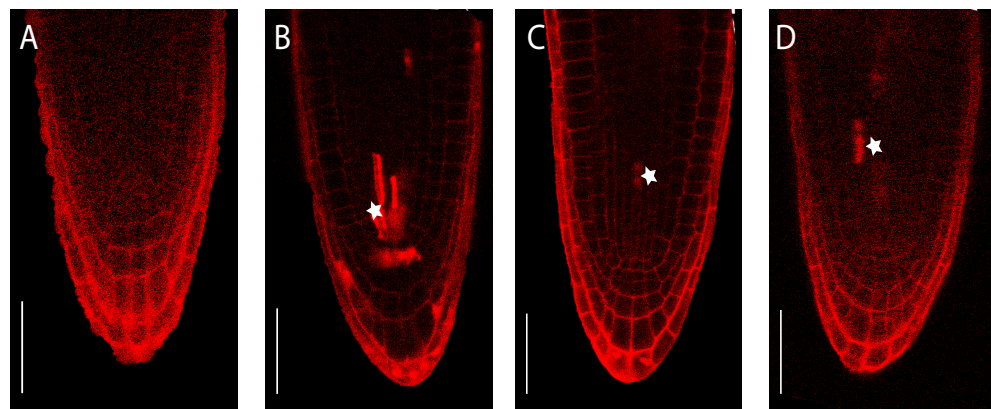


**Figure 2.1: Death of root initials is altered by cycloheximide in response to zeocin.** (A-D) Representative confocal images of root tips stained with PI. (A-B) Representative (10 plants) Col roots untreated (A) or after 24 hours in 20 µg/mL zeocin (B). (C-D) Representative (5 plants) Col roots after 24 hours in 10 µM cycloheximide (C), or 24 hours in 10 µM cycloheximide and 8 µg/mL zeocin (D). Fisher's exact test p-value = p-value = 0.007937. Scale bar = 50 µm. Asterisks indicate dead cells.

Chapter 2

Candidate Gene approach to identify components of the ATM pathway  
leading to PCD in response to DNA damage

2.2 Developmental PCD mutants have a limited effect on PCD in response to zeocin in root meristems

The discovery of plant stem cells hypersensitivity to DNA damage was accompanied by the observation of different features of the dying cells compared to apoptosis. In apoptosis, nuclear fragmentation, formation of apoptotic bodies, and engulfment and degradation of the apoptotic bodies in the lysosome of another cell is observed (van Doorn and Woltering, 2005). Instead, in *Arabidopsis* seedlings treated with zeocin, the nuclei of dying stem cells remained in a single piece, the various organelles disappeared until the cytoplasm lost its structure, and finally the cell collapsed (Fulcher and Sablowski, 2009). This morphology of dying cells resemble the features of autolysis, which has been well documented in mechanisms of developmental PCD, such as xylogenesis, or the dehiscence of anthers (van Doorn and Woltering, 2005).

To test whether ATM/SOG1 mediated PCD in plant stem cells depends on similar mechanisms than developmental PCD, zeocin response was tested in several mutants of the developmental PCD pathway.

2.2.1 A cell death marker linked to xylogenesis is not expressed in the root in response to zeocin treatment

First, we used the cell death marker line *Pro<sub>XCP2</sub>:GUS*. The *XCP2* (XYLEM CYSTEINE PROTEASE 2) gene encodes a xylem-specific cysteine protease that is believed to function as an effector during autolysis (Muñiz et al., 2008). The *Pro<sub>XCP2</sub>:GUS* line is therefore used as a marker for cell death in the xylem elements.

We looked for GUS staining at the root tip of 3 day-old *Pro<sub>XCP2</sub>:GUS* seedlings treated with zeocin for 14, 16 and 18 hours. This timeframe was shown to be when the onset of PCD occurs in response to zeocin (Fulcher and Sablowski, 2009). No GUS activity was observed at the root tip of treated

Candidate Gene approach to identify components of the ATM pathway  
leading to PCD in response to DNA damage

plants, showing the same staining pattern as the non-treated control (Figure 2.2). By contrast, the developing xylem of the root showed intense GUS staining as previously described (Ohashi-Ito et al., 2010) (figure 2.2 E). Therefore, we concluded that the XCP2 protease is not involved in PCD induced by DSB in the root stem cell niche.

Candidate Gene approach to identify components of the ATM pathway  
leading to PCD in response to DNA damage



**Figure 2.2: Evidence that a xylem element death marker is not expressed at the root tip in response to zeocin.**  
(A-E) Histochemical GUS staining of XCP2:GUS *Arabidopsis* seedlings. Images are representative of 5 seedlings imaged. (A-D) XCP2:GUS activity at the root tip after 0 hour (A), 14 hours (B), 16 hours (C) and 18 hours (D) in 8 $\mu$ g/mL zeocin. (E) XCP2:GUS activity in the xylem elements. Scale bar = 50  $\mu$ m.

Chapter 2  
Candidate Gene approach to identify components of the ATM pathway  
leading to PCD in response to DNA damage

2.2.2 A possible link between *ACL5* and zeocin response in the root meristem

Secondly, we tested the zeocin response in the *acl5* (ACAULIS 5) mutant. This gene encodes a spermine synthase and is involved in the synthesis pathway of the polyamine thermospermine (Vera-Sirera et al., 2010). Polyamines are essential for plant growth and survival, mostly by their involvement in biotic and abiotic stress responses (Kusano et al., 2008). They are also involved in vascular development linked with ROS and nitric oxide production. Thermospermine in particular has been proposed to play a role a wide role in plant development, such as stress responses, vascular definition and auxin polar transport (Clay, 2005). *ACL5* was first identified as required for internode elongation after flowering as the mutant exhibits a severe dwarf phenotype with very short internodes (Hanzawa et al., 1997) (Hanzawa et al., 2000). *ACL5* was then shown to be involved in the prevention of premature cell death during xylem specification. Indeed, in the *acl5* mutant, the vessel elements of *acl5* initiate the cell death program too early. Notably, *ProXCP2:GUS* is expressed not only in the maturing vessels but also at an earlier developmental stage in the immature vessel elements, suggesting premature onset of the cell death program in relation to the formation of the secondary cell walls in the vessel elements of *acl5*. As a result, the xylem vessel elements are small and mainly of the spiral type, without pitted vessels and xylem fibers which correspond to the normally predominant vessel elements (Muñiz et al., 2008).

We tested zeocin response in the root of two characterized *acl5* mutants, *acl5-1* and *acl5-4* (figure 2.3). Cell death was clearly reduced in the *acl5-1* mutant following zeocin treatment (2.3 D) compared to the wild-type, but not in the *acl5-4* mutant (2.3 F). These results proved inconclusive to hypothesize a role of the *ACL5* pathway in PCD in response to zeocin.

Candidate Gene approach to identify components of the ATM pathway  
leading to PCD in response to DNA damage

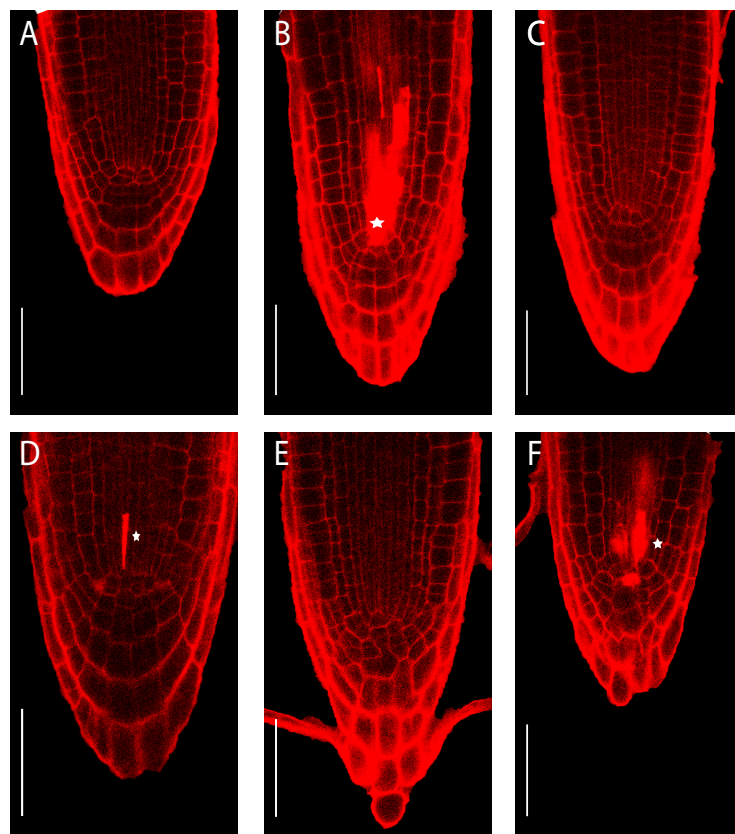


**Figure 2.3: Death of root initials in response to zeocin treatment is altered with a point mutation in the *ACL5* gene but not in an insertion line.** (A-F) Confocal images of root tips stained with PI. (A-B) Representative (10 plants) L-er roots untreated (A) or after 24 hours in 8 µg/mL zeocin (B). All plants showed the phenotype represented. (C-D) Representative (10 plants) *acl5-1* (point mutation) untreated (C) or after 24 hours in 8 µg/mL, where 3 plants showed no PCD and 7 plants showed reduced levels as presented (Fisher's exact test p-value = 1.083e-5 (D). (E-F) Representative (10 plants) *acl5-4* (insertion line) untreated (E) or after 24 hours in 8 µg/mL (F). All plants showed the phenotype represented. Scale bar = 50 µm. Asterisks indicate dead cells.

Chapter 2

Candidate Gene approach to identify components of the ATM pathway  
leading to PCD in response to DNA damage

2.2.3 A mutant protein involved in cell death in vascular tissues is not involved in PCD in response to zeocin in the root meristem

Finally, we tested the zeocin response of the VASCULAR ASSOCIATED DEATH 1 (VAD1) mutant. VAD1 is a GRAM-domain protein that plays a role in cell death and defence responses in vascular tissues. Indeed, the *vad1* mutant displays constitutive HR-like lesions in the vascular bundles, and shows an overexpression of defence genes linked to an increased resistance to *Pseudomonas* (Lorrain et al., 2004). In our conditions, the *vad-1* mutant shows a constitutive ring of dead cells in the root (figure 2.3 E), which is consistent with the description of the mutant phenotype mimicking HR lesions along the vasculature. After 24 hours of zeocin treatment, *vad-1* and Col showed no difference in cell death levels in the root initials (figure 2.3 B and C). Therefore, we concluded that VAD1 is not involved in PCD in response to zeocin in stem cells.

Candidate Gene approach to identify components of the ATM pathway  
leading to PCD in response to DNA damage

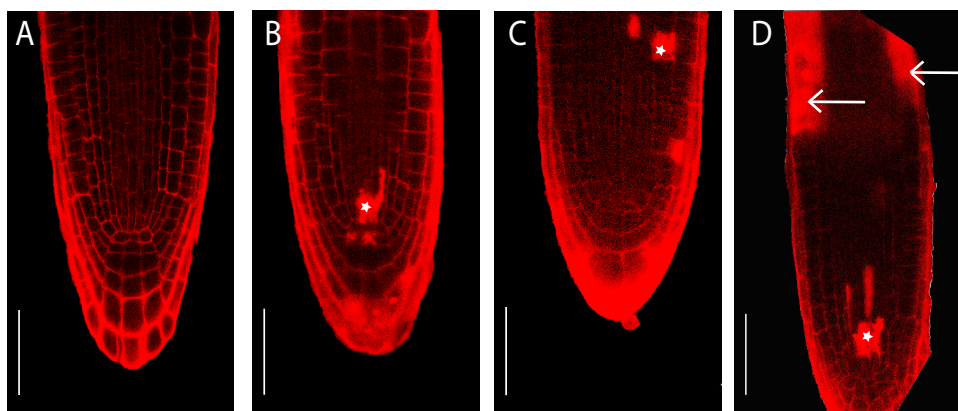


**Figure 2.4 : Death of root initials in response to zeocin is not altered in a mutant involved in vascular cell death.** (A-D) Representative (10 plants displaying the phenotype presented) of confocal images of root tips stained with PI. (A-B) Col roots untreated (A) or after 24 hours in 20 µg/mL zeocin (B). (C-D) *vad-1* roots untreated (C) or after 24 hours in 20 µg/mL zeocin (D). Scale bar = 50 µm. Asterisks indicate dead initials and arrows indicate dead cells in the vascular region.

Chapter 2

Candidate Gene approach to identify components of the ATM pathway  
leading to PCD in response to DNA damage

2.3 PCD in response to zeocin is not affected in a mitogen-activated protein kinase phosphatase mutant in the root meristem

A recent study showed that plant cell cultures treated with bleomycin, which creates DSBs in an analogous way to zeocin treated showed non apoptotic programmed cell death features and that this cell death was ATM/ATR dependent (Smetana et al., 2012). This cell death was described as having “paraptotic-like” features. Paraptosis had only been described in animal cells and protists. Its known morphological features are cytoplasmic vacuolization, “autophagy-like” vesicles and no nuclear fragmentation, but no molecular basis has been firmly established for its mechanism of action (Sperandio et al., 2000) (Sperandio et al., 2004) (Jiménez et al., 2009) (Sperandio et al., 2010). This discovery was reminiscent of the morphological features of the PCD observed in *Arabidopsis* stem cells in response to DSB provoked by zeocin. Therefore, we decided to try to identify a possible candidate gene mediating paraptosis in plant stem cells in response to zeocin. We identified the *mitogen-activated protein kinase phosphatase 1 (mkp1)* mutant as a good candidate to test this hypothesis. Indeed, one of the few identified characteristics of paraptosis is its mediation by Mitogen Activated Protein Kinases (MAPK). Mitogen Activated Protein Kinase Phosphatases are known to inactivate MAP kinases in plants (Mishra et al., 2006) and the *mkp1* mutant was shown to be hypersensitive to genotoxic stress (Ulm et al., 2001) (Ulm et al., 2002). However, no difference in zeocin response was observed in the *mkp1* mutant compared to the wild type (figure 2.4 C and D). This prompted us to conclude that this gene is not involved in PCD in response to DNA damage in cell death.

Candidate Gene approach to identify components of the ATM pathway  
leading to PCD in response to DNA damage

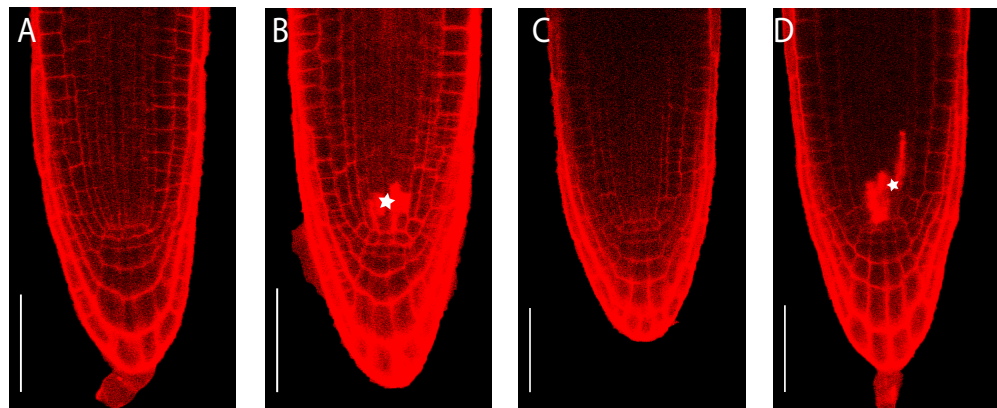


**Figure 2.5: Cell death in response to zeocin is not altered in mitogen-activated protein kinase phosphatase mutant.** (A-D) Representative (10 plants showing the phenotype presented) confocal images of root tips stained with PI. (A-B) Col roots untreated (A) or after 24 hours in 35 µg/mL zeocin. (C-D) *mkp1* roots untreated (C) or after 24 hours in 35 µg/mL zeocin (D). Scale bar = 50 µm. Asterisks indicate dead cells.

Chapter 2

Candidate Gene approach to identify components of the ATM pathway  
leading to PCD in response to DNA damage

2.4 A possible involvement of the Poly (ADP)-ribose pathway in PCD in response to zeocin

The poly (ADP)-ribose polymerase (PARP) pathway is involved in apoptotic and necrosis PCD in animals and was also shown to be activated by ATM/ATR in plants (Garcia et al., 2003). Following DNA damage, the presence of free DNA ends in a cell lead to the activation of PARP. PARP enables the synthesis of polymers of ADP-ribose on a range of nuclear proteins using NAD<sup>+</sup> as substrate, which then act as a signal for the activation of DNA repair programmes or cell death, according to the severity of the DNA injury. Cell death occurs through rapid loss of nuclear and cytoplasmic NAD, which leads to the inhibition of glycolysis. The subsequent depletion of ATP leads to a metabolic catastrophe causing necrosis (Edinger and Thompson, 2004) (Block et al., 2004).

Plants possess two PARP genes, *PARP1* and *PARP 2*. These two genes were shown to be greatly induced by ionising radiations causing DSBs (Doucet-Chabeaud et al., 2001). Using the lipophilic PARP inhibitor IAB (5-iodo-6-amino-1, 2-benzopyrone), we showed that cell death was reduced in response to zeocin when the plant was treated with 50 µM IAB (figure 2.6 F F). This treatment had no effect on root growth, and treatment of the translation fusion CYCB1;1:GFP line showed no increase in GFP accumulation (figure 2.6 G and H), suggesting that PARPs are required specifically for cell death response and does not affect cell cycle arrest in response to DNA damage.

However, no difference in the zeocin response was visible in the *parp1* and *parp2* single mutants (figure 2.7 C and D). Therefore we generated a *parp1 parp2* double mutant, which showed no difference in cell death levels compared to the wild type either (figure 2.7 D). This suggests either that the genes do not play a role in the onset of PCD in response to DNA damage, or that these insertion lines are not true loss-of-function mutants. We were not able to test *PARP2* transcript levels in either mutant, as primer efficiency

Candidate Gene approach to identify components of the ATM pathway  
leading to PCD in response to DNA damage

was very low. We were also not able to check accurately *PARP1* transcript levels in the double mutant as the Cp (see Materials and Methods) were too high to draw a definite conclusion. However, we were able to check transcript levels of *PARP1* in a *parp2* single mutant, and these were shown to be higher than in the wild type (Figure 2.7 G). This suggests the existence of a compensation mechanism between the two genes.

Other mutants involved in the PARP pathway were also tested for their zeocin response: *parg* (*poly-(ADP) ribose glucohydrolase*) and *atnudx7* (*nucleoside diphosphates linked to some moiety X 7*). These mutants are involved in providing the substrates required for the PAR response to the PARPs. PARG removes the ADP-Ribose groups from the polymer chains, modulating the PARP response (Adams-Phillips et al., 2009). AtNUDX7 shows a high affinity for ADP-Ribose and NADH as substrates *in vitro*. Therefore, the enzyme might be involved in nucleotide recycling relating to the metabolism of NADH and/or poly (ADP) ribose (Ishikawa et al., 2009). Both of these mutants displayed no difference in their zeocin response compared to the wild type (figure 2.7 E and F).

Candidate Gene approach to identify components of the ATM pathway  
leading to PCD in response to DNA damage

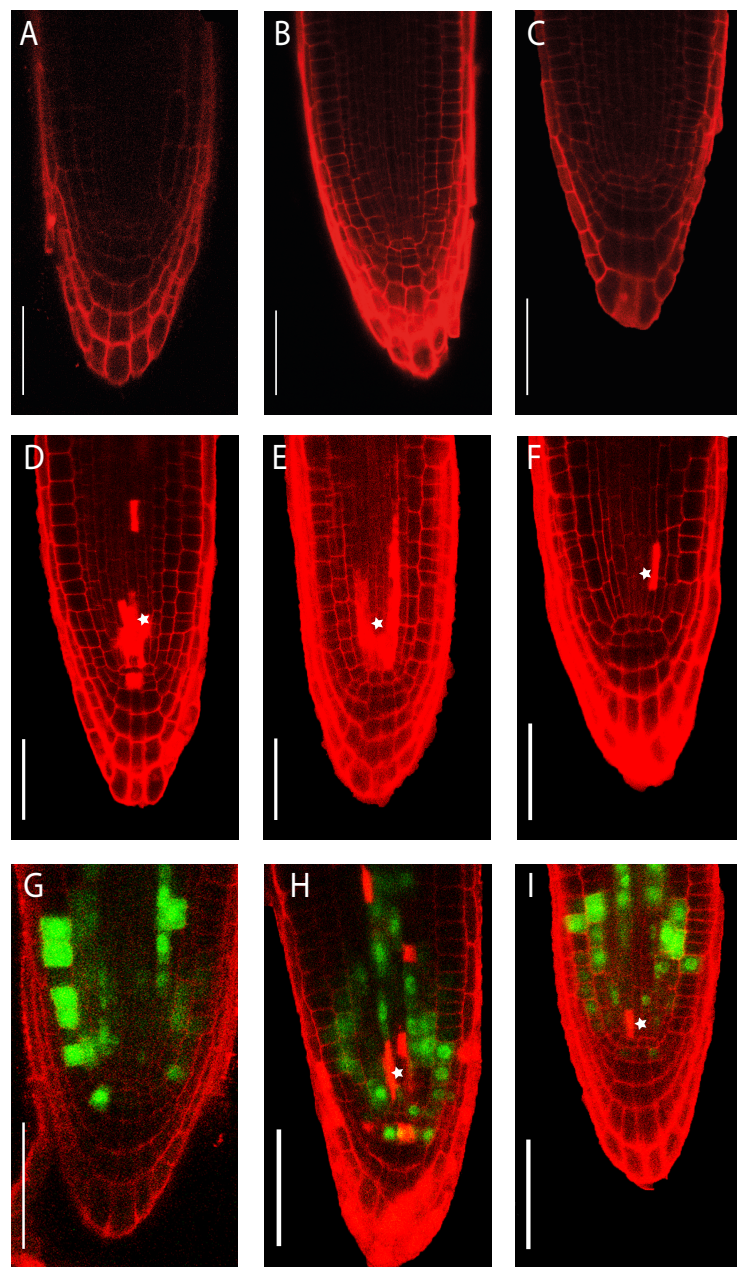


**Figure 2.6: Increasing concentrations of a lipophilic parp inhibitor alters death of root initials.**  
Representative (10 plants showing the phenotype presented) confocal images of root tips stained with (A-C) Col roots untreated (A) or after 24 hours in 20  $\mu$ M (B) or 50  $\mu$ M IAB (C). (D-F) Col roots after 24 h in 8  $\mu$ g/mL zeocin (D) or 24 hours in 8  $\mu$ g/mL zeocin and 20  $\mu$ M (E) or 50  $\mu$ M IAB (7 plants showing reduced PCD presented and 3 plants showing no PCD, Fisher's exact test p-value = 5.142e-05) (F). CYCB1;1:GFP roots wither untreated (G) after 24 hours in 8  $\mu$ g/mL zeocin (H) or 24 hours in 8  $\mu$ g/mL ze and 50  $\mu$ M IAB (3 plants showing the reduced PCD presented and 8 plants showing no PCD, Fisher's exact test p-value = 2.285e-05) (I). Scale bar = 50  $\mu$ m. Asterisks indicate dead cells.

Candidate Gene approach to identify components of the ATM pathway  
leading to PCD in response to DNA damage

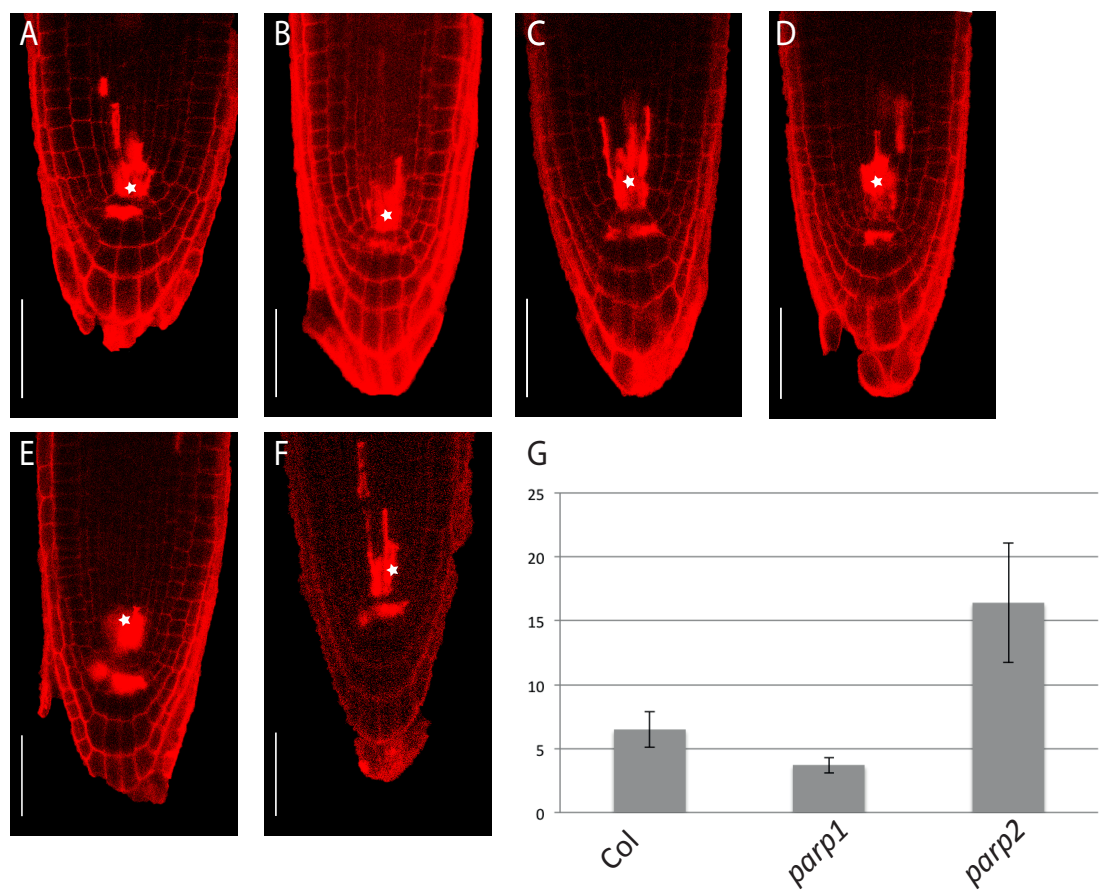


Figure 2.7: **Programmed cell death in response to zeocin is not altered in mutants of the Poly (ADP)-ribose polymerase pathway.** (A-F) Representative (10 plants showing the phenotype presented) confocal images of root tips stained with PI after 24 hours in 8  $\mu$ g/mL zeocin: Col (A), *parp1* (B), *parp2* (C), *parp1 parp2* (D), *parp1* (E), *AtNudx7* (F). Relative transcript levels of *PARP1* in comparison to actin in Col, *parp1* and *parp2*. Error bar represent standard deviation between 3 technical replicates. Scale bar = 50  $\mu$ m. Asterisks indicate dead cells.

Chapter 2

Candidate Gene approach to identify components of the ATM pathway  
leading to PCD in response to DNA damage

2.5 PCD in response to zeocin is not affected in a mutant and an over-expressor line for a plasmodesmal-localized  $\beta$ -1,3 glucanases in the root meristem

It was recently shown that changes in symplastic connectivity accompany and regulate lateral root organogenesis in *Arabidopsis*. This connectivity is dependent upon callose deposition around plasmodesmata affecting molecular flux through the channel. Two plasmodesmal-localized  $\beta$ -1,3 glucanases (PdBGs) were identified that regulate callose accumulation and the number and distribution of lateral roots (Benitez-Alfonso et al., 2013). The existence of specific genes that regulate connectivity between cells in the root apical meristem prompted us to test the link between PCD of stem cells in response to DNA damage and obstruction of the plasmodesmata through callose deposition. The hypothesis was that symplastic isolation might shut down nutrient import to the damaged cells, leading to the autophagic features described before, and at the same time might prevent leakage of any toxic products from the dying cells to their neighbours.

We decided to test the zeocin response in a mutant and overexpressor line for *At1g66250* (PdBG3), which is expressed in plasmodesmata. No difference in cell death was observed in the mutant line or the *At1g66250* overexpressor (figure 2.8 B and D). We concluded that callose deposition in plasmodesmata is not involved in PCD in cell death in response to DNA damage.

Candidate Gene approach to identify components of the ATM pathway  
leading to PCD in response to DNA damage

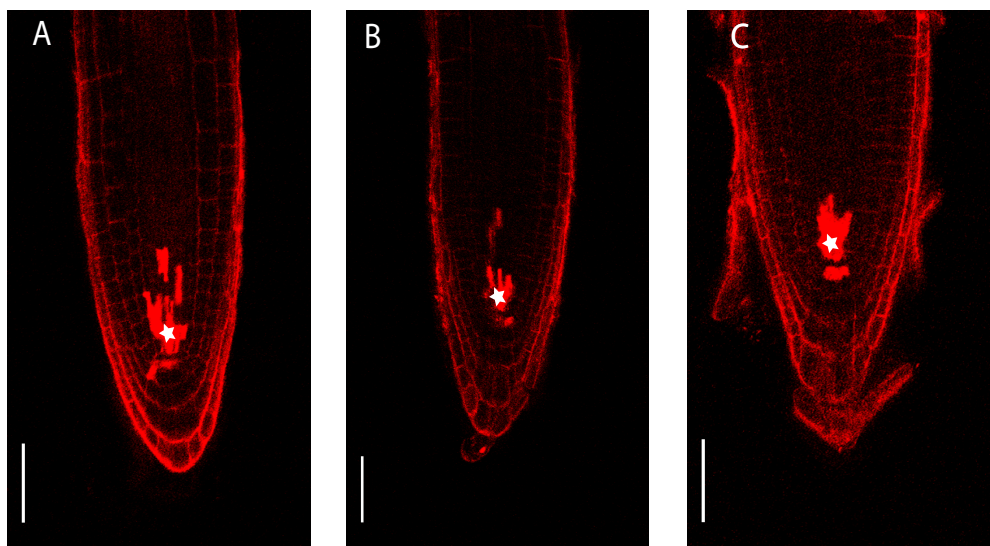


**Figure 2.8: Cell death in response to zeocin is not altered in a mutant and an over-expressor line for a plasmodesmal-localized  $\beta$ -1,3 glucanases in the root meristem.** (A-C) Representative (10 plants displaying the phenotype presented) confocal images of root tips stained with PI. (A) Col roots after 24 hours in 35  $\mu$ g/mL zeocin. (B)  $\beta$ -1,3 glucanase mutant roots after 24 hours in 35  $\mu$ g/mL zeocin. (C)  $\beta$ -1,3 glucanase overexpressor line roots after 24 hours in 35  $\mu$ g/mL zeocin. Scale bar = 50  $\mu$ m. Asterisks indicate dead cells.

Chapter 2

Candidate Gene approach to identify components of the ATM pathway  
leading to PCD in response to DNA damage

### 3. Discussion

Following the studies that showed a hypersensitivity to DNA damage of plant stem cells (Fulcher and Sablowski, 2009) (Furukawa et al., 2010), our candidate-based approach had two objectives: first to uncover components linking ATM/SOG1 and the downstream PCD pathway, and second to shed the light on the type of PCD that occurs in response to DNA damage in plant stem cells. First, we tested the requirement for *de novo* protein synthesis to trigger PCD in response to DSBs, to confirm whether intermediate changes in gene expression were required downstream of ATM/ATR/SOG1. Then, we tested the hypotheses that PCD in response to DSBs in stem cells is related to developmental PCD implicated in xylogenesis, or to the newly identified archaic PCD pathway, paraptosis. Also, we tested DNA damage responses in stem cells in relation to the Poly(ADP)-ribose polymerase pathway, which is known to have a broad role in DNA damage responses. Finally, we tested the idea that symplastic isolation due to callose deposition in plasmodesmata might be involved in cell death in response to DNA damage.

However, this approach failed to uncover clear new actors and regulators of the DNA damage pathway leading to PCD in the root stem cell.

As described in chapter 1, plants lack the core components of the apoptosis pathway described in animal cells. These differences, combined with the observation of different morphological features of dying cells suggest that plants have evolved a parallel pathway relying on ATM to induce PCD in stem cells in response to DNA damage. This concept can be developed further thanks to the study of the transcription factor SOG1. SOG1 is a major player of DNA damage responses and does not exist in animals (Yoshiyama et al., 2009). Interestingly, a study by (Furukawa et al., 2010) also showed that *atm* and *atr* mutant plants only show a delayed response to DNA

Candidate Gene approach to identify components of the ATM pathway  
leading to PCD in response to DNA damage

damage compared to the wild-type, whereas *sog1* mutants show no cell death even with an increase of the length of the DNA damage treatment, suggesting that some other pathways and molecular components feed into the SOG1 pathway for DNA damage response in stem cells. It was recently shown that phosphorylation of SOG1 by ATM is essential for the induction of DNA damage response, where p53 is also phosphorylated by ATM as one of the first steps in the DNA damage response in animals. This prompted the idea of SOG1 as the equivalent of p53 as a “guardian of the genome” even though the two proteins share no similarity (Yoshiyama et al., 2013a).

It is therefore expected the downstream elements of the ATM/SOG1 pathway leading to PCD would be different in plants.

The existence of intermediate steps of gene expression between DNA damage and PCD was confirmed by our initial experiments showing that *de novo* protein synthesis is essential for PCD after DNA damage. To identify the genes involved in these intermediate steps, we initially tested the zeocin response of several mutants implicated in developmental PCD, which shows morphological similarities to the dying cells observed in stem cells in response to zeocin.

We tested two mutant alleles of the *ACL5* gene: *acl5-1* showed reduced cell death levels and the *acl5-4* showed no difference in cell death. *acl5-1* has a point mutation replacing a glutamate at position 123 to lysine, occurring in a potential binding site for the decarboxylated S-adenosyl methionine (dcSAM), which is used as a substrate by the spermine synthase as the spermine. The *acl5-1* mutant does not show detectable thermospermine (Kakehi et al., 2008), but *ACL5* transcript levels are much higher in the *acl5-1* mutant than in the wild-type, suggesting that *ACL5* expression may be under negative feedback control (Hanzawa et al., 2000). In contrast, the *acl5-4* allele carries a large deletion of the locus and does not produce any detectable transcript, therefore it represents a null allele (Hanzawa et al., 2000). However, no thermospermine quantification was done in this mutant. In a wild-type background, thermospermine is present in high levels

Chapter 2

Candidate Gene approach to identify components of the ATM pathway  
leading to PCD in response to DNA damage

in stems and flowers but no root levels quantification has been published (Naka et al., 2010).

Because *ACL5* is required to prevent premature cell death during xylem development we were expecting more cell death in stem cells in the mutant in response to DNA damage. We obtained the opposite result in the *acl5-1* allele but no difference was observed in the *acl5-4* allele. As *acl5-1* fails to accumulate thermospermine, the results still suggested that thermospermine might regulate PCD. However, exogenous application of thermospermine did not rescue the *acl5-1* phenotype and did not increase PCD levels in the wild type (data not shown). Combined with the negative results with the *acl5-4* null mutant, the data do not support a role for *ACL5* and thermospermine in DNA-damage-induced PCD.

Paraptosis was first described as an alternative, non-apoptotic form of cell death occurring in cell cultures in response to the insulin-like growth factor I receptor (Sperandio et al., 2000). Its morphological features include cytoplasmic vacuolization, mitochondrial swelling, and the absence of caspase activation or typical nuclear changes found in apoptosis such as nuclear fragmentation (Jiménez et al., 2009). A proteome profile of mammalian cells undergoing paraptosis showed significant changes in cytoskeletal proteins  $\alpha$  and  $\beta$ -tubulin, signal transducing protein such as phosphatidyl ethanolamine and the  $\beta$ -subunit of the ATP synthase (Sperandio et al., 2010). This form of cell death has been proposed to be mediated by the MAPK and JNK pathways and prohibitin in animal cells, and inhibited by AIP-1/Alix (a protein of unknown function interacting with the cell death-related calcium-binding protein) and the phosphatidylethanolamine binding protein (PEBP-1) (Sperandio et al., 2004) (Sperandio et al., 2010). Of these candidates, we chose to focus on the MAP kinase phosphatases (MKPs) pathway. MKPs are potent inactivators of MAP kinases and are considered important regulators of MAP kinase signaling in plants (Ulm et al., 2001). In a mutant background for MPK, the MAP kinases are active and the plant is more sensitive to stress, in particular

Candidate Gene approach to identify components of the ATM pathway  
leading to PCD in response to DNA damage

the *mpk1* mutant displays a greater sensitivity to salinity and genotoxic stress induced by UV (Ulm et al., 2002). Therefore, we were expecting more cell death in the mutant than in the wild type in response to zeocin. We found no difference in cell death levels in the *mpk1* mutant compared to wild type in response to zeocin. UV-C treatment was shown not to induce PCD in stem cells (Nick Fulcher, personal communication), therefore the MAP kinase pathway could be specific to this type of stress and not broadly involved in genotoxic stress relief as we could have expected. Further work is needed to identify new components of the paraptosis pathway in plants in order to pursue this hypothesis further.

We also found no difference in cell death response in a mutant and an overexpressor line for one of the two PdBGs that regulate callose accumulation in plasmodesmata in the root meristematic region (Benitez-Alfonso et al., 2013). We could have expected more cell death in the overexpressor line and reduced cell death in the mutant line if callose deposition in the stem cell niche is linked to the onset of the PCD programme. Two other genes identified in this study, PdBG1 and 2 showed redundant localization and function for lateral root organogenesis, so a more thorough approach would be to test zeocin response in mutants for all three PdBGs and in the double or triple mutant if those are viable.

The PAR response mediated by the PARP pathway is crucial to DNA damage responses and apoptosis in animal cells (Wyllie et al., 2000). In plants, the induction of *PARP1* and *PARP2* has been linked to DSBs (Doucet-Chabeaud et al., 2001), but no link with PCD has been established. Instead, PARPs seem to be required for the response of wide variety of environmental stresses, including pathogen resistance (Adams-Phillips et al., 2010). Recently, a specific involvement of PARP in the NHEJ pathway was uncovered (Jia et al., 2013). There was no differential response to the zeocin treatment in single and double mutants for *PARP1* and *PARP2*, and similar negative results were obtained with two additional mutants in the pathway. Furthermore, single mutants and RNAi lines for both genes that were shown to increase stress

Candidate Gene approach to identify components of the ATM pathway  
leading to PCD in response to DNA damage

tolerance (Block et al., 2004) have been previously tested for their zeocin response, and showed no effect (Fulcher, personal communication). The only significant result was obtained with the lipophilic PARP inhibitor IAB that showed a clear decrease in PCD in treated plants, and this was independent of cell cycle arrest. CycB1;1 was shown to be increased in response to DNA damage (Culligan et al., 2006) but showed no difference in response to zeocin in our conditions. However, studies with chemical inhibitors without genetic support can be misleading due to non-specific effects.

Overall, these results suggest that the DNA damage response of plant stem cell is mediated by genes that are different from those implicated in known PCD pathways that are activated in development or during pathogen attack. Alternatively, the response might be multifactorial, with high levels of redundancy downstream of ATM/SOG1, which may reflect the crucial importance this pathway has in plant growth and survival. Therefore we decided to take a broader approach using a forward genetic screen in order to identify new components of the ATM/SOG1 pathway leading to PCD in response to DNA damage, as described in the next chapter.

Forward genetics approach to identify components of the ATM pathway  
leading to PCD in response to DNA damage

**Chapter 3 Forward genetics approach to identify components of the  
ATM pathway leading to PCD in response to DNA damage**

1. Introduction

The reverse genetics approach presented in chapter 2 failed to identify new components of the ATM/SOG1 pathway leading to PCD in response to DNA damage in the root stem cell niche. Therefore, we decided to use a forward genetics approach by screening for mutants showing no PCD in response to zeocin in the root stem cell niche. Our design of the screen had two main constraints: the use of an *Arabidopsis* ecotype reliably showing high levels of cell death in response to zeocin and the set-up of a workflow that would not rely on confocal microscopy for time constraints.

The advantage of a forward genetics screen approach is that it enables a non-biased way of identifying new factors of the mechanism of interest. We were therefore expecting to possibly identify new alleles of *atm*, *atr* or *sog1*, which were originally identified by forward genetic screening, but also potential new mutants involved in DNA damage sensing, repair and signalling, or new genes involved in programmed cell death. One of the pitfalls of such an approach would be the identification of mutants involved in zeocin absorption or detoxification by the cell, such as mutants with a thicker root epidermis.

Although Ethyl Methane Sulfonate (EMS mutagenesis), which induces mostly nucleotide substitutions, is useful to identify mutants with subtle effects, fast neutron bombardment is thought to lead mostly to deletions < 1 kb in size, and enables the identification of mutations with tiling arrays (Li et al., 2001) (Hazen et al., 2005). We therefore decided to use a fast-neutron mutant population in this study.

Chapter 3  
Forward genetics approach to identify components of the ATM pathway  
leading to PCD in response to DNA damage

## 2. Results

### 2.1 Design of the forward genetics screen

Experiments conducted by Nick Fulcher (John Innes Centre) showed a slight but consistent difference in PCD levels in the root meristem in response to zeocin in three *Arabidopsis* ecotypes: Col, L-*er* and Ws, with L-*er* displaying the highest levels of PCD of the three (Fulcher, personal communication). As L-*er* and Col are the two ecotypes of choice in forward genetics screening because both their genomes are fully sequenced and a plethora of markers has been developed to discriminate between the two genomes in mapping approaches, we decided to use one of these two ecotypes in our screen. As each new zeocin stock need to be calibrated to display reliable levels of PCD in the root meristem in all plants, we treated Col and L-*er* plants with an increasing concentration of zeocin for 24 hours and looked for differences in PCD levels (Figure 3.1). At a concentration of 30 µg/mL, both Col and L-*er* displayed similar levels of cell death (figure 3.1 C and I). But as the concentration of zeocin increased, the levels of cell death in Col remained unchanged while L-*er* PCD levels continued to rise. At a concentration of 35 µg/mL, high levels of cell death were observed in L-*er* and the QC remained alive (figure 3.1 K) in all 10 plants tested, but at 40 µg/mL one or the two cells of the QC were dead in 5 out of the 10 plants. Therefore, we decided to use the L-*er* background for the forward genetics screen and use zeocin at a concentration of 35 µg/mL. The lab of Dr Philip Wigge (The Sainsbury laboratory Cambridge) generated a fast neutron mutant population in the L-*er* background (Wigge, personal communication). The structure of the population is presented in Figure 3.2 (Page and Grossniklaus, 2002).

Forward genetics approach to identify components of the ATM pathway  
leading to PCD in response to DNA damage

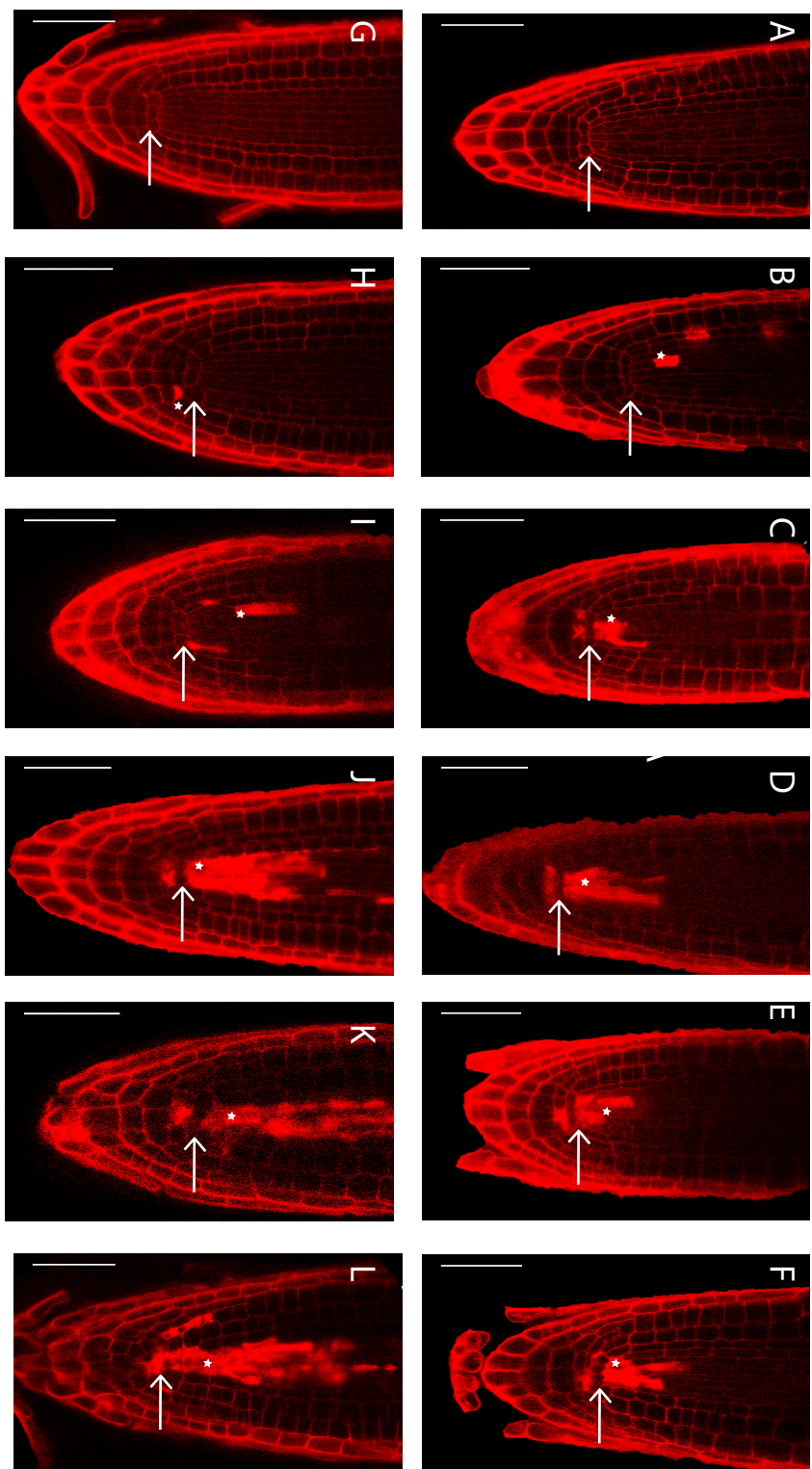


**Figure 3.1: Increasing concentrations of zeocin leads to an stronger increase in cell death in the Ler background than in the Col background.** (A-L) Representative (20 plants) confocal images of root tips stained with PI. (A-F) Col roots untreated (A) or after 24 hours in 15 (B), 20 (C), 30 (D), 35 (E) and 40 (F)  $\mu\text{g}/\text{mL}$  zeocin. (G-L) Ler roots untreated (D) after 24 hours in 15 (H), 20 (I), 30 (J), 35 (K) and 40 (L)  $\mu\text{g}/\text{mL}$  zeocin. Scale bar = 50  $\mu\text{m}$ . Asterisks indicate dead cells and arrows indicate the position of the QC cells.

Forward genetics approach to identify components of the ATM pathway  
leading to PCD in response to DNA damage

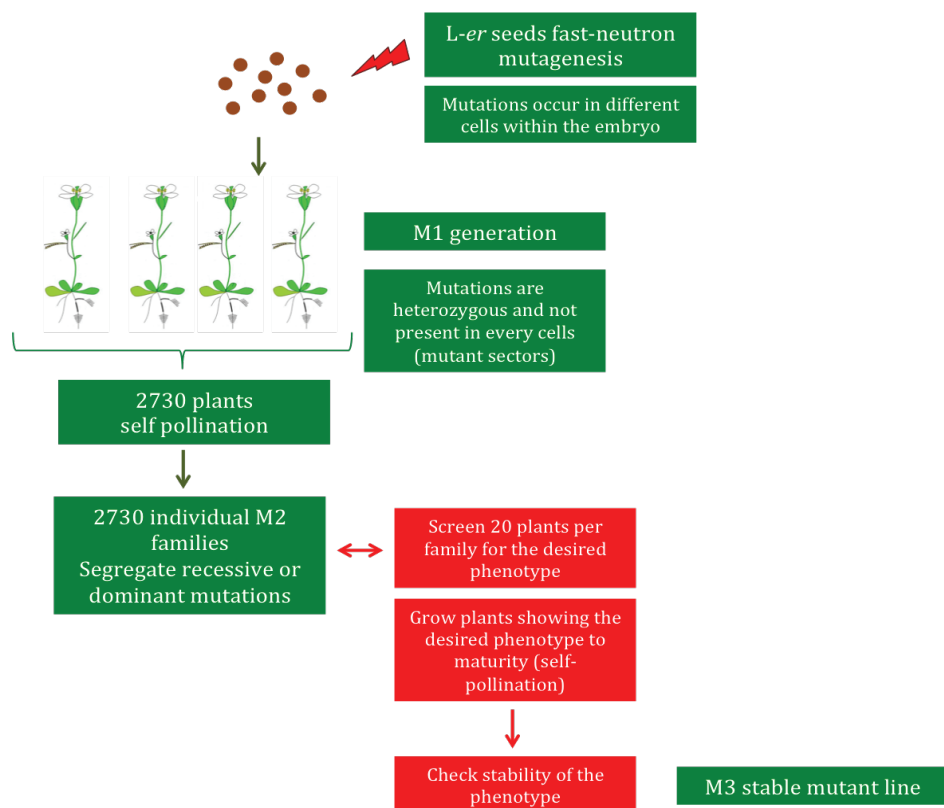


Figure 3.2: **Obtention and structure of the mutant population used in the screen.** The M1 generation and obtention of the M2 families was carried by the group of Dr Philip Wigge (Cambridge Sainsbury Laboratory). Adapted from Page and Grossniklaus, 2002.

Forward genetics approach to identify components of the ATM pathway  
leading to PCD in response to DNA damage

As time constraints did not enable the screening of the M2 families with confocal microscopy, we developed a strategy relying on the fluorescent dye SYTOX® Orange to stain dead cells in response to zeocin in the root meristem. SYTOX® Orange stains the nucleic acids in cells with compromised membranes (Truernit and Haseloff, 2008). It enables the identification of dead cells in the root meristem in response to zeocin with confocal microscopy, although it is less sensitive than propidium iodide (Fulcher, personal communication). However, with the help of Grant Calder from the Bioimaging department of the John Innes Centre, we found that the CY3 filter set of the Lumar stereomicroscope v12 (Zeiss) enables a clear identification of dead cells with SYTOX® Orange using fluorescence microscopy.

Treatment of *L-er* seedlings with zeocin at a concentration of 35 µg/mL for 24 hours followed by a 5 min stain in 1 µM SYTOX® Orange gave a reliable fluorescence signal (figure 3.3 C). The workflow of the screen is described in figure 3.3. We used 24 well plates to grow the seedlings, which enabled the screening of 22 families at once together with a *L-er* and *atm* control to check for reliable presence and absence of cell death in response to the treatment respectively without compromising the germination rate of seeds in a liquid culture under constant agitation. About 20 seeds per family were screened in order to allow the segregating phenotypes to be identified. After stratification seeds were transferred in continuous light, which showed a better germination rate and more homogenous germination. After 3 days of growth zeocin was directly added in the medium. After 24 hours of treatment the medium was removed and replaced with water and 1 µM sytox orange for imaging with the stereomicroscope. Only adding SYTOX® Orange in the GM medium prevented the identification of dead cells at the root tip, maybe from diffraction problems caused by the medium.

Out of the 2730 available M2 families from the fast-neutron mutagenesis population, 1800 could be screened. The other families showed either no

Forward genetics approach to identify components of the ATM pathway  
leading to PCD in response to DNA damage

germination or a germination rate that was too low to allow reliable screening for loss of cell death. Out of the screened families 93 showed at least 5 plants out of the 20 showing reduced or no cell death compared to the wild type. Those were defined as segregating a differential cell death response in response to zeocin as expected in the M2 generation (figure 3.2). All these 93 families were screened again under confocal microscopy to confirm the phenotype identified with the stereomicroscope and 73 families out of the 93 were confirmed.

Forward genetics approach to identify components of the ATM pathway  
leading to PCD in response to DNA damage

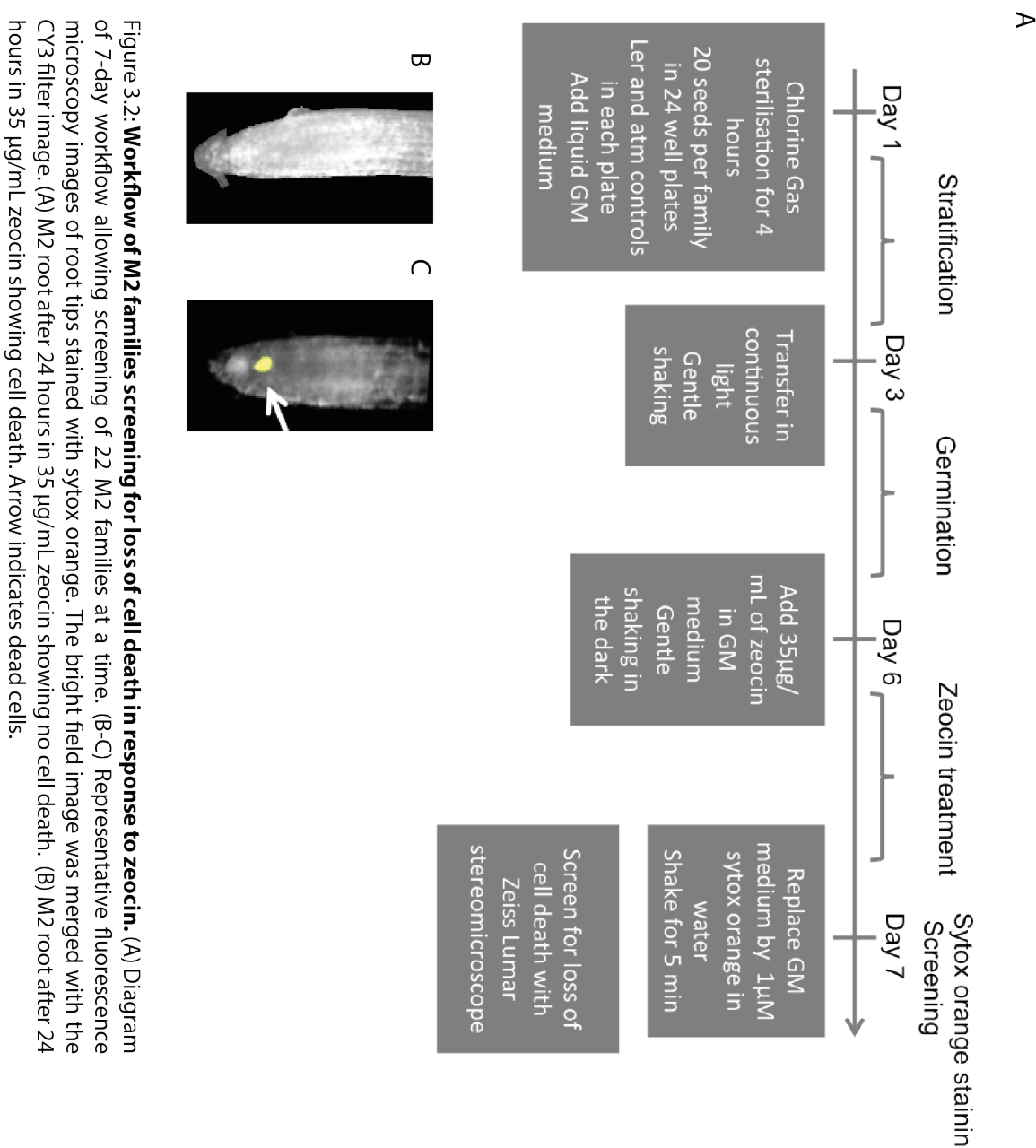


Figure 3.2: **Workflow of M2 families screening for loss of cell death in response to zeocin.** (A) Diagram of 7-day workflow allowing screening of 22 M2 families at a time. (B-C) Representative fluorescence microscopy images of root tips stained with sytox orange. The bright field image was merged with the CY3 filter image. (A) M2 root after 24 hours in 35  $\mu$ g/mL zeocin showing no cell death. (B) M2 root after 24 hours in 35  $\mu$ g/mL zeocin showing cell death. Arrow indicates dead cells.

Forward genetics approach to identify components of the ATM pathway  
leading to PCD in response to DNA damage

## 2.2 Identification of several stable mutants

From the confocal microscopy secondary screen, seedlings showing no cell death were grown on soil to maturity to check for stability of the mutations in the M3 generation. Out of the 73 identified mutants, 14 showed stability of the cell death phenotype by confocal microscopy in the M3 generation. However, most of the plants rescreened with the confocal microscope showed a decrease in cell death and not a total absence of cell death, except one : mutant 396 (Figure 3.4). These levels of cell death are comparable to what can sometimes be observed in a wild type Col background. Indeed, out the 14 mutants, we found that 5 of them were in fact Col contaminants present in the mutagenized L-*er* population used in the primary screen and did not show the morphological characteristics of L-*er* of compact inflorescences with flowers clustering at the top, short siliques and round leaves (Soga et al., 2000; Li et al., 2001). The remaining 9 stable mutants are shown in figure 3.3. All plants of mutant 396 showed no cell death, meaning that the parent was likely to be homozygous for the mutation explaining the phenotype. All other mutants showed some level of segregation of the PCD phenotype, showing that the parent plant was likely to be heterozygous for the mutation, or that several mutations would explain the observed phenotype. The segregation rates are presented in table 3.1, with the results of the Chi square test for goodness of fit with single mutations. The segregation rate of mutants 908, 958, 1596 and 1955 was compatible with the segregation of a dominant mutation (Chi square p-value > 0.05), whereas the segregation rates of mutants 970 and 989 was compatible with the segregation of a recessive mutation. The segregation of mutants 602 and 1337 was not compatible with a single recessive or dominant mutation. The reason for this could be the presence of several mutations explaining the phenotype, but also inconsistencies in zeocin response.

Forward genetics approach to identify components of the ATM pathway  
leading to PCD in response to DNA damage

**Table 3.1: Segregation of the PCD phenotype in the stable mutants.**

Mutant	Number of plants showing reduced PCD	Number of plants showing normal PCD	Chi square test p-value at 95% confidence
396	<b>25</b>	<b>0</b>	<b>1</b>
602	<b>19</b>	<b>24</b>	<b>0.0037</b>
908	<b>36</b>	<b>20</b>	<b>0.06</b>
958	<b>22</b>	<b>13</b>	<b>0.06</b>
970	<b>4</b>	<b>16</b>	<b>0.6</b>
989	<b>10</b>	<b>18</b>	<b>0.19</b>
1337	<b>8</b>	<b>7</b>	<b>0.05</b>
1596	<b>25</b>	<b>13</b>	<b>0.18</b>
1955	<b>22</b>	<b>8</b>	<b>0.8</b>

Forward genetics approach to identify components of the ATM pathway  
leading to PCD in response to DNA damage

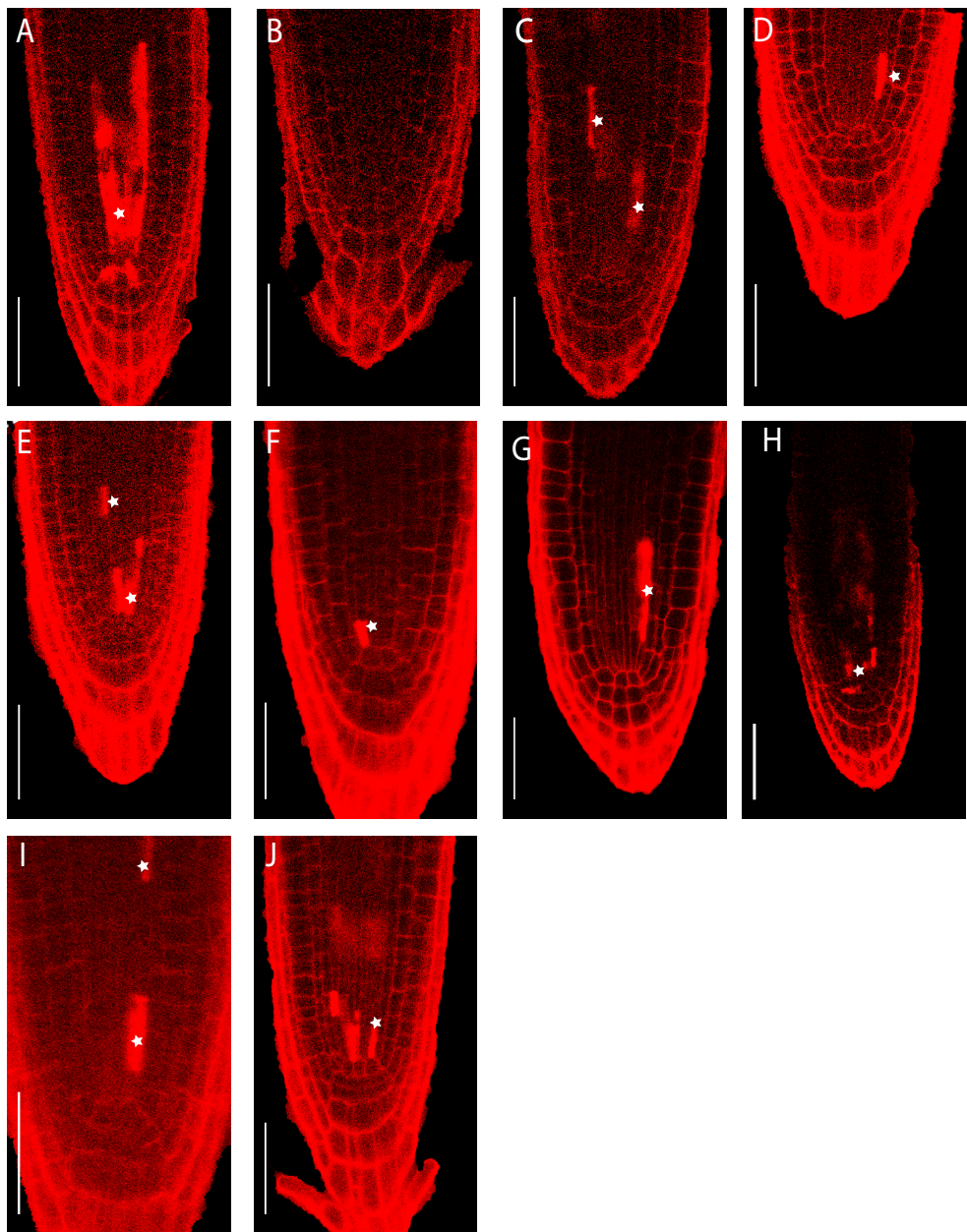


**Figure 3.4: Identification of 8 stable mutants from the forward genetics screen.** (A-J) Representative confocal images of root tips stained with PI. All plants were treated for 24 hours in 35  $\mu$ g/mL zeocin. (A) Ler control, all 20 plants showing the phenotype presented. (B-J) stable mutants in the M3 generation (B) line 396, all 20 plants showing the phenotype presented, Fisher's exact test p-value = 1.451e-11 (C) line 602, 19 plants showing the phenotype presented and 24 showing normal PCD, Fisher's exact test p-value = 0.000214 (D) line 908, 36 showing the phenotype presented and 20 showing normal PCD, Fisher's exact test p-value = 1.332.e-7 (E) line 958, 22 plants showing the phenotype presented and 13 showing normal PCD, Fisher's exact test p-value = 1.427 e-6 (F) line 970, 4 plants showing the phenotype presented and 16 showing normal cell death, Fisher's exact test p-value = 0.106 (G) line 989, 10 plants showing the phenotype presented and 18 showing normal PCD, Fisher's exact test p-value = 0.002754 (H) line 1337, 8 plants showing the phenotype presented and 7 showing normal PCD, Fisher's exact test p-value = 0.0002734 (I) line 1596, 25 plants showing the phenotype presented and 13 showing normal PCD, Fisher's exact test p-value = 4.509e-07 (J) line 1955, 22 plants showing the phenotype presented and 8 showing normal PCD, Fisher's exact test p-value = 1.255e-07. Scale bar = 50  $\mu$ m. Asterisks indicate dead cells.

Forward genetics approach to identify components of the ATM pathway  
leading to PCD in response to DNA damage

2.3 The mutant line 396 is a new *sog1* allele

The stable mutant line 396 was the only mutant identified showing a complete absence of cell death in all plants (figure 3.4 B). As this mutant did not show the macroscopic phenotype of an *atm* mutant, which is characterized by small siliques and partial sterility (Garcia et al., 2003; Hazen et al., 2005), and because the *atr* mutant can show low levels of cell death in response to zeocin (Truernit and Haseloff, 2008; Fulcher and Sablowski, 2009), we decided to test line 396 for allelism with the *SOG1* gene, the only other known mutant showing a complete absence of cell in response to zeocin in the root meristem. Therefore, we crossed line 396 with *sog1-1* and backcrossed it to the L-*er* background, and observed their cell death phenotype in response to zeocin in the F1 generation (Figure 3.5). This test showed 100 % cell death in a cross between line 396 and L-*er* (Figure 3.5 E) but no PCD in the cross between line 396 and *sog1-1*, showing that mutant 396 is in fact a new *sog1* allele (figure 3.5 D).

Forward genetics approach to identify components of the ATM pathway  
leading to PCD in response to DNA damage

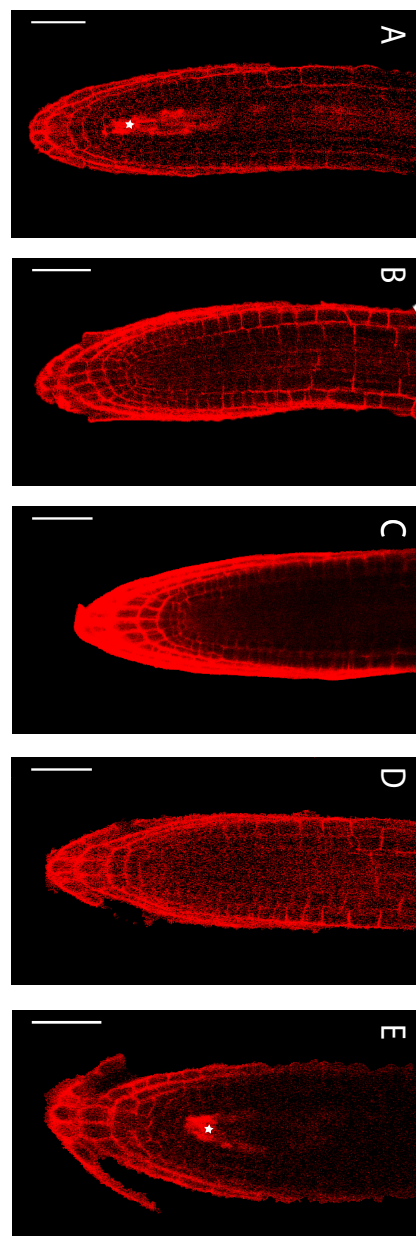


Figure 3.5: **The stable mutant line 396 is a new *sog1* allele.** (A-E) Representative (10 plants, all showing the phenotype presented) confocal images of root tips stained with PI following 24 hours in 35  $\mu$ g/mL zeocin. (A) Ler (B) line 396 (C) *sog1-1* (D) *sog1-1* crossed to line 396 F1 (E) *sog1-1* crossed to Ler F1. Scale bar = 50  $\mu$ m. Asterisks indicate dead cells.

Forward genetics approach to identify components of the ATM pathway  
leading to PCD in response to DNA damage

#### 2.4 PCD in response to X-ray irradiation in stable mutants

The remaining mutant phenotypes could be due to mutations leading to differences in cell permeability leading to a differential zeocin accumulation at the root tip, or a more global difference in zeocin metabolism in the cell and not a response to DNA damage caused by zeocin. Therefore, we decided to subject the mutants to a different source of DNA damage to confirm the origin of their phenotype. X-ray irradiation leads to a uniform degradation of DNA throughout the irradiated tissue. With the assistance of William Holmes-Smith from the Norwich and Norfolk University Hospital radiation physics team, the mutants were subjected to a 40 Gray X-ray irradiation (figure 3.6). These levels were previously described as mimicking a 24 hours zeocin treatment (Fulcher, personal communication) in terms of cell death levels in a wild type background. The reduction in cell death was confirmed by this experiment in all mutants (figure 3.6), showing that indeed these mutants show a differential cell death response to DNA damage.

Forward genetics approach to identify components of the ATM pathway  
leading to PCD in response to DNA damage

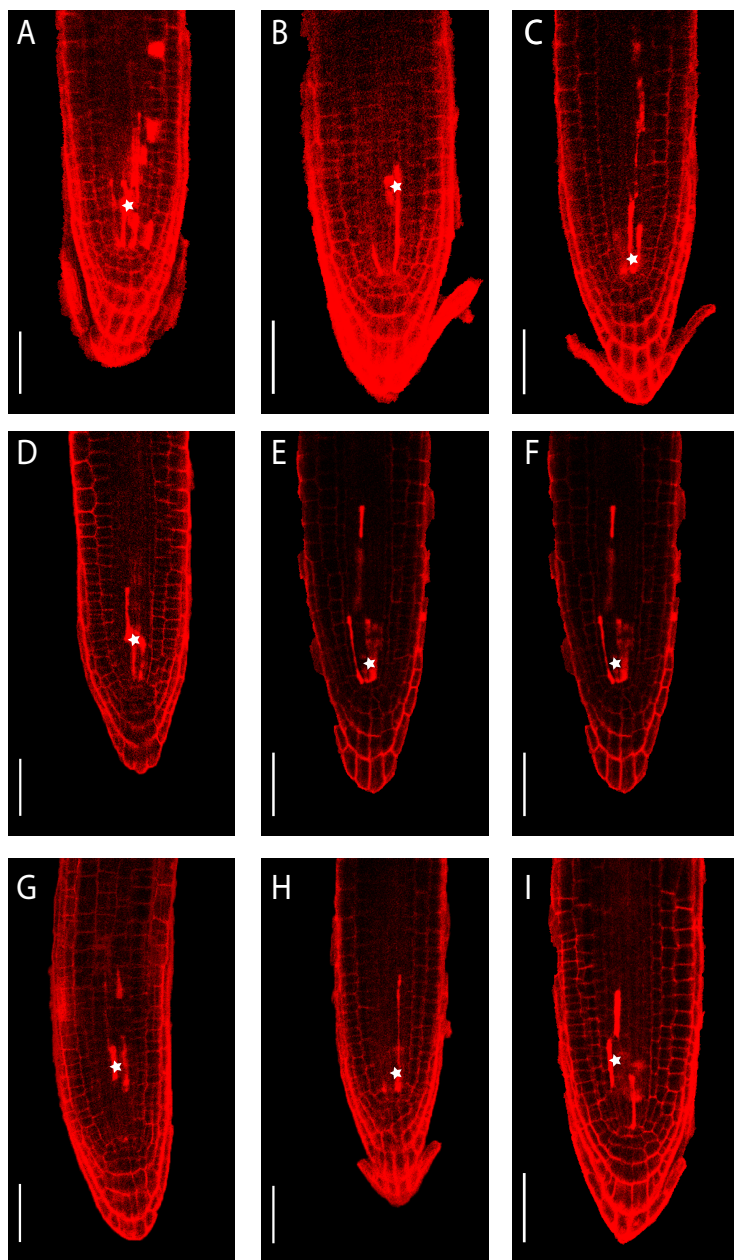


**Figure 3.6: X-ray irradiation shows the stability of the mutations.** (A-I) Representative (5 plants all displaying the phenotype presented, Fisher's exact test p-value = 0.007937) confocal images of root tips stained with PI 24 hours after an X-ray irradiation of 40 Gray. (A) Ler control (B) line 602 (C) line 908 (D) line 958 (E) line 970 (F) line 989 (G) line 1337 (H) line 1596 (I) line 1955. Scale bar = 50  $\mu$ m. Asterisks indicate dead cells.

Forward genetics approach to identify components of the ATM pathway  
leading to PCD in response to DNA damage

2.5 Test of PCD response in different *Arabidopsis* accessions and identification of an *Arabidopsis* ecotype showing decreased cell death in response to zeocin

The levels of cell death in the remaining 7 stable mutants were comparable to low levels that can be observed in a Col background. This made the generation of mapping populations for those mutants difficult, as crosses of those mutants with Col made the reliable discrimination between mutant and wild type in the F2 impossible. Therefore, as it was shown previously that Col, L-*er* and Ws show different levels of cell death, we decided to test PCD in response to zeocin in several ecotypes with sequencing data available in order to generate alternative mapping populations, in case we could identify an ecotype with cell death levels as high as L-*er* in response to the same zeocin concentration treatment.

We chose accessions that were readily available in the Dean Laboratory natural variation seed bank from the Cell and Developmental Biology Department of the John Innes Centre due to time constraints. Their origin is presented in Figure 3.7. We used several ecotypes from the Swedish accessions project (Long et al., 2013b): Bil-7, Eden-2, Nd-0, and Lov-1, together with Edi-0. We also wanted to use the Cvi ecotype from Cap Verde, but this mutant did not germinate in our experimental setting.

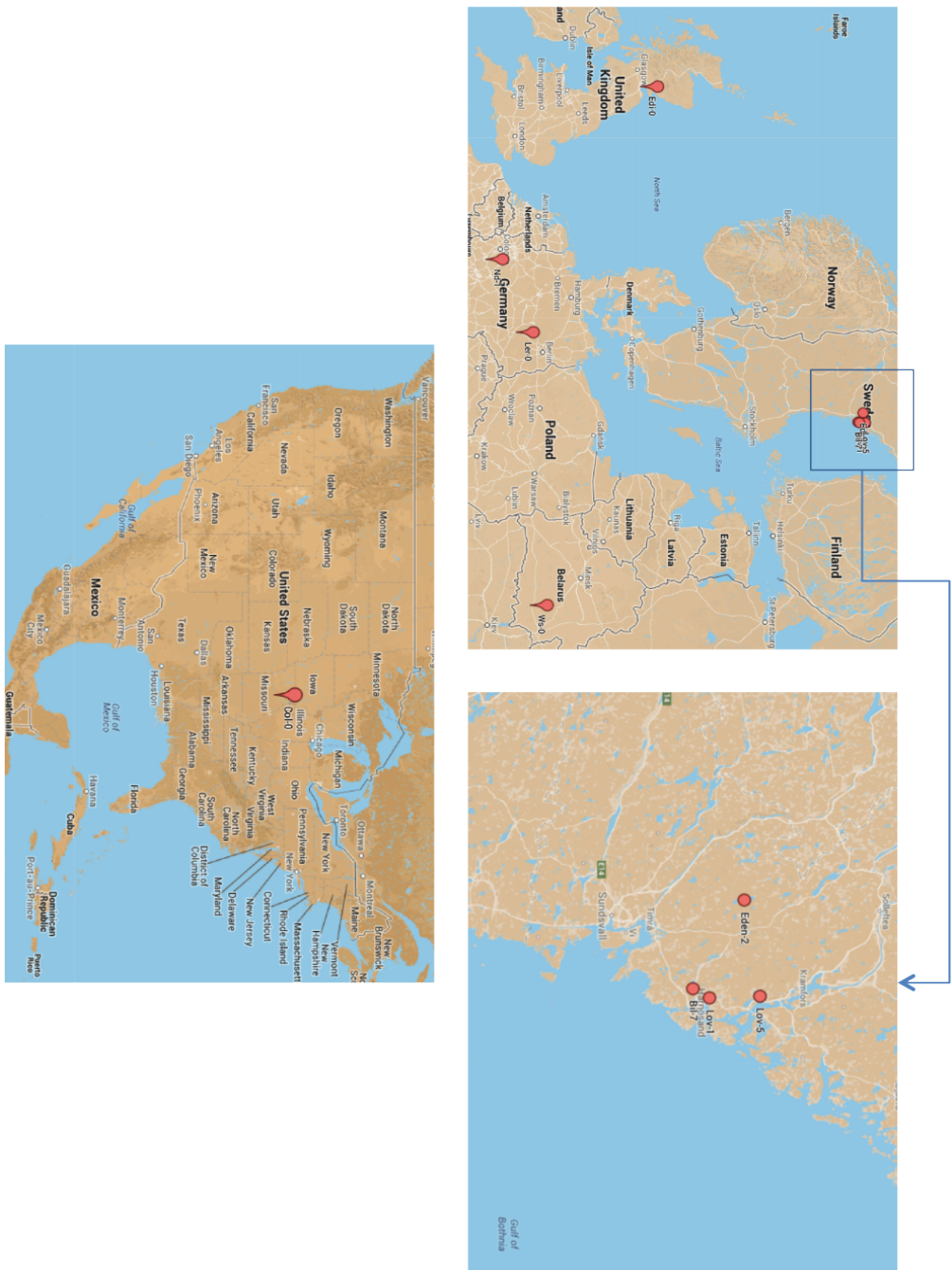
The zeocin treatment results are presented in figure 3.8. The ecotypes Nd-0 and Eden-2 were identified as good candidates for generating mapping populations, as their levels of cell death were comparable to L-*er*. Unexpectedly, the Lov-1 ecotype showed little to no cell death in response to zeocin. We confirmed this result by testing the genetically similar Lov-5 ecotype, which also showed a complete absence of cell death in response to zeocin. These levels were comparable to those seen in *atm*, *atr* and *sog1* mutants. We first checked if this phenotype could be due to a difference in

Forward genetics approach to identify components of the ATM pathway  
leading to PCD in response to DNA damage

zeocin penetrance in the cell, as the root cap of Lov-1 is extremely thick (Julia Questa, personal communication), which could lead to a difference in zeocin absorption or accumulation at the root tip. However, an irradiation of 40 Gray showed the same phenotype, suggesting that Lov-1/Lov-5 display natural polymorphism in their DNA damage response (figure 3.9).

Forward genetics approach to identify components of the ATM pathway  
leading to PCD in response to DNA damage

Figure 3.7. Location of ecotypes tested for their zecocin and X-ray response.



Forward genetics approach to identify components of the ATM pathway  
leading to PCD in response to DNA damage

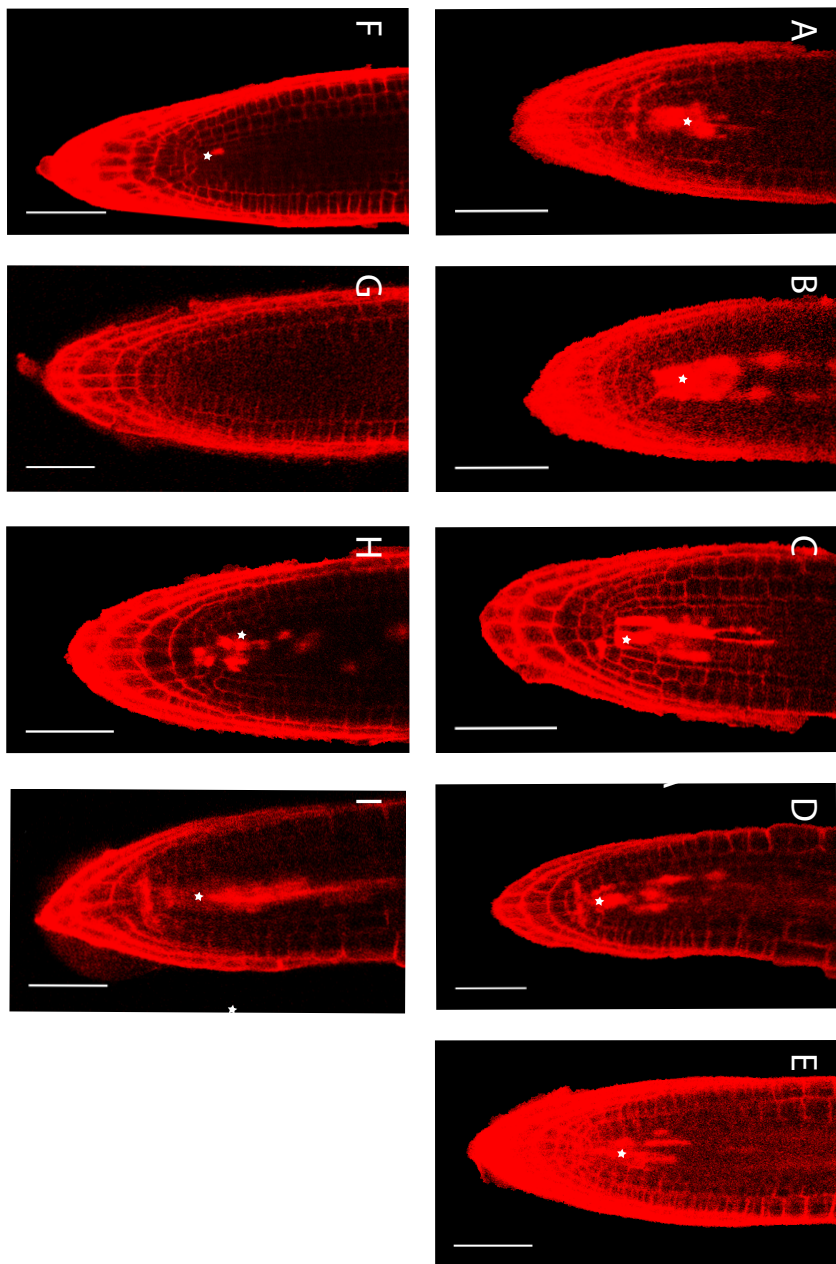


Figure 3.8: **Arabidopsis ecotypes show a differential response to zeocin.** (A-H) Representative (10 plants) confocal images of root tips stained with PI after 24 hours in 35  $\mu$ g/mL. (A) Col-0 (B) Ler (C) Ws-2 (D) Nd-1 (E) Bli-7 (F) Lov-1 (5 plants showing reduced PCD presented and 5 plants showing no PCD, Fisher's exact test p-value = 0.0001191) (G) Lov-5 (10 plants showing no PCD, Fisher's exact test p-value = 1.083e-05 (H) Edi (I) Eden-2. Scale bar = 50  $\mu$ m. Asterisks indicate dead cells.

Forward genetics approach to identify components of the ATM pathway  
leading to PCD in response to DNA damage

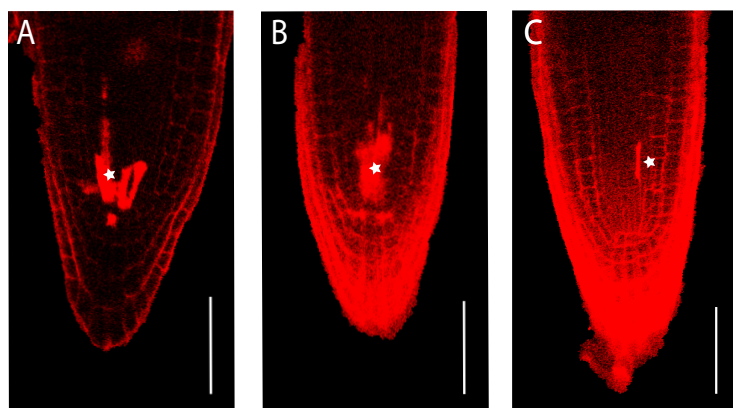


Figure 3.9: **Confirmation of Lov-1 as a zeocin response mutant after X-ray irradiation.** (A-C) Representative (10 plants) confocal images of root tips stained with PI 24 hours after an X-ray irradiation of 40 Gray. (A) Ler (B) Col (C) Lov-1 Scale bar = 50  $\mu$ m. Asterisks indicate dead cells.

Forward genetics approach to identify components of the ATM pathway  
leading to PCD in response to DNA damage

We next looked into available SNP sequencing data for the known genes *ATM*, *ATR* and *SOG1* and failed to identify unique SNPs leading to an amino acid change that could explain the phenotype in Lov-1 (data obtained from the 1001 genomes project) (Long et al., 2013a) (figure 3.10). Data from the promoter region could not be obtained due to a lack of sequencing data. The only unique SNP in the *ATM* gene identified corresponds to a region that is not conserved between *Arabidopsis* and other plants and animal species, the only somewhat conserved region being the N-terminal region (figure 3.11). Therefore, it seems that Lov-1 does not carry natural polymorphisms in *ATM*, *ATR* or *SOG1*, although we cannot conclude this with certitude for *ATM*.

Next, we decided to study the segregation of the Lov-1 cell death phenotype in order to determine if this natural polymorphism phenotype is due to one or multiple mutations. Because of time constraints, we could not generate a Col or L-*er* to Lov-1 cross ourselves. However, 250 individual F3 families are available from a Col to Lov-1 cross in the Dean Lab seed bank. We decided to look for the zeocin response of 5 plants from each of the first 30 families to check the segregation of the phenotype. The results are presented in figure 3.12. Some families showed segregation of the PCD phenotype where others showed either no cell death or cell death in all plants. A plot of the frequency of families showing either phenotype shows a clear segregation between on the one hand, families showing no cell death or cell death in all plants, and a range of families showing a segregation of the phenotype. The segregation rate is consistent with Lov-1 carrying a single mutation that abolished PCD in response to zeocin (Chi square test, p-value < 0.05).

To take the first steps towards identifying the Lov-1 natural polymorphism explaining its PCD phenotype, I used available data from the Dean lab where genetic markers spanning the 5 chromosomes of *Arabidopsis* were developed between Lov-1 and Columbia (Strange et al., 2011), spanning

Forward genetics approach to identify components of the ATM pathway  
leading to PCD in response to DNA damage

intervals of 2 to 3 Mb in length. The F2 families from which the F3 families described above were generated were genotyped using those markers and the genotyping data were provided to me by Peijin Li. In figure 3.13 are presented the data for the families in which I found either no PCD (5 families) or 100% PCD (3 families). From this small pool of plants I found that the most likely position of the natural polymorphism explaining the phenotype was between marker cd198 and marker cd41 on chromosome 2. Indeed, this position is the one that requires the less recombination events of all possible positions: no recombination event is required for line 20 and 29, and one recombination event is required for lines 10, 36, 37 (resulting in a Lov-1 genotype from an heterozygous genotype) and 40 (resulting in a Columbia genotype from an heterozygous genotype). 608 genes span this interval, corresponding to 561 loci. Most of them (51 %) are transposable element genes. Out of the characterized genes in the interval, only one was already shown to play a role in DNA damage responses: *SERPIN 2* (*SRP2*). *SRP2* is induced in response to MMS and the *srp2* mutant shows greater root length than WT in response to the MMS treatment. However, this candidate does not possess unique SNPs in the coding region for Lov1/Lov5, as they are shared with Bil-7. Moreover, this expression of the gene was localized in siliques and no differential expression of *ATM* was observed relative to the WT in *srp2* mutants exposed to MMS (Ahn et al., 2009).

Therefore, with the help of the TGAC sequencing services and Dr Cristobal Uauy (Crop Genetics Department, John Innes Centre), a sequencing strategy for Lov-1 was devised. This would start with the phenotyping of all 250 available F3 families for their zeocin response. As the preliminary data suggest one mutation is responsible for the phenotype, we expect 62.5 families to show no cell death in all plants tested. One plant per family showing no PCD and 50 plants will be pooled for DNA extraction. The DNA from plants that do not show cell death from 25 segregating families (that

Forward genetics approach to identify components of the ATM pathway  
leading to PCD in response to DNA damage

would either be heterozygous or homozygous for the mutant phenotype) will be added to provide more recombination information. Two DNA libraries will be generated from these two pools of DNA and these would be pooled at a 2:1 ratio to simulate a 150 individuals optimal population size (James et al., 2013). This pool would be sequenced with the Illumina Hiseq 2000/2500 technique using 100 bp paired-end reads, and the raw data will be analysed for SNP calling. However, this work could not be initiated due to time constraints.

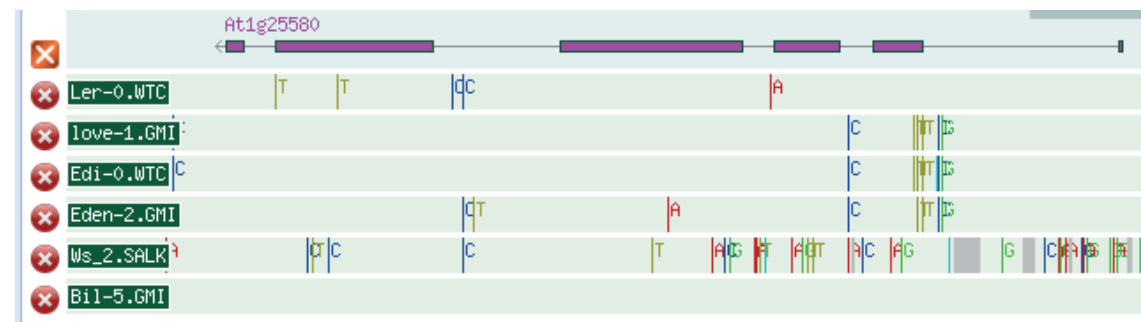
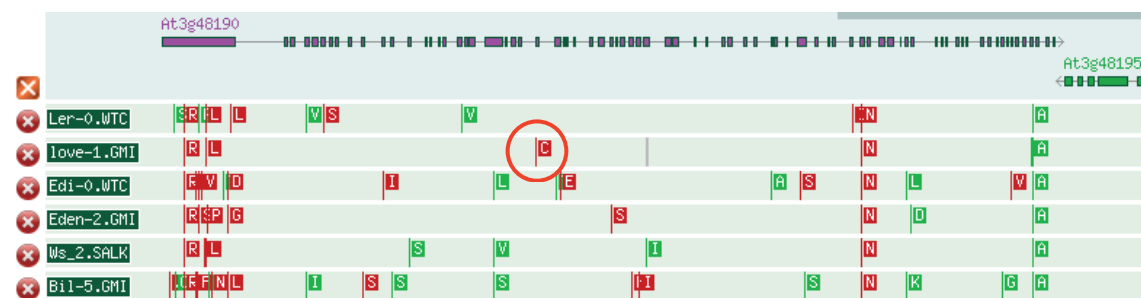
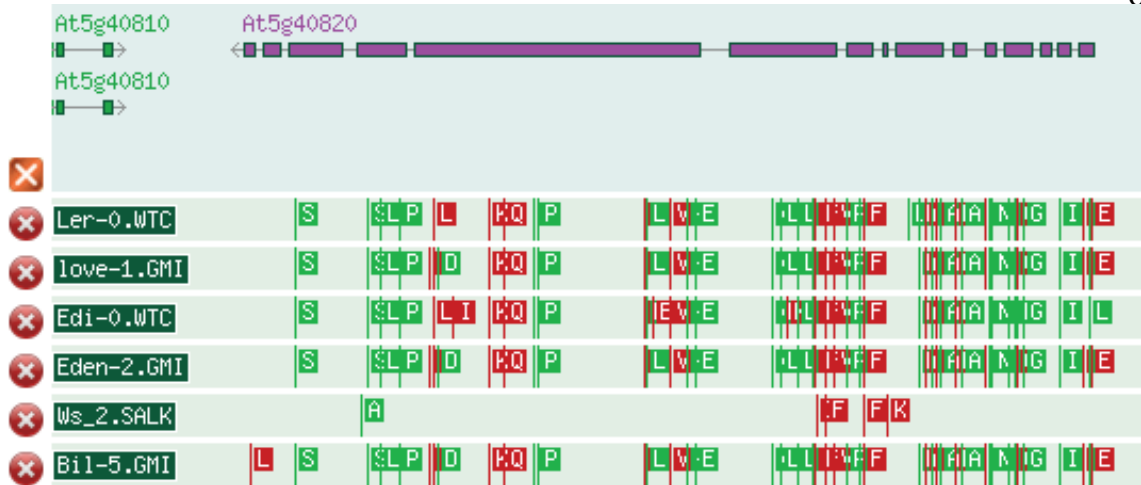


Figure 3.10: **The Lov-1 ecotype does not show any significant mutation in ATR (At5g40820), ATM (At3g48190), or SOG1 (At1g25580).** Alignment of ATM, ATR and SOG1 in ecotypes tested for their zeocin responses. Only the differences showing an amino acid change are presented. The red circle represents the only unique SNP present in Lov-1.

A

## Forward genetics approach to identify components of the ATM pathway

sp|Q62388|ATM\_MOUSE ----- -VNEAF -SQFLA  
sp|Q13315|ATM\_HUMAN ----- -VNEVF -TQFLA  
sp|Q9M3G7|ATM\_ARATH ----- ERL -LLMLS  
sp|Q9N3Q4|ATM\_CAEEL -----  
sp|Q5EAK6|ATM\_DROME LDDMLMALNSLLRIAIIKKSYTSNLTAIVRCVGLIAQRCPDIYLLENFAVICKSTAKFIT  
tr|D4ACL8|D4ACL8\_RAT ----- -VREAF -PQFLA  
tr|C5XF00|C5XF00\_SORBI -----

sp Q62388 ATM_MOUSE	DDHHQVCRM-----LAAGSVNRLFQDMRQGD--F
sp Q13315 ATM_HUMAN	RSRLKALPLKFQQTFSFNN
sp Q9M367 ATM_ARATH	DNHQVCRM-----LAAESINRLFQDT-KGD--SSRLKALPLKLQQTAFEN
sp Q9N3Q4 ATM_CAEEL	D3DYRVRF-----VLAHQIGLFLQFTWDGHEALFQDICSSFGKLVTTSKEK
sp Q5EAK6 ATM_DROME	MPTLEVRFATLFTFTTILLESNCVTSDAIGHSRTHWDPCQEL--YESIEFKKLTYNNNE
tr D4ACL8 D4ACL8_RAT	DGHHHVRM-----LAAGSISRLFLQDMRQGD--SSRSRLKALPLKFQQTFSFNS
tr C5XF00 C5XF00_SORBI	-----

B

```

sp | Q62388 | ATM_MOUSE
sp | Q13315 | ATM_HUMAN
sp | Q93M67 | ATM_ARATH
sp | Q9N304 | ATM_CAEEL
sp | Q5EAK6 | ATM_DROME
tr | D4ACL8 | D4ACL8_RAT
tr | C5XF00 | C5XF00_SORBI

EFRLAGGLNLPKI1DCVGSGDKERRQLVK-GRDDLRLQDAVMQQVFCMCNTLLQRNRTETRK
EFRLAGGLNLPKI1DCVGSGDKERRQLVK-GRDDLRLQDAVMQQVFCMCNTLLQRNRTETRK
SFTVMGMINAPKVKVVECFGSDGDKYQQLAKSGNSNDLRLQDAVMEQFFGLVNTLHNRRNTDTRK
VFTIAD1G1STPKIWE1EIGSDGKWWKTWRK--KDDVRQDVLVEQPMFVDTVNMLLE------
ETTQCGGLNAPVKIMCVGSDGDKIRALVK-GRDDLRLQDAVMQQVFG1VNLNEQNQDFE1IE
EFRLAGGLNLPKI1DCVGSGDKERRQLVK-GRDDLRLQDAVMQQVFCMCNTLLQRNRTETRK
SVMIMMGINAPKVKVVECFGSDGDKYQQLAKSGNSNDLRLQDAVMEQFFGLVNTLHNRRNTDTRK

```

```

sp | 062388 | ATM_MOUSE
sp | Q13135 | ATM_HUMAN
sp | 093M37 | ATM_ARATH
sp | Q9N3Q4 | ATM_CAEEL
sp | Q5EKA6 | ATM_HUMAN
tr | D4ACL8 | D4ACL8_RAT
tr | C5XF00 | C5XF00_SORBI

RKLITCTYKVPLSQRSGVLEWCTGTVPIGEYLVNS---EDGAHRRYRPNDFSANQCQKMM
RKLITCTYKVPLSQRSGVLEWCTGTVPIGEYLVNN---EDGAHRRYRPNDFSAQOCQKMM
RRLAVRATYKVPFTPSAGVLEWDTGTLPLGDYLGSSRGEGAHRYG1GNWYKPCREMM
-KAMLRITYVNPVLDTGCGTVEIFCCTGTSVLSKEVCMGVITREGGLHREFNSEEVSASKVSMM
RKLRLITYKVPFTLMSRSGILEWCTNSVPGHLYLV---KGKGAHARYRPNNDNNNKKRCLS
RKLITCTYKVPLSQRSGVLEWCTGTVPIGEYLVNN---EAGHAKRYPNDLSANQCQKMM
RRLIRITYKVPFTPSAGVLEWVGNTVPLGDYLGISRTGAGHRYG1GWDTYLQCREYL

```

```

sp |Q62388 |ATM_MOUSE      MEVQKKSFEEKYDFTMTCIQCNPFPVFRYFCMEKFKLDPAWFKEKRLAYTRSVATSSIVGYI
sp |Q13135 |ATM_HUMAN      MEVQKKSFEEKYDFTMVCQNCFPVFRYFCMEKFKLDPAWFKEKRLAYTRSVATSSIVGYI
sp |Q93M67 |ATM_ARATH      SSAK-----DKRKFADVFCDTNPFRVMHYYFLKEPLQADWFVFKRLAYTRSVAASSMMGYI
sp |Q9N3Q4 |ATM_CAEEL      RQVQTESTETTRQRQFVEICQQYSVPFRHFFYTFNFTSTAQIWRQKIIINYRQSLATWSIVCYI
sp |Q5EAK6  |ATM_DROME      SDHLKSPKETRYA1YK1K1CENPKFVHYFLLEKFPF1PGWFVFRERLAYTRSVATSSIVMGYI
tr |D4ACLB  |D4ACLB_8 RAT  MEVQKKSFEEKYDFTMTCIQCNPFPVFRYFCMEKFKLDPAWFKEKRLAYTRSVATSSIVGYI
tr |C5XF00  |C5XF00__SORBI MSEK-----DKRKFADVFCDTNPFRVMHYYFLERFLPDAWFQSRKRLAYTRSVAASSMMGYI

```

```

sp | Q62388 | ATM_MOUSE
sp | Q13315 | ATM_HUMAN
sp | Q9M3G7 | ATM_ARATH
sp | Q9N3Q4 | ATM_CABEL
sp | Q5EAK6 | ATM_DROME
tr | D4ACLB | D4ACLB_RAT
tr | C5XF00 | C5XF00_SORBI
LGLGDRHVQN1LINEQSAELVHIDLGVAFEGQ-KILPTPETVPFRLSRD1VDGMG1TGV
E
LGLGDRHVQN1LINEQSAELVHIDLGVAFEGQ-KILPTPETVPFRLTRD1VDGMG1TGV
E
VGLGDRHANM1LIDQATAEVHIDLGVAFEGQ-LMLKTPERVPFRLTRD1IDGMG1TGV
E
VGLGDRHASNLFDQKLC1TFVHIDLGMILEYSKR1LTPVEQPVFPR1TRDVLDP1LIEGIE
E
LGLGDRHTON1LVDQATAEVHIDLGVAFEGQ-KILPTPETVPFRLTRD1VDGMG1TGV
E
LGLGDRHVQN1LINEQSAELVHIDLGVAFEGQ-KILPTPETVPFRLTRD1VDGMG1TGV
E
VGLGDRHSN1LIDQATAEVHIDLGVAFEGQ-LMLKTPERVPFRLTRD1IDGMG1TGV
E

```

sp_062388	ATM_MOUSE	-GVRRCCEKTMVMRSSQETLLTIVEVLLYDPLFDWTMPLKALYLOQRPEDESDLHST
sp_013315	ATM_HUMAN	-GVRRCCEKTMVMRSSQETLLTIVEVLLYDPLFDWTMPLKALYLOQRPEDETLHPT
sp_09M3G7	ATM_ARATH	-GVRRCCEKTMVSMRNTKEALITTEVFIHDPLKWLALPKALQRQKETEDYDGMNLE
sp_09N3Q4	ATM_CAEEL	NGQLAEECTQIMKELKNGKVLGVASALLRTMTNFREAE--
sp_05EAKG	ATM_DROME	-GVPFKSCEATMHLRKYSSQETLLTIVEVLLYDPLFVGWLKLHKQSP--
tr_4	D4ACL8_RAT	-GVRRCCEKTMVMRSSQETLLTIVEVLLYDPLFDWTMPLKALYLOQRPEDETLHPT
tr_4	C5XF00_C5XF00_SORBI	-GVRRCCEKTMVSMRNTKEALITTEVFIHDPLKWLALPKALQRQKETEDYDGMNLE

sp_062388	ATM_MOUSE	PNADDQECKQSLSDTQSFNKAVERVLMRLQEKLKGVEEGTVL--SVGGVNLNLIQQAMD
sp_013315	ATM_HUMAN	LNADDQECKRNLSDIDQSFNKAVERVLMRLQEKLKGVEEGTVL--SVGGVNLNLIQQAID
sp_09M3G7	ATM_ARATH	-----G-LQEEEFGKNDVPRVQKLQDGYEGEMR-SIHQAOQLIQQAD
sp_09N3Q4	ATM_CAEEL	-----QAAAGRPSYI SEMAIGRLRKLRTGDTQVTAO-SSNLQIIRRLEATR
sp_05EAK6	ATM_DROME	-----QSGEEVSNLVAQARALLLWNQNLKDGRAGTMTGDSNVEAVERLINEATL
tr_04AC18	D4AC18_RAT	PSADDQECKRSLSDTQSFNKAVERVLMRLQEKLKGVEEGTVL--SVGGVNLNLIQQADM
tr_05CXF00	C5XF00_SORBI	-----D-SOEADYFGNKAARALRVLRQKLQDGYEGEMR-SVQGQVQLIQQAD

```

sp|Q62388|ATM_MOUSE      PKNLNSRLFPGWKA WV
sp|Q13315|ATM_HUMAN      PKNLNSRLFPGWKA WV
sp|Q9M3G7|ATM_ARATH      TDLRSHMFPGWGA WM
sp|Q9N3Q4|ATM_CAEEL      ADNLNSRMFCGWM PFL
sp|Q5EAK6|ATM_DROME      PSNLNSRLFPGWD PHL
tr|D4ACL8|D4ACL8_RAT    PKNLNSRLFPGWKA WV
tr|C5XF00|C5XF00_SORBI  VDRLCQMFPGWNGP WL
                                ..*.. :* ** :
```

Figure 3.11: **Conservation of the gene sequence of ATM between species.** Alignment showing conservation of the ATM sequence between the mouse, human, *Arabidopsis*, *Caenorhabditis elegans*, *Drosophila*, rat and sorghum genomes in (A) in the region where the unique SNP was identified in Lov-1 (red circle) and (B) in the N-terminal region of the gene.

## Forward genetics approach to identify components of the ATM pathway

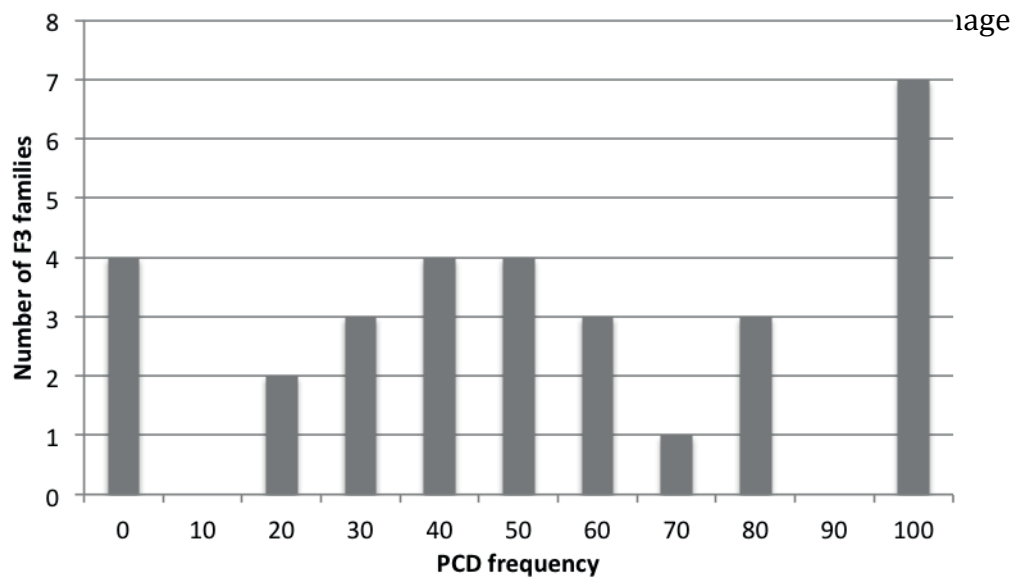


Figure 3.12: **The Lov-1 ecotype seems to segregate a single mutation explaining the PCD phenotype.** Distribution of phenotypes in F3 families of Lov-1 x Col mapping population.

Forward genetics approach to identify components of the ATM pathway  
leading to PCD in response to DNA damage

Line # phenotype	10 mut	20 mut	29 mut	36 mut	37 mut	40 wt
*cd111	H	B	H	H	H	H
*cd246	H	B	H	H	H	H
*cd137	H	B	H	H	H	H
*cd49	H	B	H	H	H	H
*cd64	H	B	H	H	H	H
*cd8	B	B	H	H	H	A
*cd173	B	B	H	H	H	A
*cd219	B	B	H	H	H	A
*cd133	H	H	H	H	H	H
*cd90	H	H	A	H	H	H
*cd24	H	H	A	H	A	H
*cd195	H	H	A	H	A	H
*cd3	H	H	A	H	A	H
*cd103	H	H	A	H	A	H
*cd249	B	H	A	A	A	H
*cd140	B	H	A	A	A	H
*cd7	B	H	A	A	A	H
*cd113	B	H	B	H	B	H
*cd71	B	B	B	H	B	H
*cd198	B	B	B	H	B	H
*cd141	H	B	B	B	H	A
*cd108	H	B	B	B	H	A
*cd65	H	B	B	B	H	B
*cd15	A	B	B	H	H	B
*cd83	A	B	H	H	H	B
*cd68	A	B	A	B	H	B
*cd46	A	B	A	B	H	B
*cd174	B	A	H	H	H	B
*cd196	B	H	B	B	H	B
*cd142	B	H	B	B	H	B
*cd88	-	H	H	B	H	B
*cd231	B	H	H	B	H	B
*cd208	H	H	H	B	B	B
*cd239	H	H	H	B	B	H
*cd2	H	B	A	B	B	H
*cd26	H	B	A	B	B	H
*cd118	H	B	A	B	B	H
*cd119	H	B	H	H	B	H
*FRI	H	A	H	H	A	A
*cd121	H	A	H	H	A	A
*cd151	H	-	H	H	-	A
*cd102	H	A	H	A	H	A
*cd125	H	A	H	H	H	A
*cd4	H	H	H	H	H	A
*cd27	H	H	H	H	H	A
*cd12	H	H	H	H	H	A
*cd19	H	H	H	H	B	H

Figure 3.13: **Preliminary rough mapping data of F2 families from a Lov1 to Col cross segregating the PCD phenotype.** (B) genotyping information of the F2 families showing either no cell death (mut) or cell death (WT) in response to zeocin in all plants in the F3. A: Col-0 genome, B: Lov-1 genome, H: Heterozygous (data obtained from Strange 2011).

## Forward genetics approach to identify components of the ATM pathway leading to PCD in response to DNA damage

### 3. Discussion

The forward genetics screen approach enabled the identification of 8 stable mutants, 7 showing a reliable decrease in PCD levels compared to the wild type, and 1 mutant showing a complete absence of PCD in response to zeocin. However, allelism tests showed that this mutant was in fact a new allele of the *sog1* mutation and not a new gene. This result seems to show how conserved and crucial for plant survival this pathway is, which makes the identification of new mutants difficult with a traditional forward genetics approach. However, we cannot conclude on the saturation of the screen, as we did not screen all of the available M2 families. Several mutants showed a sterility phenotype not unlike the *atm* mutant, but their sterility made it impossible to assess the stability of the mutation as not enough seeds were collected.

As the levels of cell death in the remaining mutants made it impossible to unmistakably select homozygous mutants from a mapping population, another screening approach was conducted. The fact that Col and L-er showed reliable differences in PCD responses prompted us to carry out a restricted natural variation screening of zeocin responses in the root stem cell niche. This approach also had the advantage of possibly enabling the identification of an ecotype displaying high levels of cell death in response to zeocin such as the ones observed in L-er. This ecotype could then be used instead of Col to generate mapping populations and enable the selection of homozygous mutants easily. We used *Arabidopsis* ecotypes available in the Cell and Developmental Biology Department and where sequencing data from the 1001 genomes project was available. This approach yielded 2 ecotypes suitable for generating mapping populations for the mutants identified in the fast neutron screen. But it also led to the identification of one ecotype showing an absence of cell death in response to zeocin in the root stem cell niche. Preliminary genotyping data and the use of the genome

Forward genetics approach to identify components of the ATM pathway  
leading to PCD in response to DNA damage

sequence points out that this ecotype could segregate a single mutation explaining its absence of PCD and no mutation in ATM/ATR/SOG1 was identified.

Interestingly, the range of mutations caused by fast neutron is different and wider than previously thought. Indeed, previous studies suggested that Fast Neutron induced mutations of about 1 kb in length (Li et al., 2001), but more recent studies show a higher frequency of single base substitutions, with a bias in favour of G:C to A:T transitions. Also, single base deletions were found to be more frequent than large base deletions (Belfield et al., 2013). This shows that this method of mutagenesis is not yet fully understood, and different mutagenesis experiments could lead to differential mutation levels.

Nevertheless, another screening approach that is more likely to yield partial loss of function mutants should be envisaged. The work presented in chapter 5 shows that the *bru1-2* mutant shows spontaneous cell death in the root initials, mimicking a zeocin treatment. This phenotype was shown to be under the control of *SOG1* but not *ATM* (figure 5.3). A screen could then be performed looking for mutants that fail to show spontaneous cell death in the *bru1-2* background. We generated a mutant population *via* EMS mutagenesis, which showed the expected signs of a successful mutagenesis in the M1, including albino sectors and aborted seeds. 2000 individual M2 families were generated.

In addition, the levels of cell death present in either the mutants identified or the ecotype screen should be better assessed by quantification experiments. So far, the studies showing quantitative data have been focusing on the number of dead cells present in the RAM in response to a zeocin treatment for instance (Furukawa et al., 2010). This type of quantification does not take into account differences in root size and/or cell

Forward genetics approach to identify components of the ATM pathway  
leading to PCD in response to DNA damage

size, especially cell volume that could affect the number of visible cells undergoing PCD. The development of new techniques of 3D imaging in our lab could therefore be used to formally quantify cell death levels in response to zeocin and pick up subtle differences (Schiessl et al., 2012).

On the other hand, the lack of cell death in response to zeocin in the Lov-1/Lov-5 ecotypes provides an interesting lead into the natural variation of DNA damage responses in plant stem cells. Lov-1 naturally grows in very harsh conditions, on a rocky, south-facing slope on the Baltic Coast (Strange et al., 2011) . One of the driving agents for the evolution of the phenotype could therefore be environmental stress such as drought or cold conditions. Drought is known to induce DNA damage (Waterworth et al., 2011), but cold stress responses linked to DNA damage has been poorly studied. It would be interesting to know if the lack of PCD in response to DNA damage is also seen in the shoot meristem of Lov-1, which could shed more light on the origin of the phenotype, as environmental stresses are expected to be very different between the root and the shoot.

Some molecular links between cold stress and DNA damage responses have been made. It has been shown that somatic homologous recombination frequencies (HRFs), which induce DNA damage are up-regulated in cold (Waterworth et al., 2011). Another study indicated that in a mutant for *UVH6*, a homolog of the XPD/RAD3 transcription factor subunit that acts as a DNA helicase to facilitate the entry of repair enzymes at the site of DNA damage in yeast and human cells, has reduced levels of several cold-stress genes (Hall et al., 2009; Ly et al., 2013). As a consequence, the *uvh6* mutant shows a hypersensitivity to cold stress.

Another gene implicated in cold stress responses that is also linked to cell cycle progression, and therefore might be relevant to DNA damage and

Forward genetics approach to identify components of the ATM pathway  
leading to PCD in response to DNA damage

programmed cell death, is the *FVE* gene, which belongs to the autonomous flowering pathway. It encodes a homologue of the mammalian Retinoblastoma Associated Protein, and is involved in transcriptional repression as part of a histone deacetylase complex. The Retinoblastoma Associated Protein pathway is involved in tumour suppression by inhibiting cell cycle progression from G1 to S phase by inhibiting the E1F transcription factors in order to avoid the replication of damaged DNA (Wachsman et al., 2011). Mutants in this gene show increased levels of *FLC* mRNA, resulting in a photoperiod-independent flowering delay. But *FVE* was also demonstrated to be a sensor of cold stress in *Arabidopsis*. For instance, the *fve* mutant exhibits ectopic expression of cold-regulated (*COR*) genes without cold treatment. In addition, it shows increased freezing tolerance, and its flowering time is not delayed by intermittent cold, indicating that *FVE* is a genetic linker between flowering time and cold response. Therefore, it was proposed that *FVE* has a dual role in regulating flowering time and the stress response to cold (Campi et al., 2011). It would be interesting to know the levels of *FVE* in Lov-1.

These candidates could therefore be tested for their zeocin response. Cold treatments were also shown to induce defence responses through the MAP kinase pathway (Mishra et al., 2006).

Another noteworthy aspect of the Lov-1 ecotype is that its genome is bigger than Columbia (170 Mb vs. 162 Mb), and most of this size difference can be accounted for ribosomal DNA repeats (Fernando Rabanal, personal communication). This genome size difference between Columbia and Lov-1 is common to other North Sweden accession where the genome size difference can be accounted for 45s and 5s rDNA repeats. Surprisingly, genetic mapping of the genome size differences with Genome Wide Association Scanning (GWAS) suggested that this variation is developmentally regulated and under the control of specific trans-acting

Forward genetics approach to identify components of the ATM pathway  
leading to PCD in response to DNA damage

loci. Indeed, the GWAS analysis identified a region that does not contain the rDNA repeats. Therefore, this trait should be considered as a phenotype rather than a genotype, meaning that it must be developmentally regulated (Long et al., 2013b)

Three interesting candidates were associated with the variability in genome size using the GWAS approach: OLA2 (At1g67630), which encodes the B subunit of DNA polymerase  $\alpha$ , MCM2/3/5 (At1g67460), which is related to the minichromosome maintenance family of proteins and *REV3* (At1g67500), which encodes the catalytic subunit of DNA polymerase  $\zeta$ . *REV3* was shown to be required for DNA damage tolerance in both yeast and *Arabidopsis* as discussed in chapter 1. In particular, *rev3* was shown to be hypersensitive to UV-irradiation,  $\gamma$  irradiation and cross-linking agents (Wang et al., 2011), notably showing cell death specifically in the stem cell niche of the root together with DNA polymerase  $\eta$  in response to UV-B irradiation (Curtis and Hays, 2007). The action of DNA polymerase  $\zeta$  was also shown to require ATR. The authors suggested that pathways dependent on ATR and/or ATM cooperate with those two polymerases to tolerate DNA damage or induce PCD depending on the severity of the damage (Curtis and Hays, 2011). Thus the zeocin response of the DNA polymerase  $\zeta$  mutant should be tested.

This discovery opens new possibilities in studying the relationship between DNA damage responses in stem cells and adaptability to varying environmental conditions.

## Chapter 4 ATM dependent silencing in response to a recombination event

### 1. Introduction

In our efforts to develop novel tools to study the ATM dependent DNA damage pathway leading to programmed cell death in stem cells, and moving away from external DNA damaging agents such as radiomimetic drugs and radiations, we decided to use intra-genomic DNA damaging agents making use of the observation in our lab that the activity of a bacterial recombinase could potentially induce DNA damage, and testing if this damage would activate the ATM pathway. We pushed this hypothesis further in chapter 5 by studying the idea of endogenous recombination as a DNA damaging agent.

The development of tools to track cell lineages has been a crucial aspect of cell biology advances for several years (Kuchen et al., 2012). One of them uses the Cre-loxP recombinase. This recombinase was identified in *Escherichia coli* bacteriophage P1. The Cre protein recognizes the loxP DNA site consisting of a 34-bp sequence containing two inverted 13-bp repeats separated by a 8-bp spacer (Abremski et al., 1986). Our laboratory developed a line based on this system that I will call GFPmosaic and the system is presented in figure 4.1 (Gallois et al., 2002). This line contains two transgenes; the first one is the Cre recombinase under the control of the promoter of Heat Shock Protein 18.2 (Sieburth et al., 1998). This makes the Cre recombinase heat shock inducible. The second transgene that I will refer to as “double reporter” consists of the loxP flanked *uidA* gene inserted between the 35S promoter and GFP (35S:lox-*uidA*-NOS-lox-GFP-NOS). As the lox sites are in opposite orientations, the transient induction of Cre by a 38°C heat shock causes the excision of *uidA* and as consequence GFP activation in random cells. The daughter cells of these cells will also inherit GFP expression under the control of the 35S promoter and this will lead to a mosaic of GFP expressing cells throughout the organ subjected to the heat

stress (figure 4.1 B). This system is very robust and has been used in many studies tracking growth patterns (Gallois et al., 2002; Gallois et al., 2004; Kuchen et al., 2012).

However, it was observed in our laboratory that when the heat shock is applied on a whole seedling at the cotyledon stage for a time long enough to ensure most if not all the cells undergo recombination, new leaves that emerge following the heat shock do not display GFP fluorescence (Sablowski, personal communication). Different hypotheses can be formulated to explain this observation. Firstly, the hsp18.2 promoter or the Cre recombinase might be inhibited in the shoot stem cells, so eventually the meristem and the new leaves would be populated with descendants of cells where recombination could not occur. Secondly, considering the fact that stem cells are known for their hypersensitivity to DNA damage, and that the true leaves would emerge from such a pool of stem cells, an attractive hypothesis would be that the recombination event could be sensed as a DNA break and therefore lead to the death of cells undergoing the recombination event, leaving alive only a few cells where Cre is not transiently expressed, which give rise to non-GFP expressing tissues.

While testing hypothesis 2, I uncovered a link between the recombination event and DNA damage processes, but this was unexpectedly not linked to cell death but gene silencing. This discovery opens new possibilities in the study of a link between gene silencing, chromatin remodelling linked to non-coding RNAs and DNA damage pathways, specifically in the context of stem cells.

The study of links between DNA damage responses and gene silencing has been booming recently in animal studies (Shanbhag et al., 2010; Francia et al., 2012; Wei et al., 2012; Altmeyer and Lukas, 2013; Fagagna, 2013; Wan et al., 2013) and I hope to provide further characterization of these new

ATM dependent silencing in response to a recombination event

pathways at the organism level and cell type level, which has not been proven in animal studies.

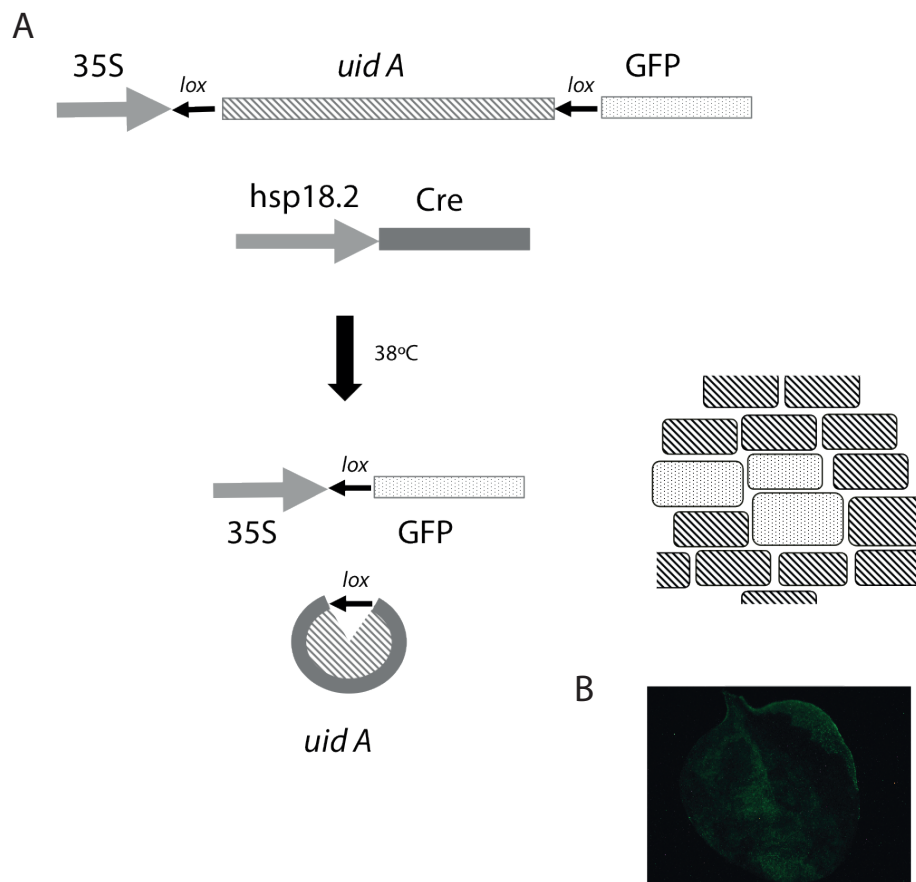


**Figure 4.1: Cre-loxP-based system for mosaic expression used in this study.** (A) The transgenic plant contains a heat-shock-inducible Cre recombinase (*hsp18.2*:*Cre*) and a reporter construct consisting of the lox-flanked *uidA* gene inserted between the 35S promoter and GFP (35S::lox-*uidA*-lox-GFP). After a heat-shock at 38°C, transient induction of Cre causes excision of *uidA* and GFP activation in random cells and their descendants (from Gallois et al., 2002). (B) GFP-expressing sectors on the cotyledon epidermis 10 days after heat shock.

## 2. Results

### 2.1 Loss of GFP expression following a recombination event was due to ATM- and SOG1-dependent transgene silencing

#### 2.1.1 GFP fluorescence cannot be observed in true leaves following a recombination event at the cotyledon stage

As mentioned above, it was observed in our lab that *Arabidopsis* seedlings subjected to a 38°C heat shock during a time sufficient for all cells to undergo recombination at the cotyledon stage did not show GFP expression in newly arising leaves, suggesting that stable GFP sectors could not be generated in the meristem (Sablowski, personal communication). Indeed, as the cotyledons kept expanding, GFP fluorescence was observed in both cotyledons as well as in the root, where fluorescence appears sooner and remains brighter than in the rest of the seedling, as it appears as early as 2 days following heat shock (figure 4.3 F). However, 10 days post heat-shock no GFP expression can be observed in any leaves that emerged post heat shock (figure 4.2 E).

With the discovery of stem cells hypersensitivity to DNA damage, it was hypothesized that the recombination event could be sensed as a DNA break, and the hypersensitivity of those cells would lead to PCD, explaining the absence of GFP fluorescence observed in true leaves emerging from this stem cell pool.

#### 2.1.2 The loss of GFP fluorescence is dependent on ATM and SOG1

As the hypersensitivity of stem cells to DNA damage is dependent on ATM (Fulcher and Sablowski, 2009; Furukawa et al., 2010), I crossed the GFPmosaic line into the *atm-2* mutant background, to see if the loss of GFP expression would be ATM dependent. I observed that 10 days post heat-shock, GFP expression in true leaves was completely lost in GFPmosaic but

## ATM dependent silencing in response to a recombination event

not in *atm-2* GFPmosaic (figure 4.2 F). Confirming this result, I also observed that loss of GFP expression was prevented in seedlings grown on the ATM inhibitor KU55933 which has been extensively used in animal and plant studies and as a therapeutic target (Amiard et al., 2010; Shanbhag et al., 2010; Amiard et al., 2011). Also, silencing was prevented in the *sog1-1* mutant background and the *mre11-4* background. MRE11 functions in DSB repair together with ATM by resecting exposed DSB ends, making them compatible for re-ligation (Paull and Gellert 1998) (see chapter 1).

The plants grown on the ATM inhibitor showed a decreased level of GFP fluorescence compared to the *atm-2* and *sog1-1* background, but the expression was still stronger than in GFPmosaic alone (figure 4.2 G). This could be attributed to the light sensitivity of the inhibitor (Shanbhag et al., 2010), which could be degraded as the plant grows in light conditions.



### 2.1.3 GFP fluorescence was lost in a pattern that suggested gene silencing

I then decided to explore further the idea of PCD as a consequence of the recombination event. First, if PCD occurred in response to the recombination event, selection against recombined cells would occur and the cells composing the newly emerging leaves would have an unrecombined double reporter transgene (Figure 4.1 A). This would mean that all cells from the true leaves would express the uidA gene under the control of the 35S promoter in the GFPmosaic line, where a mosaic of GUS sectors would be expected in the *atm-2* GFPmosaic background. However, GUS staining of the GFPmosaic seedling 10 days post heat-shock shows no GUS staining in the true leaves either (figure 4.3), whereas the *atm-2* GFPmosaic line displayed a mosaic of GUS sectors as expected. This suggested that a spreading signal inhibited expression of the double reporter transgene in all cells, regardless of whether the transgene had undergone recombination or not, and this signal was suppressed in an *atm-2* background.

I then decided to specifically monitor the time course of GFP fluorescence in newly emerging leaves, during the 7 days following heat-shock. This did not show the emergence of “dark” (non GFP expressing) leaves as I expected, but the emergence of GFP-expressing leaves followed by progressive loss of GFP fluorescence in a pattern spreading from the centre of the plant, until GFP expression is completely lost in the leaves (figure 4.4). *atm-2* GFPmosaic seedlings monitored in the same conditions did not show the spread of disappearance of GFP expression (figure 4.5).

These two experiments suggested that the loss of GFP fluorescence was caused by gene silencing, which is frequently observed in the development of transgenic lines, as the insertion of foreign DNA into the genome triggers

ATM dependent silencing in response to a recombination event

silencing mechanisms that evolved against viruses and transposons (Dalmay et al., 2000).

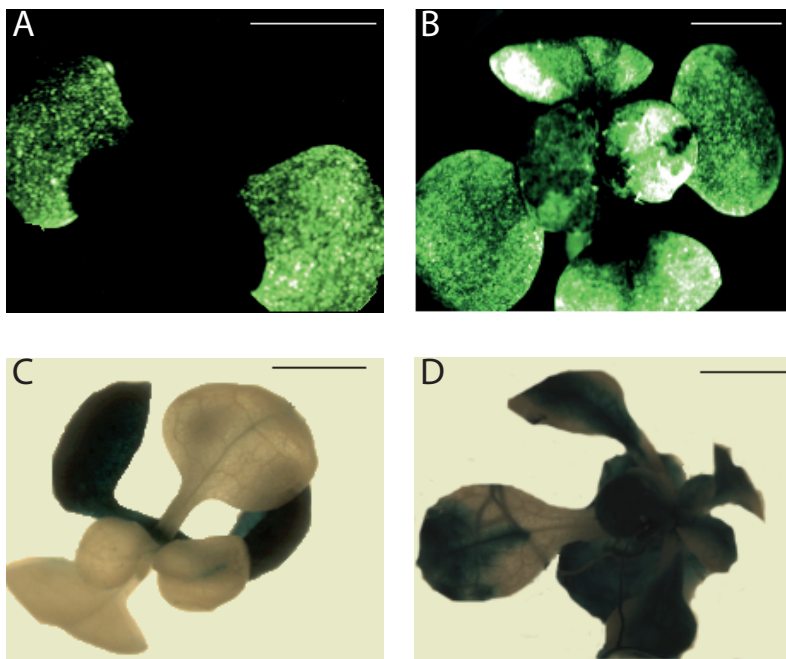
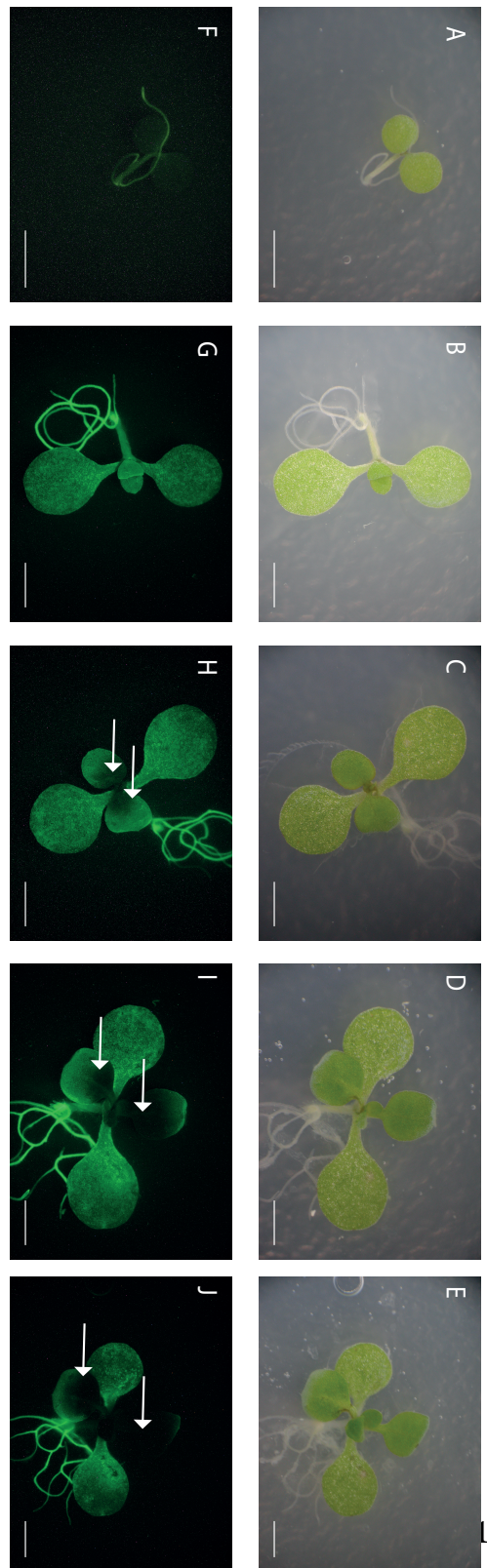


Figure 4.3: **GUS staining is not present in true leaves of the GFP mosaic line 10 days post HS but present in an *atm* background.** (A-D) Representative images of 5 seedlings 10 days post HS (A,C) GFPmosaic (B,D) *atm* GFPmos (A,B) GFP expression (C,D) GUS staining (Fisher's exact test p-value = 0.007937).



**Figure 4.4: The GFPmos line displays a loss of GFP expression in emerging leaves following heat-shock at the seedling stage.** (A-E) bright field stereomicroscopy images of seedlings 2 days (A), 4 days (B), 5 days (C), 6 days (D) and 7 days (E) following a 20 minute heat-shock at 38°C. (F-J) fluorescence stereomicroscopy images showing GFP expression in seedlings 2 days (F), 4 days (G), 5 days (H), 6 days (I) and 7 days (J) following a 20 minute heat-shock at 38°C. Scale bar = 0.2 cm. Images are representative of 3 plants imaged.



#### 2.1.4 Cre-catalysed recombination was not prevented in the GFPmosaic line

It remained possible that GFP fluorescence was lost because Cre-catalysed recombination was inhibited in the shoot stem cells, and that gene silencing additionally caused the loss of *uidA* expression. To investigate recombination events in the GFPmosaic line, I designed a multiplex semi-quantitative PCR experiment enabling the amplification of the recombined and unrecombined transgenes following the heat shock in the GFPmosaic and the *atm-2* GFP mosaic background (figure 4.6 A and B). 30 cycles were deemed optimal to detect the recombined band while the GFP band (used as an internal control) was still in the exponential phase of amplification.

Three separate experiments with individual plants showed the same ratio of recombined band/unrecombined band in GFPmosaic and in *atm-2* GFPmosaic (an example of a gel is presented in figure 4.6 C). However, the results were not comparable between experiments (Figure 4.6 D). In order to confirm this result, I repeated the experiments with three replicates of each genotype, showing again the same recombination pattern in both genotypes following the heat shock (figure 4.6 E).

In conclusion, Cre-catalysed recombination happened at the same level with or without the *atm-2* mutation in the GFPmosaic line. ATM was therefore not required for the recombination event to occur in the GFP mosaic line.

## ATM dependent silencing in response to a recombination event

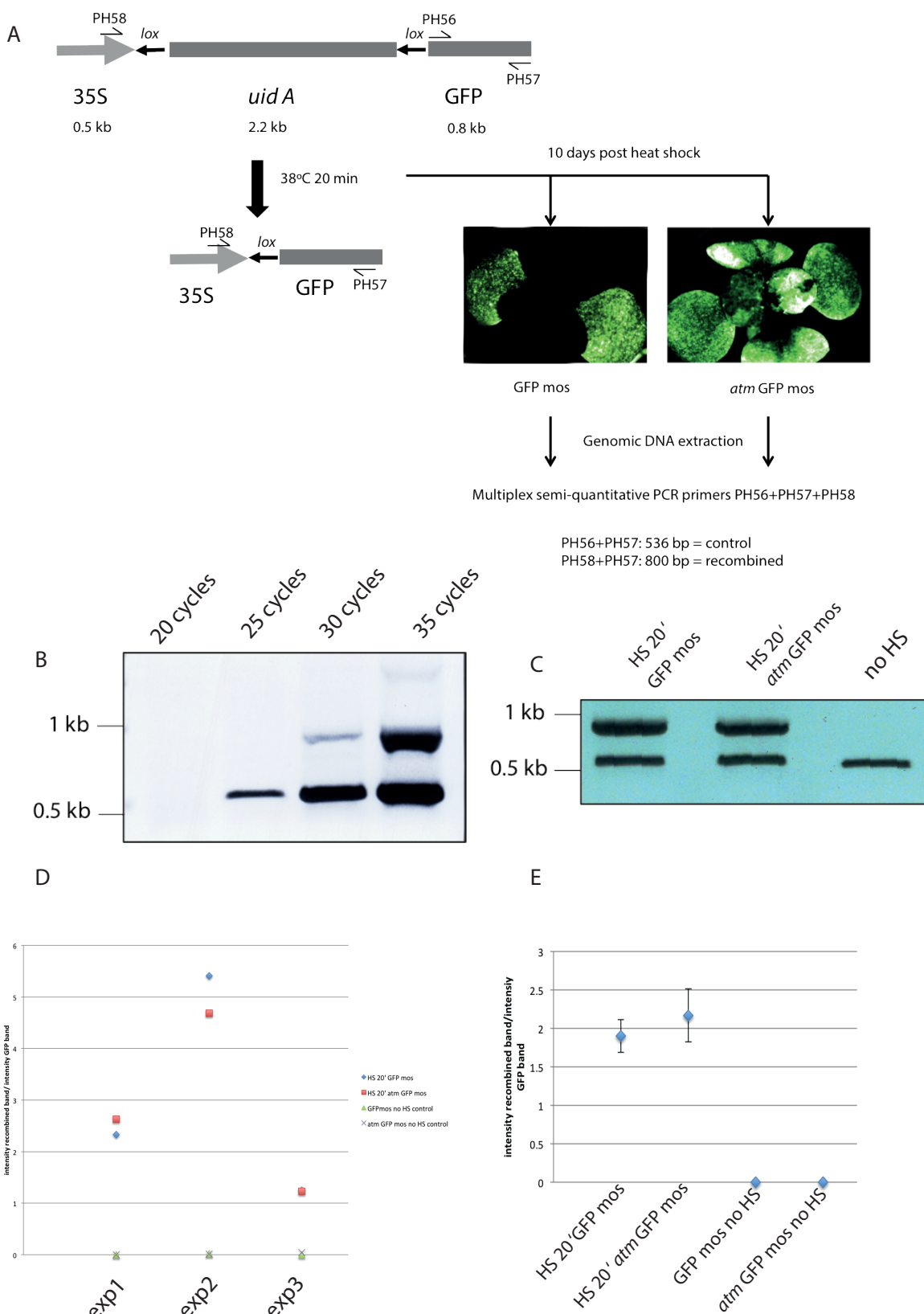


**Figure 4.6: The recombination event following HS is occurring in both GFPmosaic and *atm* GFPmosaic.** (A) Schematic representation of the experimental set-up to measure recombination by multiplex semi-quantitative PCR 10 days post HS using GFP as an internal control (B) Optimisation of the number of cycles for semi-quantitative multiplex PCR (C) Representative example of semi-quantitative multiplex PCR with 30 cycles showing similar recombination events in both GFPmosaic and *atm* GFPmosaic 10 days post HS. (D) Intensity of recombined band/intensity of GFP band 10 post HS in GFPmosaic and *atm* GFPmosaic plants in three independent experiments (E) Intensity of recombined band/intensity of GFP band 10 post HS in GFP mos and *atm* GFP mos averaging the intensity for three plants (error bar= SD).

### 2.1.5 The loss of GFP fluorescence was associated with loss of GFP expression

The experiment presented in figure 4.6 suggested that silencing of the double reporter transgene occurred in *ATM* wild-type plants but was prevented in the *atm-2* background. To confirm gene silencing at the RNA level, semi-quantitative RT-PCR was conducted with the same primers as the GFP control band presented in figure 4.6, with 30 cycles of amplification. This experiment showed very little expression of GFP in GFPmosaic seedlings 10 days post HS, while GFP expression was very high in an *atm* background (figure 4.7 A). The double reporter transgenic line alone (i.e., without the *hsp18.2:Cre* transgene) was also included to eliminate a possible effect of the heat shock itself on GFP expression. Loss of GFP mRNA in the GFPmosaic line following heat shock was consistent with ATM-dependent transgene silencing. This is likely to depend also on *SOG1*, although GFP expression in *sog1-1* GFPmosaic was not tested.

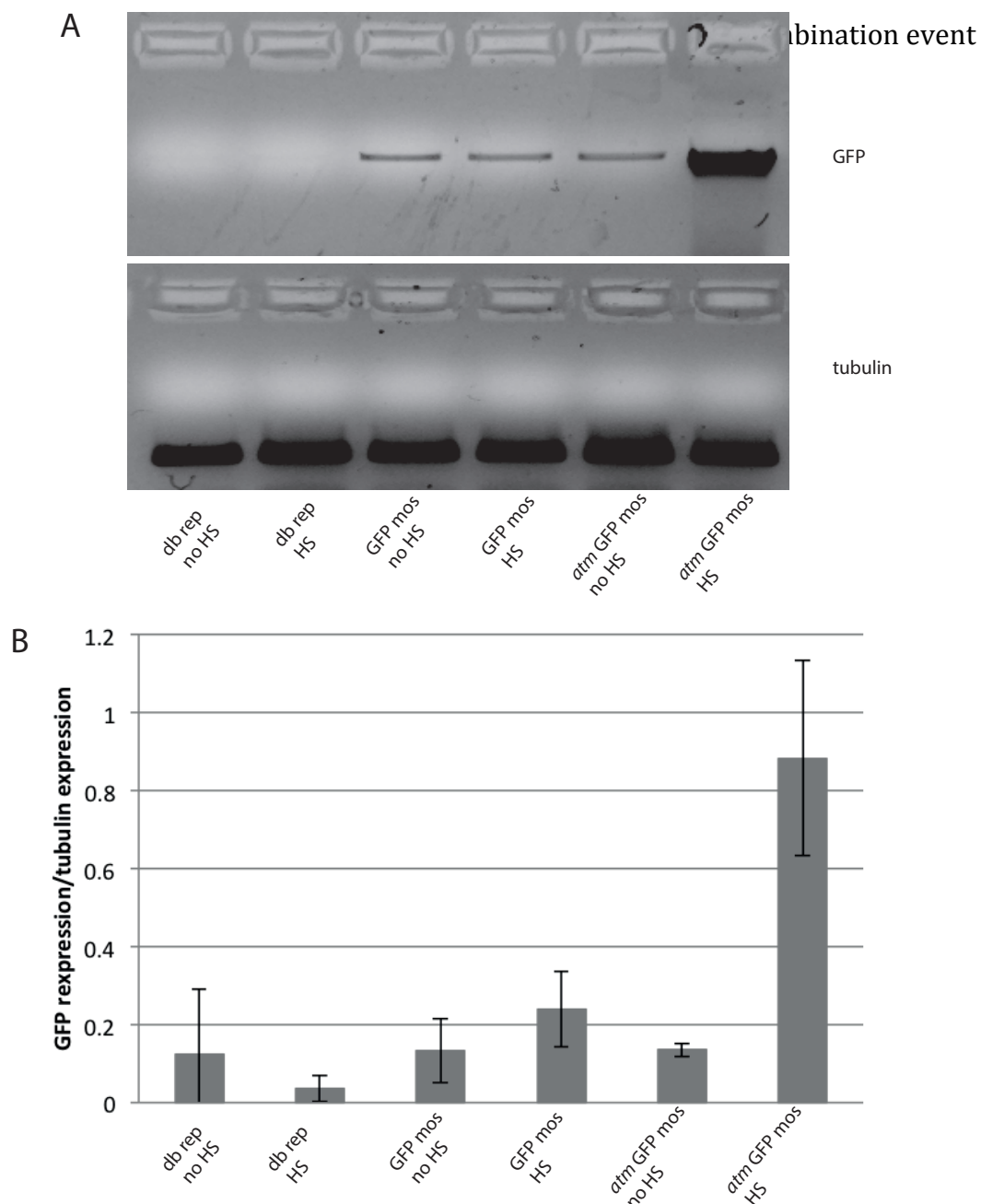
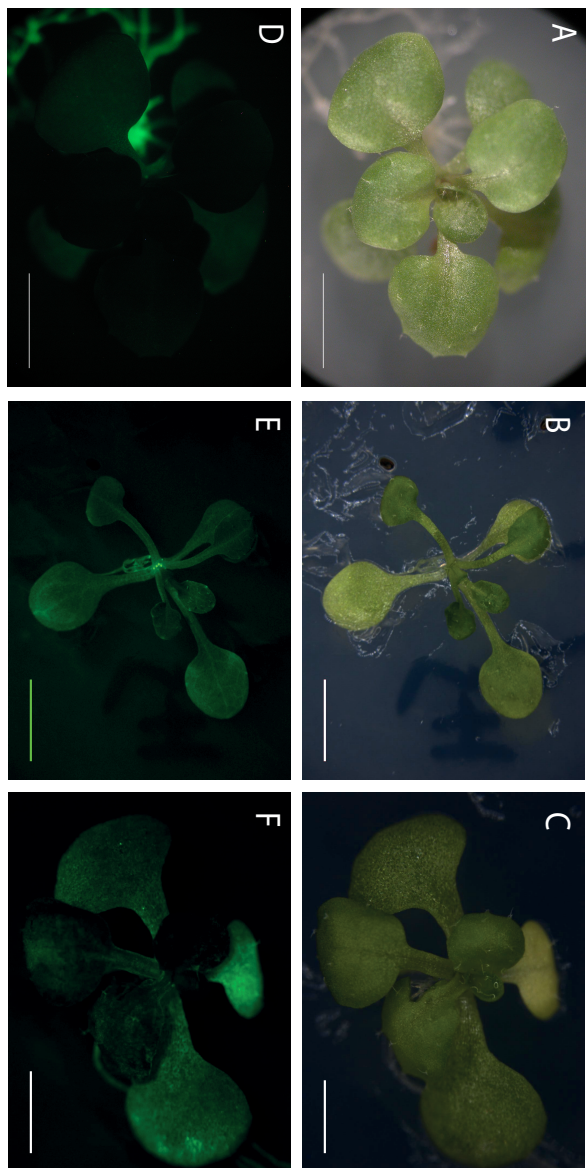


Figure 4.7: **Expression of GFP is lost in the GFPmosaic line but not in an *atm* background.** (A) Representative (3 experiments) where RNA was extracted from a single plant 10 days post HS (A) semi quantitative RT-PCR gel showing GFP and tubulin expression in db rep (GFP reporter construct without Cre recombinase construct), GFP mos and atm GFP mos plants with and without HS. (B) Relative GFP expression.

### 2.1.6 Searching for the hallmarks of DNA damage following the Cre-catalysed recombination: Silencing was prevented when the NHEJ pathway is disabled

The fact that *ATM* and *SOG1* were required for the silencing of GFPmosaic suggested that the recombination event was sensed as a DNA break by the plant as I first hypothesised. Therefore, I looked for a molecular hallmark of DNA breaks at the double reporter locus following Cre activation by crossing the GFPmosaic line to the DNA damage mutants *ku80*, and *lig4-4*. KU80 is part of the initial step of NHEJ activation by binding to DNA ends to prevent further processing and protect the DNA ends (Ramsden and Gellert 1998). LIG4 acts further down the pathway and acts to religate DBA ends (Chen *et al.* 2000).

The *ku80* GFPmosaic lines both no silencing 10 days post HS in all of 20 plants observed, and *lig4-4* showed a decrease in silencing but not as pronounced as for *ku80* in all of 20 plants observed (figure 4.8), suggesting a link between a functional NHEJ pathway and the silencing observed in the GFPmosaic line.



**Figure 4.8: GFP silencing is partially prevented in DNA repair mutant backgrounds.** (A-F) Representative (25 plants showing the phenotype presented, Fisher's exact test p-value = 1.582e-14) images of (A-C) bright field or (D-F) GFP fluorescence microscopy of (A,D) GFPmosaic, (B,E) *ku80* GFPmos (C,F) *lg4-4* GFP mos 10 days post HS. Scale bar = 200  $\mu$ m.

## 2.2 ATM-dependent production of small RNAs

The ATM-dependent silencing of GFP following the recombination event prompted me to consider which silencing pathway was affected by the *atm* mutation. RNA silencing is a central mechanism of gene regulation in all eukaryotes and relies on the action of small interfering RNAs (siRNAs). In *Arabidopsis*, two distinct classes of siRNAs have been identified: 21-nt RNAs mostly guide mRNA cleavage, whereas 24-nt siRNAs mediate chromatin modifications.

Transgene silencing has been linked to 21-nt trans-acting siRNAs as part of the PTGS mechanism that enables plants to protect themselves against viruses. PTGS operates via translational repression, often coupled to mRNA decay, or via endonucleolytic cleavage (slicing) catalysed by the AGO protein. The RNA-dependent RNA polymerases (RDRs) RDR1 and RDR6 are required in this pathway.

On the other hand, co-transcriptional silencing involves repressive chromatin modifications. This process, known as RNA-dependent DNA methylation (RdDM), acts at the chromatin level and produces the 24 nt small RNAs, many of which are associated with transposons silenced by methylation. The RNA polymerase POL-IV directs this heterochromatic silencing, together with the RNA-dependent RNA polymerase RDR2 as well as the Dicer-like protein DCL3 and the argonaute protein AGO4 (Finnegan et al., 2003; Bonnet et al., 2006; Brodersen and Voinnet, 2006; Poulsen et al., 2013).

To uncover which pathway could be activated in my context, I performed small RNA Northern blotting. Total RNAs from GFPmosaic, *atm-2* GFPmosaic and double reporter with or without *hsp18.2: Cre* were extracted from 20 day-old seedlings 10 days post heat shock or without heat shock. The small RNA fraction was enriched, purified and separated from the total RNAs. To

## ATM dependent silencing in response to a recombination event

check for the presence of small RNAs and to obtain a size marker, the blot was then first incubated with an end-labelled probe corresponding to the ubiquitous tasiRNA 255 (Xie et al., 2005). This RNA is present in an abundant 21-nt form and a less abundant 24 nt-form (figure 4.9). This enabled me to mark the location of both sizes of small RNAs on the blot. The blot was then stripped and incubated with a riboprobe corresponding to mGFP5-ER, the GFP version present in the GFPmosaic line (Gallois et al., 2002). The riboprobe was designed as a sense probe, in order to recognise antisense small RNAs targeted at the sense transcript. I was able to identify small RNAs of 24-nt in size in the GFPmosaic line 10 days post heat shock, and these small RNAs were lost in an *atm* background (figure 4.9).

Therefore, I concluded that the silencing of GFP in response to heat-shock occurred through the 24-nt small RNA pathway. This was somewhat unexpected, as experiments linked to transgene silencing usually involve the 21-nt siRNA pathway. I therefore decided to characterise this pathway further using available mutants that affect heterochromatic silencing.

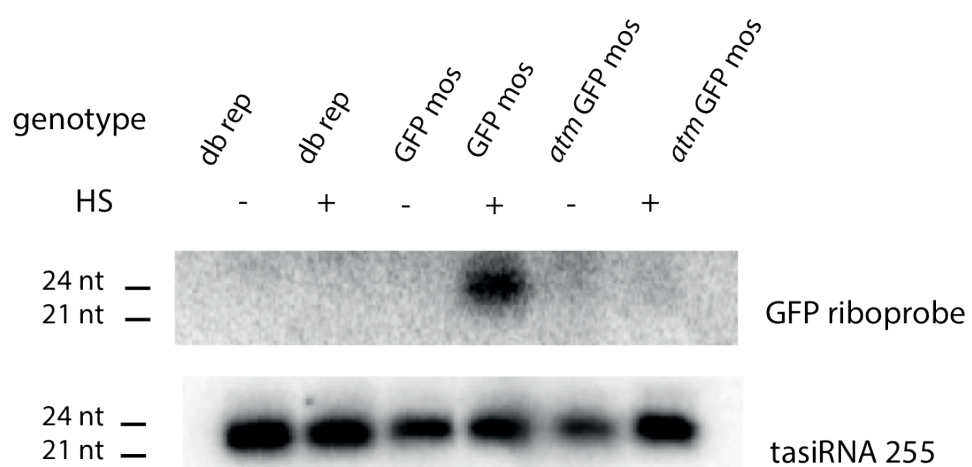


**Figure 4.9: Production of 24-nt siRNA 10 days post HS is lost in an atm background.** Representative (2 experiments) small RNA blot assay using a GFP riboprobe. The ubiquitous tasiRNA 255 was used a loading control and a size control.

### 2.3 Characterisation of the pathway leading to ATM dependent silencing

I uncovered that the ATM-mediated silencing identified in the GFPmosaic line is associated with 24-nt siRNAs, suggesting the involvement of the RdDM pathway in the silencing. Therefore, I tested GFP silencing in several mutant lines of this pathway in order to link ATM to these known genes. I first tested RDR6 to confirm the non-involvement of the 21-nt pathway and as expected, the *rdr6* GFPmosaic line showed silencing 10 days after heat shock (figure 4.10).

I then crossed the GFPmosaic line to the *nrpd1a-1* mutant, which encodes the large subunit of RNA polymerase IV (Herr et al., 2005): (figure 4.11). 10 days post heat shock, 50 % of the 50 GFPmos *nrpd1a-1* plants observed showed no silencing, where the other 50% showed silencing. However, in 50% of the plants showing silencing, the silencing was not stable: the first leaves to emerge post heat shock showed no GFP fluorescence, but subsequent leaves did express GFP (figure 4.11 F). Therefore, I concluded that the RNA pol IV is partially involved in the ATM dependent silencing of GFP.

Another important aspect of this pathway is which argonaute protein is responsible for loading the small RNAs into the dicer protein. 10 argonaute proteins have been identified in Arabidopsis. AG04, AG06, and AG09 have been linked to the DNA methylation and repressive chromatin modifications pathway with similar functions, but have different expression patterns, with AG04 playing the major role (Poulsen et al., 2013). However, in my context *ago4* GFPmosaic plants showed wild type levels of silencing 10 days post heat-shock (figure 4.12). AG06 was the only argonaute protein shown to function in RNA-mediated transcriptional gene silencing in stem cells (Eun et al., 2011) (Meister, 2013). Considering that the silencing event that I

ATM dependent silencing in response to a recombination event

observed could relate stem-cell-specific ATM responses, I also generated an *ago6* GFPmosaic line. This line showed no silencing 10 days post HS (Figure 4.12), therefore I concluded that AGO6 is required for the ATM-dependent silencing.

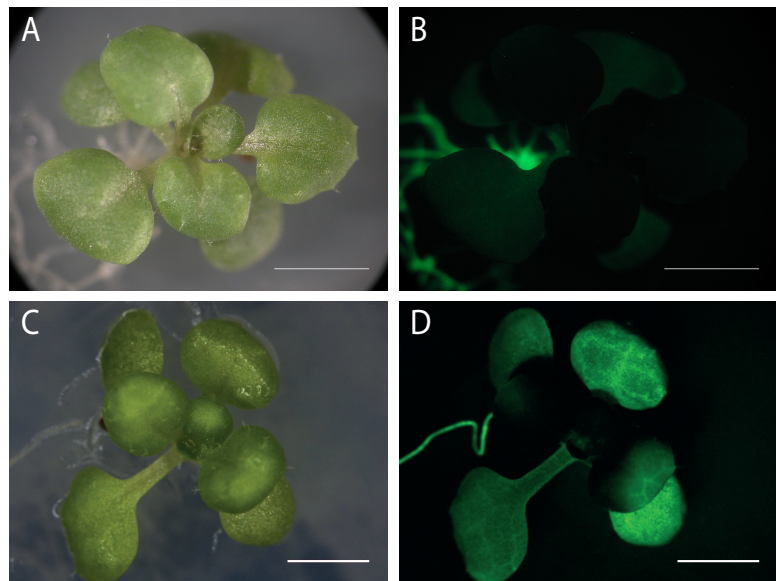
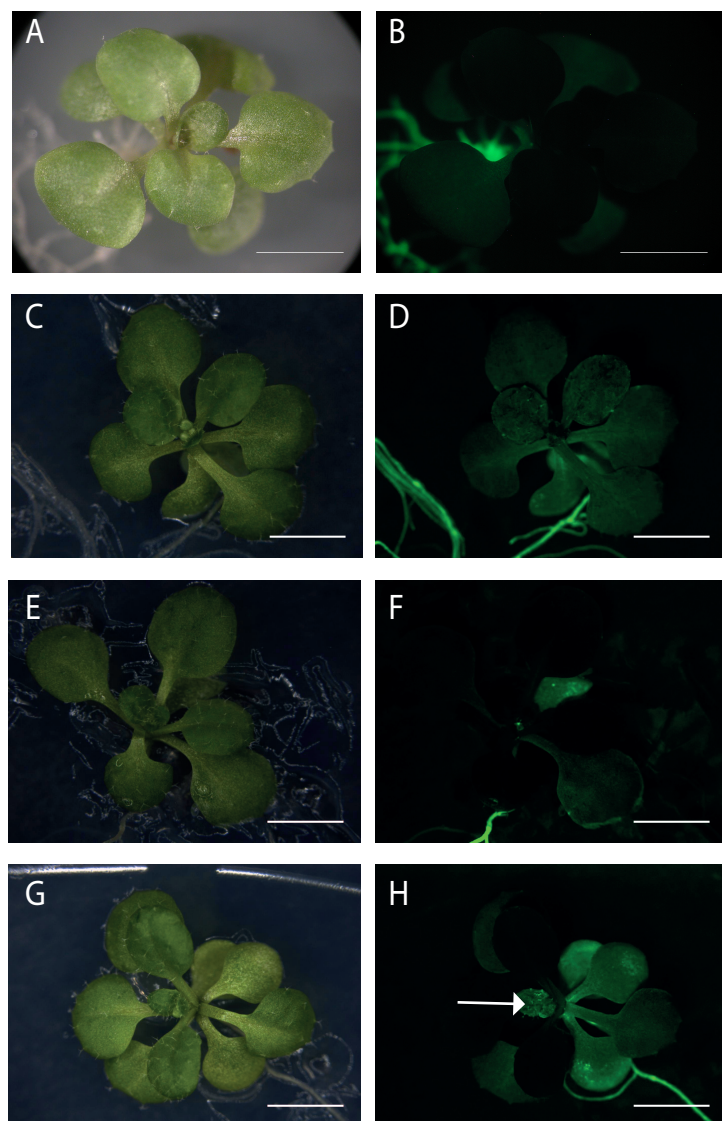


Figure 4.10: **GFP silencing is occurring in the *rdr6-16* mutant background.** (A-D) Representative (10 plants) images of (A,C) bright field or (B,D) GFP fluorescence microscopy of (A,B) GFPmosaic and (C,D) *rdr6-16* GFPmosaic 10 days post HS. Scale bar = 200  $\mu$ m.



**Figure 4.11: GFP silencing is partially prevented in the *nrpd1a* mutant background.** (A-H) Representative (50 plants) images of (A,C,E,G) bright field or (B,D,F,H) GFP fluorescence microscopy of (A,B) GFPmosaic or (C-H) *nrpd1a-1* GFPmosaic 10 days post HS. (C,D) Representative (25 plants) images of plants showing no silencing. (E,F) Representative (15 plants) images of plants showing silencing. (G,H) Representative (10 plants) images of plants showing silencing then a newly emerging leaf expressing GFP (indicated by the arrow). Scale bar = 200  $\mu$ m.

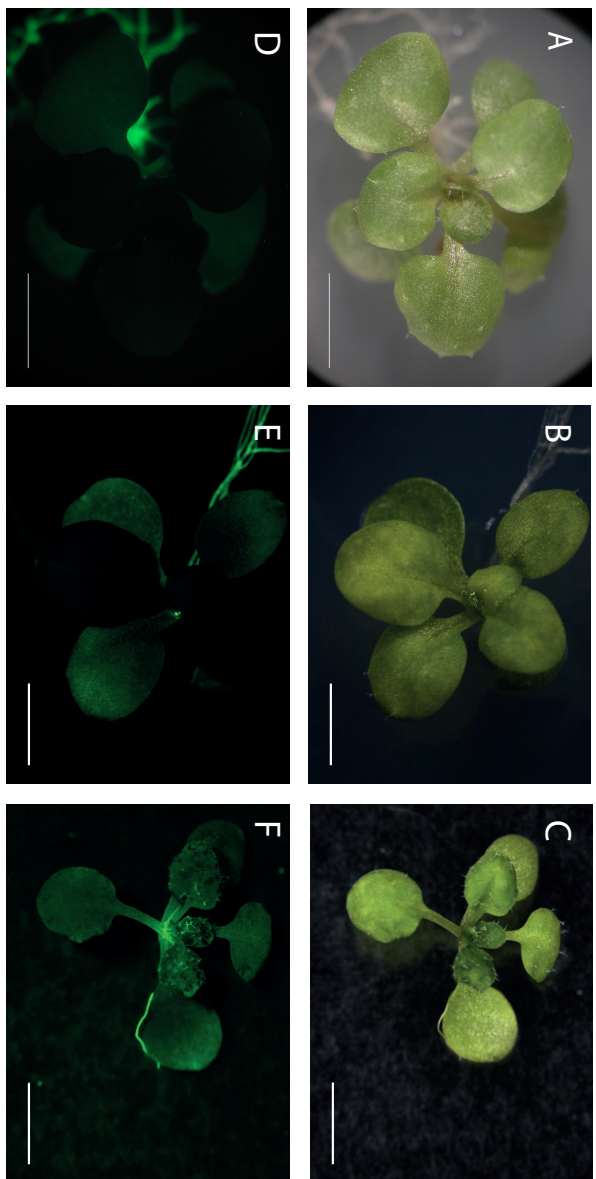


Figure 4.12: **GFP silencing is prevented in the *ago6* mutant background but not in the *ago4-1* mutant background**. (A-F) Representative (10 plants) images of (A-C) bright field or (D-F) GFP fluorescence microscopy of (A-D) GFPmosaic (B,E) *ago4-1* GFPmosaic and (C,F) *ago6* GFPmosaic 10 days post HS (Fisher's exact test p-value = 1.083e-05). Scale bar = 200  $\mu$ m.

## 2.4 Development of reporter lines for inducible DSBs

To further explore the idea that silencing was initiated in response to recombination-induced DNA damage in the shoot stem cells, two different transgenic approaches were started. The first was to replace the Cre recombinase with the I-SceI endonuclease, which has been extensively used to produce DSBs in both animal and *Arabidopsis* studies (O'Hagan et al., 2008; Michalik et al., 2012; Puchta and Fauser, 2013). I generated the same construct as presented in figure 4.1, but replacing the *loxP* sites with the I-SceI site and the Cre recombinase with the I-SceI cDNA. I was able to generate a single insertion line for I-SceI showing a good induction of I-SceI following Heat-shock (figure 4.15), but I could not generate a single insertion line for the double reporter containing the I-SceI site with one round of transformation and I could not repeat the transformation due to time constraints. However, the fact that the multi insertion line that I generated with the double reporter was showing a very strong GUS staining is encouraging.

The other approach that I started aimed to induce Cre activity specifically in the shoot stem cells. For this, the idea was to use localised expression of the heat shock response factor HSF1 to mimic a heat shock response in specific cell types. I used the pOP/LhG4 transcription system (Wielopolska et al., 2005) to express HSF1 fused to the rat glucocorticoid receptor (Gallois et al., 2004). This construct was transformed into pCLV3:LhG4, which drives expression in the central region of the SAM (Aggarwal et al., 2010). The prediction was that dexamethasone treatment would activate HSF1-GR specifically in the central region of the meristem, leading to activation of heat shock responsive promoters, including *pHSP18.2*. In combination with the GFPmosaic line, this should allow temporal control of Cre-catalysed recombination specifically in the shoot stem cells.

I tested the OP:HSF:GR system in CLV3:LhG4 in the T1 generation by

ATM dependent silencing in response to a recombination event

treating flowers with Dex and extracting the RNA 6 hours after treatment. I was able to identify several lines showing an induction of HSP18.2 (data not shown), but time constraints prevented me from completing these experiments.

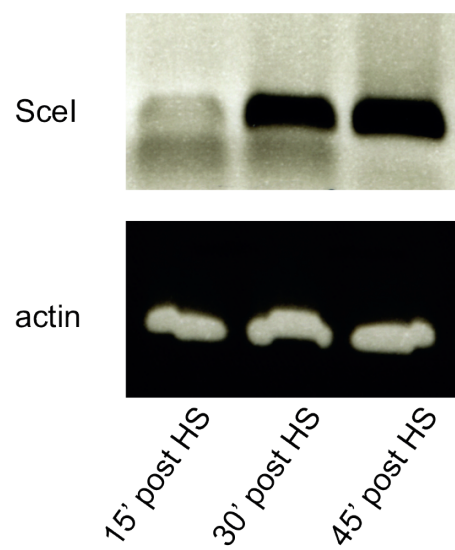


Figure 4.15 : **Induction of Scel expression following Heat Shock.** RT PCR showing: upper panel: induction of Scel expression in the pHs:Scel T1 15, 30 and 45 minutes after a 20 minute heat-shock, bottom panel: actin expression.



### 3. Discussion

The experiments described in this chapter led to the discovery of an uncharacterised phenomenon of ATM dependent silencing, which may be restricted to stem cells. Moreover, this silencing seems to be related to RNA-mediated transcriptional silencing linked to chromatin modifications, which has not been described in transgene silencing phenomena.

One limitation of my study is the use of the Cre recombinase instead of a widely used DSB inducing nuclease such as I-SceI. However, it was shown that recombination *in vitro* between a mutant lox site (with a mutation in the spacer region) and a wild type lox site with purified Cre recombinase lead to the formation of single and double stranded-breaks (Pollock and Nash, 1983). Also, the study of Cre expression in mammalian cell cultures revealed chromosome aberration and an increased number of sister chromatid exchanges, and that this toxicity was dependent on the level of Cre activity (Loonstra et al., 2000). I can therefore argue that Cre activity is likely to cause at least some DNA breaks and therefore elicit a DNA damage response.

A way to obtain a more definite answer as to whether cre recombination elicits a DSB response would be to look for the molecular hallmark of a DSB at the site of recombination: the presence of phosphorylated histone H2AX. Indeed, phosphorylation of the H2AX histone variant by ATM is the first detectable event in response to a DSB (Scully and Xie, 2013).  $\gamma$ -H2AX could be detected at the site of recombination following activation hsp18.2:Cre by heat shock by ChIP, using a specific antibody raised against the *Arabidopsis*  $\gamma$ -H2AX. First, western blotting will be used to pinpoint the time after the occurrence of a DSB when  $\gamma$ -H2AX can be detected in the histone pool. This timepoint will then be used to perform the ChIP on whole seedlings following the heat-shock. The DNA obtained from the ChIP experiment will

then be used to detect a potential enrichment of the recombined transgene by qPCR.

As I was developing this project, a number of studies linking DNA damage responses with chromatin modifications and small RNAs were published. Indeed, although it was previously thought that all factors implicated in the DDR response were protein coding genes, new evidence now points towards a crucial role of non-coding RNAs in the responses to DNA damage (Liu and Lu, 2012). First, a number of long non-coding RNAs and microRNAs were linked to DNA damage responses by targeting and modulating key genes in the DDR pathway (Wan et al., 2013) (Wang and Taniguchi, 2013). Furthermore, specific DNA-damage induced siRNAs, deemed qRNAs were described in the filamentous fungus *Neurospora crassa* (Lee et al., 2009a). Now, new studies point out a role of silencing pathways and siRNAs with similarities between plants and animals.

Specifically, Shanbhag and colleagues (Shanbhag et al., 2010) uncovered chromatin changes leading to a silencing of transcription under the control of ATM. Making use of the I-SceI inducible system and a reporter line enabling the marking of the chromosomes in a single cell together with an overview of gene transcription and protein recruitment using different fluorescent proteins, they showed in mammalian cell cultures that transcript levels in the vicinity of a DSB was lost but not because of a degradation of the transcript. Their experiments showed that there is a specific influence of ATM activity on large-scale chromatin condensation in transcriptionally active regions. Chromatin decondensation is indeed required for transcription to occur. In the context of a DSB, ATM prevents RNA polymerase II elongation at the site of DSB. Several chromatin marks are dependent on ATM, especially the ubiquitylation of histone H2A, leading to chromatin condensation, whereas if deubiquitylation is induced, transcription is restored. The conclusion was that DSBs induce transcriptional silencing in *cis* through chromatin modifications, and this

## ATM dependent silencing in response to a recombination event

can occur in multiple kb away from the damage. This study correlates with my discovery that ATM was implicated in the chromatin remodelling silencing pathway in the GFP mosaic line. Moreover, my approach expanded on this study by describing this pathway at the organism level and more importantly hinting at a stem cell-specific pathway, involving known components of the RdDM pathway. Pankotai and colleagues also showed that the occurrence of a single DSB within a transcriptional unit leads to an inhibition of transcription by PolII. This process was shown to be dependent on DNAPK, suggesting that the break does not inhibit transcription itself, but rather the activity of DNAPK (Pankotai et al., 2012).

Also, several studies showed the importance of siRNAs for an efficient repair of DNA damage. Specifically, Wei and colleagues (Wei et al., 2012) used the I-SceI system in *Arabidopsis* where the repair of the cut provoked by I-SceI would lead to the expression of the *uidA* gene. They found high levels of GUS staining at the seedling level, meaning high levels of repair in response to the induction of I-SceI, but this staining was lost in an *atr* mutant. This phenomenon was linked to siRNAs, as DCL3 was required for the repair to occur, and the production of small RNAs around the lesion site was uncovered. These derived from both sense and antisense strands of the sequence, and were 21 and 24-nt in size. Both *rdr2* and *rdr6* (involved in RdDM and *trans*-acting siRNA pathways respectively) showed a reduction in the production of those siRNAs with no effect on repair efficiency, suggesting a redundant action of the two genes. Moreover, the production of those new siRNAs, called diRNAs (for DNA damage interfering RNAs) was dependent on ATR as well. Also, the production of diRNAs was compromised in *nrpd1a* and AGO2 was found to recruit the diRNAs. There was no difference in the expression of genes involved in DNA repair linked to the production of diRNAs (MRE11, RAD50, NBS1, ATM, ATR, RAD51, RPA1, BRCA1, BRCA2, RAD54, RECQL, RAD5A, and RPA2b were tested), and no effect on the production of the histone variant H2AX. Taken together, these data suggested that siRNAs generated from sequences flanking a DSB

## ATM dependent silencing in response to a recombination event

are important for efficient repair, but this repair is not mediated by the chromatin remodelling pathway or through the regulation of known repair genes. Interestingly, this pathway seems to be conserved in animals where the knockdown of Dicer or *AGO2* leads to the loss of diRNAs following a DSB, together with a compromised repair rate (Wei et al., 2012).

Two other studies conducted in *Drosophila* and vertebrates further characterized this new pathway. The inactivation of the RNases DICER and DROSHA, which are implicated in the generation of small double stranded RNA products in animals, was reported to lead to impaired DDR caused by oncogene-induced DNA replication stress or ionizing radiation, but not the downstream elements of the RNAi pathway. The inactivation reduced the formation and DDR foci containing signalling factors such as the activated form of ATM. ATM autophosphorylation and activation were also impaired upon DICER or DROSHA inactivation and the G1/S and G2/M cell cycle checkpoints were lost leading to an escape from apoptosis. This role of DICER and DROSHA in efficient repair was also shown to require the formation of site-specific DICER- and DROSHA-dependent small RNAs, named DDRNAs, which act in a MRE11–RAD50–NBS1- complex-dependent manner (Francia et al., 2012) (Fagagna, 2013). A similar mechanism was also characterized in *Drosophila*, with the generation of small RNAs at DNA ends in the context of a double strand break. The small RNA response was amplified in the vicinity of the break by active transcription, showing that breaks are sites of transcription initiation, a novel aspect of the cellular DSB response. These small RNAs were also shown to repress homologous sequences in *trans*. Therefore, on top of their putative function in DNA repair mechanisms, these small RNAs may exert a quality control function by clearing potentially truncated messages from genes in the vicinity of the break (Michalik et al., 2012).

In my study I showed an ATM-dependent production of 24-nt siRNAs, the involvement of *AGO6* and partial involvement of Pol IV and the need for a

functional NHEJ pathway for the silencing to occur. Interestingly, the study by Wei and colleagues (Wei et al., 2012) does not mention any involvement of *ATM* in diRNAs production or repair rates, but only focuses on *ATR*. In my study I decided to focus on *ATM* because of its wider roles in stem cells hypersensitivity to DNA damage, *ATM* being required for PCD to occur in both the shoot and root where *ATR* was shown to not to be required in the shoot meristem (Fulcher and Sablowski, 2009). It would therefore be interesting to generate an *atr* GFPmosaic mutant line and look for the occurrence of GFP silencing.

This study also showed that *AGO4* was not involved in the diRNA pathway, and focused instead on *AGO2*. *AGO2* was previously linked to the miRNA pathway performed functions largely redundant to those of *AGO1*, but is also supposed to play an antiviral role as it associates with some virus-derived siRNAs (Thieme et al., 2012b). Also, the *Arabidopsis* genome contains no *DROSHA* homologue, and the small RNA biogenesis steps are carried out by the four Dicer-like proteins (Filipowicz et al., 2008). *DCL1* is involved in miRNA biogenesis, *DCL2* and *4* are involved in the *trans*-acting siRNA pathways and *DCL3* is involved in the 24-nt RdDM pathway (Xie et al., 2004). In this context, I have generated *ago2* and *dcl3* crosses in my GFP mosaic system but could not characterize them due to time constraints. The possible involvement of *DCL3* will also be crucial to decipher as it is a major player in the RdDM pathway and was also shown to be the major DCL protein involved in the diRNA pathway (Wei et al., 2012).

The Wei and colleagues study also showed that the diRNA production was greatly reduced in the *nrpd1a* mutant but slightly increased in the *nrpe1* mutant, with repair rates decreased in both mutants. *NRPE1* encodes the largest subunit of Pol V, which is also involved in the RdDM pathway but contrary to Pol IV, which is required for siRNA biogenesis, Pol V generates scaffold transcripts upon which the RdDM effectors are assembled, showing that Pol IV is involved in repair through the regulation of diRNA biogenesis

## ATM dependent silencing in response to a recombination event

and Pol V is involved in diRNA functioning. This could mean that in my experimental design, where Pol IV is partially required for silencing to occur, Pol V could also be involved and the generation of an *nrpd1a nrpe1* double mutant in the GFPmosaic line could yield some interesting information on the functioning of silencing.

The main difference between my study and the Wei study is that I linked the production of siRNAs to an ATM-dependent silencing mechanism, similar to what is described in the Shanbhag and colleagues study, whereas the Wei study described a requirement of the so-called diRNAs for an efficient DNA repair measured by GUS staining measurement. However, their study did not include the possibility of silencing occurring in response to I-SceI expression. Also, another difference is that they showed no link between diRNA production and expression known repair genes, including *MRE11*, whereas I found an effect of *MRE11* on silencing (figure 4.9). Furthermore, they did not check Ku80 and ligIV expression, while I also saw an effect on silencing, especially involving Ku80 (figure 4.9).

The fact that Ku80 is required for the silencing to occur suggests that the silencing would be a consequence of *ku80* mediated repair. One way of testing this hypothesis would be to cut the apex of heat-shocked seedlings and amplify around the *loxP* site by PCR to look for length polymorphism at the site of repair. Indeed, a non-functional NHEJ is expected to lead to aberrant repair products. For instance, it was shown in mice that a lack of Ku80 leads to aberrant rejoining of chromosome ends (Tong et al., 2002).

It would be interesting to study the expression of other repair genes in my system, such as *BRCA1* and *2* which are involved in DNA repair in both plants and animals (Abe et al., 2009). Finally, the study was done at the whole organism level, which is another difference with my system, which is focused on stem cells, where epigenetic mechanisms could be more stringent due their increased sensitivity to DNA damage. Therefore, even though the pathway described by Wei et al. could be unrelated to my system, as it does not seem to be linked to chromatin remodelling like the

## ATM dependent silencing in response to a recombination event

Shanbhag and colleagues study, intriguing similarities suggest a complex pathway involving chromatin changes, non coding RNAs and DNA repair existing in both animals and plants (Ohsawa et al., 2013).

The new phenomenon described in this chapter highlights the importance and variety of DNA damage responses in plant stem cells. It can be hypothesized that gene silencing and PCD could result from differential responses to DNA breaks in stem cells, depending on the DNA damaging agent, the length or the severity of the damage. The *in vivo* DNA damaging agents driving hypersensitivity to DNA damage of plant stem cells remain to be uncovered, and the existence of a silencing pathway linked to DNA damage responses led me to the hypothesis that endogenous DNA damaging agents such as mobile DNA elements could be involved and not necessarily exogenous agents as previously thought. The study of a potential endogenous DNA damaging agent that could lead to either PCD or gene silencing was the subject of the next chapter (Chapter 5).

## Chapter 5 Investigation of the link between DNA damage and transposon activity

### 1. Introduction

The discovery that plant stem cells are hypersensitive to DNA damage left one crucial research question unanswered: what is/are the *in vivo* DNA damaging agents that would drive the evolution of this protective mechanism? DNA damage and especially DSBs were shown to be the consequence of exogenous factors, such as cycles of heat or drought versus cold or flooding, heavy metals in the soil or UV radiation. So far, only UV-B irradiation was shown to mimic a zeocin treatment in the root in terms of DNA damage levels (Curtis and Hays, 2007) (Furukawa et al., 2010), together with  $\gamma$ -ray and X-ray irradiations that a plant is unlikely to encounter in the wild. Experiments performed in our lab failed to show a preferential effect of the toxic metals aluminium and cadmium on stem cells in the root (Fulcher, personal communication).

One problem posed by the idea of exogenous agents being responsible for stem cells hypersensitivity to DNA damage are the very different types of stress that stem cells face if they are present either in the root or in the shoot. For instance, a root is unlikely to experience UV-B induced damage although the shoot meristem will be exposed to solar radiation. On the other hand, heavy metals will only affect the root meristem and not the shoot meristem if they are not absorbed and transported *via* the xylem. Experiments using UV-B should be repeated in the shoot in order to mimic the type of stress that exposure to the sun would have on the SAM.

In this study I took a different approach considering endogenous DNA damaging agents as potential drivers of stem cells hypersensitivity to DNA damage. In maize and *Arabidopsis*, plants deficient in chromatin remodelling show increased DNA damage compared to WT plants after a

UV-B treatment (Qüesta et al., 2013). In this context, and in the light of a possible link between DNA damage response pathways and a chromatin silencing mechanism, I investigated the role of chromatin stability on stem cells hypersensitivity to DNA damage. In particular, I considered transposon mobilization as a potential endogenous DNA damaging agent, using first a candidate gene approach, and then an inducible transposon movement system in mutant backgrounds affected in the DNA damage response.

## 2. Results

### 2.1 A class of genomically unstable mutants displays spontaneous cell death

Several mutants having a broad role in chromatin stability were shown to also constitutively display activated DNA damage responses and as a consequence, hypersensitivity to DNA damaging treatments (Inagaki, 2006). I therefore decided to investigate if these genes could play a role in the hypersensitivity to DNA damage identified in stem cells, showing a link between this pathway and chromatin stability. We identified several candidates through literature search.

I first tested the *TEBICHI* gene, which encodes a homolog of the mammalian DNA polymerase  $\theta$ . This polymerase prevents spontaneous DNA double stranded breaks, and has been implicated in playing a role in resistance to ionizing radiation in animal cells (Yousefzadeh and Wood, 2013). The *tebichi* mutant in *Arabidopsis* displays a fasciation phenotype and shows constitutively activated DNA damage responses, such as an over-expression of RAD51 and BRCA1. In addition, the *tebichi* mutant is hypersensitive to the cross-linking agent mitomycin C and methyl methane sulfonate (MMS) (Inagaki, 2006; Inagaki et al., 2009). *tebichi* also over-accumulates cells expressing cyclinB1;1 in the meristems, which is known to be induced in response to DNA damage (Culligan et al., 2006). Mutations in *ATR*, *RAD51*

and *XRCC2*, but not in *ATM*, were shown to enhance the developmental phenotype of *teb*, and *atr* also suppressed the cell cycle defects of *teb*. Genes in the vicinity of the Helitron transposons genes are also up-regulated in *teb* and *teb atr* (Inagaki, 2006; Inagaki et al., 2009). I found that *tebichi* displayed statistically significant spontaneous cell death in the root initials, mimicking the effect of a mild zeocin treatment (Fisher's exact test p-value = 0.03251) (Figure 5.1 B and Table 5.1).

I next tested a gene from the *FASCIATA* group. *FASCIATA 1* encodes the large subunit of CAF1 (chromatin assembly factor1) complex and *FASCIATA 2* encodes the middle subunit. Both mutants show stem fasciation like *tebichi*, and other developmental defects such as an enlarged shoot meristem and serrated leaves, which is thought to be due to an ectopic expression of meristem regulators such as *WUSCHEL* in the shoot and *SCARECROW* in the root. The instability of the chromatin in those two mutants is associated with an increase of DSBs and homologous recombination. Mutants for *FAS1* induce an up-regulation of genes involved in the DNA damage response (Hisanaga et al., 2013) and mutants for *FAS2* also show an accumulation of cells expressing cyclinB1;1 in the meristems (Stroud et al., 2013). I found that the *fasciata2* mutant also displayed a significant level of spontaneous cell death compared to the wild type (Fisher's exact test p-value = 0.0008741) (Figure 5.1 and Table 5.1).

I next decided to consider the BRU/TSK/MG03 (BRUSHY/TONSOKU/MGOUN3) gene (Suzuki et al., 2004; Takeda et al., 2004; Guyomarc'h et al., 2006). This gene was separately identified by three teams, reinforcing the link between genome stability and chromatin stability. The *bru1* mutant is highly sensitive to DNA damage treatments, display increased levels of intrachromosomal homologous recombination and constitutively activates the *PARP2* gene. It also displays macroscopic phenotypes resembling those of *tebichi* and *fasciata* (Takeda et al., 2004),

including stem fasciation and an enlarged and disorganized meristematic region in both the root and shoot. Multiple WUS expressing centres in the SAM were identified in the mutant, and the expression of SCR disappeared in the RAM, showing that the gene is required for correct cell positioning and the determination of cell identity (Suzuki et al., 2005). The mutant was also shown to flower early, due to an reduced expression of FLC and ectopic expression of floral genes AG, PI and SEP3, associated with an alteration of histone H3 acetylation (Guyomarc'h et al., 2006). The *bru1* mutant also shows an accumulation of cells expressing cyclin B1;1, leading to the suggestion that it is required for progression of the cell cycle at the G2/M phase (Suzuki et al., 2004). As seen for *teb* and *fas2*, I found that the *bru1-2* mutant also displayed spontaneous cell death in the root meristem in all 10 plants tested (Fisher's exact test p-value = 1.083e-05), and it was also the case for the *ngo3* allele (Fisher's exact test p-value = 0.02941) (figure 5.1).

I finally tested *RPA2* (DNA replication A second subunit), which is necessary for transcriptional gene silencing and is hypersensitive to MMS (Elmayan et al., 2005). This mutant showed no spontaneous cell death in the root meristem (figure 5.1).

**Table 5.1: Spontaneous cell death observed in the root meristem of genetically unstable mutants**

Genotype	Number of plants showing spontaneous cell death	Number of plants showing no spontaneous cell death
<i>Col</i>	0	9
<i>teb</i>	5	5
<i>fas2</i>	6	1
<i>bru1-2</i>	10	0
<i>ngo3</i>	4	4
<i>rpa2</i>	0	10

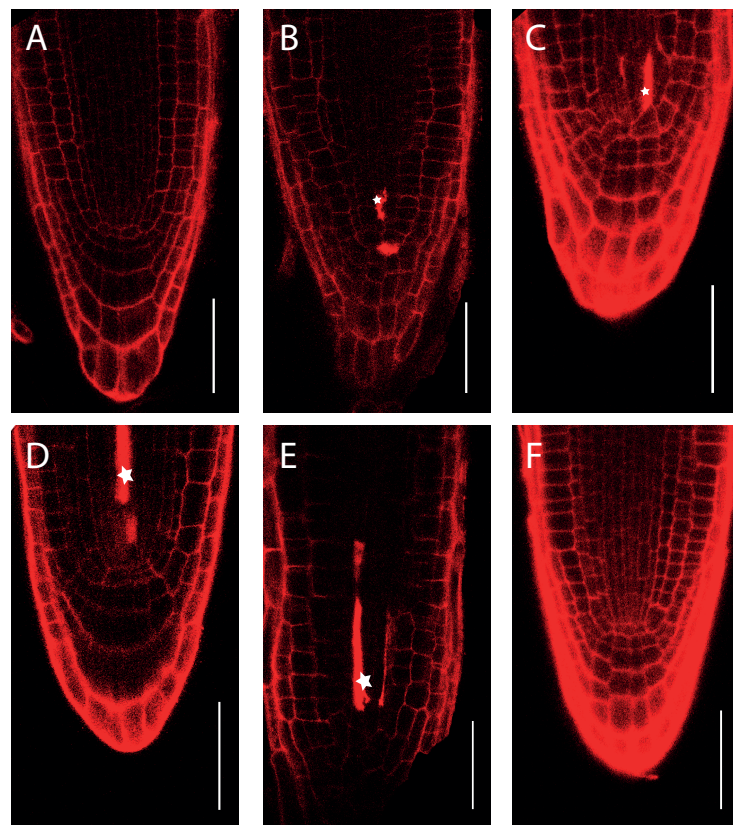


**Figure 5.1: Mutants known for genomic instability display spontaneous cell death in the root initials.** (A-F) Representative confocal microscopy images of root tips stained with PI. (A) *Col-0* (B) *teb*, 5 plants showing PCD, 5 plants showing no PCD, Fisher's exact test p-value = 0.03251 (C) *fas2*, 6 plants showing PCD, 1 plant showing no PCD, Fisher's exact test p-value = 0.0008741 (D) *bru1-2*, 10 plants showing PCD, Fisher's exact test p-value = 1.083e-05 (E) *ngo3*, 4 plants showing PCD and 4 plants showing no PCD, Fisher's exact test p-value = 0.02941 (F) *rpa2*, 10 plants showing no PCD. Scale bar = 50  $\mu$ m.

## 2.2 Partial enhancement of the *bru1-2* phenotype in *atm-2* background and partial rescue in *sog1* background

As I was developing this project, it was shown that the *fasciata1* mutant also shows spontaneous cell death in the root meristem and this death is under the control of ATM but not ATR (Hisanaga et al., 2013), showing a link between the chromatin instability of the mutant and cell death response pathways. I therefore decided to check if the same was true for *BRU1*. I crossed the mutant to *atm-2* and *sog1* and found that the *atm-2 bru1-2* double mutant still displayed spontaneous cell death in all 20 plants tested (figure 5.2), whereas the *sog1 bru1-2* double mutant showed a complete loss of spontaneous cell death in all 20 plants tested (figure 5.3). On the other hand, the developmental defects were still visible in both double mutants, such as fasciation and root length (figure 5.2 E and figure 5.3 D).

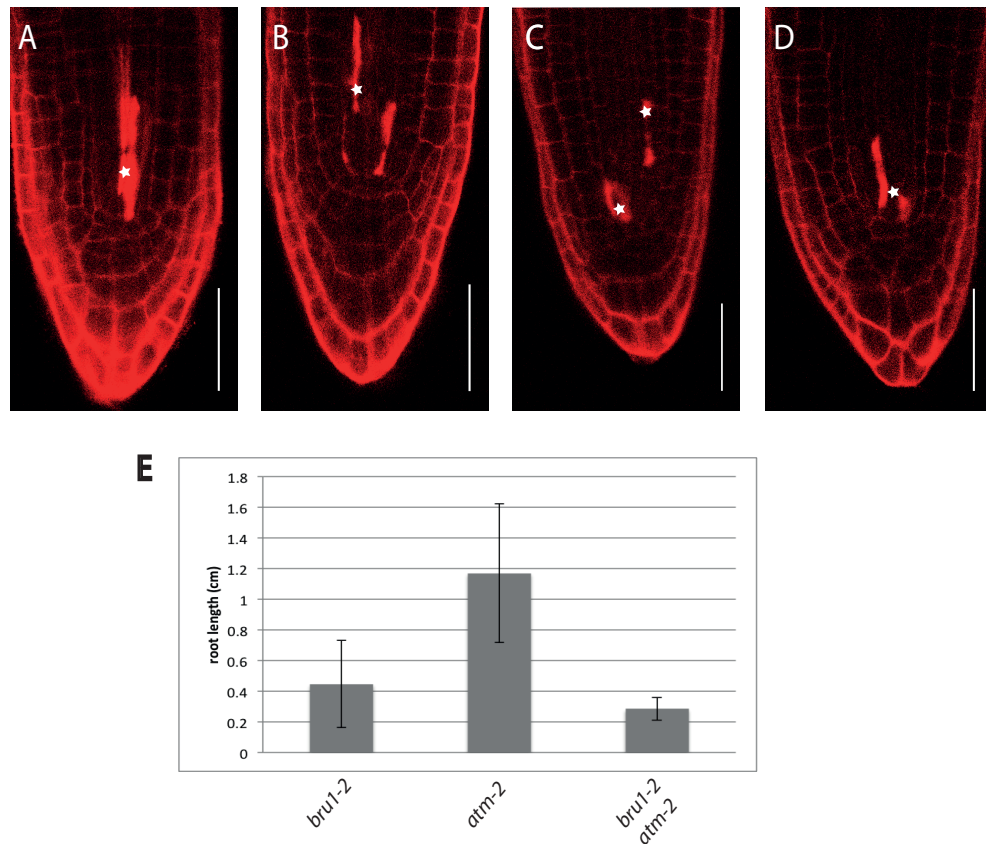


Figure 5.2 : **A mutation in ATM does not affect the PCD phenotype in *bru1-2* a.** (A-D) Representative (10 plants, all showing the phenotype presented) confocal images of root tips stained with PI. (A) *bru1-2* (B) *bru1-2 atm-2* double mutant (C) *bru1-2* with 4  $\mu$ M ATM inhibitor KU 55933 (D) *bru1-2* with 10  $\mu$ M ATM inhibitor 55933. (E) root length of 5 day old seedlings. Scale bar = 50  $\mu$ m. Asterisks indicate dead cells.

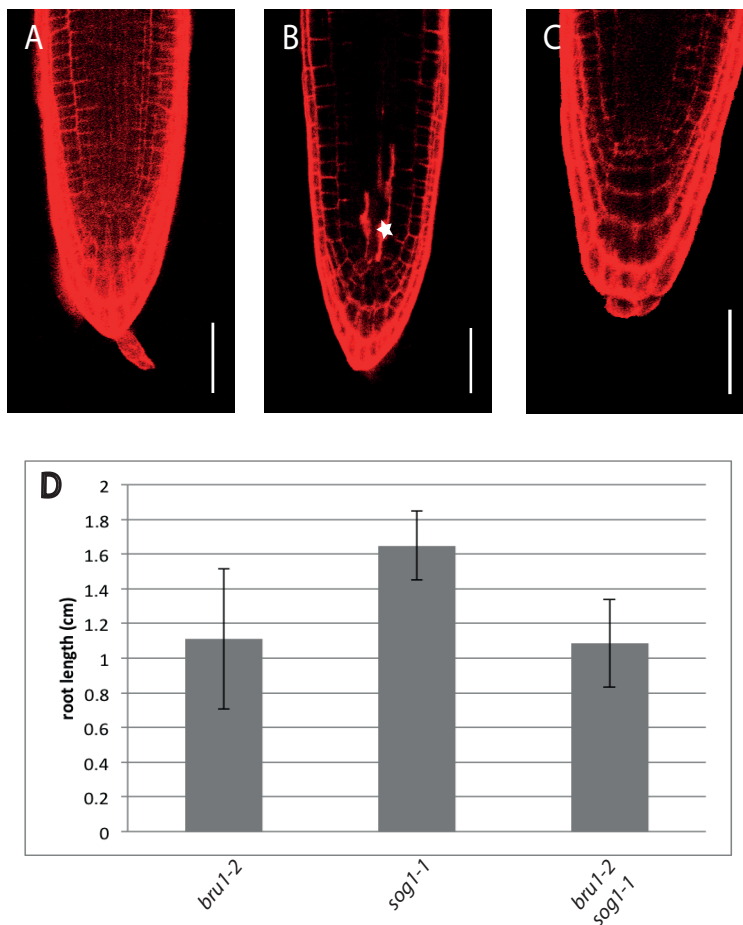


Figure 5.3 : **A mutation in *SOG1* suppresses the PCD phenotype of *bru1-2* but not the root phenotype.** (A-C) Representative confocal images of root tips stained with PI. (A) Col (B) *bru1-2* (1 showing PCD) (C) *sog1-1 bru1-2* double mutant, 19 plants showing no PCD, 3 plants showing PCD, exact test p-value = 4.433e-06. (D) root length of 5 day old seedlings. Scale bar = 50  $\mu$ m. Asterisks dead cells.

2.3 *ddm1*, but not other genes required for transcriptional gene silencing, displays spontaneous cell death in the root initials

The mutants described in 2.1 all displayed an altered chromatin stability phenotype, described as “open chromatin”, potentially making it more vulnerable to DSBs. This chromatin instability also leads to some level of release of transcriptional gene silencing in all the mutants (Elmayan et al., 2005). Transposon movement is known to require DNA repair mechanism in order to repair the break caused by transposition mechanisms, in both *Arabidopsis* and animals (Belgnaoui et al., 2006; Huefner et al., 2011). Therefore, an attractive hypothesis is that transposon movement could be a source of DNA damage in these mutants.

This link between genomic instability, release of gene silencing and spontaneous cell death lead me to consider other mutants involved in gene silencing to see if they also displayed a spontaneous cell death phenotype in the root meristem. We tested a range of mutants required for transcriptional gene silencing and acting on different aspects of chromatin stability (figure 5.4), as described below.

*MOM1* is required for transcriptional gene silencing but is not involved in methylation marks (Amedeo et al., 2000). *MET1* is required for both transcriptional and post transcriptional gene silencing (Morel et al., 2000). The mutant for the *hda6* gene shows elevated histone H3 and H4 acetylation and an increased methylation of H3K4, together with a decrease of transposable element methylation. HDA6 interacts with MET1 both *in vitro* and *in vivo*, showing that HDA6 and MET1 act together to maintain TEs silencing by modulating their histone acetylation, methylation and DNA methylation status (Liu et al., 2012). *DDM1* is part of the SWI2/SNF2-like protein family and shows a decrease in DNA methylation leading to a release of transcriptional gene silencing including transposition transcription

(Jeddeloh et al., 1999). The mutation leads to a 70% reduction of genomic cytosine methylation. Also, genes can retain a level of methylation in *ddm1* homozygous plants, but lose methylation over generations when the mutant is propagated via self-pollination (Hirochika et al., 2000). *RDR2* (RNA dependent RNA polymerase 2) is part of the RdDM pathway and the mutant also releases transcriptional gene silencing (Xie et al., 2004).

Out of all the genes mentioned above, only one showed significant occurrence of spontaneous cell death: *ddm1-2* (Fisher's exact test p-value: 0.03017), shown in figure 5.4 and table 5.2. All the other genes showed either no cell death or the increase in the frequency of PCD was not statistically significant. The latter was the case for *rdr2*, for example, which showed some level of spontaneous cell death (figure 5.4) with a Fisher's exact test p-value of 0.1544. Other genes that are involved in the RdDM pathway had already been tested in the lab and showed no occurrence of spontaneous cell death: *nrpd1a*, *ago4*, *dcl3* and *drm1drm2cmt3* (Sablowski, personal communication).

**Table 5.2: occurrence of spontaneous cell death in the *ddm1-2* and *rdr2-1* mutants.**

Genotype	PCD	No PCD
WT	0	10
<i>ddm1-2</i>	7	11
<i>rdr2-1</i>	2	14

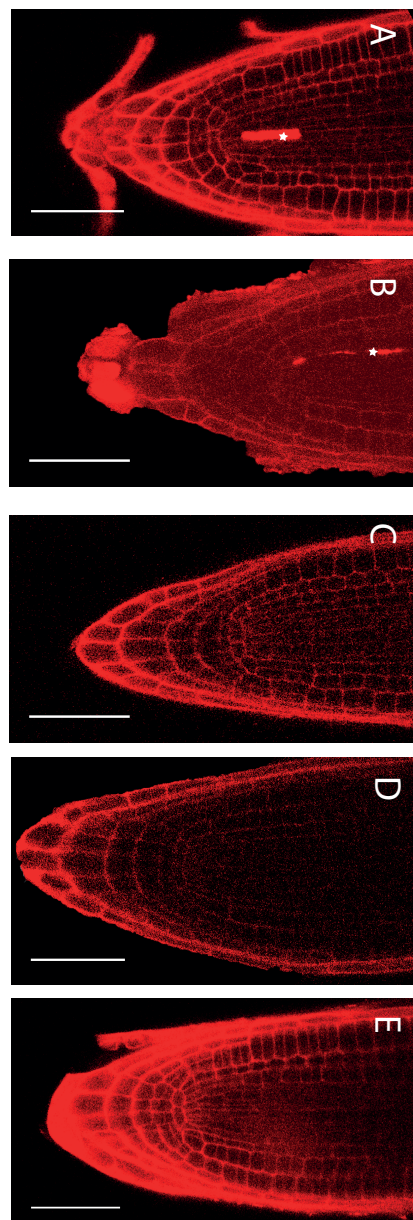


**Figure 5.4: Mutants affected in gene silencing pathways display spontaneous cell death in the root initials.** (A-C) Confocal images of root tips stained with PI. (A) Representative image of 7 out of 18 *ddm1-2* plants showing PCD (Fisher's exact test p-value 0.03017). (B) Representative image of 2 out of 7 *rdl2-1* plants showing PCD (Fisher's exact test p-value 0.1544). (C) Representative (10 plants all showing no PCD) *met1* (D) *hda6* (E) *mom-2* mutant plants. Scale bar = 50  $\mu$ m. Asterisks indicate dead cells.

As mentioned above, the mutants displaying spontaneous cell death display a significant remobilisation of transposons, notably a release of Athila retrotransposon expression (Elmayan et al., 2005). I next examined further the links between transposon movement and the spontaneous cell death phenotype in the *ddm1* mutant.

As a first step, I made use of the fact that the *ddm1* mutant is known to accumulate transposon movement over generations (Hirochika et al., 2000). I therefore crossed *ddm1-2*, which was the result of several rounds of propagation through self-pollination in the lab back to the wild-type. In the first generation following the cross, the occurrence of cell death was no longer statistically significant in homozygous *ddm1-2* seedlings (figure 5.5 and table 5.3, Fisher's exact test p-value= 0.9). Therefore, one possible conclusion is that the less transposon movement, the less cell death is occurring in the stem cells, which are more sensitive to DNA breaks than other cells. Following the pattern of spontaneous cell death following self-pollination generations of the *ddm1-2* mutant will help to test this hypothesis.

**Table 5.3: occurrence of spontaneous cell death in the *ddm1-2* mutant following backcrossing to wild-type**

Genotype	PCD	No PCD
<i>L-er WT</i>	0	10
<i>ddm1-2</i>	5	5
<i>ddm1-2 x L-er WT</i> generation 1	1	11

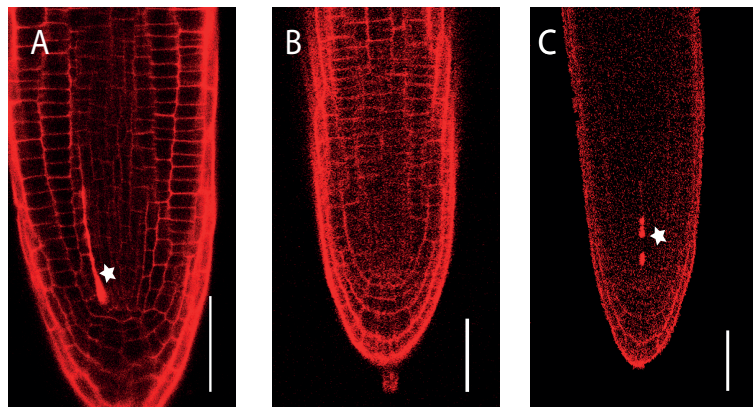


**Figure 5.5: *ddm1-2* shows a decrease in spontaneous cell death following back cross to wild type.**  
(A-C) Representative confocal images of root tips stained with PI. (A) *ddm1-2*, 5 out of 10 plants showing PCD, Fisher's exact test p-value = 0.03251 (B-C) *ddm1-2* first generation following cross to Ler wild type background showing no PCD (11 plants) (B) or PCD (1 plant, Fisher's exact test p-value = 0.9) (C). Scale bar = 50  $\mu$ m.

## 2.4 ATM-dependent reactivation of retrotransposons

If transposon mobilization were an endogenous cause of DNA damage that would lead to *ATM*- and *SOG1*-dependent defensive responses in stem cells, it would be expected that *atm* and *sog1* mutants should accumulate cells in which transposon movement has occurred. The protective responses could involve PCD, as observed after exogenously induced DSBs. Alternatively, considering the importance of chromatin silencing to prevent transposon movement, the link between *ATM/SOG1* and gene silencing described in the preceding chapter might be relevant for protection against transposon activity.

One difficulty in testing this prediction, however, is that new transposition events are expected to be rare and are diluted in a background of a large number of different mobile elements. To facilitate detecting any effects of *ATM* and *SOG1* on transposon mobilisation, I used the ONSEN retroelement. This retrotransposon is normally silent in the Columbia ecotype and is transcribed during heat stress. However, this normally does not lead to neo-insertions of transposon copies because a silencing mechanism via a 24 nt-siRNA pathway is induced following the heat-stress and transcription of the transposon. If the RdDM pathway is disabled, as in the *nrpd1a* mutant background, the silencing mechanism is prevented and neo-insertion of transposon copies occurs, which can be typically detected in the next generation of a plant subjected to heat-stress (Ito et al., 2011; Matsunaga et al., 2011; Ito et al., 2013). To test whether *ATM* or *SOG1* mediate responses to transposon activity, I monitored ONSEN movement in the *atm* and *sog1* background compared to the wild type as described below.

#### 2.4.1 Possible generational transposition event in the *atm* mutant

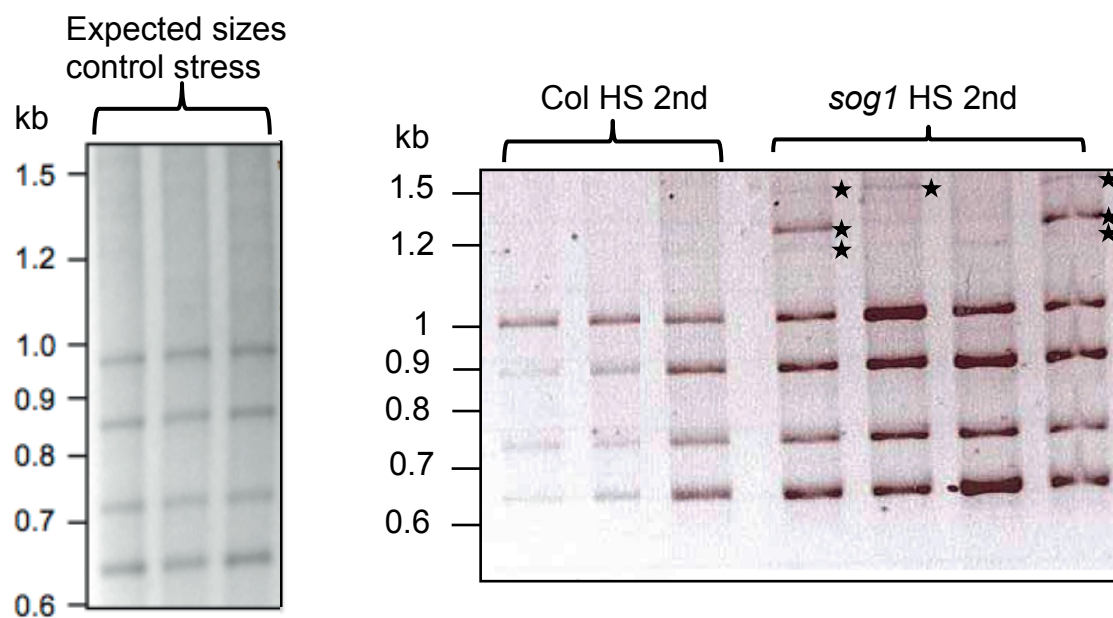
I tried to identify *de novo* retrotransposition events in the *atm* and *sog1* mutant background using the transposon display method (figure 5.6). This method uses a modified AFLP protocol. 10-day old Col, *atm* or *sog1* to heat stress and the negative control plants. The DNA was then digested with the restriction endonuclease *Dra*I and adaptors were ligated to the extremities of the fragment. A PCR was performed using a primer specific to the adapter and the other specific to the ORF of ONSEN. Running the PCR on an agarose gel or using the MultiNA nucleic acid analyser (Shimazu) enabled me to identify if *de novo* insertions had occurred between the known positions of ONSEN copies in the Col wild-type genome.

Using the restriction enzyme *Dra*I, 5 native copies of ONSEN can be detected of the following sizes: 950 bp, 837 bp, 707 bp, 638/634 bp and 429 bp (Mirouze, personal communication). The *sog1* background gave me the most promising results at first (figure 5.6 top panel), with the detection of new insertions not present into the wild-type, but because of the genetic background not being 100% Columbia (the mutant I obtained was originally a Col/L-er hybrid), I could not draw a definite conclusion, as the position of ONSEN copies in the L-er background is not published and was difficult to resolve in our conditions.

I therefore decided to focus on the *atm* background (*atm-2*) in the Columbia background. As a positive control, I included *nrpda1*, where *de novo* insertion is known to occur (Ito et al., 2011). The resolution of bands on an agarose gel proved to be difficult in our conditions, even for the positive control, therefore I decided to use the MultiNA nucleic acid analyser, where the PCR is loaded in a microchip electrophoresis system with specific size markers. To compare the result of the two experiments from the same ligation event, I used the agarose gel and the MultiNA technology on the

same set of 20 samples chosen randomly from plants subjected to the control stress and the heat stress in all genotypes. This suggested a lower level of retrotransposition than published for the *nrpd1a* background (1 clear insertion in one progeny and possible multiple insertions in 2 other progenies), and also some level of transposition in the *atm-2* background (out of 5 progenies, 1 plant with 1 insertion and 1 plant with 2 insertions). Due to the low number of plants with new insertions, however, these results are not statistically significant (Fisher's exact test p-value for *nrpd1a-1* = 0.2582 and *atm* = 0.4444). The fact that I did not identify as many neo-insertions in the *nrpd1a* mutant than published data could be explained by the fact that different alleles were used in both studies: I used the *nrpd1a-1* allele, which is linked to a large rearrangement on chromosome 1, whereas Ito and colleagues used the *nrpd1a-3* allele, which a t-DNA insertion line (Herr et al., 2005). More samples are needed to confirm this result. The new bands will also need to be cloned to identify where the insertions occurred.

A



B

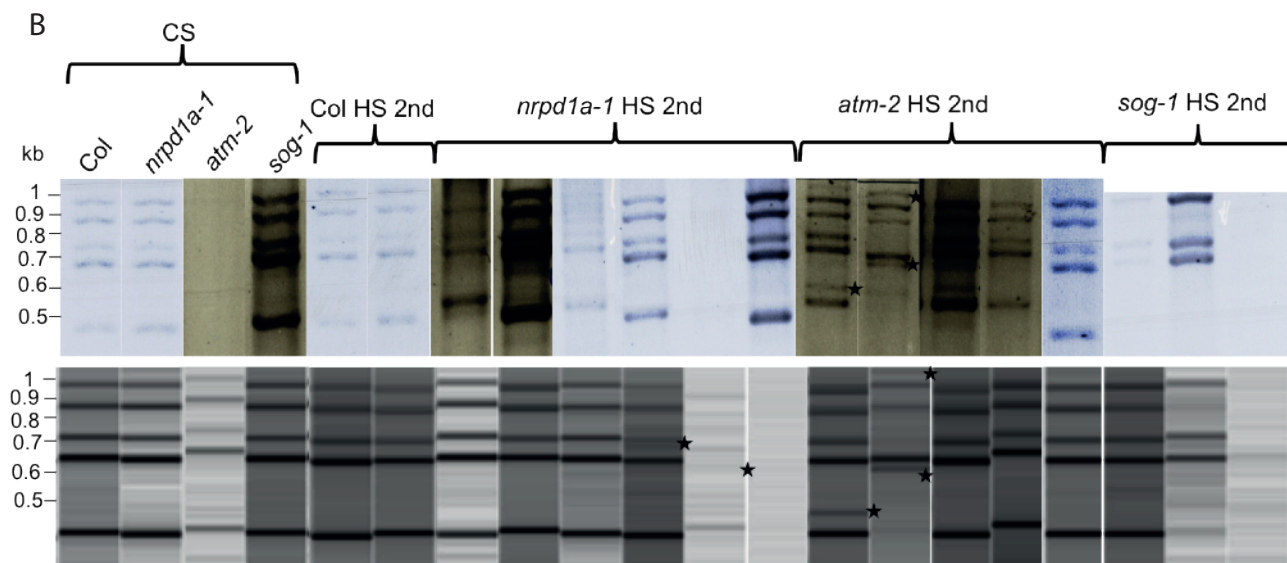


**Figure 5.6: Possible transgenerational movement of an inducible transposon in *atm-2* and *sog1* mutants.** (A) Transposon display detecting new ONSEN insertions. Col and *sog1*-1 HS 2nd (second generation) represent individual plants that are derived from bulk-harvested seeds of individual plant that were HS- treated as a 7-day-old seedling. (B) transposon display detecting new ONSEN insertions. Col, *nrpd1a-1* and *atm-2* HS 2nd (second generation) represent individual plants that are derived from bulk-harvested seeds of individual plant that were HS- treated as a 7-day-old seedling compared to a control stress (CS). The results are compared between those obtained from loading the transposon display products on an agarose gel (top panel) versus the MultiNA nucleic acid analysis system (bottom panel). Asterisks mark new ONSEN insertions.

#### 2.4.2 Detection of ONSEN expression by *in situ* hybridisation following heat-stress

To be relevant to stem cell responses to transposon activity, ONSEN would need to be expressed in the meristems. One important aspect of ONSEN biology that is still unknown, however, is its expression pattern in response to heat-stress. I therefore used *in situ* hybridisation to reveal the expression pattern of the ONSEN in the shoot meristem following heat stress.

Shoot apices in *atm*, *sog1* and Columbia were collected 24 hours following heat stress at 37°C, which was found to be when the expression of ONSEN is detectable via Northern blot (Ito et al., 2011) in four-week old plants. I used a histone H4 probe as a positive control and a GFP probe as a negative control. I could not find any visible expression in the shoot meristem following heat stress in either background tested with the ONSEN probe, whereas a strong H4 signal was found (figure 5.7) and no signal was found with the GFP probe (data not shown).

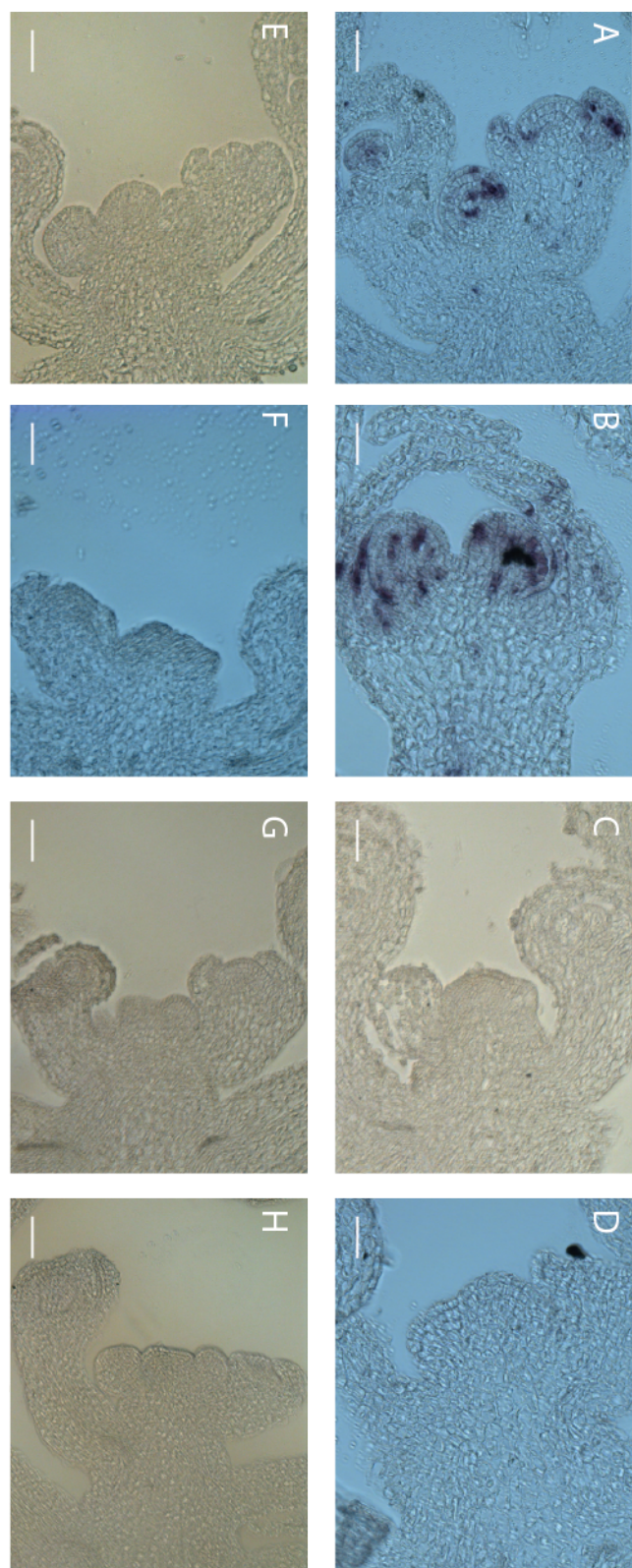


**Figure 5.7: Expression of ONSEN is not detectable 24 hours following Heat-Stress in the shoot meristem of *atm-2* and *sog1-1*.** (A-H) Representative (5 plants) *in situ* hybridisation images of meristem sections hybridised with (A-B) Histone H4 probe and (C-D) ONSEN ORF probe in (A) Col 24 hours after control stress (B) Col 24 hours after heat stress (C) Col 24 hours after control stress (D) Col 24 hours after heat stress (E) *atm-2* 24 hours after control stress (F) *atm-2* 24 hours after heat stress (G) *sog1-1* 24 hours after control stress (H) *sog1-1* 24 hours after heat stress. Scale bar = 30  $\mu$ m.

### 3. Discussion

The idea of an endogenous DNA damaging agent being responsible for the stem cell hypersensitivity to DNA damage is an attractive one, given that few exogenous agents were able to replicate the response to zeocin treatment in our conditions. In addition, both pools of stem cells responded in the same way to zeocin (with the exception of ATR not being involved in the shoot PCD), whereas the types of genotoxic stress experienced by the shoot and root meristems are likely to be different. So far, the zeocin response of the *sog1* mutant was not investigated in the shoot, and this should be performed in order to gain a more complete view of the master regulators of this pathway in stem cells.

I found that some mutants known for chromatin instability linked to hypersensitivity to DNA breaks and/or constitutive expression of DNA damage response genes also displayed spontaneous cell death in the root initials. One peculiarity of these mutants is that their chromatin instability leads to a significant release of transcriptional gene silencing. Therefore, I decided to look into the phenotype of gene silencing mutants. The study of mutants with more specific effects in gene silencing and fewer developmental defects, such as *met1*, *ddm-1*, *hda6* and *rdr2*, showed spontaneous cell death in the root meristem only in the *ddm1-2* mutant. This prompted the question of the similarities between the mutants showing spontaneous cell death compared to the mutants showing no spontaneous cell death. However, the similarities of *fas*, *bru*, *teb* and *ddm1* that would be distinct from the other mutants tested are not clear-cut enough to identify one particular factor or group of factors that would be responsible for the PCD phenotype. I will discuss these similarities and differences below.

A prominent feature shared by the mutants showing spontaneous cell death are developmental defects such as meristem enlargement and stem fasciation, although *ddm1* only shows morphological abnormalities as it accumulates secondary mutations after several generations of self-pollination (Finnegan et al., 1996). These developmental defects have been associated with changes in the expression of master regulators of meristem development, which could indirectly affect the meristem-specific responses to DNA damage, including PCD. A notable exception, however, was the *mom1* mutant, which showed similar meristem defects but did not show any spontaneous PCD. Its interaction with HDA6 means that we should look into the root meristem phenotype of the *mom1hda6* double mutant.

Interestingly, it was shown that inefficient DSB repair previously identified in the *BRCA2* gene was linked to increased fasciation phenotypes, with a greater increase of the fasciation phenotype when the mutant was treated with  $\gamma$  radiation. Fasciation was also induced by  $\gamma$  irradiation in wild-type plants. The shoot meristem of the mutant or wild-type treated plants was shown to display altered cell cycle progression, as it is the case in the *bru fas* and *teb* mutants, suggesting that inefficient DSB repair mechanisms leads to disorganization of the cell cycle of apical meristems (Abe et al., 2009). To further test the idea that meristem defects can be a consequence of DNA damage, the mutants studied in this chapter should be tested for spontaneous cell death in the shoot meristem. My first round of experiments, however, did not enable me to look into shoot meristem phenotypes, as the plants are so fragile that dissection leads to considerable user-induced cell death.

Chromatin defects might affect DNA repair and recombination, both of which could lead to DNA damage. Accordingly, the *fas*, *bru* and *teb* mutants are sensitive to DNA damaging agents such as MMS. In this respect, *ddm1-2* is the exception (Elmayan et al., 2005), but a recent study showed that *ddm1*

mutants accumulate more DNA damage in response to UV-B, showing an hypersensitivity to DNA damage of *ddm1* that was not previously described (Qüesta et al., 2013). Thus increased sensitivity to DNA damage might explain the spontaneous cell death phenotype specifically in the stem cells, although this does not hint at the upstream factor(s) explaining these phenotypes.

Also, considering the over-expression of cyclinB1;1 in the meristem of these mutants, the spontaneous cell death could be the result of cells failing to go through G2/M checkpoints, showing that the DNA damage response could activate the checkpoint, potentially promoting entry into the endocycle. It was notably shown that cells arrested by DNA damage with zeocin show an early onset of endoreduplication in undifferentiated cell suspensions, sepal cells and in the root meristem (Adachi et al., 2011). It was also reported that the a SUMO E3 ligase HIGH PLOIDY2 acts as a repressor of endocycle onset in *Arabidopsis* meristems, and the *hpy2* mutant shows severe developmental defects including fasciation (Ishida et al., 2009). This would explain the compensation phenotype observed in those mutants, where a decrease in cell number is observed, leading to bigger cells, notably in the root meristem in the *fas1* mutant (Hisanaga et al., 2013).

Finally, an attractive similarity between the set of genetically unstable mutants and *ddm1* is that all of these mutants are known to reactivate transposable elements, even if this feature is shared with other mutants showing no spontaneous cell death. The epigenetic control of transposon movement includes heavy methylation of the body of the transposable element, whereas histones are hypoacetylated and methylated on specific residues (Xu et al., 2013). Loss of methylation throughout the genome releases transposon silencing in the *ddm1* mutant (Hirochika et al., 2000), whereas changes in histone H3 acetylation (Guyomarc'h et al., 2006) could explain the release of transposon silencing in the *brushy* mutant. The

observation that mutants that affect transposon silencing through different mechanisms showed comparable cell death phenotypes in the root meristem prompted me to consider transposon movement as a possible endogenous DNA damaging agent against which plant stem cells would need to be protected.

Consistent with the idea that transposons could be an endogenous cause of DNA damage, transposon movement has been shown to induce DNA breaks that need to be repaired *via* the NHEJ pathway. This was shown in *Arabidopsis* for the class II transposable elements, which function by a “cut and paste” mechanism (Huefner et al., 2011), and also with during excision and reinsertion of the sleeping beauty transposon in mammalian cells (Yant and Kay, 2003) (Izsvák et al., 2004). It was also shown that reinsertion of the human LINE-1 retrotransposon into the genome leads to DNA damage and apoptosis in cancer cells (Belgnaoui et al., 2006) (Gasior et al., 2006). The insertion of retroviral DNA in the host genome was also shown to require a DNA repair mechanism (Skalka and Katz, 2005).

This hypothesis that transposon movement is one of the *in vivo* DNA damaging agent against which stem cells should be protected is further supported by the possible ATM dependence of the retrotransposon ONSEN movement. This should be confirmed to support a link between transposon movement and DNA damage responses in the meristem. One particularly relevant aspect of this question is the expression pattern of ONSEN. We were not able to detect ONSEN expression in the SAM after 24 hours of heat stress, and this could be due to a narrower spatiotemporal window of expression following the stress, as it is for instance the case of the *Evadé* retrotransposon. Indeed, in another inducible system using epiRIL lines in order to reconstruct *de novo* silencing of the active retrotransposon *Evadé*, it was found that *Evadé* transcripts were detectable in the L2 layer of young gynoecia, showing a tight spatiotemporal window for transmitting new

insertions to progenies (Marí-Ordóñez et al., 2013). However, the transposition events identified for ONSEN showed that within the same flowers the transposition patterns are the same. Moreover, it was not possible to find new and unique ONSEN insertions specific to a single plant, showing that transposition events must occur before the differentiation of male and female gametophytes (Ito et al., 2011). This shows that more targeted experiments to identify the location of ONSEN expression during stress are required.

As a conclusion, the *in vivo* DNA damaging agent responsible for plant stem cells hypersensitivity to DNA damage could be breaks caused by changes in chromatin stability, leading for instance to more transposon movement and/or homologous recombination, that should be avoided in the context of stem cells and the germline in particular. However, more experiments are required to link this phenomenon to prevention of cell death or gene silencing. For instance, if a DNA transposon could be part of an inducible system in stem cells it would be possible to look for hallmarks of DNA damage and/or silencing at the site of excision, such as the presence of  $\gamma$ -H2AX or stalling of RNAPolII (Shanbhag et al., 2010), and look for their dependence on *ATM* or *SOG1*.

## Chapter 6 General Discussion

### 1. Summary of results

The aim of this study was to pursue further the discovery that plant stem cells are hypersensitive to DNA damage (Fulcher and Sablowski, 2009; Furukawa et al., 2010). This project had two main objectives; first to identify new components of the ATM/SOG1 pathway leading to PCD in response to DNA damage in stem cells, and secondly to shed light on some of the *in vivo* DNA damaging agents that are relevant to this mechanism in plants.

Using a candidate gene approach (chapter 2) and a forward genetics screen (chapter 3) in the root stem cells, I was not able to identify new components of the PCD pathway leading to PCD. The candidate gene approach was focused on the downstream events following ATM and SOG1 activation and leading to PCD by studying responses to DSBs in specific PCD and stem cell function mutant. On the other hand, the forward genetics screen looked for mutants failing to induce PCD in response to DNA damage from a WT mutagenized population. Therefore, this approach could have yielded mutants involved in PCD itself, but also in the upstream events such as DNA damage signalling. Out of the mutants identified, only one showed a complete absence of PCD in response to DSB induction, and it was identified as a new *sog1* allele. Because only one new *sog1* allele was isolated, the screen may not have been saturating. However, as all other identified mutants only showed a reduction of PCD in response to DSBs, it seems that the factors downstream of ATM/SOG1 in PCD present significant levels of redundancy. Alternatively, mutations in genes with clear-cut effects on stem cell PCD (other than *SOG1*) might be lethal. This would further highlight the central importance of the mechanisms involved in the response of stem cells to genotoxicity.

A more targeted approach might make it possible to identify new mutants, specifically in a suppressor screen, for instance in the *sog1* mutant background, looking for mutants restoring the ability to display PCD in response to DSBs. Indeed, SOG1 was described as a major regulator of DNA damage responses in plants, and could receive signals and activate more targets than ATM or ATR, making it an ideal candidate for this type of screen.

The second major question that I sought to answer was the *in vivo* DNA damaging agent(s) that may have led to the evolution of this protective mechanism. It seems plausible that plants specifically evolved this mechanism in order to prevent their stem cell populations from accumulating deleterious mutations, but in practice it is difficult to establish what was the evolutionary driver for this mechanism. I pursued the hypothesis that internal DNA damaging agents would be responsible for this hypersensitivity for several reasons (chapter 5). First, it was found that both stem niches in *Arabidopsis* respond to DNA damage *via* activating an ATM-dependent cell death programme; however it is unlikely that both stem cell populations would be subjected to the same sources of DNA damaging environmental stresses. Then, it is known that regular cellular processes cause daily DNA damage that must be dealt with in a timely manner in the crucial stem cell pools (Wyllie et al., 2000).

One process that is likely to affect endogenous DNA damage is chromatin regulation. The importance of chromatin state in DNA repair mechanisms is becoming more and more clear in both plants and animals (Tran et al., 2005; Dinant et al., 2008; O'Hagan, 2013). Indeed, it was found that a more relaxed chromatin state is required for timely access to DNA repair proteins to the site of damage (O'Hagan, 2013). This means that chromatin remodelling processes participate in the crucial first steps of the DRR, but it also means that differential basal chromatin states would make certain cells more

responsive to DNA breaks. In particular, it was found that ESCs have a more relaxed chromatin state, possibly more accessible to mechanisms that protect against genomic instability, while differentiated cells show a more compact chromatin (Zhu, 2009). Interestingly, it was shown that plant stem cells might have a more compact chromatin, whereas their daughter cells would have a more relaxed chromatin (Stefanie Rosa, personal communication), which also correlates with the higher sensitivity to DNA damage in the immediate descendants of stem cells. It will be interesting to follow this field of study showing a link between chromatin state in stem cells and their suicidal tendencies linked to their importance in organism survival in both plants and animals (Zhu, 2009).

However, another aspect of chromatin relaxation that could be linked to DNA damage and the response to environmental or endogenous stresses is that a more relaxed chromatin would be more susceptible to DNA breaks themselves (Wyllie et al., 2000). Notably, it was shown that the histone variant H2AZ is required for plants to perceive ambient temperature. The presence of this histone variant confers nucleosomes with DNA-unwrapping properties, which is linked to transcriptome differences showing that plants can perceive differences in temperature as little as 1°C (Kumar and Wigge, 2010). As we could not identify mutants of the PCD pathway in response to DNA damage *via* reverse of forward genetics, we tested DSB responses in the root stem cells of several *Arabidopsis* ecotypes, and found that the Lov-1 ecotype from North Sweden shows a complete absence of PCD in response to DSBs (chapter 3). As this ecotype lives in a very cold environment, it is possible that it has evolved differences in temperature-dependent chromatin dynamics, which in turn might affect either susceptibility or responses to DNA damage.

While developing a system to induce localized DNA breaks into the genome using the Cre-induced recombination system, I uncovered that the

recombination event leads to ATM/SOG1-dependent silencing of the transgene. Moreover, this silencing was linked to TGS *via* the production of 24-nt siRNAs, and required PolIV and AGO6, linking the RdDM pathway to DNA damage sensors specifically in meristems. This discovery is significant in the light of the discovery of an ATM dependent mechanism in *cis* in response to DSBs (Shanbhag et al., 2010), and also the discovery of so-called diRNAs in both plants and animals, that seem to be required for efficient DNA repair mechanisms (Lee et al., 2009a; Wei et al., 2012).

One the most important questions linked to the discovery of these specific siRNAs is the elucidation of their mechanism of action at the site of DNA damage. For instance, they could interact with the DRR factors or modulate their function, either directly or through chromatin modification events. Also, each new damaged locus of the genome would generate a different set of siRNAs with a different sequence, as sequence complementarity is required. Thus, if protein-RNA interaction occurs it cannot depend on the RNA sequence. Also their linear structure would not bear enough information for protein interaction specificity to occur (Fagagna, 2013). This will be one of the most relevant questions to be answered concerning this new pathway.

In chapter 5, I also showed that silencing mutants showing an unstable chromatin state displayed a spontaneous cell death phenotype when grown under standard conditions. I hypothesised that transposon movement, a known consequence of this unstable chromatin state, could be sensed as DNA breaks by the plant leading to PCD specifically in plant stem cells, and studied the hypothesis that the DDR pathway could be involved in transposon silencing. Relevant to this hypothesis, the tight control of transposon movement is crucial in both animals and plants, and piRNAs were identified as linking specifically to transposon silencing in animal germ cells (Castañeda et al., 2011).

However, at least some transposition events must occur as transposon movement is known to be as a driver of genome evolution. Indeed, on top of stress induced transposon reactivation (Wang et al., 2013), transposons can be reactivated in reproducible and cell specific manner, suggesting an important role in plant development. A number of mechanisms have now been described by which transposons can alter the expression of genes that they either neighbour, or share partial complementary with *via* small RNAs (McCue and Slotkin, 2012). For instance, in *Arabidopsis*, when some *Athila* retrotransposons are reactivated, *Athila*-derived siRNAs directly target the 3'UTR of the mRNA for oligouridylate binding protein 1B (UBP1b) (McCue and Slotkin, 2012), affecting its function post-transcriptionally. It was also shown in maize that transposon activation in the SAM is linked to the transition between the juvenile and adult reproductive state (Martínez and Slotkin, 2012).

Unfortunately, I cannot conclude on the links between the PCD pathway and the silencing pathway identified in this project. An attractive hypothesis is that silencing could be used in the first instance, during low-level and targeted DNA breaks, whereas PCD would occur once a DNA damage threshold is overcome.

## 2. Perspectives and future work

In this thesis, I described several future experiments following from the work presented, such as the mapping of the mutation leading to a loss of PCD in response to DSBs in the *Lov-1* ecotype, the requirement to identify hallmarks of DNA damage at the site of the Cre-induced recombination event and the need to confirm ATM-dependent silencing of *ONSEN*, preventing transgenerational transposon movement.

For ease of imaging, I looked for mutant responses to DNA damage in the root stem cell only, where it is known that the ATM/ATR/SOG1 pathway is activated in response to DSB, promoting cell death. However, ATR was shown not to be required in the shoot meristem and it is still unknown whether SOG1 is required as well. Given that the SAM originates the germline, imaging experiments should be conducted in the SAM of the mutants described throughout the thesis, especially mutants presenting an unstable chromatin (chapter 5). Initial experiments have failed to image those mutants properly, as their pleiotropic phenotype leads to a very disorganized meristem making dissection difficult.

The hypothesis of a link between silencing pathways and DDR factors, specifically in the context of transposons, should also be explored further. Three experiments could be performed. First, the siRNA repertoire of the *atm* or *sog1* mutants could be explored by RNA-seq, and compared to a WT repertoire (Zhong et al., 2013). This would enable the identification of transposon-derived siRNAs and potentially an overall decrease of transposon-derived siRNAs, or a differential accumulation of those siRNAs in the mutants, showing that silencing mechanisms are perturbed when the DRR is disabled.

Then, the epiRILS described in chapter 5 could be used to check for EVADE (EVD) transposon movement in the *atm* and *sog1* background (Mirouze et al., 2009; Marí-Ordóñez et al., 2013). These lines were created by crossing a wild type plant to a *met-1* mutant. After selection for MET1 in the F2, the lines were selfed for many generations. Some of these lines then showed active or immobile retrotransposons, showing that *met-1* or WT epialleles had been inherited through the cross. Notably, *met-1* plants show a loss of DNA methylation near the transcriptional start in the LTR of EVD, and this was also observed in one of the line called epi12. On the other hand, in another line called epi07, DNA methylation was retained and there was no sign of EVD activity. These lines would be interesting candidates to be

crossed to the *atm* and *sog1* mutants and look for possible reactivation of EVD activity in the epi07 cross.

A transgenic approach could be taken to check if the meristem is indeed purified of transposon activity under the control of ATM or SOG1. The construct would be built with a retrotransposon fused to a reporter gene such as GFP, with an intron in the reverse orientation inside the reporter gene. If the transposon were transcriptionally activated, as expected in the *ddm1* background for instance, the intron would be lost and neo-insertions of the retrotransposon in the genome would lead to a mosaic expression of the reporter. As *de novo* silencing of those transposons would be expected, after a few generations the expression of the reporter gene would be lost. This would not be the case in the *ddm1* mutant, where transposons could not be re-methylated, and leading to a widespread expression of the reporter gene. Also, if *atm* and *sog1* were required for an efficient re-silencing of a transposon, then in a mutant background for those genes, the expression of the reporter would not be lost, showing the requirement of a functional DDR response for a purification of meristems of transposons.

## Material and Methods

### 1. Materials

#### 1.1 Plant lines

The plant lines used throughout this project are described below.

##### 1.1.1 Mutant lines

Mutant	ecotype	ID	reference
<i>parp1</i>	Columbia	GABI_382F01	n/a
<i>parp2</i>	Columbia	SALK_140392	n/a
<i>vad1</i>	Columbia	SAIL_564_e12	(Lorrain et al., 2004)
<i>atm-2</i>	Columbia	SALK_006953	(Garcia et al., 2003)
<i>rdr6-16</i>	Landsberg	n/a	M Byrne
<i>bru1-2</i>	Columbia	n/a	(Takeda et al., 2004)
<i>sog1-1</i>	Columbia	n/a	(Preuss and Britt, 2003)
<i>ddm1-2</i>	Landsberg	n/a	(Jeddeloh et al., 1999)
<i>ago4-1</i>	Landsberg	n/a	(Zilberman et al., 2003)
<i>nRPD1a-1</i>	Columbia	n/a	(Herr et al., 2005)
<i>lig4-4</i>	Columbia	SALK_095962	n/a
<i>ku80</i>	WS-2	n/a	(West et al., 2002)
<i>ago6</i>	Columbia	SALK_031553.55.00.x	n/a
<i>parg1-1</i>	Columbia	SALK_147805	n/a
<i>atnudx7</i>	Columbia	SALK_0464410	n/a

### 1.1.2 Transgenic lines

Line	Reference
pXCP2:GUS	(Funk et al., 2002)
GFPmosaic	(Gallois et al., 2002)
CYCB1;1:GFP	(Colón-Carmona et al., 1999)

### 1.2 Oligonucleotides

The oligonucleotides used throughout this project are described below.

#### 1.2.1 Genotyping oligonucleotides

Mutant	5'-3' primer
<i>parp1</i>	Forward GAAGGCATGAAATCACTCCGTCG Reverse TTAGTGCTTAGTTGTTGAATTG
<i>parp2</i>	Forward GGCCCAACTGGGACAGAGACAG Reverse CACTTCATCCTCCTGCCACAC
<i>rdr6-16</i>	Forward CGACCAGTTTGATGCGTA Reverse CCGCAAAAATCTTTCAGCA Cuts with EcoRI in mutant not in WT
<i>bru1-2</i>	Forward GATTGTGAAGCCATTCAAGAGTG Reverse CTTCATCGCAAATCTGGGGCC Cuts with ApaI in WT but not in mutant
<i>sog1-1</i>	Forward GATGTGCGCTGGCATAAGACC Reverse CCTCGCTTGACTACTAGCTG Cuts with BssSI in mutant but not in WT
<i>ddm1-2</i>	Forward GTTGGACAGTGTGGTAAATTCCGCT Reverse GAGCTACGAGCCATGGGTTGTGAAACGTA Cuts with RsaI in WT but not in mutant
<i>ago4-1</i>	Forward GACTGACAGCTGAAATGGGATGTGGAT Reverse GCCACTCCCTAGAACTCACCACCTAAGT Cuts with Avall in mutant but not in WT
<i>nRPd1a-1</i>	Forward TGGAATAGATGCTGGACGCAGCA Reverse TGTTACATACTGAGAACATGCT tDNA primer CCTCCAATTTGAAGAGAGG
<i>lig4-4</i>	Forward GTGATTGAAACTAGTCTGTG Reverse CAGCAAACCGATTTCAGAGATG lBb1.3 primer for tDNA (Alonso et al., 2003)

<i>ku80</i>	Forward CTCCAAGACGCAGCCTTACGAAG Reverse CAAGGGCTTCGCTATGGACCTCAG tDNA primer GATTCTTTATGCATAGATGCAC
<i>ago6</i>	Forward GTCTGGAAACCAAAGAGAC Reverse ACCGGAAGAACTACCACCATC lBb1.3 primer for tDNA (Alonso et al., 2003)

### 1.2.2 Other oligonucleotides

Function	Sequence	Reference
Adaptor 1 for ligation to digested DNA in transposon display	ACCAGCCC (AMINO 3')	(Ito et al., 2011)
Adapter 2 for ligation to digested DNA in transposon display	GTAATACGACTCACTATAGGGCACCGT GGTCGACGGCCGGCTGGT	(Ito et al., 2011)
Forward primer for transposon display PCR	GTAATACGACTCACTATAGGGC	(Ito et al., 2011)
Reverse primer for transposon display PCR	GCCTCCAAACTACAAAATATCTAAA	(Ito et al., 2011)
Scel primer set for RT-PCR	Forward GAACCTGGTCCGAACTCTA Reverse GGATCAGACCGATACTGCT	
GFP primer set for RT-PCR	Forward CAGTGGAGAGGGTGAAGGTG Reverse AAAGGGCAGATTGTGTGGAC	
Tubulin primer set for RT-PCR	Forward TGGGAACTCTGCTCATATCT Reverse GAAAGGAATGAGGTTCACTG	
<i>PARP1</i> primer set for RT-PCR	Forward ATGCTACTCTGGCACGGTTCAC Reverse AGGAGGAGCTATTCGCAGACCTTG	
<i>PARP2</i> primer set for RT-PCR	Forward ATGCTACTCTGGCACGGTTCAC Reverse AGGAGGAGCTATTCGCAGACCTTG	
<i>NRT2;1</i> primer set for ChIP q-PCR	Forward ATCGTCTACGATACAGCCCAGGTG Reverse TGGTTCAGGCTCATCTCTGTGC	(Arnaud et al., 2010)
GFP primer set for ChIP q-PCR	Forward AACAAAGGGCTAACGTGGATG Reverse CTGCTTCTCCTGCTCATTCC	
GUS primer set for ChIP q-PCR	Forward CAATGCTTTCAAGATAACCC Reverse AAATCGATTCCCTTAAGCTC	

35s primer set for ChIP q-PCR	Forward CTGATAGCGCGTGACAAAAA Reverse GGCACAGCACATCAAAGAGA	
GFP forward primer for multiplex PCR	ATTGTGCGTCATCCCTTACGT	
GFP reverse for multiplex PCR	CAGTGGAGAGGGTGAAGGTG	
35s forward primer for multiplex PCR	AAAGGGCAGATTGTGTGGAC	
ta-siRNA255 oligo for end-labelling for Northern blotting	GAGGAGCATCGTGGAAAAAG	(Xie et al., 2005)

### 1.3 Plasmids

The plasmids used were pGEM-T easy (Promega), pBluescript KS (-) (Agilent) and the binary vector pCGN18 (Krizek and Meyerowitz, 1996).

### 1.4 Other material

We are grateful to Holger Puchta for providing us with the cDNA for the I-SceI enzyme, Mary Byrne for *rdr6-16* seeds, Anne Britt for *sog1-1* seeds and Yoselin Benitez-Alfonso for the PdBG mutant and overexpressor line.

## 2. Methods

### 2.1 Propagation and manipulation of plants

#### 2.1.1 Seed sterilization

##### 2.1.1.1 Gas seed sterilization

Seeds were routinely surface sterilised in 1.5 mL eppendorf tubes using chlorine gas by mixing 100 mL of sodium hypochlorite (99%) with 3 mL of 12 N hydrochloric acid under a glass bell for 4 hours. The gas was then

allowed to evaporate for a few seconds prior to closing the tubes and immediately sowing the seeds on plates.

### 2.1.1.2 Liquid sterilisation

When a more thorough method of seed sterilisation was required, a liquid method was used by agitating the seeds for 20 min in 50 % (v/v) of absolute ethanol and 12.5 % of 200 mM dichlorisocyanic acid (v/v) in water. Seeds were rinsed three times in absolute ethanol and air-dried prior to sowing. For screening of M2 families, seeds placed in 24 well plates were surface sterilised for 1 hour in 100% ethanol then air-dried prior to treatments.

## 2.1.2 Growth conditions

### 2.1.2.1 *In vitro* culture

For most applications seeds were sown directly onto germination medium (GM, Murashige and Skoog salts (Sigma), 1% glucose, 0.5 g/mL 4-morpholineethanesulfonic acid (Sigma), 0.8% agar, pH 5.7) and stratified for 48 hours at 4°C in the dark. Plates were transferred to growth chambers at 21°C with 16 hours light or continuous light at 24°C vertically for root meristem imaging.

For screening M2 families seeds were grown in liquid medium (same as GM medium without sucrose and agar) in continuous light at 24°C under constant agitation.

### 2.1.2.2 Controlled Environment Room (CER) culture

For plants grown to maturity seedlings from *in vitro* culture were pricked out to soil (John Innes Compost number 2 with 4 mm grit, supplemented with the fertilizer Osmocote (Scotts) and the insecticide Exemptor (Everris)

15 days post germination. Plants were grown under 16 hours fluor light at 21°C and 70% humidity.

### 2.1.3 Crosses

Crosses were performed by dissecting secondary inflorescences with fine forceps. Mature flowers were emasculated 2 days prior to pollination of the carpel with pollen from mature flowers.

### 2.1.4 Heat Shock

Heat-shock treatment of the GFPmosaic line were performed by floating seedling plates 10 days post-germination in a 38°C water bath for 20 min. Heat-Shock of inflorescences was performed by placing mature plant inflorescences in 1.5 mL tubes with 500 µL of liquid germination media and floating then in a 38°C water bath for 20 min.

### 2.1.5 Heat stress for transposon movement

For induction of the ONSEN retrotransposon movement, 10 day-old seedlings grown on GM media at 21°C in long days were placed at 4 °C for 24 hours then at 37°C for 24 hours (heat stress), or at 21°C (control stress). Finally, all plates were placed back at 21°C until transfer onto soil until maturity and seeds collected for transposon display experiment (Ito et al., 2011).

Alternatively, when heat stress was performed on mature plants, 4 week-old plants grown in the CER were placed at 4°C for 24 hours, then either 37°C (heat stress) or back to the CER. Finally, all plants were transferred back to the CER and seeds collected for transposon display experiments.

### 2.1.6 DNA damaging treatments

For root meristem imaging, seedlings grown vertically for 3 days were transferred to  $\frac{1}{2}$  MS (2.2g/L Murashige and Skoog Salts from Sigma, agar 0.7% w/v, pH 5.9) plates supplemented with zeocin (Sigma) to the required concentration in order to observe reliable PCD in Col or *L-er* seedlings. For each new zeocin stock the concentration had to be adjusted. In the three stocks used in this project, three different concentrations were used: 8, 20 and 35  $\mu$ g/mL zeocin. The plates were then placed vertically in the dark for 24 hours prior to imaging (Fulcher and Sablowski, 2009).

For screening of M2 families, seedlings grown in liquid media for 3 days were supplemented with 35  $\mu$ g/mL of zeocin and incubated in the dark for 24 hours.

### 2.1.7 GUS staining

For GUS staining of *Arabidopsis* seedlings and organs, the tissues were collected in ice-cold 90% acetone in water (v/v) and incubated for 20 min to fix the tissues. The samples were then incubated in 50 mM sodium phosphate buffer (pH 7.2) containing 0.5 mM K-ferrocyanide (Sigma, P-8131) and 0.5mM K-ferricyanide (Sigma, P-9387) Samples were then incubated for 12h at 37°C in the same buffer containing 2 mM 5-bromo-4-chloro-3-indolyl p-D-glucuronide (Melford, MB1121) (Arnaud et al., 2010).

## 2.2 Manipulation of nucleic acids

### 2.1.1 Isolation of plant genomic DNA

#### 2.2.1.1 Rapid extraction in 96 well plates for genotyping

When the expected PCR fragment for genotyping did not exceed 500 bp in size, this rapid method was used. Small cauline leaves or inflorescences were collected in 96-well plates and lysis was performed by heating the samples at 96°C in the presence of 50  $\mu$ L of 0.25 M NaOH. The DNA was

extracted by adding 50  $\mu$ L of extraction buffer (0.5 M Tris-HCl pH8 and 0.25% NP-40) and 50  $\mu$ L 0.25M HCl and mixing by pipetting. The plate was finally incubated at 96°C for 3 min. Two microliters of extract were used in a 20 $\mu$ L PCR reaction.

#### 2.2.1.2 Clean genomic DNA extraction

For any other application than PCR genotyping with PCR fragments < 500 bp (see 2.2.1.3), this method was used. Small cauline leaves or inflorescences of *Arabidopsis* were collected and frozen immediately in liquid nitrogen and kept at -70°C until extraction. The plant tissues were ground with plastic pestles in 150  $\mu$ L of Rapid Extraction Buffer (50 mM Tris-HCl pH8, 25 mM EDTA, 250 mM NaCl, 0.5% SDS). The DNA was separated from other cellular debris by adding 150  $\mu$ L of phenol:chloroform:IAA (25:24:1 v/v/v) to the sample. The upper phase was collected after centrifugation for 10 min at 10,000 g. To remove traces of phenol, 150  $\mu$ L of chloroform:IAA (24:1 v/v) was added to the sample and the upper phase was collected after a centrifugation step of 5 min at 10,000 g. The DNA was precipitated by incubation at -20°C for 30 min in the presence of 150  $\mu$ L of isopropanol. The DNA was pelleted by centrifugation for 20 min at 10,000 g and the pellet washed with 70% ethanol. After air drying the pellet was resuspended in 30-50  $\mu$ L water depending on the quality of start material. If required, the DNA concentration was estimated using the ratio of absorbance at 260 nm and 280 nm measured with a Nanodrop © (Thermo Scientific).

#### 2.2.2 Isolation of small volumes of plant total RNA

Plant tissue was collected in 2 mL eppendorf tubes with 2 tungsten beads and frozen in liquid nitrogen. Tubes were placed on cooled metal racks in a Genogrinder© and samples were shaken at 1,300 rpm for 35 sec. The powder was homogenized in 500  $\mu$ L of TRI reagent (Sigma-Aldrich) and the samples were incubated for 10 min at room temperature. The DNA/RNA

mix was separated from other cellular debris by adding 200  $\mu$ L of chloroform/IAA (24:1 v/v) to the sample and incubating for 3 min at room temperature. The upper phase was collected by centrifugation for 15 min at 10,000g and 4°C. The DNA/RNA mix was precipitated by adding 600  $\mu$ L of absolute ethanol and 20  $\mu$ L of 3M sodium acetate pH 5.2 and incubating for 30 min at -70°C. The DNA/RNA mix was pelleted by centrifugation for 20 min at 10,000g and 4°C. After washing the pellet with ethanol 70% and air-drying, the DNA/RNA mix was resuspended in 20-50  $\mu$ L water. The RNA concentration was estimated using the ratio of absorbance at 260 nm and 280 nm measured with a Nanodrop © (Thermo Scientific).

### 2.2.3 Modified TRI protocol for small RNA Northern blotting

In order to isolate RNA for small RNA fraction enrichment, a larger scale modified version of the protocol presented in 2.2.2 was used. Whole seedlings grown on plates treated as presented in 2.1.5 were collected in 50 mL tubes and frozen in liquid nitrogen. After grinding of the samples in liquid nitrogen with a pestle and mortar, homogenization was performed with 3 volumes of TRI reagent (Sigma) per g of sample. After incubation for 10 min at room temperature, an equal volume of chloroform:IAA (24/1 v/v) was added to the samples. The upper phase was collected after centrifugation for 15 min at 4,000g and 4°C. Two volumes of chloroform:IAA were added to the samples and the same centrifugation step was performed. Three volumes of absolute ethanol were added to the upper phase with 1/10 volume of 3 M sodium acetate pH 5.2. After an overnight incubation at -70°C, the pellet was collected by centrifugation of the samples at 4,000g and 4 °C for 30 min. The pellet was washed with ethanol 70 % and after air-drying on ice the RNA was resuspended in 400  $\mu$ L water and kept at -70°C until enrichment as described in 2.2.4. The RNA concentration was estimated using the ratio of absorbance at 260 nm and 280 nm measured with a Nanodrop © (Thermo Scientific).

#### 2.2.4 Enrichment for the small RNA fraction of plant RNA

The samples prepared as described in 2.2.3 were processed further for enrichment of the small RNA fraction. The *mirVana™* miRNA Isolation Kit (Ambion) was used following the manufacturer's instructions. Briefly, 100 µg of total RNA were homogenised with the Binding Buffer and the miRNA homogenate additive from the kit. After addition of 1/3 V of absolute ethanol to the RNA mixture, the RNA mixture was passed through the filter cartridge and the filtrate was collected. The RNA fraction depleted from small RNAs was recovered by applying 100 µL of 95°C elution solution to the cartridge and spinning for 1 min at 10,000 g. The filtrate was mixed with 2/3 volume of absolute ethanol and passed through a new cartridge. The filter was then washed once with 700 µL of the miRNA Wash Solution 1 and twice with 500 µL of Wash Solution 2/3. The small RNA fraction was recovered by applying two aliquots of 50 µL of 95°C elution solution to the filter and spinning for 1 min at 10,000g. The RNA concentration was estimated using the ratio of absorbance at 260 nm and 280 nm measured with a Nanodrop © (Thermo Scientific).

#### 2.2.5 Cloning procedures

##### 2.2.5.1 Restriction enzyme digestion

Restriction enzyme digestion of plasmid or purified PCR products was performed at the temperature and buffer recommended by the manufacturers for 1 to 4 hours in a final volume of 20 µL and using 1 to 5 U of restriction enzymes. The enzymatic reaction was purified following the method described in 2.2.6.4.

##### 2.2.5.2 Dephosphorylation

Dephosphorylation of linearized plasmids was performed using 1 U of SAP (Shrimp Alkaline Phosphatase, Roche) in the buffer provided by the manufacturer at 37°C for 2 hours. The enzymatic reaction was purified following the method described in 2.2.6.4.

### 2.2.5.3 Ligation

Blunt end ligations or sticky ends ligations were performed using 1 U of T4 DNA ligase (Roche) in the buffer provided by the manufacturer overnight at 16°C. Ligation reactions were purified following the method described in 2.2.6.4.

### 2.2.5.4 Purification of nucleic acids following enzymatic reactions

Phenol:chloroform was used to purify nucleic acids from enzymatic reactions, for instance after a restriction enzyme digest or a ligation reaction. The volume of the solution was brought up to 100 µL with sterile water, and 100 µL of phenol:chloroform:IAA (25:24:1, v/v/v) was added to the reaction. After centrifugation at 10,000 g for 5 min, the upper phase containing the nucleic acids devoid of proteins was collected and mixed with an equal volume of chloroform:IAA (24:1, v/v) and a new centrifugation was performed to remove remaining traces of phenol. The nucleic acids contained in the upper phase was then precipitated by adding 3 volumes of absolute ethanol, 1/10 volume of 3M sodium acetate pH 5.2 and 1 µL of glycogen to act as a carrier. The solution was incubated at -20°C for 30 min and the nucleic acids were pelleted by centrifugation for 20 min at 10,000g. The pellet was washed in 70% ethanol and air-dried prior to resuspending in 10-20 µL of sterile water depending on the downstream experiments.

### 2.2.5.5 Transformation of electrocompetent bacteria

Forty µL of electrocompetent DH5 $\alpha$  *E.coli* cells (Genotype F-  $\Phi$ 80lacZ $\Delta$ M15  $\Delta$  (*lacZYA-argF*) U169 *recA1 endA1 hsdR17* (rK-, mK+) *phoA supE44*  $\lambda$ - *thi-1 gyrA96 relA1*) were placed in a prechilled electroporation cuvette and up to 10 µL of DNA solution were added. Cells were electroporated using the Biorad Gene pulser for 2.5 ms at 200  $\Omega$  and 250 µFD and immediately

resuspended in 900  $\mu$ L of SOC medium (LB (Lysozym Broth) supplemented with 8% glucose, 20 mM MgCl<sub>2</sub>, 20 mM MgSO<sub>4</sub>). The cells were left to recover for 45 min at 37°C under agitation then plated out on LB medium containing the appropriate antibiotics. Plates were incubated at 37°C overnight before selection of transformed cells.

### 2.2.5.6 Miniprep of plasmidic DNA

Isolation of plasmid DNA for *E.coli* was performed using the QIAprep spin Miniprep kit (Qiagen) following the manufacturer's instructions. The plasmid DNA was eluted in 50  $\mu$ L of water.

### 2.2.5.7 Sequencing

Sequencing reactions were carried out in a 10 $\mu$ L reaction using the BigDye 3.1 sequencing kit (Perkin), according to the manufacturer's instructions. Samples were submitted to the Genome Analysis Centre (Norwich, UK) for sequencing. The quality of the sequence was checked using the 4Peaks application (Mekentosj) and the sequences were processed further using the SerialCloner application (SerialBasis).

## 2.2.6 Polymerase chain reaction based techniques

### 2.2.6.1 Polymerase chain reaction (PCR)

PCRs were routinely performed in a 20 $\mu$ L reaction containing 1X Taq buffer (Roche or Promega), 10 pmol of each dNTP, 0.1 pmol of each primer, 1-500 ng of template DNA and 1 unit of Taq polymerase (Roche, Promega, or produced in the lab). Where a proof-reading polymerase was required, the Phusion® High-Fidelity DNA polymerase was used with the appropriate buffer. The PCR cycling was initiated at 94°C for 2 min for the routine PCR and 98°C for 30 sec for the Phusion polymerase were a hot-start was routinely performed by preparing the PCR reactions without the Taq, then

adding the Taq after an initial step of denaturation for 2 minutes. The rest of the cycling programme was a denaturation step at either 94°C for 1 min or 98°C for 10 sec, an annealing step at 50-60°C according to the primer melting temperature for 30 sec followed by an elongation step at 72°C for 1-4 min depending on the expected length of the PCR product. For routine PCR an extension period of 1 min per kb was used, and for Phusion PCR an extension period of 30 sec per kb was used.

#### 2.2.6.2 Production of Taq

Recombinant Taq production was performed according to (Pluthero, 1993) using the INV $\lambda$ F' *E. coli* strain (genotype not available anymore) transformed with the pTaq plasmid, which contains the Taq gene expressed under the control of the Taq promoter. A 1L overnight culture of the cells in LB with Ampicillin 80 mg/mL was grown until an OD<sub>600</sub> of 0.8 was attained; the cells were then treated for 12 hours with 125mg/mL IPTG (isopropyl- $\beta$ -D-1 thiogalactopyranoside) to induce Taq expression. The cells were then pelleted by centrifugation for 10 min at 3000g and washed in 100 mL Buffer A (50 mM Tris-HCl pH 7.9, 50 mM glucose and 1 mM EDTA). After a new centrifugation to pellet the cells they were resuspended in 50 mL prelysis buffer with 4 mg/mL lysozyme (Sigma) in Buffer A and incubated for 15 min at room temperature. Fifty mL of lysis buffer (10 mM Tris-HCl pH 7.9, 50 mM KCl, 1 mM EDTA, 1 mM PMSF, 0.5 % (v/v) Tween 20, 0.5 % (v/v) NP40) were then added to the cells and the cells were lysed for 1 hour at 75 °C. The lysis mixture lysate was centrifuged for 10 min at 10000 g and 4 °C, and the clarified lysate transferred to a new tube. The Taq polymerase was precipitated by adding 30g of ammonium sulphate and stirring at room temperature. The solution was centrifuged for 10 min at 10000g and 4°C and the protein precipitate collected as surface precipitant. The precipitant was dialyzed in storage buffer (50 mM Tris-HCl pH 7.9, 50 mM KCl, 0.1 mM EDTA, 1 mM DTT, 0.5 mM PMSF, 50% (v/v) glycerol) twice for 12 hours at 4°C. The dialysis tubing (Roth) was prepared by boiling for 10 min in 2% sodium bicarbonate and 1 mM EDTA to remove metal traces then rinsed 3

times in water and kept at 4°C in water until use. The dialyzed solution was then diluted 1:1 in storage buffer and stored in 1.5 mL tubes at -20°C.

#### 2.2.6.3 Gel purification of PCR products

PCR products were excised from the agarose gel with a scalpel and purified with the QIAquick Gel Extraction Kit (Qiagen) following the manufacturer's instructions.

#### 2.2.6.4 Semi-quantitative RT-PCR

##### *DNase treatment of RNA samples*

Five µg of input RNA prepared using the TRI reagent method were pre-treated with the DNAfree kit (Ambion) following the manufacturer's instructions.

##### *Reverse transcription*

Reverse transcription was performed on 2µg of RNA. First, the RNA was incubated with 300 ng of oligo dt (15) (Promega) and 500 µM dNTPs for 10 min at 65°C then kept on ice. Then, the RT mix was added to the mix consisting of 200 U of the SuperscriptIII reverse transcriptase (Invitrogen) in the manufacturer's buffer with DTT and 1U of RNase A inhibitor (Promega). The reverse transcription was performed with the following programme: 50 min at 50°C and 10 min at 70°C.

##### *Semi-quantitative PCR*

The PCR was performed as described in 2.2.7.1. The quality of the cDNA and the absence of genomic DNA contamination were checked by amplifying the actin gene spanning the intron. Tubulin 1 primers (see material) were used as a control.

#### 2.2.6.5 Quantitative PCR

qPCR was performed on the ChIP samples using a LightCycler ® 480 System (Roche) and the SYBR green ® kit (Roche) following the manufacturer's instructions in a final volume of 10  $\mu$ L.

#### *Primer efficiency*

The primer efficiency was checked using a series dilution of input ChIP samples and performing the following programme: 95°C for 5 min, 45 cycles of 95°C for 15 sec, 55°C for 25 sec, 72°C for 25 sec, then a melting curve with 95°C for 5 sec, 40°C for 1 min and 97°C with a ramp increase of 0.11°C/sec with 5 acquisitions per sec. The presence of only one PCR product was checked by doing a melting curve analysis with the LightCycler ® 480 software. With this analysis, the decrease in fluorescence of samples is monitored while the temperature is steadily increased to melt the DNA. The decrease in fluorescence is due to the separation of the DNA strands and release of SYBR green as a consequence. These dyes only fluoresce at 530 nm if bound to double strand DNA, so the melting curve analysis measures the decrease in fluorescence at this wavelength. The Tm obtained is defined as the point at which half the DNA is double stranded and half is single stranded. The software charts the first negative derivative of the melting curve, which displays the melting temperature as peaks, in order to easily display differences in the melting profile of the samples, i.e. if the primers amplify only one product or not. The Cp values of the samples were also obtained using the second derivative max method. With this method the Cp of a sample is defined as the point where the sample fluorescence curve turns sharply upward. This turning point corresponds to the maximum of the second derivative of the amplification curve. The PCR efficiency was calculated by plotting the Cp values of the samples as a function of log (dilution). The slope of the trend line was then used to calculate the PCR efficiency as follow:

$$\text{Efficiency} = 10^{(-1/\text{slope})}.$$

Efficiency values of 1.7-2 were considered sufficient to use the corresponding primers.

*qPCR (quantitative PCR)*

The qPCR reactions were performed using the programme described above on the input and ChIP samples. Three biological replicates and two to three technical replicates were used for each sample. The Cp values were obtained for all samples using the second derivative max calculation method and the average of the technical replicates was calculated. The percentage of input was chosen to express enrichment of DNA in a ChIP at the corresponding locus. The percentage of input is calculated as follow:

$$\% \text{ input} = 100 \times 2^{(\text{Cp input} - \text{Cp IP sample})}$$

The average of the biological replicates was used to plot the percentage of input and the standard deviation was calculated to show variation in between samples.

*RT-qPCR (reverse transcription - quantitative PCR)*

For gene expression analysis, the Cp values were obtained using the second derivative max method. From this data the relative transcript levels (RTL) were calculated as follow:

$$\text{RTL} = 1000 \times 2^{(-\Delta\text{Cp})}$$

Where  $\Delta\text{Cp} = \text{Cp (gene of interest)} - \text{Cp (housekeeping gene)}$

#### 2.2.6.6 Transposon display

In order to detect copies of the ONSEN retrotransposon in the genome, transposon display was performed. Approximately 0.5 µg of genomic DNA extracted with the method described in 2.2.1.2 were digested in the manufacturer's buffer with the rare cutting restriction endonuclease *Dra*I, which creates blunt ends at the restriction site. The reaction was carried out in 20 µL at 37°C overnight. The digested DNA was then purified using the method described in 2.2.6.4 and resuspended in 20 µL of sterile water. Adapters were then ligated to the blunt ends of the digested DNA by mixing them with 5 µL of the purified DNA, together with 1 unit of T4 DNA

polymerase (Roche) in the buffer recommended by the manufacturer. The ligation reaction was incubated at 16°C overnight and 1 µL of this solution was directly used in the PCR reaction. The forward primer recognised the untranslated region of ONSEN when the reverse primer recognised one of the adapter sequences. The PCR products were loaded on a 2% agarose gel and ran for 4 hours at 70 V. Alternatively, in order to ensure a better resolution of the samples, the PCR products were analysed using the MultiNA microchip electrophoresis system (Shimazu) following the manufacturers' instructions. The PCR product was undiluted prior to loading and the DNA1200 ladder (log2 ladder) (Promega) was used.

### 2.2.7 Radiolabelling of nucleic acids

#### 2.2.7.1 End-labelled oligonucleotide

An end-labelled oligonucleotide was used to detect the abundant siRNA tasiRNA 255 (Xie et al., 2005). Twenty pmol of oligonucleotide were labelled in a 50µL reaction containing 1X PNK buffer (New England Biolabs, composition 70mM Tris-HCl, 10mM MgCl<sub>2</sub>, 5mM DTT, pH 7.6), 30 units of polynucleotide kinase (New England Biolabs) and 100 µCi of  $\gamma$ -<sup>32</sup>P ATP. After incubation at 37°C for 1 hour, the volume was increased to 100 µL with sterile water and the labelled probe was purified using a Microspin G-25 Sephadex column (Amersham Biosciences) by centrifugation for 2 min at 650 g. Radionucleotide incorporation was measured using a ProbeCount™ (Oncor). The probe was denatured by boiling for 5 min with 2.5 mg of salmon sperm DNA, and then cooled on ice for 2 min before adding directly to the hybridization buffer.

#### 2.2.7.2 Riboprobe

RNA probes were used for the detection of siRNAs corresponding to GFP. The T7 promoter was attached to the probe sequence through cloning into

pGEM®-T Easy (Promega) which is a T7-containing vector with subsequent amplification using the M13 reverse primer upstream of the T7 site and the M13 forward primer downstream of GFP. Sense probes were produced for the detection of antisense small RNAs in a 20 µL reaction containing 2 µL of gel purified PCR product, 10 pmol of CTP, GTP and ATP, 1 µL of RNase inhibitor RNasin (Promega), 1 X T7 RNA polymerase buffer (Roche), 20 units of T7 RNA polymerase (Roche) and 50 µCi of  $\alpha$ -<sup>32</sup>P UTP. After incubation at 37°C for 1 hour, the volume was increased to 100 µL with sterile water and the labelled probe was purified using a Microspin G-25 Sephadex column (Amersham Biosciences) by centrifugation for 2 min at 650 g. Radionucleotide incorporation was measured using a ProbeCount™ (Oncor). The probe was denatured by boiling for 5 min with 2.5 mg of salmon sperm DNA, and then cooled on ice for 2 min before adding directly to the hybridization buffer.

#### 2.2.8 Gel electrophoresis of nucleic acids

##### 2.2.8.1 Agarose gels

The quality of RNA and size of DNA fragments were estimated by electrophoresis using agarose gels containing 1-3% agarose and 5 µg/mL ethidium bromide in 1X TBE (Severn Biotech) at 100 V. The 1 kb and 100 bp size markers (New England Biolabs) were used as appropriate.

##### 2.2.8.2 Polyacrylamide-urea gels

The polyacrylamide-urea gels were cast using the Biorad Minigel System with 1.5 mm spacers. The gels were prepared in 1X TBE (diluted from a 10X solution prepared from 108 g of Tris base, 55 g of boric acid, 7.5 g of EDTA in pure water) containing 42% urea ultra-pure (w/v) and 17% acrylamide (v/v), and set by adding 7 µL/mL of ammonium persulfate 10% (w/v) and 0.7 µL/mL TEMED (Tetramethylethylenediamine).

The RNA samples were prepared by adding an equal volume of 2X loading buffer from the *mirVana™* miRNA Isolation Kit (Ambion) to 5 µg of RNA enriched in small RNAs. The samples were boiled for 5 min at 96°C and kept on ice until loading on the gel.

The electrophoresis was performed in 1X TBE, first at 150 V for 5 min prior to loading, then at 300 V for 5 min following loading, and finally at 150 V until the first blue dye reaches the bottom of the gel.

The separation and quality of the samples was checked by staining the gel in 0.1mg/mL ethidium bromide for 5 min. The gel was destained by floating in sterile water for 10 min.

### 2.2.9 Hybridisation of nucleic acids

#### 2.2.9.1 Northern blotting of small RNAs

Small RNAs separated on polyacrylamide-urea gels were transferred to Hybond N+ membranes (Amersham Biosciences) by capillary transfer in 20 X SSC (prepared with 175.3g of NaCl and 88.2g of sodium citrate, pH 7.0 in 1 L of pure water) for 16 hours. The RNA was crosslinked to the membrane by using the “auto” setting on a UV Stratalinker 2400 (Stratagene) twice. The blots were kept in the dark at 4°C until hybridization.

Prior to hybridization, the blots were rinsed in 2X SSC for 5 min to rehydrate and eliminate excess salts. The blots were then pre-hybridised for 1 hour at 41°C for end-labelled probes and 68°C for riboprobes in PerfectHyb buffer (Sigma). The probes were then added directly to the hybridization buffer and incubated for 3 hours to overnight for end-labelled probes and overnight for riboprobes.

The blots were then washed twice in a low stringency buffer (2X SSC 0.1% SDS) for 5 min then according to cpm measured with a Geiger counter further washes were performed if required in high stringency buffer (0.2 X SSC 0.1 % SDS).

After washing, the blots were blot dried and wrapped in cling film (Saran) and exposed to Phosphor screen between 45 min and overnight depending on the strength of the signal. Image screens were read using a Typhoon reader (GE Healthcare) and the ImageQuant software (GE Healthcare).

#### 2.2.9.2 *in situ* hybridisation

In order to detect ONSEN expression in the shoot meristem following heat stress, non-radioactive *in situ* hybridisation was performed.

##### *Collection and fixation of samples*

In order to detect ONSEN expression in the shoot meristem following heat stress, non-radioactive *in situ* hybridisation was performed. Shoot meristem from main and secondary inflorescences from 4 week-old plants were collected following 24 hours of control stress or heat stress. The samples were infiltrated with a fixation solution containing 4% paraformaldehyde in *in situ* PBS buffer (Phosphate Buffered Saline, 130 mM NaCl, 7 mM Na<sub>2</sub>HPO<sub>4</sub>, 3 mM NaH<sub>2</sub>PO<sub>4</sub>) supplemented with 0.06% Triton X-100 and Tween-20 to facilitate infiltration. The fixative was infiltrated using a vacuum pump for 15 min and the samples were kept at 4°C overnight before dehydration.

##### *Dehydration of samples*

Fixed tissues were dehydrated by successive treatment on ice:

Solutions	Time
0.85% saline (NaCl 0.85%)	30 min
50% ethanol 0.85% saline	90 min
70% ethanol 0.85% saline	90 min
70% ethanol	Until use, keep at 4°C

The tissues were kept until embedding in plastic moulds.

##### *Embedding*

The samples were placed in a Tissue-Tek® VIP embedding apparatus (Sakura) with the following programme:

Solutions	Time	Temperature
Fixative	6 h	35°C
70% Ethanol	60 min	35°C
80% Ethanol	90 min	35°C
90% Ethanol	2 h	35°C
100% Ethanol	60 min	35°C
100% Ethanol	90 min	35°C
100% Ethanol	2 h	35°C
Xylene	30 min	35°C
Xylene	60 min	35°C
Xylene	90 min	35°C
Wax	1 hour	60°C
Wax	1 hour	60°C
Wax	2 hour	60°C
Wax	Until use	60°C

The samples were then embedded in wax and kept at 4°C until sectioning.

### *Sectioning*

The wax embedded samples were sectioned and the shoot meristem sections were placed on polysine slides (Thermo Scientific) in water and left to dry overnight.

### *Probe production*

Histone H4 cloned in pBluescript KS – (Agilent) was used as positive control. GFP in pbluescript was used as negative control and the ONSEN sequence cloned in pGEM T-easy (Promega) was used to detect ONSEN *in situ* expression. All plasmids were linearized with appropriate restriction enzyme and purified.

The *in vitro* transcription reaction was performed using the DIG RNA labelling Kit (Roche) using the SP6 RNA polymerase following the manufacturers instructions with an incubation at 37°C for 2 hours. Two µL of DNase I were then added to the sample to remove the plasmid and the sample incubated at 37°C for 15 min. Two µL of 0.2M EDTA pH 8 was added to protect the RNA from degradation. The purification of the probes was undertaken by precipitating them at -70°C for 2 hours with 100 µL 3.8 M ammonium acetate and 600µL absolute ethanol. The pellet was centrifuged for 15 min at 4°C and 10,000g and washed in ethanol 70% before resuspension in 50% 200 mM carbonate buffer (sodium carbonate in water). The probe was broken into pieces by incubation at 60°C for the duration calculated according to the following formula:

$$t_{(\text{min})} = (L_0 - L_f) / K^* L_0 * L_f$$

$L_0$  = starting length (kb), including all parts of the vector that are transcribed

$L_f$  = final length = 500 bp

$K$  = 0.11

The reaction was then stopped with 10µL acetic acid, 12 µL 3M sodium acetate pH 5.8 and 312µL absolute ethanol. The samples were precipitated overnight at -20°C and the probes were recovered by a 15 min centrifugation at 10000g at 4°C. The pellet was washed with 70% ethanol and resuspended in 50 µL TE buffer.

#### *Dot blot*

A dot blot was performed to assess the success of the probe production. Dilutions of 1/10, 1/100 and 1/1000 of the probes were prepared and 1 µL of undiluted and diluted probes were placed on a Hybond N+ membrane (Amersham Biosciences). After air-drying, the RNA was crosslinked to the membrane by using the “auto” setting on a UV Stratalinker 2400 (Stratagene) twice.

The antibody reaction was performed by incubating the blot successively in the following solutions:

Solutions	Time
-----------	------

Buffer 1 = 100 mM Tris-HCl pH 7.5, 5 min
150 mM NaCl
Buffer 1 + 0.5 % (w/v) of blocking 20 min
reagent (Roche) = buffer 2
Buffer 1 5 min twice
Buffer 1 + 1 $\mu$ L anti-DIG antibody 20 min
(Roche)
Buffer 1 5 min twice
Buffer 5 (100 mM Tris and 50mM 1 min
NaCl pH 9.5)
Buffer 5 + 9 $\mu$ L NBT + 5 $\mu$ L BCIP Until revealing of dots
(Roche)

#### *Rehydration of sections*

The slides were placed in metal racks and rehydrated in the following solutions:

Solutions	Time
Histoclear	10 min
Histoclear	10 min
Absolute ethanol	1 min
Absolute ethanol	30 sec
95% ethanol 0.85% saline (0.9% NaCl)	30 sec
85% ethanol 0.85% saline	30 sec
50% ethanol 0.85% saline	30 sec
30% ethanol 0.85% saline	30 sec
0.85% saline	2 min
<i>in situ</i> PBS buffer	2 min

#### *Proteinase K treatment of sections*

The proteins in the sections were digested and the enzymatic reaction was stopped and the sections dehydrated again by placing the sections in the following solutions:

Solutions	Time
Proteinase K (2 µg/mL in pronase buffer: 50 mM Tris-HCl pH7.5, 5 mM EDTA)	10 min
Glycine 0.2% in PBS buffer	2 min
<i>in situ</i> PBS buffer	2 min
4 % formaldehyde in PBS	10 min
<i>in situ</i> PBS buffer	2 min
<i>in situ</i> PBS buffer	2 min
Acetic anhydride (5 µL/mL in 0.1M triethanolamine	10 min
<i>in situ</i> PBS buffer	2 min
0.85% saline	2 min
30% ethanol 0.85% saline	30 sec
50% ethanol 0.85% saline	30 sec
85% ethanol 0.85% saline	30 sec
95% ethanol 0.85% saline	30 sec
Absolute ethanol	Leave at 4 °C until use

#### *Hybridisation of probes on sections*

The probes were prepared for hybridisation by preparing the following mix: 2µL probe, 2 µL pure water and 4 µL deionised formamide. The probes were denatured by placing them at 80 °C for 2 min and kept on ice. 32 µL of hybridisation buffer was added to the probe solution. The hybridisation buffer composition is as follow:

Solution	Final concentration
10 X Hybridisation salts	300 mM NaCl, 10 mM Tris-HCl pH6.8, 10 mM NaPO <sub>4</sub> , 5 mM EDTA)
Deionized formamide	50 % (v/v)

50% dextran sulphate	25 % (v/v)
tRNA 100 mg/mL	1.25 % (v/v)
50 X Denhardts salts (Thermo Scientific, 1% BSA, 1% Ficoll and 1 Polyvinylpyrrolidone in water)	2.5 % (v/v)
Water	8.75 % (v/v)

The ethanol was allowed to evaporate from the slides before placing 40  $\mu$ L of probe solution in hybridisation buffer on top of the sections. The sections were covered with plastic coverslips, wrapped in paper soaked in wash buffer (2X SCC, 50 % formamide) and placed at 50°C overnight.

#### *Washes and RNase treatment*

The slides were placed in wash buffer to allow the coverslips to be removed from the slides. The slides were then washed in wash buffer by incubation at 50°C for 30 min then the buffer was replaced twice and the slides incubated for 90 min at 50°C with each new wash.

The probes that did not hybridised were digested by incubation of the slides in the following solutions:

Solutions	Time	Temperature
NTE buffer (500 mM NaCl, 10 mM Tris-HCl pH7.5, 1 mM EDTA)	5 min	37°C
NTE buffer with 20 $\mu$ g/mL RNase A	30 min	37°C
Wash buffer	60 min	50 °C
SSC	2 min	RT
<i>in situ</i> PBS buffer	2 min	RT

#### *Antibody staining*

The slides were stained by placing them in the following solutions:

Solutions	Time
Buffer 1 (see dot blot)	5 min

Buffer 2 (see dot blot)	60 min
Buffer 1 + 1 % BSA (w/v) and 0.3 % Triton (v/v) = buffer 3	30 min
Buffer 3 + 1:3000 anti-DIG antibody = buffer 4	90 min
Buffer 3	20 min, repeat 4 times
Buffer 5 (see dot blot)	5 min twice
Buffer 5 + 2 $\mu$ L/mL NBT and 1.5 $\mu$ L/mL BCIP = buffer 6	Until signal develops

The slides were incubated in buffer 6 in the dark until a good development of the signal, from 12 to 60 hours. To stop development, the slides were rinsed in water and kept in water at 4 °C.

#### *Fixation of the slides*

The slides were placed in the following solutions for fixation:

Solutions	Time
Water	5 min
70 % ethanol	5 min
95 % ethanol	5 min
100 % ethanol	5 min
95 % ethanol	5 min
70 % ethanol	5 min
Water	5 min

The slides were kept at 4 °C in water and pictures were taken using a Leica DM6000 microscope.

### 2.3 Imaging techniques

#### 2.3.1 Confocal microscopy

For confocal microscopy of root meristems, strips of masking tape were added to microscope slide to act as spacers. Seedlings were placed vertically on the slide in 10 µg/mL of propidium iodide for 5 min prior to imaging. Imaging was performed using a SP1 Confocal Microscope (Leica). GFP and PI were excited using the 488 nm argon ion laser and emission was collected between 550 and 550 nm for GFP and between 600 and 650 nm for PI. The images were processed using the Leica Confocal Software.

### 2.3.2 Fluorescence stereomicroscopy

#### 2.3.2.1 Screening

The liquid medium with Zeocin was removed and replaced by a 1µM Sytox Orange (Sigma) solution to stain dead cells. Seedlings were imaged using a Lumar stereomicroscope v12 (Zeiss) with the CY3 filter set (Excitation: 532-558 nm, Emission: 570-640 nm).

#### 2.3.2.2 GFP expression and GUS staining

GFP expression was imaged using a M205FA fluorescent stereomicroscope (Leica) using the GFP filter and the bright field. The images were processed using the Leica Confocal Software. Scale bars were added using the Fiji image analysis suite (Schindelin et al., 2012).

### 2.4 Statistical analysis

The Fisher's exact test was used to determine whether the levels of cell death observed in various mutants in chapter 2, 3 and 5 were significantly different from wild-type levels (Quenouille, 1949). The test is designed to determine significance in contingency tables with small sample sizes, i.e the total sample size n is below 40 and/or one of the cells in the contingency table has a value of 0. The contingency table is designed as follow:

	Cell death	No cell death	Total
--	------------	---------------	-------

Wild type	a	b	a+b
Mutant	c	d	c+d
Total	a+c	b+d	n

In this test the biological hypothesis is that the number of seedlings showing cell death is similar between wild-type and mutant, and the alternative hypothesis is that there is a difference in cell death levels between wild-type and mutant.

The p-value for the test was calculated using the R statistical programming language and the Rcmdr package by applying the following equation:

$$p = \frac{(a + b)! (c + d)! (a + c)! (b + d)!}{a! b! c! d! n!}$$

The smaller the value of p, the greater the evidence for rejecting the null hypothesis, in other words the greater the evidence for wild type and mutant plants showing different levels of cell death. We decided to reject the null hypothesis if the p-value was < 0.05 (95% confidence).

The Chi square test was used in order to test the fit of segregation rates of the PCD phenotypes of the M2 families and the Lov-1 to Columbia cross F3 with single mutations (Rhoades and Overall, 1982). In this test, the biological hypothesis is that the segregation rates fit a single mutation. The statistical null hypothesis is that there is no significant difference between the observed number of plants (O) in a category (i.e. showing or not the expected phenotype, in our case PCD) and the expected number of plants (E) in a category (i.e. how many plants would display the expected phenotype in the case of the segregation of a single mutation). The value of the Chi-square is calculated as follow:

$$\chi^2 = \sum_{i=1}^n \frac{(O_i - E_i)^2}{E_i}$$

The different phenotypic groups compose the classes, which enable the calculation of the degrees of freedom df with df= (number of classes)-1.

The test statistic is then compared to the Chi-squared distribution for the df, which enables the identification of the p value. The smaller the value of p, the greater the evidence for rejecting the null hypothesis, in other words the greater the evidence for the numbers observed not to fit with the expected segregation rates for a single mutation. We decided to reject the null hypothesis if the p-value was  $< 0.05$  (95% confidence).

## References

**Abe K, Osakabe K, Ishikawa Y, Tagiri A, Yamanouchi H, Takyuu T, Yoshioka T, Ito T, Kobayashi M, Shinozaki K, et al** (2009) Inefficient double-strand DNA break repair is associated with increased fasciation in *Arabidopsis* BRCA2 mutants. *J Exp Bot* **60**: 2751–2761

**Abremski K, Wierzbicki A, Frommer B, Hoess RH** (1986) Bacteriophage P1 Cre-loxP site-specific recombination. Site-specific DNA topoisomerase activity of the Cre recombination protein. *J Biol Chem* **261**: 391–396

**Adachi S, Minamisawa K, Okushima Y, Inagaki S, Yoshiyama K, Kondou Y, Kaminuma E, Kawashima M, Toyoda T, Matsui M, et al** (2011) Programmed induction of endoreduplication by DNA double-strand breaks in *Arabidopsis*. *Proc Natl Acad Sci USA* **108**: 10004–10009

**Adams-Phillips L, Briggs AG, Bent AF** (2009) Disruption of Poly(ADP-ribosyl)ation Mechanisms Alters Responses of *Arabidopsis* to Biotic Stress. *Plant Physiol* **152**: 267–280

**Adams-Phillips L, Briggs AG, Bent AF** (2010) Disruption of poly(ADP-ribosyl)ation mechanisms alters responses of *Arabidopsis* to biotic stress. *Plant Physiol* **152**: 267–280

**Aggarwal P, Yadav RK, Reddy GV** (2010) Identification of novel markers for stem-cell niche of *Arabidopsis* shoot apex. *Gene Expression Patterns* **1–6**

**Ahn J-W, Atwell BJ, Roberts TH** (2009) Serpin genes AtSRP2 and AtSRP3 are required for normal growth sensitivity to a DNA alkylating agent in *Arabidopsis*. *BMC Plant Biol* **9**: 52

**Aichinger E, Kornet N, Friedrich T, Laux T** (2012) Plant Stem Cell Niches. Annual review of plant biology. doi: 10.1146/annurev-arplant-042811-105555

**Aida M, Beis D, Heidstra R, Willemsen V, Blilou I, Galinha C, Nussaume L, Noh Y-S, Amasino R, Scheres B** (2004) The PLETHORA genes mediate patterning of the *Arabidopsis* root stem cell niche. *Cell* **119**: 109–120

**Alonso JM, Stepanova AN, Leisse TJ, Kim CJ, Chen H, Shinn P, Stevenson DK, Zimmerman J, Barajas P, Cheuk R, et al** (2003) Genome-wide insertional mutagenesis of *Arabidopsis thaliana*. *Science* **301**: 653–657

**Altman J, Das GD** (1965) Autoradiographic and histological evidence of postnatal hippocampal neurogenesis in rats. *J Comp Neurol* **124**: 319–

**Altmeyer M, Lukas J** (2013) To spread or not to spread—chromatin modifications in response to DNA damage. *Current Opinion in Genetics & Development*. doi: 10.1016/j.gde.2012.11.001

**Amedeo P, Habu Y, Afsar K, Mittelsten Scheid O, Paszkowski J** (2000) Disruption of the plant gene MOM releases transcriptional silencing of methylated genes. *Nature* **405**: 203–206

**Amiard S, Charbonnel C, Allain E, Depeiges A, White CI, Gallego ME** (2010) Distinct Roles of the ATR Kinase and the Mre11-Rad50-Nbs1 Complex in the Maintenance of Chromosomal Stability in *Arabidopsis*. *Plant Cell*. doi: 10.1105/tpc.110.078527

**Amiard S, Depeiges A, Allain E, White CI, Gallego ME** (2011) *Arabidopsis* ATM and ATR Kinases Prevent Propagation of Genome Damage Caused by Telomere Dysfunction. *Plant Cell*. doi: 10.1105/tpc.111.092387

**Arnaud N, Girin T, Sorefan K, Fuentes S, Wood TA, Lawrenson T, Sablowski R, Østergaard L** (2010) Gibberellins control fruit patterning in *Arabidopsis thaliana*. *Genes Dev* **24**: 2127–2132

**Ba Z, Qi Y** (2013) Small RNAs: Emerging key players in DNA double-strand break repair. *Sci China Life Sci*. doi: 10.1007/s11427-013-4552-7

**Bakkenist CJ, Kastan MB** (2003) DNA damage activates ATM through intermolecular autophosphorylation and dimer dissociation. *Nature* **421**: 499–506

**Barton MK, Poethig RS** (1993) Formation of the shoot apical meristem in *Arabidopsis thaliana*: an analysis of development in the wild type and in the shoot meristemless mutant. *Development*

**Battu A, Ray A, Wani AA** (2011) ASF1A and ATM regulate H3K56-mediated cell-cycle checkpoint recovery in response to UV irradiation. *Nucleic Acids Res*. doi: 10.1093/nar/gkr523

**Belfield EJ, Gan X, Mithani A, Brown C, Jiang C, Franklin K, Alvey E, Wibowo A, Jung M, Bailey K, et al** (2013) Genome-wide analysis of mutations in mutant lineages selected following fast-neutron irradiation mutagenesis of *Arabidopsis thaliana*. *Genome Res* **22**: 1306–1315

**Belgnaoui SM, Gosden RG, Semmes OJ, Haoudi A** (2006) Cancer Cell International | Full text | Human LINE-1 retrotransposon induces DNA damage and apoptosis in cancer cells. *Cancer Cell Int* **6**: 13

**Benitez-Alfonso Y, Faulkner C, Pendle A, Miyashima S, Helariutta Y, Maule A** (2013) Symplastic Intercellular Connectivity Regulates Lateral Root Patterning. *Dev Cell* **26**: 136–147

**Bitomsky N, Hofmann TG** (2009) Apoptosis and autophagy: Regulation of apoptosis by DNA damage signalling - roles of p53, p73 and HIPK2. *FEBS Journal* **276**: 6074–6083

**Blevins T, Pontes O, Pikaard CS, Meins F** (2009) Heterochromatic siRNAs and DDM1 independently silence aberrant 5S rDNA transcripts in *Arabidopsis*. *PLoS ONE* **4**: e5932

**Block MD, Verduyn C, Brouwer DD, Cornelissen M** (2004) Poly(ADP-ribose) polymerase in plants affects energy homeostasis, cell death and stress tolerance. *The Plant Journal* **41**: 95–106

**Bonnet E, van de Peer Y, Rouzé P** (2006) The small RNA world of plants. *New Phytologist* **171**: 451–468

**Brand U, Grünwald M, Hobe M, Simon R** (2002) Regulation of CLV3 Expression by Two Homeobox Genes in *Arabidopsis*. *Plant Physiol*

**Bray CM, West CE** (2005) DNA repair mechanisms in plants: crucial sensors and effectors for the maintenance of genome integrity. *New Phytol* **168**: 511–528

**Brodersen P, Voinnet O** (2006) The diversity of RNA silencing pathways in plants. *Trends Genet* **22**: 268–280

**Bucher E, Reinders J, Mirouze M** (2012) Epigenetic control of transposon transcription and mobility in *Arabidopsis*. *Curr Opin Plant Biol*. doi: 10.1016/j.pbi.2012.08.006

**Buisine N, Quesneville H, Colot V** (2008) Improved detection and annotation of transposable elements in sequenced genomes using multiple reference sequence sets. *Genomics* **91**: 467–475

**Bunz F, Dutriaux A, Lengauer C, Waldman T, Zhou S, Brown JP, Sedivy JM, Kinzler KW, Vogelstein B** (1998) Requirement for p53 and p21 to sustain G2 arrest after DNA damage. *Science* **282**: 1497–1501

**Byrne ME, Kidner CA, Martienssen RA** (2003) Plant stem cells: divergent pathways and common themes in shoots and roots. *Current opinion in genetics & ...*

**Byrne ME, Simorowski J, Martienssen RA** (2002) ASYMMETRIC LEAVES1 reveals knox gene redundancy in *Arabidopsis*. *Development* **129**: 1957–1965

**Campi M, D' Andrea L, Emiliani J, Casati P** (2011) Participation of Chromatin Remodeling Proteins in the repair of UV-B damaged DNA. *Plant Physiol*. doi: 10.1104/pp.111.191452

**Cao X, Aufsatz W, Zilberman D, Mette MF, Huang MS, Matzke M,**

**Jacobsen SE** (2003) Role of the DRM and CMT3 methyltransferases in RNA-directed DNA methylation. *Curr Biol* **13**: 2212–2217

**Castañeda J, Genzor P, Bortvin A** (2011) piRNAs, transposon silencing, and germline genome integrity. *Mutation Research/Fundamental and Molecular Mechanisms of Mutagenesis* **714**: 95–104

**Chankova SG, Dimova E, Dimitrova M, Bryant PE** (2007) Induction of DNA double-strand breaks by zeocin in *Chlamydomonas reinhardtii* and the role of increased DNA double-strand breaks rejoining in the formation of an adaptive response. *Radiat Environ Biophys* **46**: 409–416

**Chaudhary PM, Roninson IB** (1991) Expression and activity of P-glycoprotein, a multidrug efflux pump, in human hematopoietic stem cells. *Cell* **66**: 85–94

**Clark SE, Jacobsen SE, Levin JZ, Meyerowitz EM** (1996) The CLAVATA and SHOOT MERISTEMLESS loci competitively regulate meristem activity in *Arabidopsis*. *Development* **122**: 1567–1575

**Clay NK** (2005) *Arabidopsis* thickvein Mutation Affects Vein Thickness and Organ Vascularization, and Resides in a Provascular Cell-Specific Spermine Synthase Involved in Vein Definition and in Polar Auxin Transport. *Plant Physiol* **138**: 767–777

**Coll NS, Vercammen D, Smidler A, Clover C, Van Breusegem F, Dangl JL, Epple P** (2010) *Arabidopsis* Type I Metacaspases Control Cell Death. *Science* **330**: 1393–1397

**Colón-Carmona A, You R, Haimovitch-Gal T, Doerner P** (1999) Technical advance: spatio-temporal analysis of mitotic activity with a labile cyclin-GUS fusion protein. *Plant J* **20**: 503–508

**Cui X, Jin P, Cui X, Gu L, Lu Z, Xue Y, Wei L, Qi J, Song X, Luo M, et al** (2013) Control of transposon activity by a histone H3K4 demethylase in rice. *Proc Natl Acad Sci USA* **110**: 1953–1958

**Culligan K, Tissier A, Britt A** (2004) ATR regulates a G2-phase cell-cycle checkpoint in *Arabidopsis thaliana*. *Plant Cell* **16**: 1091–1104

**Culligan KM, Robertson CE, Foreman J, Doerner P, Britt AB** (2006) ATR and ATM play both distinct and additive roles in response to ionizing radiation. *The Plant Journal* **48**: 947–961

**Curtis MJ, Hays JB** (2007) Tolerance of dividing cells to replication stress in UVB-irradiated *Arabidopsis* roots: requirements for DNA translesion polymerases eta and zeta. *DNA Repair* **6**: 1341–1358

**Curtis MJ, Hays JB** (2011) Cooperative responses of DNA-damage-activated protein kinases ATR and ATM and DNA translesion polymerases to

replication-blocking DNA damage in a stem-cell niche. *DNA Repair* **10**: 1272–1281

**Dalmay T, Hamilton A, Rudd S, Angell S, Baulcombe DC** (2000) An RNA-Dependent RNA Polymerase Gene in *Arabidopsis* Is Required for Posttranscriptional Gene Silencing Mediated by a Transgene but Not by a Virus. *Cell* **101**: 543–553

**Dandoy E, Schnys R, Deltour R, Verly WG** (1987) Appearance and repair of apurinic/apyrimidinic sites in DNA during early germination of *Zea mays*. *Mutation Research/Fundamental and Molecular Mechanisms of Mutagenesis* **181**: 57–60

**De Veylder L, Beeckman T, Beemster GT, Kroes L, Terras F, Landrieu I, van der Schueren E, Maes S, Naudts M, Inze D** (2001) Functional analysis of cyclin-dependent kinase inhibitors of *Arabidopsis*. *Plant Cell* **13**: 1653–1668

**Dinant C, Houtsmuller AB, Vermeulen W** (2008) Chromatin structure and DNA damage repair. *Epigenetics Chromatin* **1**: 9

**Dobbelstein M, Strano S, Roth J, Blandino G** (2005) p73-induced apoptosis: a question of compartments and cooperation. *Biochem Biophys Res Commun* **331**: 688–693

**Dolan L, Janmaat K, Willemsen V, Linstead P, Poethig S, Roberts K, Scheres B** (1993) Cellular organisation of the *Arabidopsis thaliana* root.  
...

**Doucet-Chabeaud G, Godon C, Brutesco C, de Murcia G, Kazmaier M** (2001) Ionising radiation induces the expression of PARP-1 and PARP-2 genes in *Arabidopsis*. *Mol Genet Genomics* **265**: 954–963

**Edinger A, Thompson C** (2004) Death by design: apoptosis, necrosis and autophagy. *Current Opinion in Cell Biology*

**Elmayan T, Proux F, Vaucheret H** (2005) *Arabidopsis* RPA2: a genetic link among transcriptional gene silencing, DNA repair, and DNA replication. *Curr Biol* **15**: 1919–1925

**Emery JF, Floyd SK, Alvarez J, Eshed Y, Hawker NP** (2003) Radial Patterning of *Arabidopsis* Shoots by Class III HD-ZIP and KANADI Genes. *Current Biology*

**Eun C, Lorkovic ZJ, Naumann U, Long Q, Havecker ER, Simon SA, Meyers BC, Matzke AJM, Matzke M** (2011) AGO6 Functions in RNA-Mediated Transcriptional Gene Silencing in Shoot and Root Meristems in *Arabidopsis thaliana*. *PLoS ONE* **6**: e25730

**Fagagna FDD** (2013) A direct role for small non-coding RNAs in DNA

damage response. *Trends Cell Biol.* doi: 10.1016/j.tcb.2013.09.008

**Fang W, Wang X, Bracht JR, Nowacki M, Landweber LF** (2012) Piwi-Interacting RNAs Protect DNA against Loss during *Oxytricha* Genome Rearrangement. *Cell* **151**: 1243–1255

**Fedoroff NV** (2012) Classic Perspective: McClintock's challenge in the 21st century. *Proc Natl Acad Sci USA* **109**: 20200–20203

**Fernandez-Capetillo O, Murga M** (2008) Why cells respond differently to DNA damage: a chromatin perspective. *Cell Cycle* **7**: 980–983

**Filipowicz W, Bhattacharyya SN, Sonenberg N** (2008) Mechanisms of post-transcriptional regulation by microRNAs: are the answers in sight? *Nat Rev Genet* **2008**: 102–114

**Finnegan EJ, Margis R, Waterhouse PM** (2003) Posttranscriptional Gene Silencing Is Not Compromised in the *Arabidopsis* CARPEL FACTORY (DICER-LIKE1) Mutant, a Homolog of Dicer-1 from *Drosophila*. *Current Biology* **13**: 236–240

**Finnegan EJ, Peacock WJ, Dennis ES** (1996) Reduced DNA methylation in *Arabidopsis thaliana* results in abnormal plant development. *Proc Natl Acad Sci USA* **93**: 8449–8454

**Fong YW, Cattoglio C, Tjian R** (2013) The Intertwined Roles of Transcription and Repair Proteins. *Mol Cell* **52**: 291–302

**Francia S, Michelini F, Saxena A, Tang D, de Hoon M, Anelli V, Mione M, Carninci P, d'Adda di Fagagna F** (2012) Site-specific DICER and DROSHA RNA products control the DNA-damage response. *Nature* **488**: 231–235

**Fulcher N, Sablowski R** (2009) Hypersensitivity to DNA damage in plant stem cell niches. *Proc Natl Acad Sci USA* **106**: 20984–20988

**Funk V, Kositsup B, Zhao C, Beers EP** (2002) The *Arabidopsis* xylem peptidase XCP1 is a tracheary element vacuolar protein that may be a papain ortholog. *Plant Physiol* **128**: 84–94

**Furukawa T, Curtis MJ, Tominey CM, Duong YH, Wilcox BWL, Aggoune D, Hays JB, Britt AB** (2010) A shared DNA-damage-response pathway for induction of stem-cell death by UVB and by gamma irradiation. *DNA Repair* **1–9**

**Gallagher KL, Paquette AJ, Nakajima K, Benfey PN** (2004) Mechanisms Regulating SHORT-ROOT Intercellular Movement. *Current Biology*

**Gallois J-L, Nora FR, Mizukami Y, Sablowski R** (2004) WUSCHEL induces shoot stem cell activity and developmental plasticity in the root

meristem. *Genes Dev* **18**: 375–380

**Gallois J-L, Woodward C, Reddy GV, Sablowski R** (2002) Combined SHOOT MERISTEMLESS and WUSCHEL trigger ectopic organogenesis in *Arabidopsis*. *129*: 3207–3217

**Garcia V, (null), (null), (null), (null), (null)** (2003) AtATM Is Essential for Meiosis and the Somatic Response to DNA Damage in Plants. *Plant Cell* **15**: 119

**Gasior SL, Wakeman TP, Xu B, Deininger PL** (2006) ScienceDirect.com - Journal of Molecular Biology - The Human LINE-1 Retrotransposon Creates DNA Double-strand Breaks. *Journal of Molecular Biology*

**Gonfloni S** (2013) Targeting DNA damage response: Threshold, chromatin landscape and beyond. *Pharmacology & Therapeutics* **138**: 46–52

**González-García M-P, Vilarrasa-Blasi J, Zhiponova M, Divol F, Mora-García S, Russinova E, Caño-Delgado AI** (2011) Brassinosteroids control meristem size by promoting cell cycle progression in *Arabidopsis* roots. *Development* **138**: 849–859

**Goodarzi AA, Jeggo P, Lobrich M** (2010) The influence of heterochromatin on DNA double strand break repair: Getting the strong, silent type to relax. *DNA Repair* **9**: 1273–1282

**Grieneisen VA, Xu J, Marée AFM, Hogeweg P, Scheres B** (2007) Auxin transport is sufficient to generate a maximum and gradient guiding root growth. *Nature* **449**: 1008–1013

**Guyomarc'h S, Benhamed M, Lemonnier G, Renou J-P, Zhou D-X, Delarue M** (2006) MGOUN3: evidence for chromatin-mediated regulation of FLC expression. *J Exp Bot* **57**: 2111–2119

**Hall JD, Cobb J, Iqbal M, Abidali M, Liu Z, Mount DW** (2009) UVH6, a plant homolog of the human/yeast TFIIH transcription factor subunit XPD/RAD3, regulates cold-stress genes in *Arabidopsis thaliana*. *Plant Molecular Biology Reporter* **27**: 217–228

**Hanzawa Y, Takahashi T, Komeda Y** (1997) ACL5: an *Arabidopsis* gene required for internodal elongation after flowering. *Plant J* **12**: 863–874

**Hanzawa Y, Takahashi T, Michael AJ, Burtin D, Long D, Pineiro M, Coupland G, Komeda Y** (2000) ACAULIS5, an *Arabidopsis* gene required for stem elongation, encodes a spermine synthase. *EMBO J* **19**: 4248–4256

**Hazen SP, Borevitz JO, Harmon FG, Pruneda-Paz JL, Schultz TF, Yanovsky MJ, Liljegren SJ, Ecker JR, Kay SA** (2005) Rapid array mapping of circadian clock and developmental mutations in

Arabidopsis. *Plant Physiol* **138**: 990–997

**Herr AJ, Jensen MB, Dalmay T, Baulcombe DC** (2005) RNA polymerase IV directs silencing of endogenous DNA. *Science* **308**: 118–120

**Hirochika H, Okamoto H, Kakutani T** (2000) Silencing of retrotransposons in arabidopsis and reactivation by the *ddm1* mutation. *Plant Cell* **12**: 357–369

**Hisanaga T, Ferjani A, Horiguchi G, Ishikawa N, Fujikura U, Kubo M, Demura T, Fukuda H, Ishida T, Sugimoto K, et al** (2013) The ATM-dependent DNA damage response acts as an upstream trigger for compensation in the *fas1* mutation during Arabidopsis leaf development. *Plant Physiol* **162**: 831–841

**Hoffman PD, Leonard JM, Lindberg GE, Bollmann SR, Hays JB** (2004) Rapid accumulation of mutations during seed-to-seed propagation of mismatch-repair-defective Arabidopsis. *Genes Dev* **18**: 2676–2685

**Huefner ND, Mizuno Y, Weil CF, Korf I, Britt AB** (2011) Breadth by depth: Expanding our understanding of the repair of transposon-induced DNA double strand breaks via deep-sequencing. *DNA Repair*. doi: 10.1016/j.dnarep.2011.07.011

**Inagaki S** (2006) Arabidopsis TEBIChI, with Helicase and DNA Polymerase Domains, Is Required for Regulated Cell Division and Differentiation in Meristems. *Plant Cell* **18**: 879–892

**Inagaki S, Nakamura K, Morikami A** (2009) A Link among DNA Replication, Recombination, and Gene Expression Revealed by Genetic and Genomic Analysis of TEBIChI Gene of Arabidopsis thaliana. *PLoS Genet* **5**: e1000613

**Irwin M, Marin MC, Phillips AC, Seelan RS, Smith DI, Liu W, Flores ER, Tsai KY, Jacks T, Vousden KH, et al** (2000) Role for the p53 homologue p73 in E2F-1-induced apoptosis. *Nature* **407**: 645–648

**Ishida T, Fujiwara S, Miura K, Stacey N, Yoshimura M, Schneider K, Adachi S, Minamisawa K, Umeda M, Sugimoto K** (2009) SUMO E3 Ligase HIGH PLOIDY2 Regulates Endocycle Onset and Meristem Maintenance in Arabidopsis. *Plant Cell* **21**: 2284–2297

**Ishikawa K, Ogawa T, Hirosue E, Nakayama Y, Harada K, Fukusaki E, Yoshimura K, Shigeoka S** (2009) Modulation of the Poly(ADP-ribosyl)ation Reaction via the Arabidopsis ADP-Ribose/NADH Pyrophosphohydrolase, AtNUDX7, Is Involved in the Response to Oxidative Stress. *Plant Physiol* **151**: 741–754

**Ito H, Gaubert H, Bucher E, Mirouze M, Vaillant I, Paszkowski J** (2011) An siRNA pathway prevents transgenerational retrotransposition in

plants subjected to stress. *Nature* **472**: 115–119

**Ito H, Yoshida T, Tsukahara S, Kawabe A** (2013) Evolution of the ONSEN retrotransposon family activated upon heat stress in Brassicaceae. *Gene* **518**: 256–261

**Izsvák Z, Stüwe EE, Fiedler D, Katzer A, Jeggo PA, Ivics Z** (2004) Healing the Wounds Inflicted by Sleeping Beauty Transposition by Double-Strand Break Repair in Mammalian Somatic Cells. *Mol Cell* **13**: 279–290

**Jamalkandi SA, Masoudi-Nejad A** (2009) Reconstruction of *Arabidopsis thaliana* fully integrated small RNA pathway. *Funct Integr Genomics* **9**: 419–432

**James GV, Patel V, Nordström KJ, Klasen JR, Salomé PA, Weigel D, Schneeberger K** (2013) User guide for mapping-by-sequencing in *Arabidopsis*. *Genome Biol* **14**: R61

**Jasinski S, Piazza P, Craft J, Hay A, Woolley L, Rieu I, Phillips A, Hedden P, Tsiantis M** (2005) KNOX action in *Arabidopsis* is mediated by coordinate regulation of cytokinin and gibberellin activities. *Curr Biol* **15**: 1560–1565

**Jeddeloh JA, Stokes TL, Richards EJ** (1999) Maintenance of genomic methylation requires a SWI2/SNF2-like protein. *Nat Genet* **22**: 94–97

**Jia Q, Dulk-Ras den A, Shen H, Hooykaas PJJ, de Pater S** (2013) Poly(ADP-ribose)polymerases are involved in microhomology mediated back-up non-homologous end joining in *Arabidopsis thaliana*. *Plant Mol Biol* **82**: 339–351

**Jiménez C, Capasso JM, Edelstein CL, Rivard CJ, Lucia S, Breusegem S, Berl T, Segovia M** (2009) Different ways to die: cell death modes of the unicellular chlorophyte *Dunaliella viridis* exposed to various environmental stresses are mediated by the caspase-like activity DEVDase. *J Exp Bot* **60**: 815–828

**Kakehi JI, Kuwashiro Y, Niitsu M, Takahashi T** (2008) Thermospermine is Required for Stem Elongation in *Arabidopsis thaliana*. *Plant Cell Physiol* **49**: 1342–1349

**Kaya H, Shibahara KI, Taoka KI, Iwabuchi M, Stillman B, Araki T** (2001) FASCIATA genes for chromatin assembly factor-1 in *arabidopsis* maintain the cellular organization of apical meristems. *Cell* **104**: 131–142

**Kimura S, Sakaguchi K** (2006) DNA repair in plants. *Chem Rev* **106**: 753–766

**Kimura S, Tahira Y, Ishibashi T, Mori Y, Mori T, Hashimoto J, Sakaguchi**

**K** (2004) DNA repair in higher plants; photoreactivation is the major DNA repair pathway in non-proliferating cells while excision repair (nucleotide excision repair and base excision repair) is active in proliferating cells. *Nucleic Acids Res* **32**: 2760–2767

**Klapholz B, Dietrich BH, Schaffner C, Hérédia F, Quivy J-P, Almouzni G, Dostatni N** (2009) CAF-1 is required for efficient replication of euchromatic DNA in *Drosophila* larval endocycling cells. *Chromosoma* **118**: 235–248

**Klattenhoff C, Theurkauf W** (2008) Biogenesis and germline functions of piRNAs. *Development* **135**: 3–9

**Klekowski EJ Jr** (1997) Klekowski Jr: Somatic mutation theory of clonality - Google Scholar. ... ecology and evolution of clonal ...

**Krizek BA, Meyerowitz EM** (1996) The *Arabidopsis* homeotic genes APETALA3 and PISTILLATA are sufficient to provide the B class organ identity function. *Development* **122**: 11–22

**Kuchen EE, Fox S, de Reuille PB, Kennaway R, Bensmihen S, Avondo J, Calder GM, Southam P, Robinson S, Bangham A, et al** (2012) Generation of leaf shape through early patterns of growth and tissue polarity. *Science* **335**: 1092–1096

**Kumar SV, Wigge PA** (2010) H2A.Z-Containing Nucleosomes Mediate the Thermosensory Response in *Arabidopsis*. *Cell* **140**: 136–147

**Kunz BA, Straffon AFL, Vonarx EJ** (2000) DNA damage-induced mutation: tolerance via translesion synthesis. *Mutation Research/Fundamental and Molecular Mechanisms of Mutagenesis* **451**: 169–185

**Kusano T, Berberich T, Tateda C, Takahashi Y** (2008) Polyamines: essential factors for growth and survival. *Planta* **228**: 367–381

**la Chaux de N, Tsuchimatsu T, Shimizu KK, Wagner A** (2012) The predominantly selfing plant *Arabidopsis thaliana* experienced a recent reduction in transposable element abundance compared to its outcrossing relative *Arabidopsis lyrata*. *Mobile DNA* **3**: 2

**Lal A, Pan Y, Navarro F, Dykxhoorn DM, Moreau L, Meire E, Bentwich Z, Lieberman J, Chowdhury D** (2009) miR-24-mediated downregulation of H2AX suppresses DNA repair in terminally differentiated blood cells. *Nat Struct Mol Biol* **16**: 492–498

**Lang-Mladek C, Popova O, Kiok K, Berlinger M, Rakic B, Aufsatz W, Jonak C, Hauser M-T, Luschnig C** (2010) Transgenerational inheritance and resetting of stress-induced loss of epigenetic gene silencing in *Arabidopsis*. *Molecular Plant* **3**: 594–602

**Lario L, Ramirez-Parra E, Gutierrez C, Spampinato C, Casati P** (2013) ASF1 Proteins are Involved in UV-induced DNA Damage Repair and are Cell Cycle Regulated by E2F Transcription Factors in *Arabidopsis thaliana*. *Plant Physiol.* doi: 10.1104/pp.112.212837

**Laux T** (2003) The stem cell concept in plants: a matter of debate. *Cell* **113**: 281–283

**Lee H-C, Chang S-S, Choudhary S, Aalto AP, Maiti M, Bamford DH, Liu Y** (2009a) qRNA is a new type of small interfering RNA induced by DNA damage. *Nature* **459**: 274–277

**Lee HO, Davidson JM, Duronio RJ** (2009b) Endoreplication: polyploidy with purpose. *Genes Dev*

**Lenhard M, Jürgens G, Laux T** (2002) The WUSCHEL and SHOOTMERISTEMLESS genes fulfil complementary roles in *Arabidopsis* shoot meristem regulation. *Development* **129**: 3195–3206

**Li X, Song Y, Century K, Straight S, Ronald P, Dong X, Lassner M, Zhang Y** (2001) A fast neutron deletion mutagenesis-based reverse genetics system for plants. *Plant J* **27**: 235–242

**Lindahl T** (1996) DNA Ligase IV from HeLa Cell Nuclei. *Journal of Biological Chemistry* **271**: 24257–24261

**Lisch D** (2009) Epigenetic regulation of transposable elements in plants. *Annual review of plant biology* **60**: 43–66

**Lissy NA, Davis PK, Irwin M, Kaelin WG, Dowdy SF** (2000) A common E2F-1 and p73 pathway mediates cell death induced by TCR activation. *Nature* **407**: 642–645

**Liu X, Yu CW, Duan J, Luo M, Wang K, Tian G, Cui Y, Wu K** (2012) HDA6 directly interacts with DNA methyltransferase MET1 and maintains transposable element silencing in *Arabidopsis*. *Plant Physiol* **158**: 119–129

**Liu Y, Lu X** (2012) Non-coding RNAs in DNA damage response. *Am J Cancer Res* **2**: 658–675

**Long JA, Moan EI, Medford JI, Barton MK** (1996) A member of the KNOTTED class of homeodomain proteins encoded by the STM gene of *Arabidopsis*. *Nature* **379**: 66–69

**Long Q, Rabanal FA, Meng D, Huber CD, Farlow A** (2013a) Massive genomic variation and strong selection in *Arabidopsis thaliana* lines from Sweden. *Nature*

**Long Q, Rabanal FA, Meng D, Huber CD, Farlow A, Platzer A, Zhang Q,**

**Vilhjálmsdóttir BJ, Korte A, Nizhynska V, et al** (2013b) Massive genomic variation and strong selection in *Arabidopsis thaliana* lines from Sweden. *Nat Genet*. doi: 10.1038/ng.2678

**Loonstra A, Vooijs M, Beverloo HB, Allak Al B, van Drunen E, Kanaar R, Berns A, Jonkers J** (2000) Illegitimate Cre-dependent chromosome rearrangements in transgenic mouse spermatids. *Proc Natl Acad Sci USA* **97**: 13702–13707

**Lorrain S, Lin B, Auriac MC, Kroj T, Saindrenan P, Nicole M, Balagué C, Roby D** (2004) Vascular associated death1, a novel GRAM domain-containing protein, is a regulator of cell death and defense responses in vascular tissues. *Plant Cell* **16**: 2217–2232

**Ly V, Hatherell A, Kim E, Chan A, Belmonte MF, Schroeder DF** (2013) Interactions between *Arabidopsis* DNA repair genes UVH6, DDB1A, and DDB2 during abiotic stress tolerance and floral development. *Plant Sci* **213**: 88–97

**Lydall D, Whitehall S** (2005) Chromatin and the DNA damage response. *DNA Repair* **4**: 1195–1207

**Mace PD, Riedl SJ** (2010) Molecular cell death platforms and assemblies. *Current Opinion in Cell Biology* **22**: 828–836

**Marí-Ordóñez A, Marchais A, Etcheverry M, Martin A, Colot V, Voinnet O** (2013) Reconstructing de novo silencing of an active plant retrotransposon. *Nat Genet*. doi: 10.1038/ng.2703

**Martínez de Alba AE, Elvira-Matelot E, Vaucheret H** (2013) Gene silencing in plants: A diversity of pathways. *Biochimica et Biophysica Acta (BBA) - Gene Regulatory Mechanisms* **1829**: 1300–1308

**Martínez G, Slotkin RK** (2012) Developmental relaxation of transposable element silencing in plants: functional or byproduct? *Curr Opin Plant Biol* **15**: 496–502

**Matsunaga W, Kobayashi A, Kato A, Ito H** (2011) The effects of heat induction and the siRNA biogenesis pathway on the transgenerational transposition of ONSEN, a copia-like retrotransposon in *Arabidopsis thaliana*. *Plant Cell Physiol*. doi: 10.1093/pcp/pcr179

**McConnell JR, Emery J, Eshed Y, Bao N, Bowman J, Barton MK** (2001) Role of PHABULOSA and PHAVOLUTA in determining radial patterning in shoots. *Nature* **411**: 709–713

**McCue AD, Nuthikattu S, Reeder SH, Slotkin RK** (2012) Gene expression and stress response mediated by the epigenetic regulation of a transposable element small RNA. *PLoS Genet* **8**: e1002474

**McCue AD, Slotkin RK** (2012) Transposable element small RNAs as regulators of gene expression. *Trends Genet* **28**: 616–623

**Mehrotra S, Maqbool SB, Kolpakas A, Murnen K, Calvi BR** (2008) Endocycling cells do not apoptose in response to DNA rereplication genotoxic stress. *Genes Dev* **22**: 3158–3171

**Meister G** (2013) Argonaute proteins: functional insights and emerging roles. *Nat Rev Genet* **14**: 447–459

**Michalik KM, Bottcher R, Forstemann K** (2012) A small RNA response at DNA ends in Drosophila. *Nucleic Acids Res* **40**: 9596–9603

**Mirouze M, Reinders J, Bucher E, Nishimura T, Schneeberger K, Ossowski S, Cao J, Weigel D, Paszkowski J, Mathieu O** (2009) Selective epigenetic control of retrotransposition in Arabidopsis. *Nature* **461**: 427–430

**Mishra NS, Tuteja R, Tuteja N** (2006) Signaling through MAP kinase networks in plants. *Arch Biochem Biophys* **452**: 55–68

**Morel JB, Mourrain P, Béclin C, Vaucheret H** (2000) DNA methylation and chromatin structure affect transcriptional and post-transcriptional transgene silencing in Arabidopsis. *Curr Biol* **10**: 1591–1594

**Muñiz L, Minguez EG, Singh SK, Pesquet E, Vera-Sirera F, Moreau-Courtois CL, Carbonell J, Blázquez MA, Tuominen H** (2008) ACAULIS5 controls Arabidopsis xylem specification through the prevention of premature cell death. *Development* **135**: 2573–2582

**Naka Y, Watanabe K, Sagor GHM, Niitsu M, Pillai MA, Kusano T, Takahashi Y** (2010) Quantitative analysis of plant polyamines including thermospermine during growth and salinity stress☆. *Plant Physiology and Biochemistry* **48**: 527–533

**Nelson JR, Lawrence CW, Hinkle DC** (1996) Thymine-Thymine Dimer Bypass by Yeast DNA Polymerase zeta. *Science* **272**: 1646–1649

**Norbury CJ, Zhivotovsky B** (2004) DNA damage-induced apoptosis. *Oncogene* **23**: 2797–2808

**O'Hagan HM** (2013) Chromatin modifications during repair of environmental exposure-induced DNA damage: A potential mechanism for stable epigenetic alterations. *Environ Mol Mutagen* n/a-n/a

**O'Hagan HM, Mohammad HP, Baylin SB** (2008) Double Strand Breaks Can Initiate Gene Silencing and SIRT1-Dependent Onset of DNA Methylation in an Exogenous Promoter CpG Island. *PLoS Genet* **4**: e1000155

**Ohashi-Ito K, Oda Y, Fukuda H** (2010) Arabidopsis VASCULAR-RELATED

NAC-DOMAIN6 Directly Regulates the Genes That Govern Programmed Cell Death and Secondary Wall Formation during Xylem Differentiation. *Plant Cell* **22**: 3461–3473

**Ohsawa R, Seol JH, Tyler JK** (2013) At the intersection of non-coding transcription, DNA repair, chromatin structure, and cellular senescence. *Frontiers in Genetics*. doi: 10.3389/fgene.2013.00136

**Page DR, Grossniklaus U** (2002) The art and design of genetic screens: *Arabidopsis thaliana*. *Nat Rev Genet* **3**: 124–136

**Pankotai T, Bonhomme C, Chen D, Soutoglou E** (2012) DNAPKcs-dependent arrest of RNA polymerase II transcription in the presence of DNA breaks. *Nat Struct Mol Biol* **19**: 276–282

**Phelps-Durr TL, Thomas J, Vahab P, Timmermans MCP** (2005) Maize rough sheath2 and Its *Arabidopsis* Orthologue ASYMMETRIC LEAVES1 Interact with HIRA, a Predicted Histone Chaperone, to Maintain knox Gene Silencing and Determinacy during Organogenesis.

**Pluthero FG** (1993) Rapid purification of high-activity Taq DNA polymerase. *Nucleic Acids Res* **21**: 4850

**Pollock TJ, Nash HA** (1983) Knotting of DNA caused by a genetic rearrangement: Evidence for a nucleosome-like structure in site-specific recombination of bacteriophage lambda. *Journal of Molecular Biology* **170**: 1–18

**Polo SE, Jackson SP** (2011) Dynamics of DNA damage response proteins at DNA breaks: a focus on protein modifications. *Genes Dev* **25**: 409–433

**Poulsen C, Vaucheret H, Brodersen P** (2013) Lessons on RNA silencing mechanisms in plants from eukaryotic argonaute structures. *Plant Cell* **25**: 22–37

**Preuss SB, Britt AB** (2003) A DNA-damage-induced cell cycle checkpoint in *Arabidopsis*. *Genetics* **164**: 323–334

**Puchta H, Fauser F** (2013) Synthetic nucleases for genome engineering in plants: prospects for a bright future. *Plant J.* doi: 10.1111/tpj.12338

**Quenouille MH** (1949) JSTOR: *Biometrics*, Vol. 5, No. 2 (Jun., 1949), pp. 162–164. *Biometrics*

**Qüesta JI, Fina JP, Casati P** (2013) DDM1 and ROS1 have a role in UV-B induced- and oxidative DNA damage in *A. thaliana*. *Front Plant Sci.* doi: 10.3389/fpls.2013.00420

**Ramsden DA** (1998) Ku protein stimulates DNA end joining by mammalian DNA ligases: a direct role for Ku in repair of DNA double-strand breaks.

EMBO J **17**: 609–614

**Rhoades HM, Overall JE** (1982) A sample size correction for Pearson chi-square in 2??2 contingency tables. *Psychological Bulletin* **91**: 418–423

**Riha K** (2001) Living with Genome Instability: Plant Responses to Telomere Dysfunction. *Science* **291**: 1797–1800

**Rossi M, De Laurenzi V, Munarriz E, Green DR, Liu Y-C, Vousden KH, Cesareni G, Melino G** (2005) The ubiquitin-protein ligase Itch regulates p73 stability. *EMBO J* **24**: 836–848

**Sablowski R** (2004) Plant and animal stem cells: conceptually similar, molecularly distinct? *Trends Cell Biol* **14**: 605–611

**Sablowski R** (2007) The dynamic plant stem cell niches. *Curr Opin Plant Biol* **10**: 639–644

**Satina S, Blakeslee AF, Avery AG** (1940) JSTOR: American Journal of Botany, Vol. 27, No. 10 (Dec., 1940), pp. 895-905. American Journal of Botany

**Sánchez-Calderón L, López-Bucio J, Chacón-López A, Cruz-Ramírez A, Nieto-Jacobo F, Dubrovsky JG, Herrera-Estrella L** (2005) Phosphate starvation induces a determinate developmental program in the roots of *Arabidopsis thaliana*. *Plant Cell Physiol* **46**: 174–184

**Scheres B, van den Berg C, Willemsen V, Hendriks G, Weisbeek P** (1997) Short-range control of cell differentiation in the *Arabidopsis* root meristem. *Nature* **390**: 287–289

**Schiessl K, Kausika S, Southam P, Bush M, Sablowski R** (2012) JAGGED controls growth anisotropy and coordination between cell size and cell cycle during plant organogenesis. *Curr Biol* **22**: 1739–1746

**Schindelin J, Arganda-Carreras I, Frise E, Kaynig V, Longair M, Pietzsch T, Preibisch S, Rueden C, Saalfeld S, Schmid B, et al** (2012) Fiji: an open-source platform for biological-image analysis. *Nature Methods* **9**: 676–682

**Schneider-Poetsch T, Ju J, Eyler DE, Dang Y, Bhat S, Merrick WC, Green R, Shen B, Liu JO** (2010) Inhibition of eukaryotic translation elongation by cycloheximide and lactimidomycin. *Nat Chem Biol* **6**: 209–217

**Schoof H, Lenhard M, Haecker A, Mayer KF, Jürgens G, Laux T** (2000) The stem cell population of *Arabidopsis* shoot meristems is maintained by a regulatory loop between the CLAVATA and WUSCHEL genes. *Cell* **100**: 635–644

**Scofield S, Murray JAH** (2006) KNOX Gene Function in Plant Stem Cell

Niches. *Plant Mol Biol* **60**: 929–946

**Scully R, Xie A** (2013) Double strand break repair functions of histone H2AX. *Mutation Research/Fundamental and Molecular Mechanisms of Mutagenesis*. doi: 10.1016/j.mrfmmm.2013.07.007

**Shanbhag NM, Rafalska-Metcalf IU, Balane-Bolivar C, Janicki SM, Greenberg RA** (2010) ATM-dependent chromatin changes silence transcription in cis to DNA double-strand breaks. *Cell* **141**: 970–981

**Shiloh Y, Ziv Y** (2013) The ATM protein kinase: regulating the cellular response to genotoxic stress, and more. *Nat Rev Mol Cell Biol* –

**Shroff R, Arbel-Eden A, Pilch D, Ira G, Bonner WM, Petrini JH, Haber JE, Lichten M** (2004) Distribution and Dynamics of Chromatin Modification Induced by a Defined DNA Double-Strand Break. *Current Biology* **14**: 1703–1711

**Sieburth LE, Drews GN, Meyerowitz EM** (1998) Non-autonomy of AGAMOUS function in flower development: use of a Cre/loxP method for mosaic analysis in *Arabidopsis*. *Development* **125**: 4303–4312

**Skalka AM, Katz RA** (2005) Retroviral DNA integration and the DNA damage response. *Cell Death Differ* **12**: 971–978

**Slotkin RK, Martienssen R** (2007) Transposable elements and the epigenetic regulation of the genome. *Nat Rev Genet* **8**: 272–285

**Slotkin RK, Vaughn M, Borges F, Tanurdžić M, Becker JD, Feijó JA, Martienssen RA** (2009) Epigenetic reprogramming and small RNA silencing of transposable elements in pollen. *Cell* **136**: 461–472

**Smetana O, Siroky J, Houlne G, Opatrny Z, Chaboute ME** (2012) Non-apoptotic programmed cell death with paraptotic-like features in bleomycin-treated plant cells is suppressed by inhibition of ATM/ATR pathways or NtE2F overexpression. *J Exp Bot*. doi: 10.1093/jxb/err439

**Smith J, Tho LM, Xu N, Gillespie DA** (2010) The ATM-Chk2 and ATR-Chk1 pathways in DNA damage signaling and cancer. *Adv Cancer Res* **108**: 73–112

**Soga K, Wakabayashi K, Hoson T, Kamisaka S** (2000) Flower stalk segments of *Arabidopsis thaliana* ecotype Columbia lack the capacity to grow in response to exogenously applied auxin. *Plant Cell Physiol* **41**: 1327–1333

**Sozzani R, Cui H, Moreno-Risueno MA, Busch W, van Norman JM, Vernoux T, Brady SM, Dewitte W, Murray J, Benfey PN** (2010) Spatiotemporal regulation of cell-cycle genes by SHORTROOT links patterning and growth. *Nature* **466**: 128–132

**Sperandio S, de Belle I, Bredesen DE** (2000) An alternative, nonapoptotic form of programmed cell death. *Proc Natl Acad Sci USA* **97**: 14376–14381

**Sperandio S, Poksay K, de Belle I, Lafuente MJ, Liu B, Nasir J, Bredesen DE** (2004) Paraptosis: mediation by MAP kinases and inhibition by AIP-1/Alix. *Cell Death Differ* **11**: 1066–1075

**Sperandio S, Poksay KS, Schilling B, Crippen D, Gibson BW, Bredesen DE** (2010) Identification of new modulators and protein alterations in non-apoptotic programmed cell death. *J Cell Biochem* **111**: 1401–1412

**Stahl Y, Wink RH, Ingram GC, Simon R** (2009) A Signaling Module Controlling the Stem Cell Niche in *Arabidopsis* Root Meristems. *Current Biology* **19**: 909–914

**Strange A, Li P, Lister C, Anderson J, Warthmann N, Shindo C, Irwin J, Nordborg M, Dean C** (2011) Major-Effect Alleles at Relatively Few Loci Underlie Distinct Vernalization and Flowering Variation in *Arabidopsis* Accessions. *PLoS ONE* **6**: e19949

**Stroud H, Greenberg MVC, Feng S, Bernatavichute YV, Jacobsen SE** (2013) Comprehensive Analysis of Silencing Mutants Reveals Complex Regulation of the *Arabidopsis* Methylome. *Cell* **152**: 352–364

**Suzuki T, Inagaki S, Nakajima S, Akashi T, Ohto M-A, Kobayashi M, Seki M, Shinozaki K, Kato T, Tabata S, et al** (2004) A novel *Arabidopsis* gene TONSOKU is required for proper cell arrangement in root and shoot apical meristems. *The Plant Journal* **38**: 673–684

**Suzuki T, Nakajima S, Inagaki S, Hirano-Nakakita M, Matsuoka K, Demura T, Fukuda H, Morikami A, Nakamura K** (2005) TONSOKU is expressed in S phase of the cell cycle and its defect delays cell cycle progression in *Arabidopsis*. *Plant Cell Physiol* **46**: 736–742

**T Carter IVISWLSD** (1990) A DNA-activated protein kinase from HeLa cell nuclei. *Mol Cell Biol* **10**: 6460

**Takeda S, Tadele Z, Hofmann I, Probst AV, Angelis KJ, Kaya H, Araki T, Mengiste T, Mittelsten Scheid O, Shibahara K-I, et al** (2004) BRU1, a novel link between responses to DNA damage and epigenetic gene silencing in *Arabidopsis*. *Genes Dev* **18**: 782–793

**Thieme CJ, Schudoma C, May P, Walther D** (2012a) Give It AGO: The Search for miRNA-Argonaute Sorting Signals in *Arabidopsis thaliana* Indicates a Relevance of Sequence Positions Other than the 5'-Position Alone. *Front Plant Sci.* doi: 10.3389/fpls.2012.00272

**Thieme CJ, Schudoma C, May P, Walther D** (2012b) Give It AGO: The Search for miRNA-Argonaute Sorting Signals in *Arabidopsis thaliana*

Indicates a Relevance of Sequence Positions Other than the 5'-Position Alone. *Front Plant Sci* **3**: 272

**Tong W-M, Cortes U, Hande MP, Ohgaki H, Cavalli LR, Lansdorp PM, Haddad BR, Wang Z-Q** (2002) Synergistic role of Ku80 and poly(ADP-ribose) polymerase in suppressing chromosomal aberrations and liver cancer formation. *Cancer Res* **62**: 6990–6996

**Tran RK, Zilberman D, de Bustos C, Ditt RF, Henikoff JG, Lindroth AM, Delrow J, Boyle T, Kwong S, Bryson TD, et al** (2005) Chromatin and siRNA pathways cooperate to maintain DNA methylation of small transposable elements in *Arabidopsis*. *6*: R90

**Truernit E, Haseloff J** (2008) A simple way to identify non-viable cells within living plant tissue using confocal microscopy. *Plant methods*

**Ulm R, Ichimura K, Mizoguchi T, Peck SC, Zhu T, Wang X, Shinozaki K, Paszkowski J** (2002) Distinct regulation of salinity and genotoxic stress responses by *Arabidopsis* MAP kinase phosphatase 1. *EMBO J* **21**: 6483–6493

**Ulm R, Revenkova E, di Sansebastiano GP, Bechtold N, Paszkowski J** (2001) Mitogen-activated protein kinase phosphatase is required for genotoxic stress relief in *Arabidopsis*. *Genes Dev* **15**: 699–709

**van Doorn WG, Woltering EJ** (2005) Many ways to exit? Cell death categories in plants. *Trends Plant Sci* **10**: 117–122

**Vazquez F** (2006) *Arabidopsis* endogenous small RNAs: highways and byways. *Trends Plant Sci* **11**: 460–468

**Vera-Sirera F, Minguez EG, Singh SK, Ljung K, Tuominen H, Blázquez MA, Carbonell J** (2010) Role of polyamines in plant vascular development. *Plant Physiology and Biochemistry* **48**: 534–539

**Vogelstein B, Lane D, Levine AJ** (2000) Surfing the p53 network. *Nature* **408**: 307–310

**Wachsman G, Heidstra R, Scheres B** (2011) Distinct Cell-Autonomous Functions of RETINOBLASTOMA-RELATED in *Arabidopsis* Stem Cells Revealed by the Brother of Brainbow Clonal Analysis System. *Plant Cell*. doi: 10.1105/tpc.111.086199

**Walker JR, Corpina RA, Goldberg J** (2001) Access : Structure of the Ku heterodimer bound to DNA and its implications for double-strand break repair : *Nature* **412**: 607–614

**Wan G, Liu Y, Han C, Zhang X, Lu X** (2013) Noncoding RNAs in DNA Repair and Genome Integrity. *Antioxid Redox Signal*. doi: 10.1089/ars.2013.5514

**Wang S, Wen R, Shi X, Lambrecht A, Wang H, Xiao W** (2011) RAD5a and REV3 function in two alternative pathways of DNA-damage tolerance in *Arabidopsis*. *DNA Repair* **10**: 620–628

**Wang X, Weigel D, Smith LM** (2013) Transposon variants and their effects on gene expression in *Arabidopsis*. *PLoS Genet* **9**: e1003255

**Wang Y, Taniguchi T** (2013) MicroRNAs and DNA damage response: Implications for cancer therapy. *Cell Cycle* **12**: 32–42

**Ward IM, Minn K, van Deursen J, Chen J** (2003) p53 Binding protein 53BP1 is required for DNA damage responses and tumor suppression in mice. *Mol Cell Biol* **23**: 2556–2563

**Watanabe N, Lam E** (2011) *Arabidopsis* metacaspase 2d is a positive mediator of cell death induced during biotic and abiotic stresses. *Plant J* **66**: 969–982

**Waterworth WM, Drury GE, Bray CM, West CE** (2011) Repairing breaks in the plant genome: the importance of keeping it together. *New Phytol* **192**: 805–822

**Waterworth WM, Masnavi G, Bhardwaj RM, Jiang Q, Bray CM, West CE** (2010) A plant DNA ligase is an important determinant of seed longevity. *The Plant Journal* **63**: 848–860

**Wei H, Ben Zhou, Zhang F, Tu Y, Hu Y, Zhang B, Zhai Q** (2013) Profiling and Identification of Small rDNA-Derived RNAs and Their Potential Biological Functions. *PLoS ONE* **8**: e56842

**Wei W, Ba Z, Gao M, Wu Y, Ma Y, Amiard S, White CI, Rendtlew Danielsen JM, Yang Y-G, Qi Y** (2012) A role for small RNAs in DNA double-strand break repair. *Cell* **149**: 101–112

**West CE, Waterworth WM, Story GW, Sunderland PA, Jiang Q, Bray CM** (2002) Disruption of the *Arabidopsis* AtKu80 gene demonstrates an essential role for AtKu80 protein in efficient repair of DNA double-strand breaks *in vivo*. *The Plant Journal* **31**: 517–528

**White K, Grether ME, Abrams JM, Young L, Farrell K, Steller H** (1994) Genetic control of programmed cell death in *Drosophila*. *Science* **264**: 677–683

**Wielopolska A, Townley H, Moore I, Waterhouse P, Helliwell C** (2005) A high-throughput inducible RNAi vector for plants. *Plant Biotechnology Journal* **3**: 583–590

**Wildwater M, Campilho A, Perez-Perez JM, Heidstra R** (2005) The RETINOBLASTOMA-RELATED Gene Regulates Stem Cell Maintenance in *Arabidopsis* Roots. *Cell*

**Wyllie AH, Rich T, Allen RL** (2000) Defying death after DNA damage. *Nature* **407**: 777–783

**Xie Z, Allen E, Wilken A, Carrington JC** (2005) DICER-LIKE 4 functions in trans-acting small interfering RNA biogenesis and vegetative phase change in *Arabidopsis thaliana*. *Proc Natl Acad Sci USA* **102**: 12984–12989

**Xie Z, Johansen LK, Gustafson AM, Kasschau KD, Lellis AD, Zilberman D, Jacobsen SE, Carrington JC** (2004) Genetic and Functional Diversification of Small RNA Pathways in Plants. *PLoS Biol* **2**: e104

**Xu Y, Wang Y, Stroud H, Gu X, Sun B, Gan E-S, Ng K-H, Jacobsen SE, He Y, Ito T** (2013) A Matrix Protein Silences Transposons and Repeats through Interaction with Retinoblastoma-Associated Proteins. *Current Biology* **23**: 345–350

**Yadav RK, Girke T, Pasala S, Xie M, Reddy GV** (2009) Gene expression map of the *Arabidopsis* shoot apical meristem stem cell niche. *Proc Natl Acad Sci USA* **106**: 4941–4946

**Yadav RK, Perales M, Gruel J, Girke T, Jönsson H, Reddy GV** (2011) WUSCHEL protein movement mediates stem cell homeostasis in the *Arabidopsis* shoot apex. *Genes Dev* **25**: 2025–2030

**Yadav RK, Tavakkoli M, Reddy GV** (2010) WUSCHEL mediates stem cell homeostasis by regulating stem cell number and patterns of cell division and differentiation of stem cell progenitors. *Development* **137**: 3581–3589

**Yamada Y, Coffman CR** (2005) DNA damage-induced programmed cell death: potential roles in germ cell development. *Ann N Y Acad Sci* **1049**: 9–16

**Yanai O, Shani E, Dolezal K, Tarkowski P, Sablowski R, Sandberg G, Samach A, Ori N** (2005) *Arabidopsis* KNOXI proteins activate cytokinin biosynthesis. *Curr Biol* **15**: 1566–1571

**Yant SR, Kay MA** (2003) Nonhomologous-End-Joining Factors Regulate DNA Repair Fidelity during Sleeping Beauty Element Transposition in Mammalian Cells. *Mol. Cell. Biol.*

**Yao Y, Bilichak A, Golubov A, Blevins T, Kovalchuk I** (2010) Differential sensitivity of *Arabidopsis* siRNA biogenesis mutants to genotoxic stress. *Plant cell reports* **29**: 1401–1410

**Yokota Y, Shikazono N, Tanaka A, Hase Y, Funayama T, Wada S, Inoue M** (2005) Comparative Radiation Tolerance Based on the Induction of DNA Double-Strand Breaks in Tobacco BY-2 Cells and CHO-K1 Cells Irradiated with Gamma Rays. *Radiation Research* **163**: 520–525

**Yoshiyama K, Conklin PA, Huefner ND, Britt AB** (2009) Suppressor of gamma response 1 (SOG1) encodes a putative transcription factor governing multiple responses to DNA damage. *Proc Natl Acad Sci USA* **106**: 12843–12848

**Yoshiyama KO, Kobayashi J, Ogita N, Ueda M, Kimura S, Maki H, Umeda M** (2013a) ATM-mediated phosphorylation of SOG1 is essential for the DNA damage response in *Arabidopsis*. *EMBO Rep* –

**Yoshiyama KO, Sakaguchi K, Kimura S** (2013b) DNA Damage Response in Plants: Conserved and Variable Response Compared to Animals. *Biology*

**Yousefzadeh MJ, Wood RD** (2013) DNA polymerase POLQ and cellular defense against DNA damage. *DNA Repair* **12**: 1–9

**Zellinger B, Akimcheva S, Puizina J, Schirato M, Riha K** (2007) Ku suppresses formation of telomeric circles and alternative telomere lengthening in *Arabidopsis*. *Mol Cell* **27**: 163–169

**Zhang Z, Hu L, Kong X** (2013) MicroRNA or NMD: Why have two RNA silencing systems? *Journal of Genetics and Genomics*

**Zhao Z, Andersen SU, Ljung K, Dolezal K, Miotk A, Schultheiss SJ, Lohmann JU** (2010) Hormonal control of the shoot stem-cell niche. *Nature* **465**: 1089–1092

**Zhong S-H, Liu J-Z, Jin H, Lin L, Li Q, Chen Y, Yuan Y-X, Wang Z-Y, Huang H, Qi Y-J, et al** (2013) Warm temperatures induce transgenerational epigenetic release of RNA silencing by inhibiting siRNA biogenesis in *Arabidopsis*. *Proc Natl Acad Sci USA*. doi: 10.1073/pnas.1219655110

**Zhu J-K** (2009) Active DNA demethylation mediated by DNA glycosylases. *Annu Rev Genet* **43**: 143–166

**Zilberman D, Cao X, Jacobsen SE** (2003) ARGONAUTE4 control of locus-specific siRNA accumulation and DNA and histone methylation. *Science* **299**: 716–719